



UNIVERSITAT DE
BARCELONA

Development of Epstein-Barr Virus-Specific T cells expressing anti-CD19 Chimeric Antigen Receptor for cancer immunotherapy

Ana Gabriela Lara de León

ADVERTIMENT. La consulta d'aquesta tesi queda condicionada a l'acceptació de les següents condicions d'ús: La difusió d'aquesta tesi per mitjà del servei TDX (www.tdx.cat) i a través del Dipòsit Digital de la UB (diposit.ub.edu) ha estat autoritzada pels titulars dels drets de propietat intel·lectual únicament per a usos privats emmarcats en activitats d'investigació i docència. No s'autoritza la seva reproducció amb finalitats de lucre ni la seva difusió i posada a disposició des d'un lloc aliè al servei TDX ni al Dipòsit Digital de la UB. No s'autoritza la presentació del seu contingut en una finestra o marc aliè a TDX o al Dipòsit Digital de la UB (framing). Aquesta reserva de drets afecta tant al resum de presentació de la tesi com als seus continguts. En la utilització o cita de parts de la tesi és obligat indicar el nom de la persona autora.

ADVERTENCIA. La consulta de esta tesis queda condicionada a la aceptación de las siguientes condiciones de uso: La difusión de esta tesis por medio del servicio TDR (www.tdx.cat) y a través del Repositorio Digital de la UB (diposit.ub.edu) ha sido autorizada por los titulares de los derechos de propiedad intelectual únicamente para usos privados enmarcados en actividades de investigación y docencia. No se autoriza su reproducción con finalidades de lucro ni su difusión y puesta a disposición desde un sitio ajeno al servicio TDR o al Repositorio Digital de la UB. No se autoriza la presentación de su contenido en una ventana o marco ajeno a TDR o al Repositorio Digital de la UB (framing). Esta reserva de derechos afecta tanto al resumen de presentación de la tesis como a sus contenidos. En la utilización o cita de partes de la tesis es obligado indicar el nombre de la persona autora.

WARNING. On having consulted this thesis you're accepting the following use conditions: Spreading this thesis by the TDX (www.tdx.cat) service and by the UB Digital Repository (diposit.ub.edu) has been authorized by the titular of the intellectual property rights only for private uses placed in investigation and teaching activities. Reproduction with lucrative aims is not authorized nor its spreading and availability from a site foreign to the TDX service or to the UB Digital Repository. Introducing its content in a window or frame foreign to the TDX service or to the UB Digital Repository is not authorized (framing). Those rights affect to the presentation summary of the thesis as well as to its contents. In the using or citation of parts of the thesis it's obliged to indicate the name of the author.



UNIVERSITAT DE
BARCELONA

**Development of Epstein-Barr Virus-Specific T cells
expressing anti-CD19 Chimeric Antigen Receptor for
cancer immunotherapy**

Ana Gabriela Lara de León



UNIVERSITAT DE
BARCELONA

Department of Medicine

Doctoral program in Biomedicine

Immunology

**Development of Epstein-Barr Virus-Specific T cells
expressing anti-CD19 Chimeric Antigen Receptor for
cancer immunotherapy**

Doctoral thesis dissertation presented by

Ana Gabriela Lara de León

A handwritten signature in black ink, appearing to read "Ana Gabriela Lara de León".

to obtain the degree of

Doctor in Philosophy by the University of Barcelona

September 2024

Supervision: **Francesc Rudilla Salvador**

(Banc de Sang i Teixits, Barcelona, España)

Tutorship: **Manel Juan Otero**

(Institut d'Investigacions Biomèdiques August Pi i Sunyer (IDIBAPS), Barcelona,
Espanya)

*To my parents,
brothers,
and grandparents.*

*“To achieve great things, we must not only act but also dream, not only plan but also
believe”*

Anatole France

ACKNOWLEDGMENTS/AGRADECIMIENTOS

Lo más bonito de este viaje llamado vida son las personas con las que coincidimos en el camino. He tenido la fortuna de coincidir con personas maravillosas en esta etapa de mi vida profesional quienes con su apoyo y cariño han hecho que esta experiencia sea menos dura y mucho más alegre. No podría estar más agradecida con Dios por haberlos puesto en mi camino, por la oportunidad de realizar este doctorado y darme la sabiduría para salir adelante cada día.

Manel y Francesc, muchas gracias por la oportunidad que me habéis dado, por confiar en mí para este proyecto y por la colaboración que surgió entre ambos centros. Francesc, moltes gràcies per guiar-me, pels teus consells, per escoltar-me, per la teva paciència, esforç, temps i dedicació. He après molt i sempre valoraré i estaré molt agraïda per tot el que m'has ensenyat. Espero que la vida ens segueixi donant oportunitats de continuar col·laborant.

Sergi Querol, gracias por permitir desarrollar el proyecto de mi tesis doctoral en el Banc de Sang i Teixits en colaboración con el IDIBAPS, Hospital Clínic.

VSTs-team: Rut, moltes gràcies per ensenyar-me no només coses pràctiques de laboratori, sinó també a desenvolupar un pensament crític, per les idees al llarg del projecte, per resoldre els meus dubtes i guiar-me quan ho he necessitat, però sobretot, moltes gràcies per ser una amiga i un suport. Emma y Mireia, Gràcies per la vostra ajuda, col·laboració i temps en el processament i anàlisi de les mostres de TCR. Maria, gràcies per fer els meus dies més alegres, per les rialles, aventures, per les paraules d'ànim, per la teva bonica amistat i pel suport al laboratori quan no donava a l'abast (canvis de medi, marcatges intracel·lulars però sobretot per les compensacions jajaja). Miriam, gràcies pel suport experimental i els ànims a la recta final. Gràcies a totes per donar-me suport i anims sempre, per les discussions i idees en els lab meetings, les quals m'ajudaven a créixer professionalment i aportaven millores al projecte.

CAR-T-team: Mario, Blanca, Rober, Sergio, Ari, Mireia, Iñaki, Berta, Maria, Cristina, Lorena, Sergi, Valeria, Mercedes, Alexis, Alejandro, Joan, Ane, Andrea, Erik, Elisabet, Montse y Nela, gracias por compartir conmigo, hacerme sentir cómoda e incluida cada vez que iba al CEK y por tomarme en cuenta en los planes fuera del lab. Sois unas personas increíbles. Mario, trabajar contigo en el proyecto de Yamanaka ha sido una experiencia que no sólo nos ha retado profesionalmente, sino que también generó una bonita amistad profesional y personal. Gracias por ser un gran amigo, por la confianza que nos tenemos, el apoyo que nos hemos dado mutuamente, por compartir dramas y experiencias. Estoy muy feliz de haberte conocido y porque sé que esta amistad continuará, sin importar a donde nos lleve la vida. Blanca, gracias por tus

ánimos, por tu amistad tan bonita tanto dentro como fuera del laboratorio y por tu ayuda técnica con las contraseñas jaja. Al grupo Gyala, por dejarme espacio en vuestra cabina jeje. Sergio y Rober, gracias por enseñarme el proceso de transducción y darme alícuotas de LV. Ari, gracias por ser una buena roommate de congreso, eres una persona increíble, gracias por tu ayuda y consejos. Mireia e Iñaki, gracias por vuestra ayuda y resolver mis dudas en el mundo de las CART. Montse, muchas gracias por todo tu apoyo y eficiencia en las comandas del material y reactivos para llevar a cabo la parte experimental de la tesis, así como solucionar cualquier problema con el papeleo administrativo. Eres una gran persona, todo sería más fácil si todos tuvieran una Montse Cofán en su vida.

Joan M. y Oriol (mieloma team), gracias por vuestra buena vibra cada vez que iba al lab. Joan M. por coincidir en cabina algunos de los viernes por la tarde, haciendo que fueran menos largos y duros.

Al grupo de inmunoterapia del Hospital Clínic: Mariona, Natalia, Maria, Dani, Azu, Raquel, Leticia, Marta, Sergio, Juajo, Paula, Libertad y Carol, gracias por dejarme utilizar vuestras instalaciones tanto el citometro como las salas blancas. Gracias por ayudarme a solventar mis dudas en la logística y funcionamiento de una sala blanca. Natalia, muchas gracias por tu tiempo y tu ayuda en el escalado de las VSTs en sala blanca. Contigo las horas encerradas en pleno verano dentro de sala blanca fueron más amenas. Gracias también por incluirme en el grupo y compartir comidas en el Hospital. Maria, gracias por las alícuotas de LV de los excedentes de ARI-0001.

A Miriam Aylagas, has hecho que el mundo de producción en sala blanca fuera más fácil. Gracias por tu guianza, tus conocimientos y tu apoyo en enseñarme los mejores tips. Eres una persona maravillosa, gracias por ser una colega y amiga. Por demostrarme tu cariño e interés sin importar donde estés.

Al grupo de HLA del BST: Maria José, Elena, Pepi, Albert, Claudia, Laura, Silvia, Marta y Cristina por procesar la solicitud y realizar el tipaje de HLA de cada donante. Gracias por vuestro tiempo.

Al personal de subministrament del BST, muchas gracias por procesar cada solicitud y darme las bolsas de sangre de cada donante utilizada en este estudio.

Al personal del laboratorio celular del BST, por facilitarme el trabajo en el laboratorio.

Mike, thank you for your support and sharing your expertise in T cell reprogramming.

Al Departamento de Hematología de Leiden University, Medical Center, the Netherlands por proporcionar los tetrameros y al proyecto T-Celbanc por la cesión de los tetrámeros de EBV utilizados en este estudio.

A los donantes, por su generosa donación voluntaria, sin la cual no sería posible investigar y comprender el sistema inmunitario para el desarrollo y avances de las terapias.

A mis compis de planta, despacho y laboratorio: Laia Ruíz, José, Laura (tejidos team); Helena, Alba (FTA team); Laia Miquel y Sergio (inmunohemato team); Quim, Raquel, Irene, Ángela, Carmen, Victor y Sara (mesenquimales team); Belén, Rubén, Kenia y Miquel (iPSC team); Laia Closa, Laura, Perla (imunocoagulopatías team), muchas gracias por vuestro cariño, ánimos, por coincidir más de algún fin de semana o festivo en el laboratorio, y por vuestro apoyo durante este tiempo. Carmen, Rubén, Kenia Ángela, Irene, Maria y Victor gracias por vuestra amistad, por las aventuras tanto dentro como fuera del laboratorio, jamás olvidaré todos los momentos que hemos compartido. Habéis hecho que mis días sean divertidos y menos estresantes. Gracias por distraerme, por escucharme, motivarme, por calmarme cuando me enfado jaja, por estar conmigo en esta recta final, por las idas al Cake Man y al súper. Por ser compis no solo de laboratorio sino también catadores de comida, de escalada, de gym y de lectura. Kenia y Rubén gracias por ayudarme con la portada de esta tesis. Todos sois unas personas maravillosas y no he podido tener mejores compañeros de laboratorio y despacho que vosotros. Siempre os tendré en mi corazón y estoy segura que nuestra amistad seguirá creciendo. Os quiero!

Ester, gràcies per ser una guia i consellera, no només en l'àmbit laboral sinó també en la vida, però sobretot moltes gràcies per la teva amistat tan bonica i sincera. La teva amistat és un regal que valoro molt en la meva vida, i no puc estar més agraïda d'haver coincidit amb tu. T'estimo molt. Gràcies per les teves paraules de motivació, per escoltar-me, per compartir el teu temps i la teva experiència (laboral, personal i gastronòmica). T'admiro molt.

Diego, gracias por las increíbles clases de inmunología, que hicieron que me gustara aún más el mundo tan complejo, pero maravilloso, de las inmunoterapias. Gracias por ser un excelente profesor y amigo.

Marta, Paola, Cristian e Ingrid, gracias por estar siempre. Gracias por vuestra paciencia, ánimos, consejos y apoyo incondicional...no hay mejores terapueutas que vosotros. Cada viaje, cada experiencia compartida con vosotros ha sido inolvidable. No sois solo amigos, sois mi familia, gracias por demostrarme vuestro cariño y aguantarme cada día. Vuestra amistad es un regalo y una luz en mi vida. Marta, gracias por la revisión cruzada, por tu complicidad y por compartir

esta etapa juntas, no podría haber elegido mejor amiga/hermana. Os quiero para siempre, sin importar a donde nos lleven nuestros sueños y metas, estoy segura que nuestra amistad seguirá creciendo con el paso de los años.

A mis bioquis y farmas favoritos, Quetza, Elena, Luisa, Analu, Katia, Paula, Lula, Mariana y Cristian, muchas gracias por esos mensajes que a pesar de la distancia se sentían cercanos, gracias por ser unos amigos excepcionales, por creer en mí, compartir mis sueños y logros. No puedo estar más agradecida de haber coincidido con ustedes en la uni. Paula y Katia, gracias por los ánimos y la idas a tomar algo para distraerme en la recta final. Los quiero!

Por último y más importante, a mi familia, sin ellos este sueño no hubiera sido posible. A pesar de la distancia, siempre han estado a mi lado. Gracias por todo su amor y apoyo incondicional, por enseñarme a soñar en grande y a luchar por lo que quiero. Gracias por creer en mí, guiarme, por inculcarme buenos valores y principios, por escucharme y darme los mejores consejos. Mamá gracias por ser mi refugio y calma en los momentos difíciles. Papá, gracias por enseñarme la importancia del equilibrio en la vida y para saber tomar buenas decisiones. Pablo, aunque seas mi hermano pequeño, siempre aprendo algo nuevo contigo. Eres un regalo para todos nosotros y llenas nuestras vidas de alegría cada día. Jony, no hay mejor hermano mayor que tú. Eres la persona más humilde, paciente y trabajadora. Te admiro y no puedo estar más orgullosa de ser tu hermana. Gracias por cuidarme, apoyarme, escucharme y aguantarme en mis momentos de estrés, por cocinarme, por motivarme, animarme y ayudarme a sobrevivir mientras escribía la tesis. A mis abuelos, gracias por las palabras llenas de amor, ánimos y sabiduría. Cada consejo y enseñanza de vida me inspiran a ser mejor persona cada día. Los amo con todo mi corazón!!

TABLE OF CONTENTS

LIST OF FIGURES	xiii
LIST OF TABLES.....	xv
LIST OF ABBREVIATIONS	xvii
ABSTRACT	xix
RESUMEN.....	xx
INTRODUCTION.....	23
1. B-cell hematological neoplasms	24
1.1. Acute Lymphoblastic Leukemia	24
1.2. Chronic Lymphocytic Leukemia.....	25
1.3. Non-Hodgkin Lymphomas.....	26
1.4. Hodgkin Lymphomas.....	27
2. Tumor immunity	27
3. Major Histocompatibility Complex	29
4. T Cell Receptor	30
5. Immunotherapy: Adoptive Cell Therapy	30
6. Chimeric Antigen Receptor T cell immunotherapy	32
6.1 Structure of CAR	33
6.2. Evolution of CARs development.....	35
6.3. Transfection of CARs constructs into viral vectors	37
6.4. CAR-T approved as treatment	39
6.5. ARI-0001	41
6.6. Side effects in the anti-CD19 CAR-T cell therapy	43
6.7. Limitations and challenges.....	45
7. Virus-Specific T cell	50
7.1. VST manufacturing.....	50
7.2. VSTs donor sources	54
7.3. Generation of Third-party “ <i>off the shelf</i> ” banks for VSTs	55
7.4. VST clinical efficacy and safety	57
8. EBV-specific T cells (EBVSTs).....	58
8.1. EBV or Human herpesvirus 4 (HHV-4).....	58
8.2. Clinical evidence of EBVSTs immunotherapy for treating lymphomas.....	63
8.3. Banked EBVSTs	66
9. CAR-VSTs Therapy.....	68
10. Partial reprogramming T cells with Yamanaka Factors	69
10.1. Yamanaka factors	70
10.2. Cell source.....	70
10.3. Reprogramming strategies	71
10.4. Evidence of partial reprogramming in T cells.....	73
HYPOTHESIS AND OBJECTIVES.....	75

MATERIALS AND METHODS	79
1. Samples, cells lines and vectors.....	80
2. High-resolution HLA typing.....	81
3. Isolation of PBMCs.....	83
4. Optimization of EBVST generation.....	83
5. Large-scale of EBVSTs production.....	88
6. Optimization of EBVSTs transduction.....	89
7. Flow cytometry.....	92
8. <i>In vitro</i> cytotoxicity assay.....	96
9. Interferon-gamma (IFN- γ) ELISpot assay.....	97
10. DNA extraction and TCR- β sequencing.....	98
11. Cryopreservation.....	99
12. EBVSTs thawing and stability.....	99
13. Statistical analysis.....	99
RESULTS	101
Chapter I: <i>In vitro</i> optimization of the activation and expansion of EBVSTs.....	102
1.1. Optimization 1.....	102
1.2. Optimization 2.....	104
1.3. Optimization 3.....	106
1.4. Optimization 4.....	108
1.5. Optimization 5 and 6.....	110
1.6. Selected condition.....	114
1.7. Selected condition using different stimuli for PBMC activation.....	123
Chapter II: Large-scale activation and expansion of EBVSTs under GMP.....	131
Chapter III: Transduction <i>in vitro</i> of anti-CD19 CAR in thawed EBVSTs.....	138
Chapter IV: <i>In vitro</i> optimization of cell culture conditions for anti-CD19 CAR transduction in thawed EBVSTs.....	140
4.1. Stability of large-scale manufactured EBVSTs.....	140
4.2. Thawed EBVSTs potency.....	140
4.3. Optimizing the expansion and culture conditions of post-thaw EBVSTs.....	141
4.4. Transduction.....	147
4.5. Proof of concept: Partially reprogram EBVST cells with Yamanaka factors.....	152
DISCUSSION	157
CONCLUSIONS	171
BIBLIOGRAPHY	173
ANNEXES	191

LIST OF FIGURES

Figure 1. First line treatment of B-cell acute lymphoblastic leukemia.....	25
Figure 2. Immune response against a tumor.	28
Figure 3. Structure of HLA molecules.....	29
Figure 4. Structure of the TCR-CD3 complex.....	30
Figure 5. CAR-T cell therapy process.	33
Figure 6. Structure and evolution of CARs development.....	35
Figure 7. Generations of LV plasmid systems.	39
Figure 8. CAR-T CD19, ARI-0001.....	41
Figure 9. ARI-0001 cells production and dose infusion.	43
Figure 10. Strategies for manufacturing VST.	51
Figure 11. Comparison of Banked-VSTs strategy and Recipient-specific VSTs.....	55
Figure 12. Virus latent infection in B lymphocytes.	60
Figure 13. Latency states and frequency of EBV in different types of lymphomas.	61
Figure 14. Advancement of methods for producing EBVSTs.	65
Figure 15. Age reprogramming.....	69
Figure 16. mRNA-delivery strategies.	72
Figure 17. Diagram of A3B1 CAR.CD19 (ARI-0001) construct.	81
Figure 18. Protocol developed and optimized for the small-scale production of EBVSTs.	87
Figure 19. Protocol developed and optimized for large-scale production of EBVSTs.....	88
Figure 20. Protocol for the first transduction of CAR.CD19 (ARI-0001) into EBVSTs.....	89
Figure 21. Phenotypic characterization in the 1 st expansion of EBVSTs.	102
Figure 22. IFN- γ specificity and degranulation marker in the 1 st expansion of EBVSTs.....	103
Figure 23. T cell differentiation phenotypes in the 1 st expansion of EBVSTs.....	104
Figure 24. Phenotypic characterization and IFN- γ specificity in the 2 nd expansion of EBVSTs.....	105
Figure 25. T cell differentiation phenotypes in the 2 nd expansion of EBVSTs.	106
Figure 26. Phenotypic characterization and IFN- γ specificity in the 3 rd expansion of EBVSTs.	107
Figure 27. T cell differentiation phenotypes in the 3 rd expansion of EBVSTs.	108
Figure 28. Phenotypic characterization and IFN- γ specificity in the 4 th expansion of EBVSTs.	109
Figure 29. Percentage of degranulation marker in the 4 th expansion of EBVSTs.	110
Figure 30. Phenotypic characterization and IFN- γ specificity in the 5 th expansion of EBVSTs.	111
Figure 31. Phenotypic characterization and IFN- γ specificity of the 6 th expansion of EBVSTs.....	113
Figure 32. T cell differentiation phenotypes in the 6 th expansion of EBVSTs.	113
Figure 33. Optimized protocol to produce EBVSTs and characterization of the expanded product.	115
Figure 34. Polyfunctional EBV-specific T cells.	116
Figure 35. Comparative analysis of EBVSTs TCR- β diversity pre- and post-expansion.....	117
Figure 36. Comparison of V and J gene segments usage frequencies in TCR- β analysis of PBMCs from different donors.	118
Figure 37. Comparison of V and J gene segments usage frequencies in TCR- β from expanded EBVSTs from different donors.	119
Figure 38. Comparison of TCR- β clonotypes diversity in expanded EBVSTs from 7 donors.....	120

Figure 39. HLA class I tetramer analysis of EBV-specific CD8 ⁺ T cells in the expanded EBVSTs.	121
Figure 40. T cell differentiation phenotypes in the optimized condition for generating EBVSTs.	122
Figure 41. Expression of exhaustion markers in CD4 ⁺ and CD8 ⁺ T cells from EBVSTs.	123
Figure 42. Comparison of the fold expansion of EBVSTs with different stimuli.	124
Figure 43. Comparison of EBVSTs characterization and specificity under different stimuli.	125
Figure 44. PHA-blast cytotoxicity assay in the final EBVSTs product.	126
Figure 45. Comparison of TCR-β analysis and tetramer assay of EBVSTs under different stimuli.	127
Figure 46. Tetramer assay of expanded EBVSTs with EBNA-1+PepTivator [®] EBV consensus stimuli. .	128
Figure 47. Comparison of T cell differentiation phenotypes under different stimuli.	129
Figure 48. Expression of exhaustion markers in CD8 ⁺ and CD4 ⁺ T cells from EBVSTs stimulated with PepTivator [®] EBV consensus/EBNA-1.	130
Figure 49. Phenotypic characterization in EBVSTs expanded on a large scale.	131
Figure 50. Specificity and degranulation marker of EBVSTs expanded on a large scale.	132
Figure 51. ELISpot assay comparison before and after stimulation and expansion of EBVSTs.	133
Figure 52. PHA-blast cytotoxicity assay of EBVSTs expanded on a large scale.	134
Figure 53. TCR-β diversity pre- and post-large-scale expansion of EBVSTs.	135
Figure 54. TCR-β clonotypes and tetramer assay of EBVSTs expanded on a large scale.	136
Figure 55. Comparison of T cell differentiation phenotype pre- and post-expansion.	136
Figure 56. Expression of T cell exhaustion markers pre- and post-expansion of EBVSTs on a large scale.	137
Figure 57. Expansion and characterization of CAR.CD19 (ARI-0001)-transduced EBVSTs.	138
Figure 58. Expression of CAR.CD19 (ARI-0001) and final product potency.	139
Figure 59. Comparison of EBVSTs stability at room temperature and at 4°C.	140
Figure 60. Comparison of T cell phenotype and potency pre- and post-thawing.	141
Figure 61. Comparison of the fold expansion of EBVSTs stimulated with Dynabeads [™]	142
Figure 62. Comparison of phenotype and potency of EBVSTs stimulated with Dynabeads [™]	143
Figure 63. Comparison of the characterization of post-thaw EBVSTs stimulated with Dynabeads [™]	144
Figure 64. Comparison of the characterization of post-thaw EBVSTs stimulated with different stimuli.	146
Figure 65. Characterization of EBVSTs stimulated with anti-CD3 and transduced with CAR.CD19.	148
Figure 66. CAR.CD19 expression and characterization at different time points during culture.	149
Figure 67. Comparison of CAR.CD19 expression using different detection methods.	149
Figure 68. Comparison of T cell subpopulations in transduced conditions.	150
Figure 69. Characterization of transduced EBVSTs with different stimuli and culture media.	151
Figure 70. Comparison of the fold expansion in cryopreserved EBVSTs on days 12, 15, and 20.	152
Figure 71. Expression of Yamanaka factors in HEK 293T cells transfected with RNAiMAX.	153
Figure 72. Yamanaka factors expression in transfected CD3 ⁺ T cells.	154
Figure 73. Fold expansion and viability in EBVSTs transfected using chemical methods.	155
Figure 74. Transfection of PBMCs with mRNA encoding GFP using TransIT [®]	156
Figure 75. Comparison of Yamanaka factors expression in EBVSTs transfected via TransIT [®]	156

LIST OF TABLES

Table 1. Current adoptive cell therapies in cancer treatment	32
Table 2. Characteristic of Retroviridae family vectors.....	37
Table 3. Comparison of autologous CAR-T cell FDA-approved therapies	40
Table 4. Currently allogenic CAR-T products under clinical evaluation.....	47
Table 5. Summary of methods for presenting different types of viral antigens	52
Table 6. Advantages and disadvantages of different rapid culture techniques.....	54
Table 7. Clinical experiences using VSTs therapy in HSCT.....	58
Table 8. Summarize of viral proteins of EBV	62
Table 9. Donor-Banked EBVSTs to treat EBV lymphomas.....	67
Table 10. Advantages and disadvantages of different reprogramming methods.....	71
Table 11. Initial criteria for starting material.....	80
Table 12. HLA class I alleles in the studied cohort	81
Table 13. HLA class II alleles in the studied cohort.....	82
Table 14. Approximation of the number of cells to be obtained per unit of blood volume	83
Table 15. Conditions tested in each optimization.....	85
Table 16. Parameters tested with different chemical reagents for transfection.....	91
Table 17. Cytometry panels and antibodies information.....	94
Table 18. List of peptide-MHC tetramers used	95
Table 19. CDR3 amino acid sequences shared in expanded products on day 20.....	120

LIST OF ABBREVIATIONS

A

aa: Amino acid
ACT: Adoptive cell therapy
AdV: Adenovirus
AEMPS: Agencia Española de Medicamentos y Productos Sanitarios
ALL: Acute lymphoblastic leukemia
AICD: Activation-induced cell death
APCs: Antigen-presenting cells
ATCC: American type culture collection

B

BCMA: B-cell maturation antigen
BCR: B-cell receptor
BKV: BK virus
BL: Burkitt lymphoma

C

CAR-T: Chimeric antigen receptor T cell therapy
CAR: Chimeric antigen receptor
CAR.CD19-EBVSTs: Chimeric antigen receptor targeting CD19 expressed by EBV-specific T cells
CB: Cord blood
CDR: Complementarity-determining region
CFSE: Carboxyfluorescein succinimidyl ester
CHOP: A chemotherapy regimen used to treat non-Hodgkin lymphomas, consisting of cyclophosphamide, hydroxydaunorubicin, oncovin (vincristine), and prednisone.
CLL: Chronic lymphocytic leukemia
CMV: Cytomegalovirus
CRS: Cytokine release syndrome
CTL: Cytotoxic T lymphocytes
CTLA-4: Cytotoxic T-lymphocyte-associated protein 4

D

DB: Dynabeads™ CD3/CD28
DCs: Dendritic cells
DLBCL: Diffuse large B-cell Lymphoma
DMEM: Dulbecco's modified eagle medium
DNA: Deoxyribonucleic acid

E

EBNA: EBV nuclear antigen
EBV: Epstein-Barr virus
EBVSTs: EBV-specific T cells
ELISpot: Enzyme-linked ImmunoSpot
EM: Expansion medium, composed with 45% RPMI 1640, 45% Click's EHAA and 10%hSAB
EMA: European Medicine Agency

F

FasL: Fas ligand
FDA: Food and Drug Administration

G

GFP: Green fluorescent protein
GMP: Good manufacturing practices
GRV: Gamma retroviral
GvHD: Graft-versus-host disease
Gy: Grays

H

HHV-6: Human herpes virus 6
HHV-8: Human herpesvirus 8
HIV: Human immunodeficiency virus
HL: Hodgkin's lymphomas
HLA: Human leukocyte antigen
HSA: Human serum albumin
hSAB: Human serum AB
HSCT: Hematopoietic stem cell transplantation
HTLV: Human T cell lymphotropic virus. A virus linked to certain types of leukemia and lymphomas

I

ICANS: Immune effector cell-associated neurotoxicity syndrome
IFN- γ : Interferon gamma
IgG: Immunoglobulin G
IgM: Immunoglobulin M
IL: Interleukin
iNKT: Invariant natural killer T cells
iPSCs: Induced pluripotent stem cells
IQR: Interquartile range
ITAMs: Immunoreceptor tyrosine-based activation motifs

J

JCV: John Cunningham virus

K

KLF4: Krüppel-like factor 4

L

LAG-3: Lymphocyte activation gene-3

LCLs: Lymphoblastoid cell lines

LMP2: Latent membrane protein

LV: Lentivirus

M

mAB: Monoclonal antibody

MHC: Major histocompatibility complex

MM: Multiple myeloma

MOI: Multiplicity of infection

mRNA: messenger RNA

N

NALM6: A human B-cell leukemia cell line

NFAT: Nuclear factor of activated T cells

NHL: Non-Hodgkin's lymphomas

NK: Natural killer

NP: Non-pulse

O

O/N: Overnight

OKSM: OCT4, KLF4, SOX2, MYC – The four main transcription factors used to create induced pluripotent stem cells (iPSCs).

OKSMNL: OCT4, KLF4, SOX2, MYC, NANOG, LIN28 – A combination of factors used to reprogram cells into pluripotent stem cells.

OKT3: Clone of monoclonal antibody targeting CD3, used to activate T cells

P

P: Pulsed

PBMCs: Peripheral blood mononuclear cells

PCR: Polymerase chain reaction

PD-1: Programmed death-1

PHA-P: Phytohemagglutinin-P

PTLD: Post-transplant lymphoproliferative disorder

R

REDECAN: Red Española de Registros de Cáncer

R/R: Relapsed/Refractory

RNA: Ribonucleic acid

RT: Room temperature

RV: Retrovirus

S

ScFV: Single-chain variable fragment

SFU: Spot-forming units

SOT: Solid organ transplantation

STAT3: Signal transducer and activator of transcription 3

SV40: Simian virus 40

T

T_{CM}: Central memory T cells

TCR-β: T cell receptor β chain

TCR-T: T cell receptor therapy

TCR: T cell receptor

TD: Transduced

T_{EM}: Effector memory T cells

T_{EMRA}: Terminally differentiated effector memory T cell

TIGIT: T cell immunoreceptor with Ig and ITIM domains

TILs: Tumor-infiltrating lymphocytes

TIM-3: T cell immunoglobulin and mucin-domain containing-3

TLS: Tumor lysis syndrome

T_N: Naïve T cells

TNF: Tumor necrosis factor

T_{SCM}: Stem cell memory T cells

U

UCB: Umbilical cord blood

UTD: Untransduced

UTR: Untranslated region

V

VSTs: Virus-specific T cells

W

WHO: World Health Organization

ABSTRACT

T cells expressing chimeric antigen receptors (CAR-T) targeting the CD19 antigen have been proven to be one of the most promising treatments for B cell neoplasms. However, CAR-T therapy presents certain limitations, such as lack of proliferation and persistence *in vivo*. A potential strategy to extend and enhance the activity of CAR-T cells is to co-express the CAR in virus-specific T cells. The aim of this doctoral thesis was to optimize a protocol to produce Epstein-Barr virus-specific T cells capable of expressing the CAR.CD19 construct from ARI-0001.

Peripheral blood mononuclear cells (PBMCs) from healthy EBV-seropositive donors were activated using a pool of overlapping peptides derived from 15 viral antigenic proteins. Various culture conditions were tested using 24-well G-Rex[®] plates. The selected condition was replicated in 7 donors, achieving over 95% CD3⁺ T cells, with 93.5% of them being CD8⁺ T cells. On day 20 of culture, the median IFN- γ production was 89% for both CD3⁺ and CD8⁺ T cells, which also produced TNF- α and IL-2. EBV-specific CD8⁺ T cells expressed 24% of the degranulation marker in the presence of EBV antigens. Flow cytometry analysis revealed that most of the expanded cells displayed an effector memory phenotype. The production of EBV-specific T cells was successfully scaled up under good manufacturing practices, yielding results comparable to those obtained at a smaller scale. PBMCs were also stimulated with peptides from EBNA-1 and LMP2A proteins, producing a higher percentage of CD4⁺ T cells by day 20. The *in vitro* cytotoxicity assay demonstrated specific lysis between 54-69% against PHA-blasts pulsed with viral antigen peptides. TCR- β sequencing revealed increased clonality in the expanded products and allowed for the detection of EBV-specific clonotypes presented by donor HLA molecules, confirmed by tetramers assay. EBV-specific T cells transduced demonstrated the ability to co-express CAR.CD19 and eliminate target cells (NALM6) in co-culture. However, it was observed that stimulation with Dynabeads[™] CD3/CD28 reversed the CD4:CD8 ratio and decreased specificity, whereas soluble anti-CD3 antibody preserved both the phenotype and specificity but decreased CAR.CD19 co-expression. Cellular expansion was limited due to the use of pre-activated and thawed EBVSTs as starting source. Different *in vitro* conditions were evaluated, including a proof of concept in which T cells were transfected with Yamanaka factors to induce partial reprogramming with the aim of modifying the cell differentiate state and enhancing their proliferative and antitumor capacity. Although Yamanaka factor expression was not detected, the results provided valuable insights for future process optimizations.

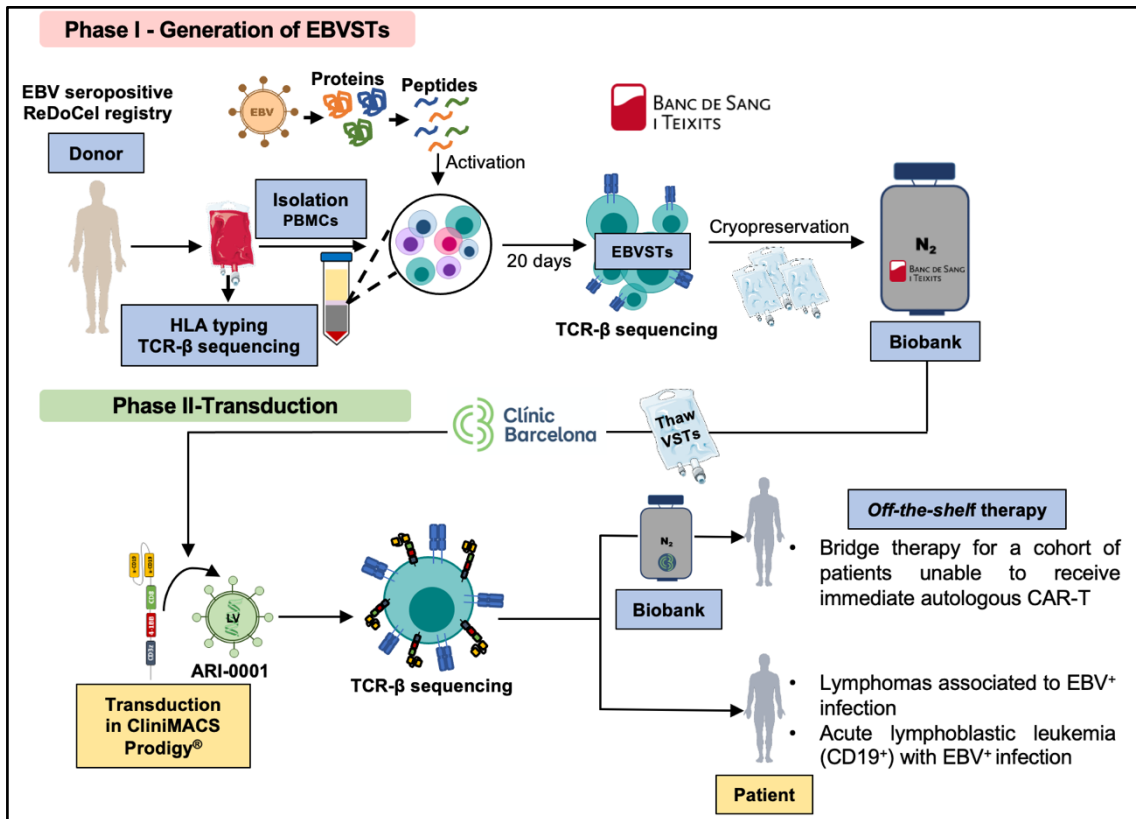
In conclusion, a scalable protocol under good manufacturing practices has been described for producing EBV-specific T cells, resulting in a highly pure and polyfunctional product with high specificity, capable of co-expressing the CAR.CD19 and eliminate target cells. These findings open new opportunities to explore "*off-the-shelf*" immunotherapy strategies, where T cells can be educated or directed, improve their persistence, proliferation, and safety *in vivo*.

RESUMEN

Las células T que expresan receptores de antígeno quimérico (CAR-T) dirigidas contra el antígeno CD19 han demostrado ser un tratamiento prometedor para neoplasias de células B. No obstante, la terapia CAR-T presenta algunas limitaciones, como la falta de proliferación y persistencia *in vivo*. Una posible estrategia para prolongar y potenciar la acción de células CAR-T, es co-expresar el CAR en células T específicas de virus. El objetivo de esta tesis doctoral fue optimizar un protocolo para la producción de células T específicas del virus de Epstein-Barr capaces de expresar el constructo del CAR.CD19 del ARI-0001.

Se activaron células mononucleares de sangre periférica (PBMCs) de donantes sanos EBV seropositivos mediante un pool de péptidos superpuestos derivados de 15 proteínas antigénicas del virus. Se evaluaron distintas condiciones de cultivo usando placas G-Rex® de 24 pocillos. La condición seleccionada se replicó en 7 donantes, obteniendo más del 95% de células T CD3⁺, con un predominio del 93.5% de células T CD8⁺. A día 20 de cultivo, la mediana de producción de IFN- γ fue del 89% para las células T CD3⁺ y T CD8⁺, además de producir TNF- α e IL-2. Las células T CD8⁺ específicas expresaron un 24% del marcador de desgranulación en presencia de antígenos de EBV. El estudio del fenotipo por citometría de flujo reveló que la mayoría de las células expandidas exhibían un fenotipo de memoria efectora. La producción de células T específicas se escaló con éxito bajo buenas prácticas de manufactura, obteniendo resultados comparables a los obtenidos a pequeña escala. También se estimularon PBMCs con péptidos de las proteínas EBNA-1 y LMP2A, logrando a día 20 un porcentaje más elevado de células T CD4⁺. El ensayo de citotoxicidad *in vitro* mostró una lisis específica entre el 54-69% contra PHA-blastos pulsados con péptidos de los antígenos del virus. La secuenciación del TCR- β mostró una mayor clonalidad en los productos expandidos y permitió detectar clonotipos específicos de antígenos del EBV presentados por moléculas HLA del donante, confirmados por ensayo de tetrámeros. Las células T específicas de EBV transducidas demostraron ser capaces de co-expresar el CAR.CD19 y eliminar a las células diana (NALM6) en co-cultivo. No obstante, se observó que el estímulo de las Dynabeads™ CD3/CD28 invertía el ratio CD4:CD8 y disminuía la especificidad, mientras que el anticuerpo soluble anti-CD3 preservaba tanto el fenotipo como la especificidad, pero disminuía la co-expresión CAR.CD19. La expansión celular fue limitada debido al uso de EBVST pre-activadas y descongeladas como fuente de partida. Se evaluaron diferentes condiciones *in vitro*, incluyendo una prueba de concepto, en las que se transfectaron las células T con factores de Yamanaka para inducir una reprogramación parcial con el objetivo de modificar el estado de diferenciación celular y potenciar su capacidad proliferativa y antitumoral. Aunque no se observó la expresión de los factores de Yamanaka, los resultados obtenidos aportan información valiosa para futuras optimizaciones del proceso.

En conclusión, se ha descrito un protocolo transferible a gran escala y bajo buenas prácticas de manufactura para producir células T específicas contra el virus de EBV, logrando un producto polifuncional de alta pureza y especificidad, con potencial de co-expresar el CAR.CD19 y eliminar a las células diana. Estos hallazgos abren nuevas oportunidades para explorar estrategias de inmunoterapia “*off-the-shelf*”, en las que se pueda educar o dirigir a las células T, mejorando su persistencia, proliferación y seguridad *in vivo*.



Graphical abstract. Proposal for the development of Epstein-Barr virus-specific T cell expressing CAR.CD19 for cancer immunotherapy: Epstein-Barr virus-specific T cells (EBVSTs) will be derived from EBV seropositive donors (e.g. ReDoCel registry) and cryopreserved to create an EBVSTs biobank. After thawing, these cells will be transduced with the CAR.CD19 construct (ARI-0001). The final CAR.CD19-EBVSTs product can be infused immediately after completing manufacturing process without an additional cryopreservation, or stored for later infusion (“*off-the-shelf*”). Institutional collaboration will facilitate flexible and coordinated production, ensuring effective patient treatment. Figure created by the author.

INTRODUCTION

1. B-cell hematological neoplasms

Cancer has been a leading cause of morbidity and mortality worldwide for many years, making it one of the most important diseases for public health. The number of cancers diagnosed in Spain in 2024 is estimated to reach 286,664 cases according to REDECAN calculations for the year 2023.¹

Cancer is a pathological accumulation of clonally expanded cells derived from the same precursor,² in which there has been a DNA mutation in cell growth or DNA repair genes. The etiology of cancer is multifactorial, involving the interaction of genetic, medical, and lifestyle factors.³ Conventional treatment includes strategies such as chemotherapy,⁴ radiotherapy, surgery, and palliative care,⁵ which in certain types of cancer can be helpful and effective but have many side effects and, in metastatic stages, are not functional. In recent years, cancer treatment approaches have been evolving, with immunotherapy being a promising and potent advance.⁶

Hematologic neoplasms, or cancers of blood-forming cells, are a group of diseases arising from heterogeneous affections originating in bone marrow cells and the lymphatic system. Hematologic neoplasms of B-cell lineage can be divided into three groups: leukemias, lymphomas, and plasma cell neoplasms.⁷ The world health organization (WHO) has classified hematologic tumors according to myeloid or lymphoid lineage. Within the lymphoid classification, the following stand out: B-type precursors, mature B-cell and Hodgkin's lymphomas.⁸ B-cell neoplasms are highly prevalent tumors that arise from the transformation of B lymphocytes at different stages of their differentiation. The most common B-cell neoplasms of lymphoid lineage are acute lymphoblastic leukemia (ALL), chronic lymphocytic leukemia (CLL), non-Hodgkin's lymphomas (NHL) and Hodgkin's lymphomas (HL).

1.1. Acute Lymphoblastic Leukemia

It is an unregulated growth of clonal lymphoid cells, where 80-85% of cases occur at an early stage of differentiation (Pre-B cells) and less common in T cells (10-15%) and mature B cells (<5%).⁹ It may invade the bone marrow, blood and extramedullary sites.¹⁰ More than 95% of B cells in ALL express the CD19 antigen, 90% CD22, 20-50% CD20 and 70% CD52 respectively.^{10,11} Worldwide, more than 250,000 people are diagnosed with leukemia each year, representing 2.5% of all cancers.⁷ ALL primarily affects children aged 1 to 4 years and adults aged more than 80 years.^{7,12} It is slightly more common in men than in women. There are environmental and genetic risk factors that predispose the population to develop ALL. Genetic alterations that predispose to ALL include chromosomal alterations such as aneuploidy (e.g. Down syndrome, Fanconi anemia, Bloom syndrome, ataxia telangiectasia, and Nijmegen

breakdown syndrome), inherited gene variants (*ARID5B*, *IKZF1*, *CEBPE*, *CDKN2A* or *CDKN2B*, *PIP4K2A*, *ETV6*), constitutional Robertsonian translocation, or single nucleotide polymorphisms. As for predisposition due to environmental factors, pediatric ALL could be initiated during pregnancy due to the impact of exposure to pesticides, ionizing radiation,¹⁰ solvents, or viruses such as Epstein-Barr virus (EBV) and Human Immunodeficiency virus (HIV).¹³

The first line of treatment for B-cell ALL includes 4 phases, which can last 2 to 3 years: induction, consolidation, intensification, and long-term maintenance (**Figure 1**). In addition, a preventive treatment for the central nervous system is administered. Allogeneic hematopoietic cell transplantation (HSCT) is reserved for patients with high-risk disease or minimal persistent residual disease.¹⁰

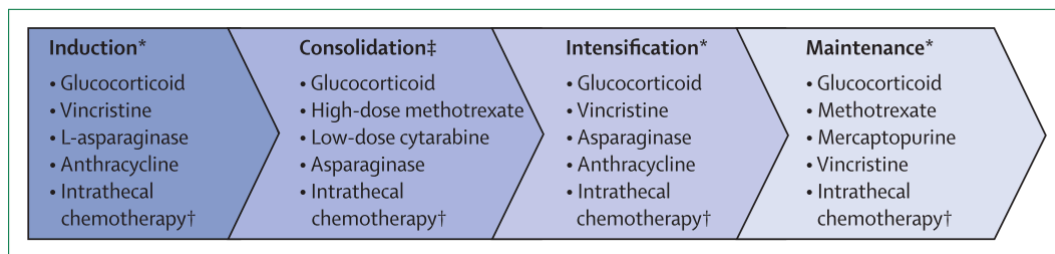


Figure 1. First line treatment of B-cell acute lymphoblastic leukemia.

†Intrathecal chemotherapy consists of methotrexate alone or combined with cytarabine and hydrocortisone.

Figure obtained from Malard & Mohty. *Lancet* (2020).¹⁰

During the last 10 years, several targeted therapies have been developed, such as monoclonal antibodies (e.g. Rituximab, Ofatumumab, Epratuzumab, and Alemtuzumab), bi-specific antibodies (e.g. Blinatumomab) and more recently, CAR-T cell immunotherapy. Obtaining survival results of a median of 6-19 months, depending on the treatment.¹⁰ While 85-90% of patients go into remission after induction therapy, there are a percentage who are refractory. Patients who achieve complete remission, most of them relapse. In these cases, relapsed/refractory (R/R) ALL patients are treated with salvage chemotherapy, followed by allogeneic stem cell transplantation or new monoclonal antibodies, which in some cases can extend life by a few more years.¹³ Therefore, there is still much to be understood in order to improve response rates and overall survival in ALL patients.

1.2. Chronic Lymphocytic Leukemia

It mainly affects older adults, with a high prevalence rate in Western countries. B-cell CLL is the result of an excessive clonal expansion of mature CD5⁺ B cells in blood, bone marrow, and lymphoid tissues,¹⁴ co-expressing low levels of surface membrane immunoglobulin (smIg) of a single type of immunoglobulin light chain (L) and CD79b, CD20 and CD23.¹⁵ In some patients,

the cancer remains stable, causing no significant morbidity and a life expectancy like a healthy person, while other patients may die within 2-3 years of diagnosis. There is still no treatment to cure B-cell CLL.¹²

Chemotherapy with targeted monoclonal antibodies (e.g. fludarabine, cyclophosphamide, and rituximab) is one of the treatments for patients <65 years of age and with a good prognosis. Because B-cell CLL functionally expresses B-cell receptor (BCR) on their surface, therapeutic strategies targeting BCR signaling have been developed. The application of CAR-T against the CD19 antigen to treat CLL is also being investigated.¹⁴ However, further research and improvement is still needed to make the effectiveness of the therapy applicable to most people with CLL, reducing side effects and preventing CLL from transforming into higher grade non-Hodgkin's lymphoma, such as diffuse large B-cell lymphoma (DLBCL).¹⁵

1.3. Non-Hodgkin Lymphomas

NHLs account for 90% of malignant lymphomas, while the remaining 10% are HLs.¹⁶ 25% of cases are in extranodal regions¹⁷ and have a wide range of histological appearances and clinical characteristics at the time of presentation, which makes diagnosis difficult.¹⁸ NHL is divided into 36 subtypes, where 21 of them are B-type and 15 are T-type. The most common subtypes of NHL are diffuse large B-cell lymphoma (about 30%) and follicular lymphoma (about 20%). The remaining lymphomas have a frequency of less than 10%,¹⁶ with Burkitt's lymphoma (BL) constituting 1-5% of NHL in adults.¹⁹ In Spain, 3% of cases are of NHL.¹

Central pathogenic mechanisms in the development of NHL include immunosuppression, especially in relation to T cell function and loss of control of latent EBV infection.¹⁷ Upon severe immunodeficiency, the control mechanisms of the immune system that regulate EBV infection are altered, leading to EBV-driven B-cell proliferation and the development of B-cell lymphoma. Latent EBV-encoded genes are capable of transforming B cells *in vitro* by altering cellular gene transcription and key cell signaling processes. In the case of BL, there are three subtypes: sporadic, endemic, and immunodeficiency associated. Endemic BL is associated with EBV infection, while immunodeficiency-associated BL is associated with HIV infection as well as solid organ transplantation.¹⁹ Other risk factors that may increase the likelihood of developing NHL are ultraviolet radiation, other viruses and pathogens (HTLV, HHV-8, Hepatitis C, SV40, *Helicobacter pylori*), chronic autoimmune and inflammatory disorders (e.g. rheumatoid arthritis and Sjogren's syndrome), exposure to pesticides and pesticides,¹⁷ blood transfusions, organ transplantation,¹⁶ exposure to tobacco, alcohol, and diet, among others.²⁰

Low-grade or indolent lymphomas, which account for 20-40% of NHL and include follicular lymphoma, small lymphocytic lymphoma and marginal zone lymphomas, can be treated with chemotherapy. Aggressive lymphomas, which account for 40% of all NHL, including DLBCL and BL, are treated with CHOP chemotherapy in combination with anti-CD20 monoclonal antibodies (Rituximab).¹² Approximately 20-30% of patients who survived first-line therapy relapse or are refractory. After R/R, salvage chemotherapy followed by autologous hematopoietic progenitor transplantation is applied; however, 50-60% relapse occurs, so there remains a need for improved treatments. CD19-targeted CAR therapy has generated high remission rates (>2 years) in some patients with refractory DLBCL (e.g. of the ongoing studies ZUMA-1 JULIET, TRANSCEND, and SCHOLAR-1); however, there is still a need to boost therapy to decrease the adverse effects of therapy.^{21,22}

1.4. Hodgkin Lymphomas

A rare B-cell malignant composed of less than 1% Reed-Sternberg tumor cells.²³ It is a disease of bimodal distribution, with a higher incidence in young adults as well as in people older than 55 years. There are no defined risk factors, so the cause remains unknown²⁴. However, some of the factors that may be associated with HL include exposure to viruses, suppression of the immune system, and family history. Epidemiological and serological studies have shown the involvement of EBV in the etiology of HL and the EBV genome has been detected in tumor samples from patients with HL.²⁵ In the last four decades, advances in radiotherapy and combination chemotherapy have increased the remission rate in patients with HL, where more than 80% (under 60 years of age) are likely to be cured. However, the rest have refractory disease in the first line of treatment or relapse. In these cases, chemotherapy followed by autologous HSCT or more innovative treatments such as inhibitor molecules, anti-PD-1 monoclonal antibodies, artificial antibodies against the CD30 protein (e.g. brentuximab vedotin) or the combination of nivolumab and ipilimumab are used.²⁴ Another promising approach for patients with HL is CAR-T therapy against the CD30 antigen, but it is still in the early stages of development. However, it has promising clinical activity.²⁶

2. Tumor immunity

The immune system is composed of cells, tissues, and molecules that act in a coordinated manner to ensure the maintenance or re-establishment of homeostasis in the different tissues of the organism. In the presence of a tumor, immunosurveillance detects malignant cells, eliminates them, and prevents their proliferation, involving both the innate and adaptive immune systems. Immune surveillance against tumors is important to prevent tumor growth. However, most tumors develop in immunocompromised patients, where the immune system is unable to control and

eliminate the tumor.²⁷ In the immune response, the first line of action is carried out by the innate immune system (macrophages, neutrophils, basophils, eosinophils, natural killer (NK) cells, and dendritic cells), which generates an immediate response that acts in minutes to days. Subsequently, if the disease is not eliminated or controlled, the adaptive system comes into play (CD8⁺ T lymphocytes, CD4⁺ T lymphocytes, and B lymphocytes).²⁷

The main mediators of the antitumor response are CD8⁺ or cytotoxic T lymphocytes (CTL) and CD4⁺ or helper T lymphocytes. The activation of these mediators occurs when antigen-presenting cells (APCs) of the host recognize, process, and integrate tumor antigens. Following this APC-antigen contact, mature dendritic cells migrate to the peripheral or secondary lymphoid organs (lymph nodes or spleen) and present the processed antigens to the T cells via class I major histocompatibility complex (MHC) molecules. At this synapse, the MHC and the T cell receptor (TCR) of the T cells come into contact (signal 1), leading to the activation of the T-lymphocytes. The activation process induces the expression of co-stimulatory molecules (signal 2) and the production of cytokines (signal 3), generating a clonal expansion of specific T lymphocytes capable of migrating to the affected tissue and eliminating the tumor cells (**Figure 2**).^{27,28}

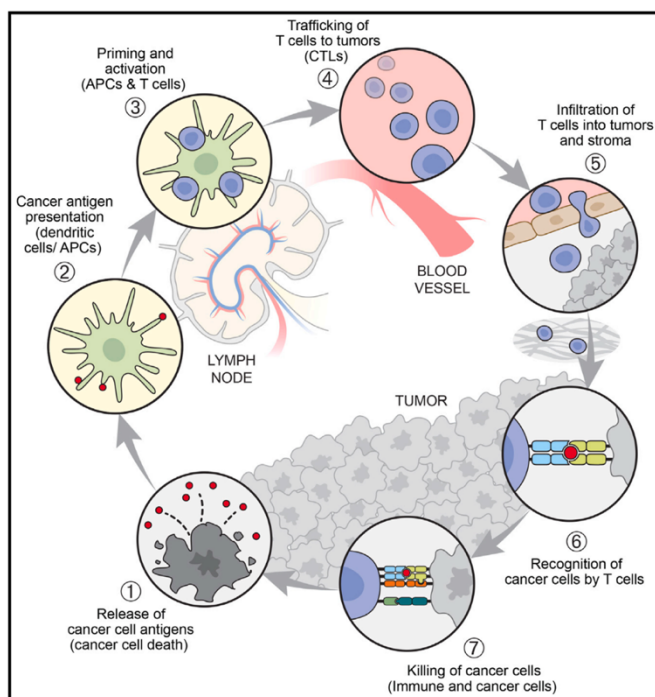


Figure 2. Immune response against a tumor.

It starts with the (1) release of tumor antigens (2) which are recognized by the antigen-presenting cells, which par excellence are the dendritic cells (DCs). (3) The DCs with the antigen migrate towards the lymph nodes and present it to the T lymphocytes to activate them. (4) Active cytotoxic T lymphocytes migrate towards the tumor, (5) infiltrate into the tumor, (6) recognize the cancer cells, (7) and eliminate them. Figure obtained from Abbas et al. *Elsevier*. (2016).²⁷

DCs are also capable of presenting antigens by MHC class II, activating CD4⁺ T cells. This T cell subtype helps to regulate the immune response by inducing an increased response from CD8⁺ T cells. Additionally, CD4⁺ T cells can activate B cells, favoring the production and maturation of immunoglobulins.²⁷

3. Major Histocompatibility Complex

The MHC, or human leukocyte antigen (HLA) in humans, are molecules located on the short arm of chromosome 6 (6p21.3) and contain the most polymorphic group of genes in the entire human genome (**Figure 3A**). They consist of 3 regions that have been designated as class I, class II and class III, depending on gene structure and function. HLA class I molecules (HLA-A, -B, and -C) consist of an α -chain non-covalently associated with a protein called β 2-microglobulin. The α -chain consists of 3 extracellular domains (α 1, α 2 and α 3), followed by short transmembrane and cytoplasmic domains. The amino-terminal domains α 1 and α 2 of the α -chain molecule form an 8-9 amino acid long peptide binding groove, which is endogenously presented to CD8⁺ T cells because the α 3 domain is invariant and binds to the co-receptor of CD8⁺ T cells (**Figure 3B**). Additionally, there are non-classical HLA class I molecules (HLA-E, -F, and -G). HLA class II molecules (HLA-DR, -DP, and -DQ) are heterodimers composed of two transmembrane chains, called α and β . Each chain has two extracellular domains. The domains α 1 and β 1, which are characterized by containing polymorphic residues that form a large cleft or groove to bind peptides of 10-30 amino acids, are presented exogenously to CD4⁺ T lymphocytes because the non-polymorphic α 2 and β 2 domains contain the binding site for the CD4⁺ T lymphocyte co-receptor (**Figure 3C**). In the case of HLA class III molecules, they are less polymorphic, but are also polygenic, in which genes encoding complement factors C3, C4 and C5, heat shock proteins and the TNF family have been found (**Figure 3A**).^{27,29}

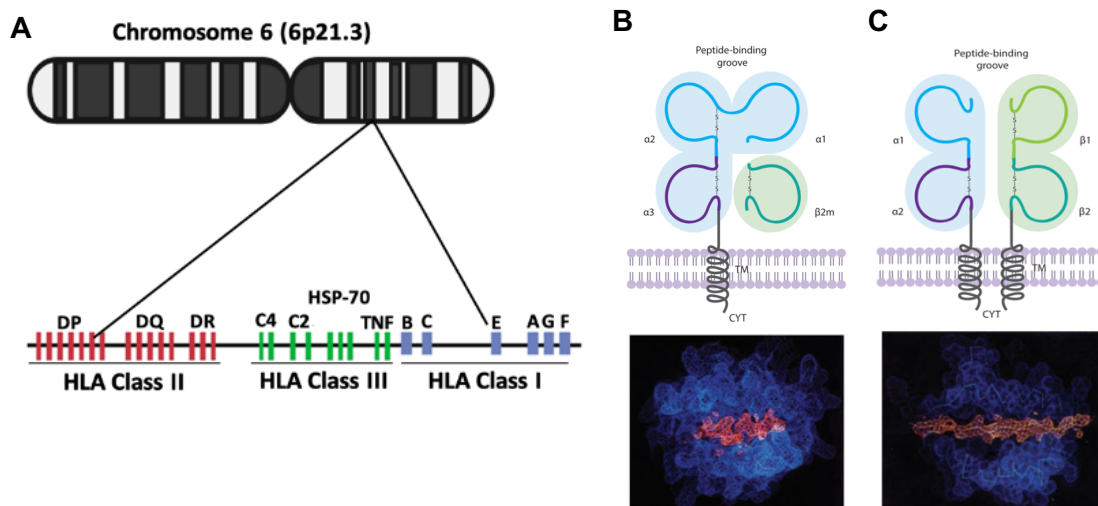


Figure 3. Structure of HLA molecules.

(A) Chromosome 6p21.3, which contains the 3 regions of the genes that belong to HLA class I, HLA class II and HLA class III. (B) Structure of the HLA class I molecules and graphic representation of the peptide binding groove of 8-9 amino acids long. (C) Structure of the HLA class II molecules and graphical representation of the binding groove for peptides 10-30 amino acids long. Figure adapted from Abbas et al. *Elsevier*. (2016).²⁷

4. T Cell Receptor

The T cell receptor (TCR), is a heterodimer, composed of an α chain and a β chain. Each of the chains contains an immunoglobulin (Ig)-like extracellular variable (V) and constant (C) domain, a membrane-proximal connecting peptide, a single transmembrane region, and a short cytoplasmic tail (**Figure 4**). Furthermore, it is non-covalently associated with the following invariant dimers: CD3 $\epsilon\gamma$, CD3 $\epsilon\delta$ and CD3 $\zeta\zeta$, forming the TCR-CD3 complex. The main function of the TCR is to mediate the recognition of peptide fragments that are bound to MHC/HLA molecules on APCs.³⁰

TCRs engage peptide-MHC ligands via their complementarity-determining region (CDR) loops, three from the V α domain and three from the V β domain. The first two (CDR1 and CDR2) are encoded within the TCR V segments, whereas CDR3 is formed by DNA recombination involving the juxtaposition of V α and J α segments for α chain gene and V β , D and J β segments for β chain genes. These rearrangements generate many different permutations and combinations of the V, D, and J gene segments, allowing a combinatorial and binding diversity to the TCR.³¹ Each clone has a unique specificity, potential for $>10^{11}$ different specificities.²⁷ For the activation process, following TCR binding to peptide-MHC, the CD3 molecules, which contain the immunoreceptor tyrosine-based activation motifs (ITAMs), undergo phosphorylation by the Src kinase Lck, initiate the down-stream signaling cascade to activate the T cells.³¹

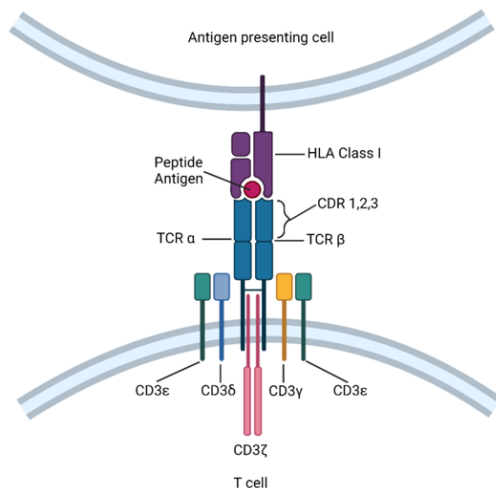


Figure 4. Structure of the TCR-CD3 complex.

The TCR complex is a heterodimer with two different peptide chains (TCR α and TCR β) and is associated with four CD3 chains. Figure also represents how the MHC class I molecule presents an intracellular antigenic peptide for recognition by the T cell receptor Figure obtained from Y. Sun et al. *Cells*. (2021).³²

5. Immunotherapy: Adoptive Cell Therapy

Previously, the most common B-cell neoplasms and first-line treatments were presented, which are usually external (radiotherapy and surgery) or systemic (chemotherapy), and act directly on the tumor from outside the patient's body or a general level on the whole body, respectively. However, immunotherapy has advantages over external and systemic treatments, as it can

stimulate and utilize the intrinsic potential of the patient's immune system to eradicate residual or disseminated tumor cells and restore weakened immune function. Additionally, it has been clinically demonstrated to have promising potential in treating various malignant neoplasms, prolonging survival, and improving the patient's quality of life.³³

There is a wide range of immunotherapies to combat cancer, such as monoclonal antibody therapy and immune checkpoint inhibitors, cytokine therapy, the use of oncolytic viruses, cancer immunomodulators, and adoptive cell therapy (ACT). Monoclonal antibody therapy has been one of the most widely used treatments for cancer; however, it has limited biodistribution, a variety of effector mechanisms, and low *in vivo* persistence, which have restricted its clinical potency. In contrast, ACT has the ability to effectively reach distant tumor sites, recruit multiple cellular and humoral effector mechanisms that help control and remit the disease.^{34,35}

The initial developments in ACT are based on using cells, specifically T cells/lymphocytes, extracted directly from the patient (autologous approach) or from healthy donors (allogeneic approach) for therapeutic purposes. This therapy has been applied to treat tumors or infections. Among the ACTs, we find TIL, TCR-T, CAR-T (**Table 1**). The following section delves deeper into CAR-T therapy, which is one of the therapies that this study aims to enhance.

Table 1. Current adoptive cell therapies in cancer treatment

Adoptive cell therapy	TIL	TCR-T	CAR-T
Effector cell	Mainly Th and CTL	Th/CTL	Th/CTL
Marker	CD3 ⁺ CD4 ⁺ / CD3 ⁺ CD8 ⁺	CD3 ⁺ CD4 ⁺ / CD3 ⁺ CD8 ⁺	CD3 ⁺ CD4 ⁺ / CD3 ⁺ CD8 ⁺
Cell source	Isolated from tumor tissue	PBMC, iPSC	PBMC, iPSC, UCB
Tumor recognition pattern	Natural multi-antigen recognition	Engineered TCR-dependent, low antigen density threshold	CAR-dependent
Tumor killing pattern	Perforin/granzyme, cytokine	Perforin/granzyme, cytokine	Perforin/granzyme, cytokine
Safety	High: naturally selected <i>in vivo</i>	High: MHC restriction, may cause GvHD and off-tumor toxicities	Moderate: may cause CRS, ICANS, GvHD and off-tumor toxicities
Infiltrating ability	High: have mature tumor chemotaxis system	Low	Low
<i>In vivo</i> persistence	Low: have been extensively expanded <i>in vitro</i>	Moderate	Moderate
Improve TME	Low	Low	Low
Gene transfer	Not apply	Easy (RV, LV)	Easy (RV, LV)
Potential for off-the-shelf products	Not apply	Low	Low
Research progress	Phase 3	Phase 2	6 products have been marketed
Manufacture cost	High	Moderate	Moderate
Manufacture time	Long	Moderate	Moderate
Antigen pool	Not apply	Large: all antigens that can be presented by TCR	Limited: only extracellular antigens

TME, Tumor microenvironment; PBMCs, Peripheral blood mononuclear cells; iPSC: induced pluripotent stem cells; UCB, umbilical cord blood; RV, retrovirus; LV, lentivirus; MHC, major histocompatibility complex; GvHD, graft-versus-host disease; CRS: cytokine release syndrome; ICANS: Immune effector cell-associated neurotoxicity syndrome. Adapted from P. Zhang et al. *Journal of Hematology & Oncology*. (2023).³⁵

6. Chimeric Antigen Receptor T cell immunotherapy

CAR-T cell therapy is an adoptive cell-transfer-based immunotherapy developed by genetically modifying T cells. The CAR was developed to circumvent MHC/HLA restriction, since tumor cells frequently downregulate the expression of these molecules, evading recognition by T cells, and also to mitigate rejection by the hosts' immune system. So, CARs are modular synthetic receptors or genetically modified fusion proteins, that combine the binding specificity of monoclonal antibodies with the effector function given by different signaling domains capable of

activating T cells independently of HLA restriction, to induce an antitumor immune response.^{36,37} CAR-T cell therapy uses genetic transduction techniques to give T cells the ability to precisely attack tumors by introducing antigen-specific CAR molecules into them.³⁵

The source of T cells for CAR T cell production can be the patient (autologous) or a donor (allogeneic). Blood is collected by apheresis from the patient or the donor. T cells are isolated from collected blood, activated and subjected to genetic engineering. T cells are typically engineered to express CAR by transducing the patient's T cells with a virus that contains a DNA construct. The resulting CAR-T cells are then expanded and infused into the patient (**Figure 5**).³⁸

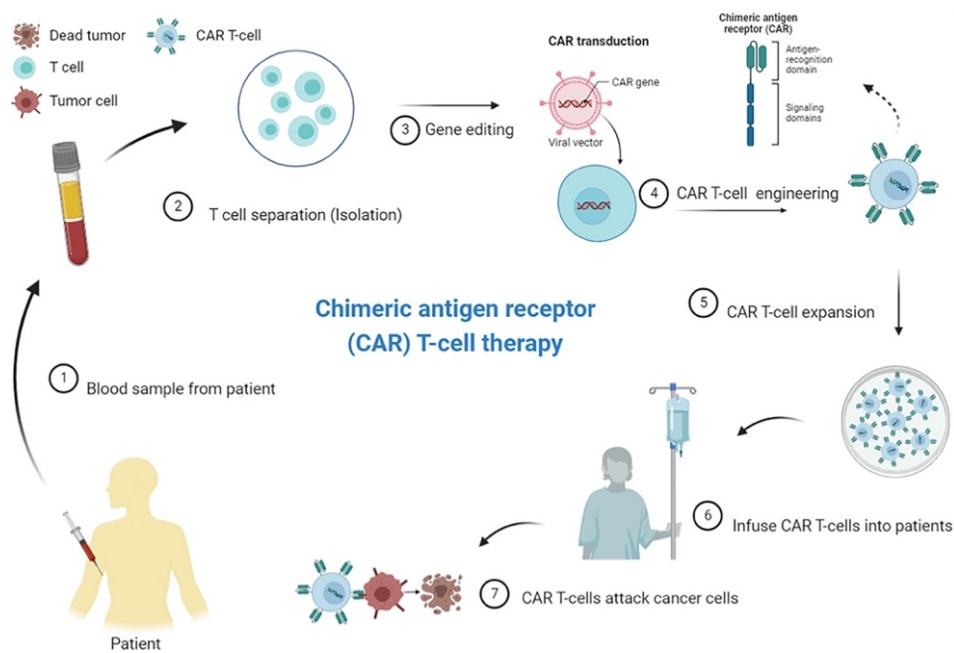


Figure 5. CAR-T cell therapy process.

(1) Blood is drawn from the patient or donor, (2) T cells are isolated and activated (3) and (4) T cells are modified by viral vector transfection, such as lentivirus transfection or retrovirus transfection, to express specific CARs on the surface of T cells. (5) After amplification and control quality, (6) CAR-T cells are infused into the patient's body (7) to enhance antitumor capacity. Figure obtained from Ghazi, El Ghanmi, Kandoussi, Ghouzlani, & Badou. *Front. Immunol.* (2022).³⁹

6.1 Structure of CAR

The function of CAR-T cells is determined by the structure of the CAR molecule. CARs consist of four main components: (1) extracellular target-binding domain (2) hinge region (3) transmembrane domain, and (4) intracellular signal domain (comprising the CD3 ζ T cell activation domain and the signaling of costimulatory receptors), which vary depending on the type of CAR-T generation (**Figure 6A**).^{40,41}

Extracellular target-binding domain: It is derived from a single-chain antibody fragment, known as single-chain variable fragment (scFv), which is responsible for identifying and conferring the targeting specificity to CAR-T cells. In addition to specificity, the binding affinity of this domain to the target is another key factor affecting how well a CAR performs. Also, charge density, epitope location and target antigen density will be considered while designing a CAR.³⁵ Lately, other strategies are also being designed that involve the use of a known receptor or ligand for a specific target protein (e.g. IL13R α 2), using a system based on streptavidin-biotin, and/or incorporating CARs with more than one scFv region in tandem.⁴²

Hinge domain: It is located extracellularly and serves as a linker connecting the target-binding domain to the transmembrane domain. The length of the hinge may affect the binding of the CAR to target cells, since the target may be located proximal or distal to the plasma membrane. The most employed hinge regions are derived from amino acid sequences from CD8, CD28, IgG1 or IgG4.⁴⁰

Transmembrane domain: The main function is to anchor the CAR to the T cell membrane, but there is also speculation that the transmembrane domain can be active in signaling or synapse formation and dimerize with endogenous signaling molecules. Most transmembrane domains are derived from natural proteins: CD3 ζ , CD4, CD8 α or CD28.⁴⁰

Intracellular signal domain: It is responsible for triggering cell activation after the interaction of the CAR with the antigen.⁴² It involves signal transduction and costimulatory molecules to transmit activation signals to T cells. The signal transduction is usually CD3 ζ or immunoglobulin Fc receptor Fc ϵ RI γ , which contains ITAM, mimicking the signal transduction of the TCR.³⁵ The ITAM domain of CD3 ζ alone is not sufficient to induce the expression and persistence of the effector T lymphocyte, which is why costimulatory molecules are necessary, to create synergy and enhance intracellular activation signals.⁴²

Costimulatory domains are derived from the CD28 family (CD28, ICOS) or the tumor necrosis factor receptor family (4-1BB, OX40, CD27).^{35,43} The two most common costimulatory domains, CD28 and 4-1BB (CD137), approved by the Food and Drugs Administration (FDA), are associated with high response rates.⁴⁰

6.2. Evolution of CARs development

The first CARs were generated around 30 years ago and subsequently underwent a stepwise evolution in their development. Five generations can be distinguished, based on the structure and composition of the intracellular signaling domain⁴⁴ (**Figure 6B**).

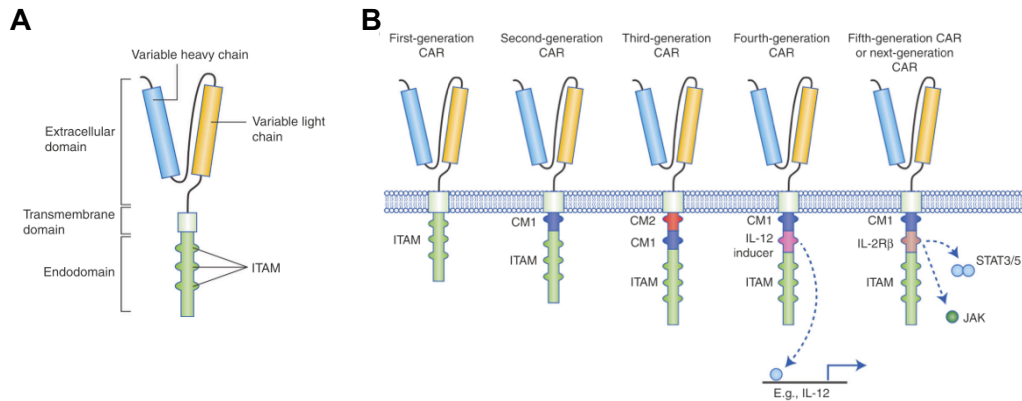


Figure 6. Structure and evolution of CARs development.

(A) Structure and components of CARs. (B) Evolution of the development of CARs from the first generation, in which only the CD3 ζ intracellular signaling (with its three ITAMs) was present. The second generation introduced one costimulatory molecule to enhance proliferation and cytotoxicity. The third generation incorporated two costimulatory molecules. The fourth generation, also called TRUCKs, can activate downstream transcription factors to induce cytokine production upon recognizing target antigens. The fifth generation has a β -fragment of the IL-2 (IL-2R β), which has a STAT3/5 binding site and is capable of activating cytokine signaling via JAK/STAT. Figure obtained from Tokarew et al. *British Journal of Cancer*. (2019).⁴⁴

The **first generation** of CAR contained a single CD3 ζ intracellular domain, with three ITAMs, which are phosphorylated by lymphocyte-specific protein tyrosine kinase (Lck) within the cytoplasmic domain of CD3.⁴⁵ Initial experiments with this generation showed low cytotoxicity and proliferation due to a lack of costimulatory signaling and cytokines.⁴⁴ It was developed between 1989-1993 by the immunologists Zelig Eshhar and Gideon Gross.³⁵

Thereafter, a **second generation** was generated to enhance T cell proliferation and cytotoxicity by adding one costimulatory domain (CD28 or 4-1BB).⁴⁴ It has been observed that CARs containing a CD28 costimulatory molecule, cause stronger activation than CAR-4-1BB, but less sustained, with a more effector phenotype, high production of IL-2, greater cytolytic capacity and enhances glycolytic metabolism. While CARs with 4-1BB molecules are more persistent, with a mostly central memory phenotype, less exhaustion, a positive regulation of Bcl-2 family members and mitochondrial biogenesis is selectively induced.⁴³ The second generation CAR was developed by June et al. who introduced 4-1BB as costimulatory domain in the first generation CAR. Recent findings have shown that patients treated with second-generation CD19 CAR-T cell not only achieve complete remission but also maintain CAR-T cells *in vivo* for up to 10 years after therapy,

demonstrating that the costimulatory domain has greatly improved persistence of CAR-T cells, facilitating long-term tracking and elimination of tumor cells.³⁵

The **third generation**, contains two costimulatory domains, such as CD28/4-1BB or CD28/OX40. Despite the third generation of CAR-T cell therapy showing improved persistence and proliferation compared to the second generation, it did not exhibit better *in vivo* antitumor activity against hematological malignancies. Consequently, second generation constructs are the most widely used.³⁵

The **fourth generation**, based on the second generation, incorporates the expression of the protein interleukin 12 (IL-12) through the synthetic NFAT promoter (by activation of the T cell and response to IL-2). T cells transduced with this generation are referred to as T cells redirected for universal cytokine-mediated killing (TRUCKs). This co-expression of IL-12 increases T cell activation and allows the production and release of specific cytokines to recruit innate immune cells to enhance tumor elimination through various synergistic mechanisms such as exocytosis (perforin and granzyme) or death ligand-death receptor (Fas-FasL, TRAIL) systems.^{44,46}

The **fifth generation** of CAR is also based on the second generation but includes a truncated cytoplasmic IL-2 receptor β -chain domain with a binding site for the transcription factor STAT3. So, when the T cell is activated through the CAR, this receptor simultaneously activates the TCR, through CD3 ζ , CD28 costimulatory domain and the JAK-STAT3/5 signaling pathway, mimicking the three intrinsic physiological activation pathways of the T lymphocytes.^{44,47} Its effectiveness and safety continue to be investigated.

Additional variants of the aforementioned CARs have been generated, to further improve the limitations (described later), specificity and control of transfused T cells.

Within these variants, there are **CARs with different ectodomains**: ScFv, single-domain antibodies (SdAbs), natural receptor, natural ligand; and **endogenously programmed CAR-T cells**, which includes OR, AND/NOT-CARs. OR, is designed to prevent antigen escape rather than increase specificity. The CAR-T cell is activated when one of the antigens is present. In this category are the multi-target CARs such as Pooled CARs (two different types of CAR-T cells), Duo-CARs (same cell that expresses two types of CAR) and Tandem-CARs (expresses two ScFVs, that can activate the CAR-T cell). AND/NOT are designed to increase tumor specificity, and only when both antigens are present will the CAR-T cell be activated. An example of this are the Split-CARs, SynNotch CAR, SUPRA-CAR, among others. **Universal CARs**, which have been created to modulate the response against any antigen by adding a specific adapter.³⁵

6.3. Transfection of CARs constructs into viral vectors

Although viruses are commonly associated with disease, genetic engineers have discovered how to use their natural biology to alter or complement the genetic code of host cells, thus developing a new class of gene delivery tools called viral vectors.⁴⁸ The viral vector particles are not infective; therefore, they do not infect but transduce the target cell and do so in a very efficient manner.⁴⁹ The components of a viral vector are:

1. Capsid, which envelopes the genetic material and defines the tropism (cell type to be modified).
2. Transgenes of interest to be expressed in the target cells.
3. Expression and packaging regulator cassette, which contains the enhancer, promoter and necessary elements to be packaged in the viral particle, expressed, and/or integrated in the target cells.

Gamma retroviral (GRV) and lentiviral (LV) vectors, originating from enveloped RNA viruses of the *Retroviridae* family, have been widely used in research and clinical use due to their ability to insert genetic material into the host cell genome and express transgenes in a stable manner, making them particularly suitable for transducing rapidly replicating cells, such as immune cells.⁴⁸ The RNA genome of the *Retroviridae* family is retrotranscribed into DNA by the enzyme reverse transcriptase. This DNA is integrated into the host cell genome, allowing long-term expression of the gene of interest in both infected cells and their progeny. GRV is derived from Moloney murine leukemia virus or murine stem cell virus, while LV are mainly derived from HIV-1.⁴⁹ **Table 2** describes the main characteristics of each viral vector.

Table 2. Characteristic of Retroviridae family vectors

Characteristic	Gamma-retroviral	Lentivirus
Size	~80-100nm	~80-100nm
Genome	ssRNA	ssRNA
Packing capacity	10kb	8kb
Transduction	Dividing cells	Dividing and non-dividing cells
Transduction efficiency	Moderate	Moderate
Integration	Integrating	Integrating
Expression	Stable	Stable
Biosafety level	BSL-2	BSL-2
Immunogenicity	Moderate-high	Low

In the production of retroviral vectors, packaging cells are used, which act as factories of viral particles by assembling the different components of the vector and also provide the virus membrane. For their production, the packaging cells (usually HEK 293T cells) are transfected

with 3 or 4 plasmids,^{48,49} depending on the generation (**Figure 7**). The plasmid that can be used are:

1. **Envelope plasmid** expresses the selected envelope protein, usually the vesicular stomatitis virus fusogenic envelope glycoprotein G (VSV-G).
2. **Packaging plasmid** contains the necessary genes *gag*, *pol*, *rev* and *tat*. In the case of second generation vectors, it contains all four genes on one plasmid, while third generation vectors contain one plasmid with the *gag* and *pol* genes and another plasmid with *rev* (regulatory plasmid).
3. **Transgene plasmid** contains the mRNA including the packaging signal (ψ), reverse transcription and integration signals, promoter and the gene of interest.

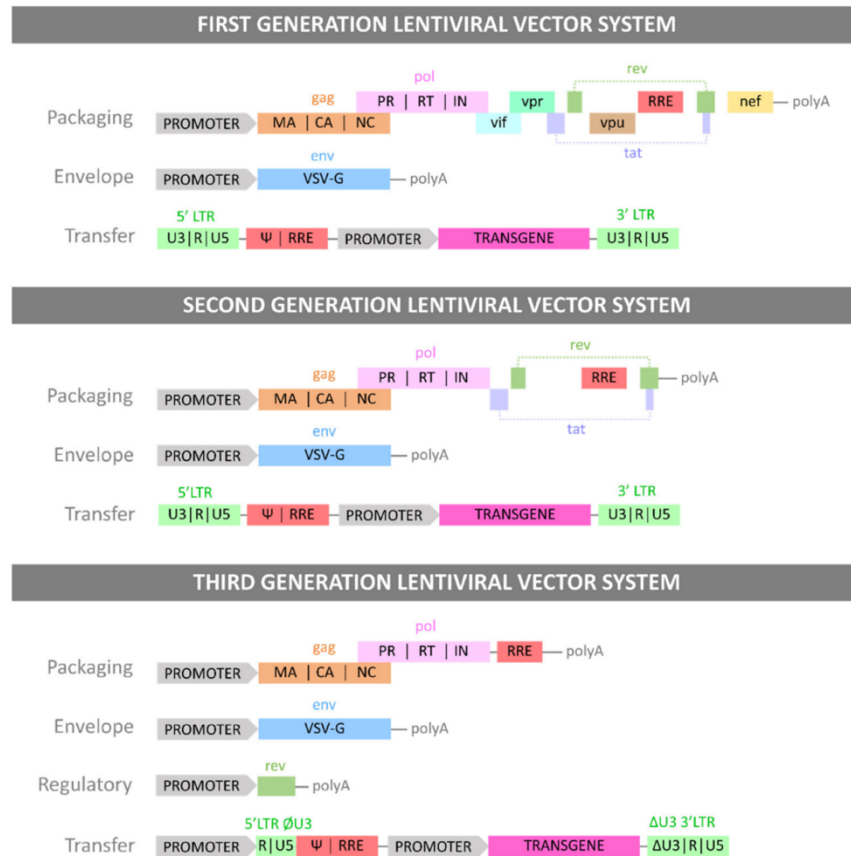


Figure 7. Generations of LV plasmid systems.

First generation, are designed with only the viral genes essential for virus replication. They have certain limitations in terms of transduction efficiency and safety. Second generation viral accessory genes have been removed, along with the incorporation of additional regulatory elements and the improvement of gene expression capacity to improve safety and transduction efficiency. Third generation, are even more refined in terms of safety and efficiency. They usually include controlled gene expression induction systems, such as specific promoters or transcriptional regulators, which allow more precise control over the expression of the inserted gene. In addition, improvements in gene loading capacity and vector stability. Figure obtained from Labbé et al. *Viruses*. 2021.⁴⁸

6.4. CAR-T approved as treatment

In the last three decades, CARs have progressed from their initial characterization until FDA approval for use in patients.⁴⁴ CAR-Ts can be designed to target any extracellular antigen, however those that have been designed against the CD19 antigen (which is expressed in lymphomas and B-cell ALL) are those that represent the greatest clinical success at the moment.⁵⁰ Currently, CAR-T cell therapies are primarily approved for hematologic tumors for domestic and international markets. Of the six approved therapies, four are against CD19 antigen, targeting relapsed or refractory (R/R) B-cell lymphoma and ALL, whereas the remaining two are against anti-B-cell maturation antigen (BCMA) to treat R/R multiple myeloma (MM) (Table 3).^{51–53}

Table 3. Comparison of autologous CAR-T cell FDA-approved therapies

	Kymriah® Tisagenlecleucel	Yescarta® Axicabtagene ciloleucel	Tecartus® Brexucabtagene autoleucel	Breyanzi® Lisocabtagene maraleucel	Abecma® Idecabtagene vicleucel	Carvykti® Ciltacabtagene autoleucel
FDA approved date	August 30, 2017	October 18, 2017	July 24, 2020	February 5, 2021	March 26, 2021	February 28, 2022
Target/ScFv antibody	CD19/mouse FMC63	CD19/mouse FMC63	CD19/mouse FMC63	CD19/mouse FMC63	BCMA/mouse BB2121	BCMA/dual camel single domains antibodies
Hinge/transmembrane domain	CD8 α /CD8 α	CD8 α /CD8 α	CD28/CD28	IgG4/CD28	CD8 α /CD8 α	CD8 α /CD8 α
Intracellular domain	4-1BB + CD3 ζ	CD28 + CD3 ζ	CD28 + CD3 ζ	4-1BB + CD3 ζ	4-1BB + CD3 ζ	4-1BB + CD3 ζ
Vector/ promoter	Lentiviral/EE1 α	Gammaretroviral/LTR	Gammaretroviral/LTR	Lentiviral/EE1 α	Lentiviral/MND	Lentiviral/EE1 α
Source	PBMCs	PBMCs	T cells (CD4 ⁺ and CD8 ⁺)	T cells (CD4 ⁺ and CD8 ⁺ , ratio 1:1)	PBMCs	T cells (CD4 ⁺ and CD8 ⁺)
Manufacturing time	22 days	19 days	15 days	24 days	4 weeks	32 days
Targeted cancers	R/R B-ALL R/R DLBCL	R/R DLBCL	R/R MCL R/R B-ALL	R/R DLBCL	R/R MM	R/R MM
Pivotal trial	ELIANA NCT02228096	ZUMA-1 NCT02348216	ZUMA-2 NCT02601313	Transcend NHL001 NCT02631044	KarMMa NCT03361748	CARTITUDE-1 NCT03548207
No. of patients	75	108	68	269	128	97
Outcomes	81% overall remission rate	58% complete response	67% complete response	53% complete response	33% complete response	82.5% complete response
Persistence	1-9 years	3 moths	3-24 months	2 years	13-20 months	12 months
Cost	373,000-475,000\$	373,000\$	373,000\$	410,300\$	419,500-545,000\$	465,000\$

B-ALL, B-cell lymphoblastic leukemia; LTR, long terminal repeats. Adapted from Mitra et al., *Front. Immunol.* (2023).⁵²

In Spain, and in parallel to commercial development, CAR-T against CD19 antigen is being developed in academic institutions. The first public centers to promote this strategy were the Hospital Clínic and Hospital Sant Joan de Déu in Barcelona, for pediatric patients with B-cell ALL and adults with CD19⁺ lymphoid neoplasms.⁵⁰

6.5. ARI-0001

It is the first CAR designed and developed by the academy, approved in March 2021 by the Spanish Medicines Agency (AEMPS), as an advanced therapy medicinal product for non-industrial manufacturing, developed by the Hospital Clínic and the Institut d' Investigacions Biomèdiques August Pi i Sunyer (IDIBAPS). The name ARI is due to Ariana Benedé, a young patient with ALL who died at the age of 18 in 2016 and, thanks to her and her mother, propelled the research of CAR-T cell therapy to get it implanted in Spain.

ARI-0001 is a second-generation CAR containing a scFv binding domain anti-hCD19 A3B1 monoclonal antibody (mAB), with an EF1 α promoter, a CD8 α hinge and transmembrane domain, a CD3 ζ signal and 4-1BB costimulatory domain as an intracellular domain (**Figure 8**). Transduction of the CAR construct is performed with a third generation lentivirus in autologous T cells, mainly in isolated CD4 and CD8 T cells. It has been approved as an autologous treatment for R/R B-cell ALL in patients older than 25 years, generating 70% complete remissions and 50% versus NHL.⁵⁴

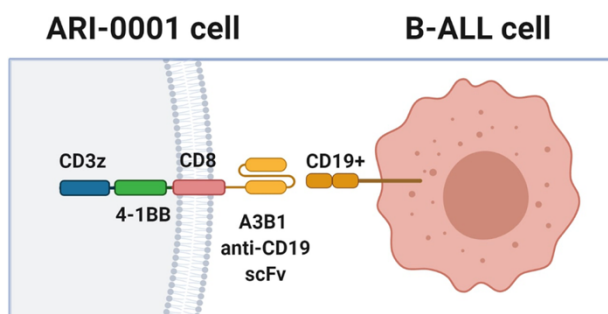


Figure 8. CAR-T CD19, ARI-0001. ARI-0001 cells, highlighting the CAR construct and its interaction with the tumor cells (ALL). Figure obtained from Ortiz-Maldonado et al. *Am. J. Hematol.* (2022).⁵⁵

6.5.1. ARI-0001 large-scale production

The manufacturing process begins with peripheral blood leukapheresis, obtained from the patient. This leukapheresis is connected to the ClinicMACs Prodigy[®] system (Miltenyi Biotec) using a specific tubing set. Erythrocytes and platelets are removed through density gradient centrifugation in the CentriCult unit. The remaining cells are then selected using CD4 and CD8-coated magnetic beads. These selected T cells are eluted in the “reapplication bag”. From this bag, 1×10^8 T cells are used to initiate cell culture. The remaining cells are cryopreserved in bags and vials for quality assays and as a backup. Cells are activated with TransACT[®] GMP grade (T cell activation via anti-CD3/anti-CD28) and transduced 24 hours later using CAR19-containing in a third generation

lentivirus at multiplicity of infection (MOI) = 10. Cells are cultured in TexMACS[®] media supplemented with 3% human serum AB and with 155U/mL IL-7 and 290U/mL IL-15. T cell expansion with IL-7 and IL-15 has been shown to promote the naïve T cells (T_N) and stem cell-like memory T cells (T_{SCM}) phenotype more than when using expansion with IL-2, which favors the effector T cell (T_{EM}) phenotype. A cell culture wash is programmed 48h after transduction. The cells are maintained in culture with increasing shaking until the desired cell number is reached (typically 7-10 days after culture initiation). Finally, cells are eluted in 100ml 0.9% NaCl and 1%HSA, aliquoted according to the desired ARI-0001 cell dose, and cryopreserved until infusion (**Figure 9A**). Prior to infusion, microbiological and immunological characterization and quality analyses are performed, as required for a GMP product. The aim of each production is to achieve two doses of ARI-0001 cells/patient. The cell dose is dependent on the patient's disease. Typically, 0.5-1x10⁶ ARI-0001 cells/kg for patients with ALL and 5x10⁶ ARI-0001 cells/kg for NHL/CLL patients.^{54,56} The cost of this therapy is around 90,000-100,000€.

During the production process, the patient undergoes lymphodepletion under a preventive chemotherapy regimen (with cyclophosphamide/fludarabine), with the aim of reducing the number of tumor cells and favoring the *in vivo* expansion of the CAR-T cells administered. Usually, the patient receives a single dose of CAR-T cells. But it has been observed in the CART19-BE-01 clinical trial, which included patients with ALL, NHL and 1 patient with CLL, that when the dose was fractionated into three parts: 10% at day 0, 30% and 60% in the second and third fractions, side effects such as cytokine release syndrome (CRS), were better controlled (**Figure 9B**).^{55,57,58}

There are many different systems to use for the *ex vivo* transduction and expansion of CAR-T cells. For ARI-0001 was choose the ClinicMACs Prodigy[®] system because (1) is a semi-automated system that allows magnetic cell separation, cell activation, transduction and expansion in a single machine, and (2) it is a close GMP-compliant system. In addition, the results of each production have been found to be robust and reproducible.^{54,56}

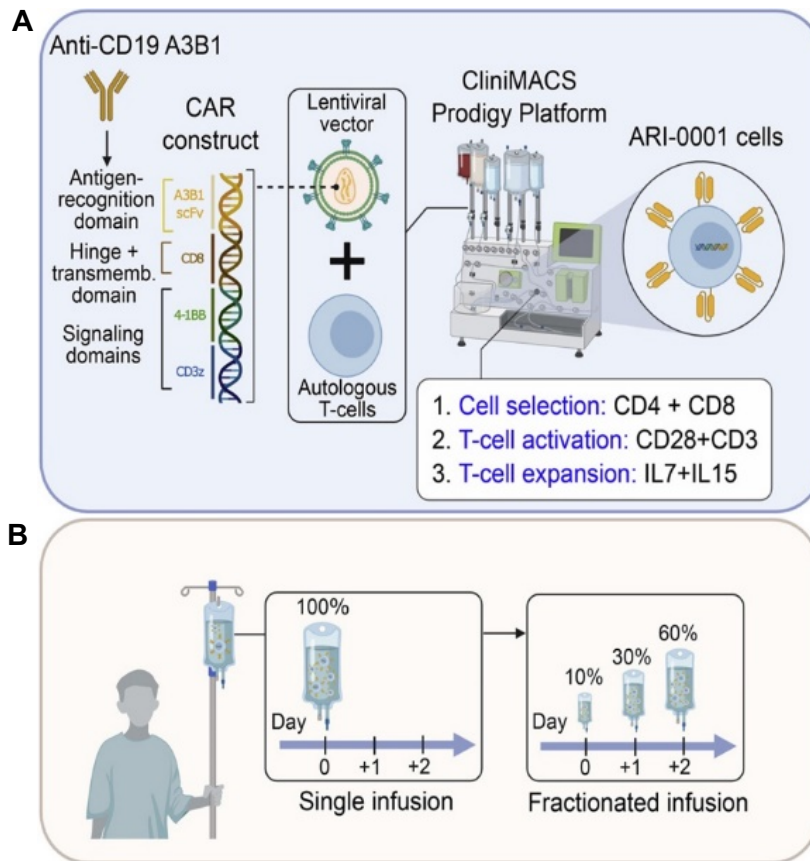


Figure 9. ARI-0001 cells production and dose infusion.

(A) Steps of manufacturing ARI-0001 in a semi-automatic system: CliniMACs Prodigy[®]. (B) Usually, the patient receives a single dose of CAR-T cells, but the administered dose of ARI-0001 has been fractionated in 3 parts: 10% at day 0, 30%, and 60% in the second and third fractions, to reduce and control side effects such as CRS. Figure obtained from Ortiz-Maldonado et al. *Molecular Therapy Cell Press* (2021).⁵⁷

6.6. Side effects in the anti-CD19 CAR-T cell therapy

Despite the promising results of CAR-T therapy against the CD19 antigen, there are severe side effects, including CRS, Graft-versus-host disease (GvHD), tumor lysis syndrome (TLS) and immune effector cell associated syndrome (ICANS).³⁸ On the other hand, there are certain limitations, such as lack of cell proliferation, persistence, antigen escape, immunosuppression microenvironment, and exhaustion, among others.⁴⁰ These limitations compromise the efficacy of CAR-T therapy, causing treated patients to not achieve complete remission in the long term.

CRS: Is a life-threatening systemic inflammatory response triggered by the release of proinflammatory cytokines such as: IL-1, IL-2, IL-6, TNF- α , IFN- γ , GM-CSF, MCP-1 and MIP-1 β . The frequency and severity of CRS correlate with antigen-dependent T cell activation and expansion.⁵⁹ CRS can cause long-term fever, hypotension, dyspnea and organ problems. Usually, the reaction and symptoms arise during the first two days after CAR-T cell infusion, and its

maximum intensity is recorded one to two weeks after infusion.⁶⁰ The use of lymphodepletion chemotherapy, a higher dose of CAR-T cells, disease burden, and elevated baseline inflammatory markers are factors associated with severe CRS. Previous studies report that by not using lymphodepletion chemotherapy when administering CAR-T cells, cytotoxicity decreases, but so does the effectiveness of the therapy.⁶¹⁻⁶³

ICANS: It is characterized by elevated levels of cytokines in the cerebrospinal fluid and disruption of the blood-brain barrier.⁴⁰ Clinical manifestations are confusion, headache, attention deficit, word-finding difficulties, focal neurological deficits, encephalopathy to life-threatening cerebral edema, transient coma, or seizures. Neurotoxicity after CAR-T cell therapy is common and can occur in up to 67% and 62% of patients receiving treatment for leukemia and lymphoma, respectively.⁶⁴

B cell aplasia and cytopenia: Since CD19 is present on normal B cells, hypogammaglobulinemia may arise due to long-term B cell aplasia. Cytopenia has been observed in ZUMA-1 and JULIET clinical trials.⁶⁵

TLS: The high efficiency of killing tumor cells causes the release of a large number of intracellular ions and metabolic products into the bloodstream that can generate acute and systemic renal failure.^{62,65}

Anaphylaxis and immunogenicity: Since CARs have a non-human part (ScFv, of murine origin) in their construct, there may be a risk of allergic reaction.⁶⁶

GvHD: At the moment, the therapies approved by the FDA and AEMPS are autologous, so the risk of GvHD is almost zero. However, in cases where the T cells for CAR-T therapy come from a donor (allogeneic), the risk of GvHD may be a concern. This scenario can occur in patients who have received an allogeneic stem cell transplant, where the donor's T cells are used for CAR-T modification. In the trials, NCT01626495 and NCT01029366, with Tisagenlecleucel (Kymriah®), where 18 patients who had previously received an allogeneic stem cell transplant received tisagenlecleucel, no development of GvHD was observed after infusion of CAR-T cells, even though the donor's chimerism was 100%. In another study, the occurrence of acute GvHD was not reported when CAR-T cells were provided by the patient's transplant donor (NCT01087294).⁶⁷

6.7. Limitations and challenges

Antigen escape: Although a CAR-T directed against a single antigen can offer high response rates, tumor cells have developed various strategies for partial or complete loss of expression of the target antigen.⁴⁰ Mechanisms of CD19 loss include mutations and splice variants of the CD19 gene, as well as the switch of tumor cells from lymphoid lineage (B cells) to myeloid CD19.⁶⁸ In addition, there is also the mechanism of trogocytosis, where when the CAR comes into contact with the antigen, the target is transferred to the CAR-T cell membrane itself. This mechanism generates a cooperative death (fratricide), where a CAR-T cell lyses a CD19⁺ CAR-T cell, and T cell exhaustion.⁶⁹

Evasion of the immune system and immunosuppressive microenvironment: Many cell types that drive immunosuppression can infiltrate lymphomas and solid tumors, including myeloid-derived suppressor cells (MDSCs), tumor-associated macrophages (TAMs), and regulatory T cells (Tregs). These infiltrates and tumor cells drive the production of cytokines, chemokines, and tumor-facilitating growth factors. Furthermore, immune checkpoint pathways, such as PD-1 or CTLA-4, may serve to diminish antitumor immunity.^{40,70} Another resistance mechanism is the loss of receptor signaling (FADD, BID and TRAIL2) in tumor cells. This loss makes them more resistant to the effectiveness of CAR-T targeting CD19, both *in vitro* and *in vivo*.⁷¹

Exhaustion, lack of persistence and cell proliferation: Extensive *in vitro* expansion, repetitive stimulation by tumor cells, and the inhibitory tumor microenvironment all lead to CAR-T cell exhaustion and a subsequent loss of antitumor function. Exhausted CAR-T cells display increased levels of inhibitory receptors (such as PD-1, LAG-3, TIM-3, CTLA-4, and TIGIT), reduced secretion of IL-2, TNF- α , and IFN- γ , altered metabolism, and epigenetic modifications.³⁵ Physiologically, exhaustion prevents overactivation of T cells when they are repeatedly stimulated by self-peptide/MHC and become inactivated. Likewise, continued exposure to the antigen causes T cells to become exhausted and susceptible to activation-induced cell death (AICD), decreasing their cytotoxic potential, proliferation and persistence *in vivo*. On the other hand, a study of responders and non-responders (with primary resistance) to CAR-T cells targeting CD19 in CLL patients showed that T cells from non-responders had a more effector, glycolytic, exhausted, and apoptotic phenotype. While the phenotype of the responding patients had T cells with a memory phenotype, greater expression of IL-6R, and activator of transcription 3 (STAT3).⁴³

Cell source: Until now, the CAR-Ts targeting the CD19 antigen, that have been approved by the FDA, European Medicines Agency (EMA) and AEMPs are based on an autologous T cell product, to avoid GvHD. Being an autologous product, the long time required for manufacturing and the variability of the final product between patients are limitations. Furthermore, patients, before

starting CAR-T therapy, undergo intensive treatments and lymphocytopenia, which makes it difficult to collect an adequate number of initial T cells to start the manufacturing process. Therefore, one of the advances in CAR-T therapy the use of allogeneic CAR-T. This approach requires editing or non-editing strategies to eliminate the TCR or HLA intrinsic to the T cells or using cells that do not mediate GvHD as the initial population, like invariant Natural Killer T cells (iNKT).⁷²

Among the advantages offered by an allogeneic CAR-T are several patients were treated from a single donor, worldwide availability of cellular products and easier automation. On the other hand, there are disadvantages, like the cost is higher than autologous process, greater human labor in activities such as research and development, and more steps in its construction to inactivate endogenous TCR.⁷³

Table 4 shows the different allogeneic CAR-T products currently available on the market, under clinical evaluation in Phase I or Phase I/II studies by various groups.⁷²

Table 4. Currently allogeneic CAR-T products under clinical evaluation

Allogeneic Technology	Target Antigen	Strategy for GvHD	Strategy for HvG	Product Name	Developers	Trial Names, Phase and Number
$\alpha\beta$ T cells (from PBMCs)						
TALEN	CD19	Disruption of TRAC	Disruption Of CD52 and use of anti-CD52	ALLO-501/UCART19	Collectis (Paris, France); Allogene Therapeutics (San Francisco, CA, USA)	CALM Phase 1 NCT02746952 PALL Phase 1 NCT02808442 ALPHA Phase 1 NCT03939026
	CD19	Disruption of TRAC	Disruption Of CD52 and use of anti-CD52	ALLO-501A	Collectis (Paris, France); Allogene Therapeutics (San Francisco, CA, USA)	ALPHA 2 Phase 1/2 NCT04416984
	BCMA	Disruption of TRAC	Disruption of CD52 and use of anti-CD52	ALLO-715	Allogene Therapeutics (San Francisco, CA, USA); Collectis (Paris, France)	UNIVERSAL Phase 1 NCT04093596
	CD70 TALEN	Disruption of TRAC	Disruption Of CD52 and use of anti-CD52 CD70 CAR designed to avoid fratricide	ALLO-316	Allogene Therapeutics (San Francisco, CA, USA); Collectis (Paris, France)	TRAVERSE Phase 1 NCT04696731
	CD123	Disruption of TRAC	Disruption of CD52 and use of anti-CD52	UCART123	Collectis (Paris, France)	AMELI-OI Phase 1 NCT03190278 Phase 1 NCT04106076 ABC12.3 Phase 1 NCT03203369
	CD22	Disruption of TRAC	Disruption of CD52 and use of anti-CD52	UCART22	Collectis (Paris, France)	BALLI-OI Phase 1 NCT04150497
	SLAMF7	Disruption of TRAC	Disruption of CS1 gene to avoid fratricide	UCARTCSI	Collectis (Paris, France)	MELANI-OI Phase 1 NCT04/42619

Table 4 (continued)

ARCUS	CD19	Disruption of TCR	-	PBCAR0191 /Azercabtagene zapreleucel	Precision BioSciences (Durham,NC,USA)	Phase 1/2 NCT03666000
	CD19	Disruption of TCR	shRNA against β 2M and HLA-E transgene	PBCAR19B	Precision BioSciences (Durham NC, USA)	Phase 1 NCT04649112
	BCMA	Disruption of TCR	-	PBCAR269A	Precision BioSciences (Durham,NC,USA)	Phase 1 NCT04171843
	CD20	Disruption of TCR	-	PBCAR20A	Precision BioSciences (Durham,NC,USA)	Phase 1/2 NCT04030195
CRISPR/Cas9	CD19	Disruption of TRAC		CB-OIO	Caribou Biosciences (Berkeley, CA, USA)	ANTLER Phase 1 NCT04637763
	CD19	Disruption of TRAC	Disruption of β 2M	CTX110	CRISPR Therapeutics (Zug, Switzerland)	CARBON Phase 1/2 NCT04035434
	BCMA	Disruption of TRAC	Disruption of β 2M	CTX120	CRISPR Therapeutics (Zug, Switzerland)	Phase 1 NCT04244656
	CD70	Disruption of TRAC	Disruption of β 2M + CD70 disruption to avoid fratricide	CTX130	CRISPR Therapeutics (Zug, Switzerland)	COBALT-RCC Phase 1 NCT04438083 COBALT-LYM Phase 1 NCT04502446
	CD19	Disruption of TRAC	Disruption of CD52 and use of anti-CD52	CTAIOI	Nanjing Bioheng Biotech (Nanjing, China)	Phase 1 NCT04154709 NCT04227015
	CD19/CD7	Disruption of TRAC	CD7 disruption to avoid fratricide	GC502	Gracell Biotechnologies (Suzhou, China)	Early Phase 1 NCT05105867
	CD7	Disruption Of TRAC	CD7 disruption to avoid fratricide	WU CART 007	Wugen (St Louis, MO, USA)	Phase 1/2 NCT04984356

Table 4 (continued)

Cas- CLOVERTM	BCMA	Disruption of TCR- β chain 1	Disruption of β 2M	P-BCMA- ALLOI	Poseida Therapeutics (San Diego, CA, USA)	Phase 1 NCT04960579
	FKBP12; MUCI-C	Disruption of TCR	Disruption of β 2M	P-MUCIC- ALLOI	Poseida Therapeutics (San Diego, CA, USA)	Phase 1 NCT05239143
Base-pair editing	CD7	Disruption of TRAC	Disruption of CD52 and CD7 to avoid fratricide	BE-CAR7	Great Ormond Street Hospital (London, UK)	Phase 1 ISRCTN15323014
Peptide-based (TIM8)	NKG2DL	Negative competition with CD3 ζ	-	CYAD-101	Celyad Oncology (Mont-Saint- Guibert, Belgium)	alloSHRINK Phase 1 NCT03692429 CYAD-101-002 Phase 1 NCT04991948
miRNA-based shRNA	BCMA	Knock-down of CD3 ζ	-	CYAD-211	Celyad Oncology (Mont-Saint- Guibert, Belgium)	IMMUNICY-I Phase 1 NCT04613557
Non-gene editing	CD19	Intracellular retention of TCR /CD3 complex via KDEL-tagged anti-CD3 scFv	Decreasing surface HLA-A and HI- A-B by HCMV US11 protein	ThisCART19 cells	Fundamenta Therapeutics (Suzhou, China)	Phase 1 NCT04384393
Cytolytic T-lymphocytes (from PBMCs)						
Zinc Finger Nuclease	IL13-zetakine	Disruption of the glucocorticoid receptor	Use of dexamethasone	GRm13Z40-2	City of Hope (Duarte, CA, USA)	Phase 1 NCT01082926
$\alpha\beta$ T cells (from iPSCs)						
CRISPR/Cas	CD19	Disruption of TRAC	-	FT819	Fate Therapeutics (San Diego, CA, USA)	Phase 1 NCT04629729

iPSC: Induced pluripotent stem cells; TRAC, T cell receptor alpha constant. Adapted from Lonez & Breman. *Cells* (2024).⁷²

As mentioned in previous sections, new variants and modifications of CAR-T therapy have been designed to minimize the side effects, limitations and challenges. However, functional and manufacturing improvements are still needed.

One of the recent strategies to prolong and enhance CAR-T is using virus-specific T cells (VSTs), as a cellular source for subsequent transduction. The combination of these two therapies can generate a specific cytotoxicity and long-term persistence against the antigen. Additionally, it could become an allogeneic therapy “*off the shelf*”.

7. Virus-Specific T cell

VSTs are T cells designed to recognize and attack cells infected by specific viruses. These cells use their native TCR to identify multiple epitopes on viral antigens, reducing the chances of viral immune escape. The use of VSTs as an adoptive therapy has been studied for over two decades and represents an innovative and promising approach for treating viral infections in immunocompromised patients, particularly those who have undergone hematopoietic stem cell transplantation (HSCT) and solid organ transplantation (SOT). VSTs have proven effective in preventing or treating viral infections caused by viruses such as EBV, Cytomegalovirus (CMV), Adenovirus (AdV), BK virus (BKV), John Cunningham virus (JCV), and Human Herpes virus (HHV).⁷⁴ VSTs can be obtained from various sources. They can be patient-derived (autologous) or donor-derived and third-party donors (allogeneic). Currently, banks of allogeneic VSTs are being developed to provide “*off-the-shelf*” therapies, enabling faster access to treatment.^{75,76}

Their effectiveness has been demonstrated in clinical trials. In the context of transplantation, VSTs were capable of restoring antiviral immunity and treating infections. VSTs have also shown promise outside of the transplant context, particularly in treating virus-associated malignancies such as EBV and human papillomavirus (HPV)-related cancers. Moreover, VSTs can target multiple epitopes of various tumor antigens, effectively addressing the issue of tumor heterogeneity.⁷⁷

7.1. VST manufacturing

It has been over 20 years since Riddell and colleagues conducted the pioneering protocol in which VSTs were infused into a patient, without significant side effects.⁷⁸ They generated CMV-specific CD8⁺ T cells by *ex vivo* culture of PBMCs in the presence of CMV-infected autologous fibroblasts, followed by clonal expansion and depletion of CD4⁺ T cells.^{76,78,79}

Over time, various *in vitro* strategies have been tested to optimize the generation of VSTs for clinical use (**Figure 10**). Typically, VST production begins with the isolation of PBMCs or T cells using density gradient centrifugation or apheresis techniques, respectively. Once isolated, there are two primary approaches:

1. **Direct Selection:** Specific T cells can be directly selected using various technologies such as multimer staining, IFN- γ capture, surface marker identification, or magnetic enrichment. These selected cells can either be expanded to increase their numbers or directly infused into the patient.
2. **Rapid and classic *ex vivo* expansion:** T cells can be activated by exposure to specific viral antigens, such as overlapping peptides, viral lysate, or antigen-presenting cells (APCs) transduced with viral vectors or plasmids encoding the target antigen. Following activation, the T cells are cultured under controlled conditions to promote their expansion, ensuring a sufficient number of antigen-specific T cells are produced. Finally, the expanded VSTs are infused into the patient, where they can recognize and attack virus-infected cells or virus-associated tumor cells, thereby restoring and enhancing T cell immunity.^{75,76,79,80}

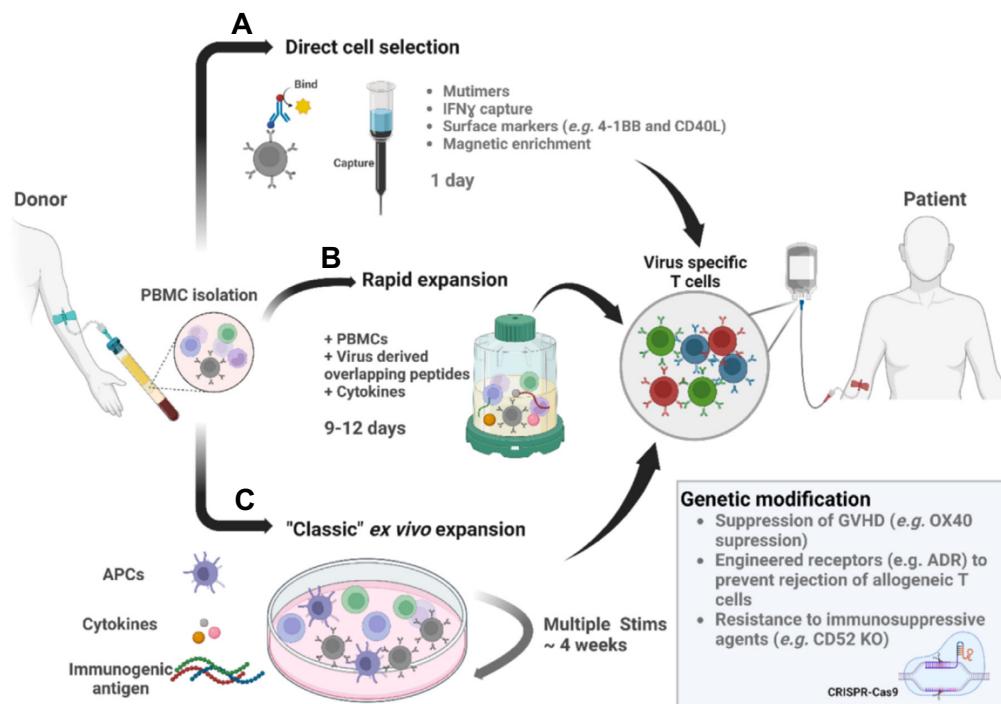


Figure 10. Strategies for manufacturing VST.

PBMCs isolated from blood donors can be manipulated using different strategies such as: (A) direct selection, (B) rapid expansion, which involves stimulating the cells with viral-derived overlapping peptides and maintaining the cell culture for a few days (9-12 days); and (C) the “classic” *ex vivo* expansion, which requires multiple stimulations of T cells with APCs pulsed with immunogenic antigens and expansion for approximately four weeks. Subsequently, VSTs can be infused into the patient. APCs, antigen-presenting cells; GvHD, graft vs host disease; PBMCs, peripheral blood mononuclear cell; VSTs, virus-specific T cells. Figure adapted from Motta, Keller & Bollard. *Elsevier*. (2023).⁷⁵

The phases for the manufacturing of VSTs are described in more detail below:

Antigen selection

The production and *ex vivo* expansion of VSTs for clinical applications require two key elements: (1) a defined antigen with immunogenic properties, and (2) an antigen-presenting cell that can effectively present this antigen to T cells along with appropriate costimulatory signals. Therefore, it is crucial to identify which viral antigens are immunodominant and capable of inducing protective responses *in vivo*. For example, some latent viruses, such as CMV and EBV, the immunodominant epitopes at different stages of infection are well established.⁸¹

Antigen presentation

Defined immunogenic antigens must be presented by APCs that express MHC molecules to display virus-derived peptides, along with sufficient costimulatory molecules to induce T cell activation and expansion.⁸¹ The choice of APC depends on the type of viral antigen used and the proposed delivery method (**Table 5**).

Table 5. Summary of methods for presenting different types of viral antigens

Viral antigens	Presentation	Notes
Whole virions or viral lysates	Infected fibroblasts** APCs (pulsed DCs, LCLs)	Can complicate the transition to clinical trials due to the risk of infection
Vectors or plasmids	APCs	-
Individual peptides	Peptide-HLA multimer	Can lead escape mutants and is limited to patients with specific HLA types.
Whole proteins	APCs, irradiated PBMCs ^{*/**}	Protein must be universally expressed and immunogenic (e.g. pp65 or EBNA-1).
Peptide mix (Overlapping peptides)	APCs, Artificial APC (e.g. KATpx, K562) Irradiated PBMCs ^{*/**}	Peptide libraries covering complete protein sequences of target viral antigens. GMP format. It has been validated in numerous preclinical and clinical studies.

*Recently, irradiated PBMCs have been used as APCs because they include lymphocytes (T cells, B cells, and NK cells), monocytes, and dendritic cells. PBMCs are irradiated, to prevent their proliferation but remain viable and capable of producing cytokines and other soluble factors, which can also act as a feeder's layer to provide metabolites supporting cell growth.^{82,83} **They may present antigens under special conditions but are not considered APC. LCLs, Lymphoblastoid cell lines. Table compiled the information obtained from Bollard & Heslop. *Blood*. (2016).⁸¹

Manufacturing techniques

Direct selection allows for the rapid production of VST. This method involves the direct selection of VSTs from the donor's peripheral blood using (1) peptide-HLA multimers (2) cytokine (IFN- γ)-capture system (3) surface markers or (4) magnetic enrichment.⁷⁶ Peptide-HLA multimers enable the isolation of T cells based on the ability of their receptor to bind to a complex of recombinant HLA class I and class II molecules loaded with synthetic peptides. However,

multimers are more easily produced with HLA class I antigens, which may limit the duration of an immune response after adoptive transfer in the absence of CD4⁺ T cells. This approach is HLA-restricted and requires knowledge of which epitopes are immunodominant. Additionally, the donor must have a high frequency of T cells specific to the peptide used.⁸¹ The Cytokine (IFN- γ)-capture system is a rapid method (12-24 hours) for isolating CD4⁺ and CD8⁺ antigen-specific T cells in an HLA-unrestricted manner. This method is based on activation-induced release of IFN- γ after stimulation with viral antigens. Populations of IFN- γ -secreting cells are then captured by labeling them with an anti-IFN- γ monoclonal antibody conjugated to a leukocyte-specific (CD45) antibody, followed by magnetic selection.^{81,84-87} A limitation or challenge of this strategy is that it requires a critical number of cells circulating, in order to detect and collect clinically relevant T cell numbers. Therefore, this method is usually limited to the antigens that induce a large memory T cell pool.⁸⁸ Other approaches involve isolating specific T cells based on surface marker molecules (CD137 (4-1BB) and CD154 (CD40L) or enrichment using magnetic column.⁷⁵ Additionally, the cost of equipment and reagents for direct selection strategies is very high.

Ex vivo expansion is a widely used technique for generating VSTs. Initially, this process involved complex protocols using defined immunogenic antigens (e.g. virus lysates) and APCs (e.g. LCL lines), requiring a long manufacturing time of approximately 3 months.^{75,89} To address these challenges, the strategy has been refined over the past two decades to reduce production time (**short/rapid *ex vivo* culture**) and cost while optimizing *in vivo* function. The update approach involves stimulating PBMCs with peptide libraries representing viral antigens of interest. After a single stimulation, virus-reactive T cell populations are selectively amplified and expanded in culture for 10 to 14 days in the presence of pro-survival cytokines.⁹⁰ The final VST product contains a high number of polyclonal CD4⁺ and CD8⁺ T cells capable of targeting one or multiple viruses simultaneously.^{91,92} This method requires only a small volume of donor blood and can produce effective T cells even from low levels of circulating VST and unexposed sources.^{75,93,94} Additionally, these cells exhibit minimal alloreactivity and GvHD.⁷⁹

Table 6 summarizes the advantages and disadvantages of 3 of the most common and rapid expansion strategies used.

Table 6. Advantages and disadvantages of different rapid culture techniques

Method	Advantages	Disadvantages
Short <i>ex vivo</i> culture	Expand low frequency VSTs; not restricted by HLA type	Still 10-14 days culture period; not yet available when donor seronegative
Multimer selection	Rapid manufacturing; already in late phase trials	Restricted to certain HLA types; few class II multimers available; not available when donor seronegative or has low frequency of circulating T cells specific for the peptides
Cytokine IFN-γ capture system	Rapid manufacturing; not restricted to certain HLA types; will select polyclonal T cells recognizing multiple epitopes	Large volume of blood required; will not select T cells producing other cytokines; may still require <i>ex vivo</i> culture to expand; not available when donor seronegative

Adapted from Bollard & Heslop. *Blood*. (2016).⁸¹

7.2. VSTs donor sources

VSTs can be sourced from patient-derived (autologous) and healthy seropositive donors (allogenic). This second group can be either "donor-derived" (from the original HSCT donor) or "third-party" (from an unrelated donor).^{74,90}

- 1. Donor-Derived VSTs:** High HLA matching with the recipient, which improves viral antigen recognition, enhances antiviral activity, promotes VST persistence, and reduces the risk of GvHD.^{74,90,95}
- 2. Third-Party VSTs:** Generally available "*off the shelf*" and suitable for SOT recipients who are typically limited to third-party sources. They are chosen based on shared HLA alleles and overall, HLA match, but usually match fewer HLA alleles (4/10) compared to donor-derived VSTs.^{74,90,96-98} Currently, there are registries for selecting potential donors of allogeneic T cells:
 - **AlloCELL**, established at Hannover Medical School over the past three years, this registry compiles screening results for the specific memory T cell repertoire of potential donors in response to CMV, EBV, AdV, and now extends to include BK and HHV-6. Its aim is to accelerate the development and application of adoptive T cell therapy. The registry was created to provide personalized antiviral T cell immunotherapies for patients in need, identify suitable T cell donors, and monitor pathogen-specific T cell programs both before and after T cell therapy (<https://www.allocell.org/>).^{84,99}
 - **ReDoCel**, was started in 2017 and established between 2019 and 2023 by the Banc de Sang i Teixits of Catalonia and the Centre de Transfusió de la Comunitat Valenciana, Spain. This registry includes 597 healthy donors from Catalonia and Valencia, all of whom are HLA-typed and screened for CMV and EBV. Nearly 65%

of donors were CMV-seropositive, while less than 5% were EBV-seronegative. Of the CMV-seropositive donors, 98% were also EBV-seropositive. This registry facilitates the availability and the selection of the optimal donor to produce advanced cell therapies that use allogenic sources of lymphocytes.¹⁰⁰

Another donor source that has emerged as an effective alternative for adoptive transfer of *ex vivo*-expanded VSTs is **umbilical cord blood (CB)**.¹⁰¹ Although CB donors have not been previously exposed to the virus, T cells obtained have shown the ability to recognize viral epitopes with efficacy comparable to that of T cells from seropositive donors. The process, now optimized to be completed in under 30 days and compliant with GMP standards, has been validated in clinical trials, demonstrating that CB T cells can be effectively expanded and persist long-term.^{93,102} Recently, BK virus has been added to the CB-derived VST product in an ongoing clinical study (NCT03594981).^{75,103}

7.3. Generation of Third-party “off the shelf” banks for VSTs

Over the years, the idea and interest in the use of banked-VSTs have grown significantly. This refers to cryopreserved VSTs that can be expanded exponentially *in vitro* from the blood of selected healthy donors. Banking-VSTs can be characterized by phenotype, specificity, and function, and are immediately available for clinical use to treat one or more patients (**Figure 11**).^{104–108}

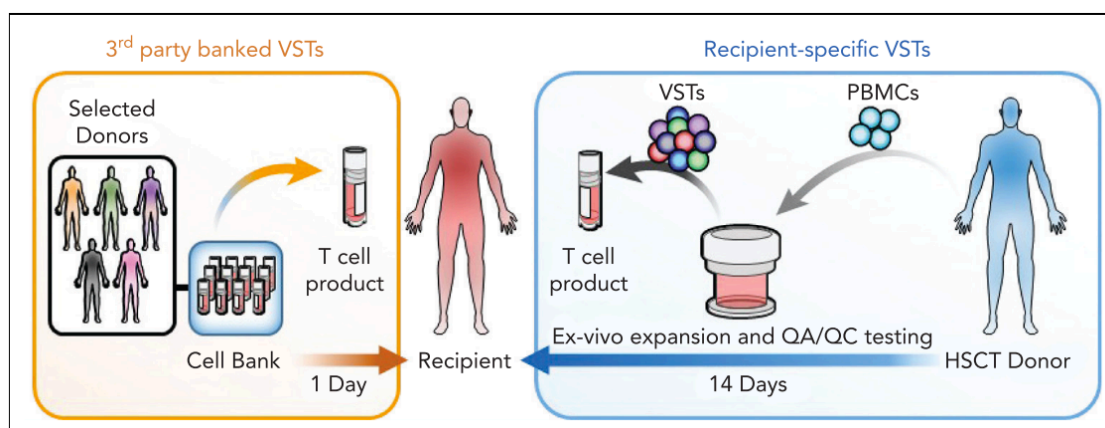


Figure 11. Comparison of Banked-VSTs strategy and Recipient-specific VSTs.

Banking-VSTs are expanded *in vitro* by a limited number of donors and stored in a cryopreserved bank, ready to be thawed and used immediately for multiple recipients. In contrast, recipient-specific VSTs, derived from the HSCT donor, take up to 4 weeks or more to manufacture and undergo QA/QC testing, and are intended for use with a single recipient only. Figure obtained from Quach et al. *Blood*. (2023).⁷⁴

Nevertheless, the use of banked-VSTs is not without limitations. Key challenges of allogeneic therapies include HLA restriction and alloreactivity. For effective infusion, VSTs must recognize

viral peptides through “shared” HLA alleles. Given that a specific VST line is unlikely to recognize viral peptides across all 12 possible HLA class I and II surface alleles, it is essential to identify the HLA antigens presented by the viral peptides recognized by each VST line. Consequently, VST banks should include a diverse range of products from donors with various HLA types to adequately cover the HLA profiles of the recipient population. Additionally, HLA molecules are highly immunogenic, which can lead to GvHD and allogeneic cells may be rapidly rejected if administered to HLA-mismatched hosts.^{74,81} However, the TCR repertoire of VSTs is smaller compared to CD3-activated T cells typically used for CAR-T cell generation, which helps reduce alloreactivity and contributes to the lower incidence of GvHD reported in multiple trials. This underscores the suitability of VSTs as a safe, commercially available cell therapy and supports the development of VST banks.^{74,109}

In HSCT settings, Leen et al. (2013) banked-multivirus-specific T cells, targeting CMV, AdV and EBV, achieving complete or partial responses in 74% of patients.¹⁰⁸ In 2017, Tzannou et al. infused a single dose of 2×10^7 banked-VSTs/m² (multivirus-specific T cells targeting CMV, AdV, BKV, HHV-6 and EBV), which resulted in a cumulative response rate of 92% and rarely induced GvHD (<10% de novo). However, not all lines recognized all five viruses, with only 59% of them identifying at least three.¹¹⁰ In SOT settings, Haque et al. (2002) observed that the patients require multiple infusions of partially HLA-matched banked-VSTs to result in complete responses for the treatment EBV-associated post-transplant lymphoproliferative disease (PTLD).¹¹¹ Regarding the persistence of banked-VSTs, persistence using genetic markers has not yet been confirmed.⁷⁴ Nevertheless, the TCR- β of VSTs can be sequenced to classify and track VST populations in patients. Keller and colleagues sequenced the TCR- β in PBMCs and VSTs products from 12 patients who received CMV/EBVST after HSCT to prevent or treat viral infections. After infusion, the TCR- β repertoire in 8 patients showed an expansion of CMV/EBV-specific clonotypes present in the administered VSTs within 3 months. 7 of these patients achieved complete responses against the targeted virus. In responding patients, CMV/EBV-specific clonotypes represented a median of 0.03% of the TCR- β repertoire at 6 months, 0.07% at 12 months, and remained detectable up to 4 years after infusion.¹¹² These findings demonstrate that allogeneic VSTs can persist *in vivo* and therefore can be tracked by TCR- β sequencing. Also, it suggests that the diversity of the T cell receptor repertoire may be critical for the control of CMV/BEV reactivation after HSCT.¹¹²

Another effective and safe banking strategy, developed by Rut Mora and colleagues at the Banc de Sang i Teixits, involves cryopreserving whole blood as the starting material and adapting a T cell activation and expansion protocol to generate VSTs. This approach provides an antiviral

therapeutic option that can be available on the market. The resulting VSTs can be stored for later use, in particular maintaining viability and antigen specificity after cryopreservation.¹¹³

7.4. VST clinical efficacy and safety

VSTs have proven to be highly effective against various viruses, such as CMV, EBV, AdV, and BKV, particularly in immunocompromised patients, such as those who have undergone organ or stem cell transplants.⁹⁰ In HSCT settings, clinical trials have shown that responses observed after VSTs infusions can persist for several months and even years, providing long-term antiviral surveillance. Heslop et al. (2010) demonstrated that, after infusing EBV-specific T cells (EBVSTs) combined with a genetic marking component into patients to prevent or treat EBV-PTLD, the EBVSTs persisted for up to 12-15 years. Additionally, 79 patients were still alive after 3 to 15 years of follow-up⁹⁵. Similarly, various studies using different manufacturing methods and VST sources have reported high rates of complete response, as shown in **(Table 7)**. In cases where a complete response was not achieved, a high rate of partial response was observed. Prockop et al. (2020) have noted that, in some cases, it may be necessary to administer third-party VSTs more frequently to achieve the same response seen with donor-derived VSTs.⁹⁶ In SOT recipients, autologous VSTs expanded *ex vivo* have been successfully used to treat CMV infections and EBV-related PTLD. However, using autologous VSTs is often impractical due to lengthy manufacturing and quality control processes. A key challenge with third-party VSTs in SOT patients is their higher level of immunocompetence compared to HSCT recipients, leading to limited expansion and persistence of the VSTs. Despite these challenges, most CMV infections and EBV-related PTLD cases after SOT have responded well to VST therapy.⁹⁰ Regarding safety, VST infusions are generally well tolerated, with infusion-related adverse reactions being rare and limited to mild, transient symptoms like fever, chills, headache, myalgia, and fatigue. There have been no reported cases of cytokine release syndrome associated with VST administration, nor have any deaths been attributed to this therapy. The incidence of de novo GvHD attributable to this therapy is significantly low, below 10%. This is likely due to the fact that VST products predominantly consist of cells with a central memory and effector phenotype, which are less likely to become alloreactive compared to naïve T cells. Consequently, de novo GvHD cases are typically mild (grade 1), primarily affecting the skin, and resolve with topical treatment.^{95,97,98,110,114,115}

Table 7. Clinical experiences using VSTs therapy in HSCT

Virus	Study/year	Method	Source	N ^a	CR	PR	aGvHD
EBV	(S. Prockop et al., 2020) ⁹⁶	EVE	3P	33	19 (58%)	3 (9%)	1 (3%)
	(Dobrovina et al., 2012) ¹¹⁶	EVE	Donor	12	8 (73%)	0 (0%)	0 (0%)
	(Dobrovina et al., 2012) ¹¹⁶	EVE	3P	5	4 (80%)	0 (0%)	0 (0%)
	(Heslop et al., 2010) ⁹⁵	EVE	Donor	13	11 (85%)	0 (0%)	1 (8%)
	(Icheva et al., 2013) ¹¹⁷	GC	Donor	10	7 (70%)	0 (0%)	4 (40%)
CMV	(A. M. Leen et al., 2013) ¹⁰⁸	EVE	3P	9	2 (22%)	4 (44%)	1 (11%)
	(S. E. Prockop et al., 2023) ¹¹⁸	EVE	3P	59	20 (34%)	18 (31%)	1 (2%)
	(Pei et al., 2017) ¹¹⁹	EVE	Donor	32	27 (84%)	5 (16%)	1 (3%)
	(Withers et al., 2017) ¹⁰⁵	EVE	3P	28	22 (79%)	5 (18%)	2 (7%)
	(Jiang et al., 2022) ¹²⁰	EVE	3P	27	25 (93%)	2 (7%)	4 (15%)
ADV	(Pfeiffer et al., 2023) ⁹⁸	EVE	3P	24	11 (46%)	12 (50%)	4 (17%)
	(Feucht et al., 2015) ¹²¹	GC	Donor	30	18 (60%)	3 (10%)	2 (7%)
	(Rubinstein et al., 2021) ¹²²	EVE	3P	19	8 (42%)	6 (32%)	1 (5%)
	(Rubinstein et al., 2021) ¹²²	EVE	Donor	7	6 (86%)	1 (14%)	0 (0%)
	(A. M. Leen et al., 2013) ¹⁰⁸	EVE	3P	17	7 (41%)	7 (41%)	3 (18%)
BKV	(Pfeiffer et al., 2023) ⁹⁸	EVE	3P	12	6 (50%)	4 (33%)	2 (17%)
	(Creidy et al., 2016) ¹²³	GC	Donor	6	3 (50%)	0 (0%)	0 (0%)
	(Olson et al., 2021) ⁹⁷	EVE	3P	57	33 (58%)	10 (18%)	2 (4%)
	(Nelson et al., 2020) ¹¹⁴	EVE	3P	24	18 (75%)	4 (17%)	1 (4%)
	(Nelson et al., 2020) ¹¹⁴	EVE	Donor	14	7 (50%)	4 (29%)	0 (0%)
	(Pfeiffer et al., 2023) ⁹⁸	EVE	3P	27	0 (0%)	27 (100%)	8 (30%)
	(Papadopoulou et al., 2014) ⁹¹	EVE	Donor	6	4 (67%)	1 (17%)	0 (0%)

3P, third-party; CR, complete response; EVE, *ex vivo* expansion; GC, gamma capture (IFN- γ); PR, partial response; aGvHD, acute graft-versus-host disease N^a, Evaluable patients. Adapted from Green et al. *Journal of the Pediatric Infectious Diseases Society*. (2024).⁹⁰

There are several studies and clinical evidence against different viruses such as CMV, AdV, BKV, JCV and EBV. However, from now on, we will only focus on the evidence for EBV, since it is the virus of interest in this doctoral thesis.

8. EBV-specific T cells (EBVSTs)

8.1. EBV or Human herpesvirus 4 (HHV-4)

It is a member of the gamma herpesvirus family. It was discovered in 1964 associated to Burkitt lymphoma and later was associated with other types of B-cell lymphoma, including HL, NHL in posttransplant patients, HIV-infected individuals, T cell lymphoma, NK/T cell lymphoma, epithelial cancers including nasopharyngeal carcinoma and a subset of gastric cancers. In addition, EBV is linked with non-malignant diseases including infectious mononucleosis, oral hairy leukoplakia, system lupus erythematosus and multiple sclerosis.¹²⁴

The prevalence of EBV in the human population is over 95%. The first infection is usually asymptomatic and occurs at an early age (childhood). Transmission occurs primarily through saliva but can also be through breast milk or body fluids, after allogeneic-HSCT or organ transplantation. EBV establishes lifelong persistence in the human host by infecting B cells and residing in memory B cells in healthy individuals, where it remains asymptomatic and does not cause disease. However, both intrinsic factors (e.g. mutations and genetic deficiencies) and extrinsic factors (e.g. immunosuppression, HIV infection, and a diet rich in salted or canned fish) can trigger the development of EBV-associated cancers.¹²⁵

The EBV genome is a linear, double-stranded DNA molecule, approximately 172 kb, which encodes more than 85 genes. EBV has a complex life cycle, with two different replications, depending on the stage of infection: the latency phase and the lytic phase.^{126,127}

During the **latent phase**, EBV remains inactive within the host's cells. The virus genome resides in the nucleus as a circular episome attached to the host chromatin by the viral protein EBNA-1. Only a small fraction of the viral genes is expressed. The expression pattern of latent genes (latency 0, I, II and III) varies depending on the type of infected cell and environmental conditions (**Figure 12**).¹²⁷ In this stage, the virus uses the host's DNA replication machinery to passively replicate its genome during cell division. Latency in B cells can be established through direct infection of memory B cells or through infection of naïve B cells, which then become memory B cells by passing through the germinal center (GC) of lymph nodes.¹²⁶ Latency allows EBV to establish a lifelong infection in the host, with only sporadic episodes of reactivation.¹²⁸

In the **lytic phase**, EBV reactivates and produces new viral particles. All viral genes are expressed during this phase. A complete lytic gene expression program is initiated that includes genes responsible for viral DNA replication, capsid assembly, and virus release. The virus actively replicates its genome. New viral particles are assembled and released to infect new cells. Lytic replication usually results in the lysis of the host cell.^{124,125,127}

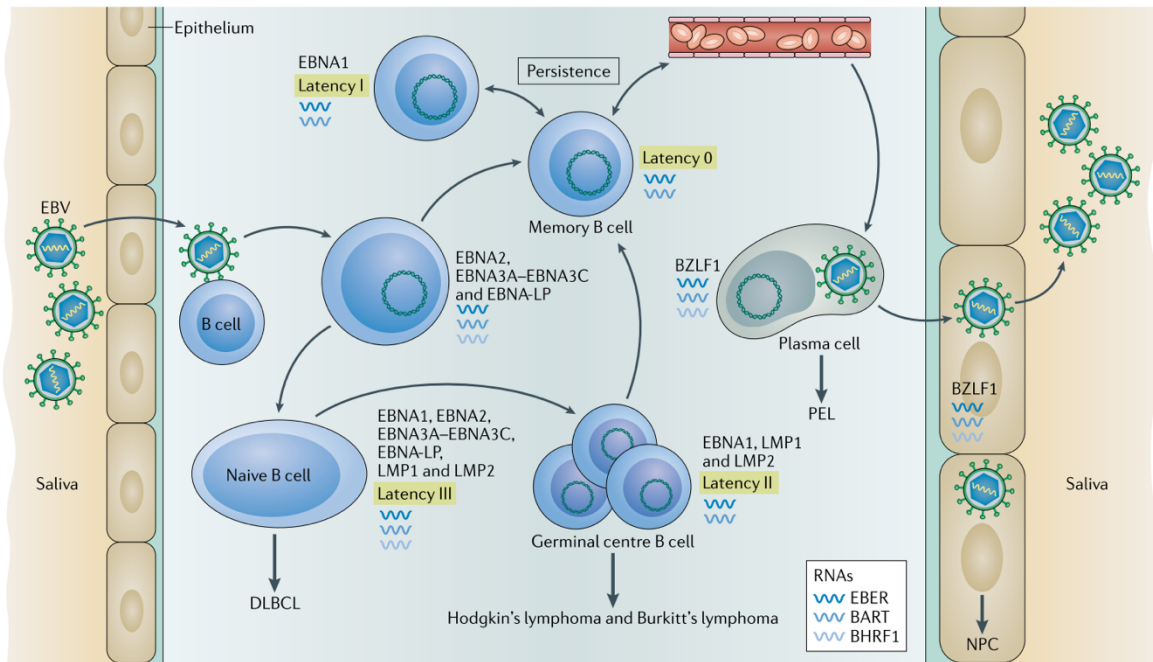


Figure 12. Virus latent infection in B lymphocytes.

EBV persists in circulating memory B cells without viral protein expression (latency 0). During homeostatic proliferation of these memory B cells, EBNA1 is transiently expressed. EBV transmitted via saliva establishes a primary lytic replication in the oropharyngeal mucosal epithelium, infecting B cells. This infection leads to EBNA2-dependent proliferation of infected cells. Infected memory B cells may differentiate directly into latency 0 after infection. Alternatively, EBV drives naive B cells into full latency III transformation (during which EBNA1, EBNA2, EBNA3A–EBNA3C, EBNA-LP, LMP1 and LMP2 are expressed) and this activation leads to their differentiation via latency II-expressing germinal center B cells (in which EBNA1, LMP1 and LMP2 are expressed) to latency 0 memory B cells. This germinal center differentiation pathway is thought to provide premalignant precursors of the EBV-DLBCL, Hodgkin's lymphoma and Burkitt's lymphoma. From circulating memory B cells, EBV reactivates lytic replication upon plasma cell differentiation and elevated lytic EBV replication can also be found in the EBV-associated plasmacytoma primary effusion lymphoma (PEL). This lytic reactivation most likely allows epithelial cell infection from the basolateral side for efficient shedding into the saliva and virus transmission. This epithelial cell infection gives rise to EBV-associated carcinomas, for example nasopharyngeal carcinoma (NPC). Expression of the viral non-coding RNAs (EBV- encoded small RNAs (EBERs), BART and BHRF1 microRNAs) is also present in the cycle. Figure obtained from Münz. *Nature Reviews Microbiology*. (2019).¹²⁷

The viral proteins of EBV can be categorized into nuclear antigens, latent membrane antigens, and functional small non-coding RNAs. Each viral antigen is associated with a diverse variety of malignant neoplasms, which exhibit three general patterns of latent gene expression (I, II, III), with type III latency the most immunogenic (**Figure 13** and **Table 8**).¹²⁹

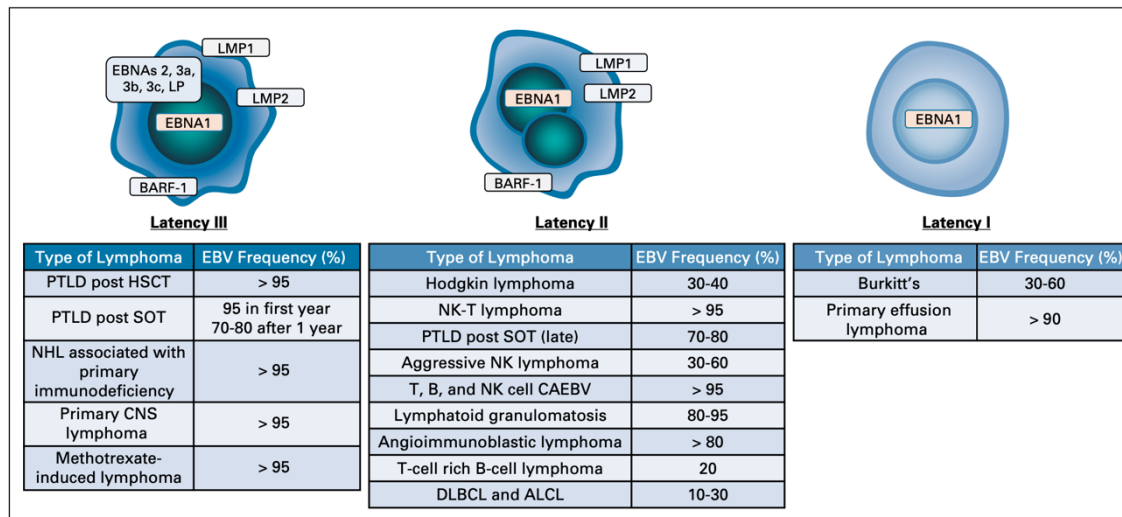


Figure 13. Latency states and frequency of EBV in different types of lymphomas.

Type 3 latency is the most immunogenic, as it expresses all latency-associated proteins that lead to B-cell transformation. This type is typically seen in lymphomas in individuals with severe immunosuppression, such as after stem cell transplantation. Type 2 latency, found in some Hodgkin and non-Hodgkin lymphomas, expresses EBV nuclear antigen 1 (EBNA1), latent membrane protein 1 (LMP1), and LMP2, and has moderate immunogenicity. Burkitt's lymphoma exhibits type 1 latency, expressing only EBNA1, making it less responsive to EBV-specific T cells. Additionally, there can be transitions between latency states, with changes in the expression of latency and lytic genes. PTLD, post-transplant lymphoproliferative disorder; CNS, Central nervous system; CAEBV, Chronic active Epstein–Barr virus; ALCL, Anaplastic large cell lymphoma. Figure obtained from Heslop, Sharma, & Rooney. *American Society of Clinical Oncology*. (2021).¹²⁹

Table 8. Summarize of viral proteins of EBV

Viral proteins	Function	Latency type	EBV-associated disease
EBV-Encoded Nuclear Antigens (EBNAs)			
EBNA-1	<ul style="list-style-type: none"> Essential for EBV double stranded DNA maintenance and replication Enhances cell survival Inhibit apoptosis Induces B cell neoplasia Regulation of gene expression Avoids CTL surveillance Mimics the central nervous system protein glial cell adhesion molecule in multiple sclerosis. 	I II III	Burkitt lymphoma Gastric carcinoma Hodgkin lymphoma NK/T cell lymphoma Nasopharyngeal carcinoma DLBCL HIV-associated lymphomas PTLD
EBNA-2	<ul style="list-style-type: none"> Transcriptional activation of viral and cellular genes Rewires host gene regulatory programs in autoimmune disease Functionally replaces the intracellular region of Notch receptor 	III	DLBCL HIV-associated lymphomas PTLD
EBNA-LP	<ul style="list-style-type: none"> Assists EBNA-2 mediated transcriptional activation Suppresses the innate cell response to viral DNA 	III	DLBCL HIV-associated lymphomas PTLD
EBNA-3A/ EBNA-3C	<ul style="list-style-type: none"> Required for efficient transformation of B cells <i>in vitro</i> Mediate inhibition of various cyclin-dependent kinase inhibitors Epigenetically control gene transcriptions 	III	DLBCL HIV-associated lymphomas PTLD
EBNA-3B	<ul style="list-style-type: none"> Functions as a tumor suppressor 	III	
EBV-Encoded Latent Membrane Antigens			
LMP1	<ul style="list-style-type: none"> The main transforming antigen of EBV Mimics CD40 signaling Prevents p53-mediated apoptosis Prompts cell proliferation Activates signaling pathways that contribute to invasion and metastasis Escape from immune surveillance 	II III	Hodgkin lymphoma NK/T cell lymphoma Nasopharyngeal carcinoma HIV-associated lymphomas PTLD
LMP2A	<ul style="list-style-type: none"> Drives proliferation and survival of B cells by mimicking the BCR signaling Affects apoptosis and cell cycle checkpoints Enhances adhesion and motility Circumvents the innate immune response by attenuates signaling (IFN receptors type I and II) 	II III	Hodgkin lymphoma NK/T cell lymphoma Nasopharyngeal carcinoma HIV-associated lymphomas PTLD
LMP2B	<ul style="list-style-type: none"> Modulates the effects of LMP2A on BCR function 	II III	Hodgkin lymphoma NK/T cell lymphoma Nasopharyngeal carcinoma HIV-associated lymphomas PTLD

Table 8 (continued)

EBV-Encoded Functional Small Non-Coding RNAs			
EBERs (EBER1 and EBER2)	• Maintenance of latency and transformation		Healthy individuals Burkitt lymphoma
	• They can increase tumorigenicity	0	Gastric carcinoma
	• Promote cell survival	I	Hodgkin lymphoma
	• Induce interleukin-10 (IL-10) expression in Burkitt lymphoma cell lines	II	NK/T cell lymphoma
		III	Nasopharyngeal carcinoma DLBCL HIV-associated lymphomas PTLD
BHRF1 miRNAs	• Modulation of Apoptosis		DLBCL
	• Regulation of the Immune Response		HIV-associated lymphomas PTLD
	• Promotion of Cellular Proliferation		
	• Interaction with Cellular Signaling Pathways	II/III	
	• Support for Viral Latency • Contribution to Oncogenesis		
BARTs miRNAs	• Regulation of gene expression		Healthy individuals
	• Immune system evasion		Burkitt lymphoma
	• Promotion of cellular survival and proliferation	0	Gastric carcinoma
	• Contribution to oncogenesis	I	Hodgkin lymphoma
	• Modulation of the viral microenvironment	II III	NK/T cell lymphoma Nasopharyngeal carcinoma DLBCL HIV-associated lymphomas PTLD

Adapted from Damania et al. *Cell*. (2022) and H. Yu & Robertson. *Viruses* (2023).^{124,125}

8.2. Clinical evidence of EBVSTs immunotherapy for treating lymphomas

Latency III - Post-transplant lymphoproliferative disease (PTLD)

As mentioned in sections 7.3 and 7.4, VSTs have demonstrated potent activity against various viruses, including EBV. Consequently, lymphomas associated with the EBV, by expressing viral antigens, become a potential target for T cell immunotherapy. This makes EBVSTs not only powerful antiviral agents but also effective in antitumor activity. This interest in exploring the antitumor potential of EBVSTs has led to a series of studies evaluating the adoptive transfer of EBVSTs in the treatment of EBV-associated lymphomas.

To mitigate the risk of alloreactivity in infusion of unmanipulated donor T cells, Rooney and colleagues established in 1996-1998 the first EBVSTs. The study consisted in generating *ex vivo* EBVSTs by repetitive stimulation of donor-derived PBMCs with irradiated autologous EBV-transformed B cell lines for the treatment of EBV-associated PTL. In 26 patients, gene marking showed that these LCL-stimulated EBVSTs expanded significantly after infusion, could target disease sites, persist for up to 10 years, and displayed memory cell characteristics by contracting and re-expanding in response to viral reactivation.¹³⁰

In 2009, a multi-institutional and long-term study where 114 HSCT patients were candidates for EBVSTs therapy to prevent or treat PTLD. None of the 101 patients who received prophylactic infusions developed PTLD, and 11 of 13 patients with active disease achieved sustained remission. No alloreactivity or de novo GvHD was observed, and the only significant adverse effect was localized swelling during the therapeutic response in four patients with bulky active disease. In one non-responding patient, a tumor evasion mechanism was discovered, where the infused EBVSTs were biased towards A11-restricted epitopes, allowing tumor cells with a deletion in EBNA-3B to proliferate.¹¹⁵

Researches at Memorial Sloan Kettering Cancer reported similar responses to LCL-induced EBVSTs, with an overall response rate of 68% and no symptoms of GvHD in a study of 47 patients with EBV-PTLD. However, in some cases, restricted specificity of the infused line or antigenic differences between the EBV strain causing PTLD and the B95-8 strain allowed tumor evasion. In such cases, using EBVST lines from another donor should be considered.¹¹⁶ Other studies with fewer patients were performed and supported the potency and safety of EBVSTs cells obtained by LCLs.¹³¹

At the end of 2022, the European Commission approved the commercialization of Tabelecleucel (Ebvallo[®]), an allogeneic T cell immunotherapy specifically targeting EBV. It is indicated as a monotherapy for adult and pediatric patients aged two years and older with relapsed or refractory EBV-positive post-transplant lymphoproliferative disorder (EBV + PTLD) who have received at least one prior treatment. For patients with solid organ transplants, prior treatment includes chemotherapy unless deemed inappropriate. It is the first “*off-the-shelf*”, allogeneic, EBV-specific T cell immunotherapy to receive approval for this disorder. EBVSTs are produced from PBMCs collected from healthy, EBV-seropositive donors. Donor B cells were infected with EBV to produce EBV-transformed B-lymphoblastoid cell lines (EBV-BLCLs), which are capable of presenting a broad range of EBV antigens. After irradiation and extended culture with acyclovir, the EBV-BLCLs were co-cultured with T cells from the same donor to stimulate a polyclonal T cell population. The ALLELE trial is currently underway. It is a global, multicenter, single-arm, open-label, phase 3 trial of Tabelecleucel in patients with relapsed or refractory EBV-positive post-transplant lymphoproliferative disease following HSCT or SOT.¹³²

Although these studies showed impressive response rates, the manufacturing process took up to 12 weeks or less than 30 days in the case of Tabelecleucel, limiting the broader application of these donor-specific products. Furthermore, advancements in manufacturing have simplified the production and development of both autologous and allogeneic EBVSTs (donor-derived or third-party donor), while also increasing the number of viruses targeted (multi-VST therapy) by the

resulting product. An example of this multi-VST therapy is Posoleucel (AlloVir), an allogeneic (partially HLA-matched) for direct use against six common viral infections in allogeneic-HSCT recipients: AdV, BKV, CMV, EBV, HH6 JCV.⁹⁸ Consequently, various APCs and antigen sources were evaluated (**Figure 14**), to reduce manufacturing time to 10 days while maintaining consistent outcomes in trials.¹²⁹

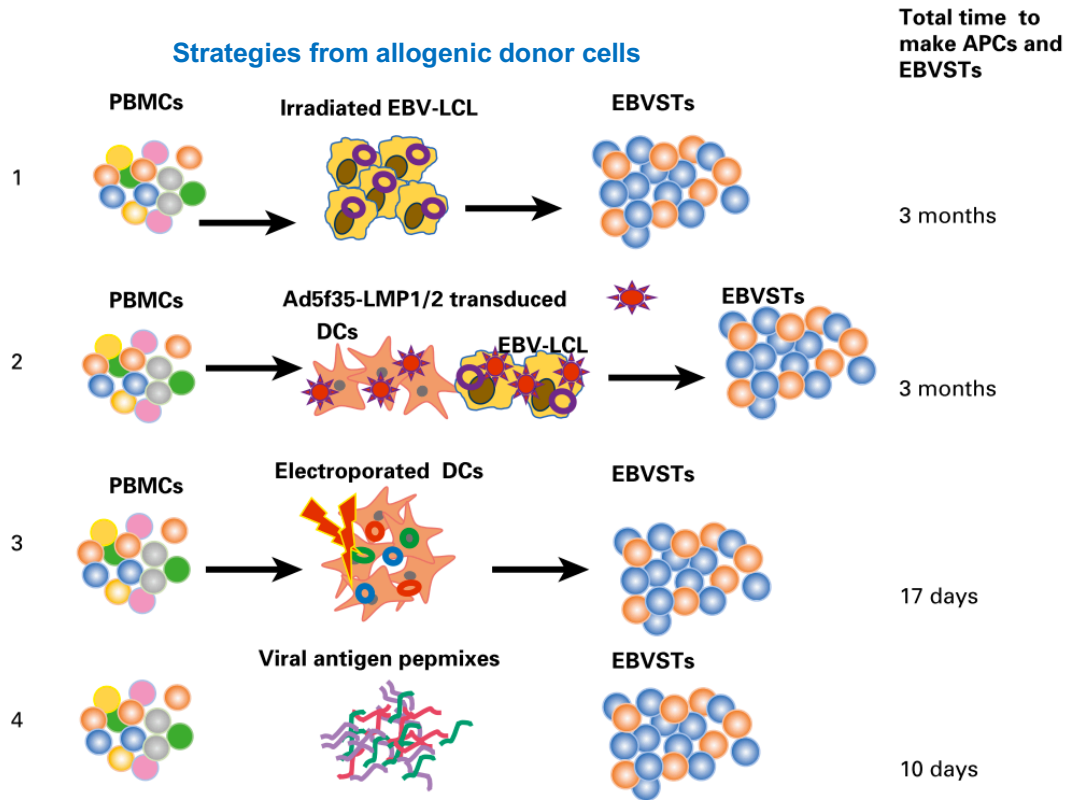


Figure 14. Advancement of methods for producing EBVSTs.

(1) Early clinical studies utilized EBV-transformed B lymphoblastoid cell lines (LCLs) as antigen-presenting cells (APCs). Later, (2) adenovirus vectors were used to introduce Cytomegalovirus (CMV) antigens into dendritic cells (DCs) for initial stimulation, followed by stimulation with Adenovirus (Ad)-LMP1/2-transduced LCLs. This process took at least 6 weeks for LCL production and 4 weeks for expanding EBVSTs, leading to extended manufacturing times (3) The use of DNA plasmids for electroporation into DCs reduced the manufacturing time to 17 days (4) Further reduction to 10 days was achieved by pulsing PBMCs with overlapping peptide libraries and using optimized cytokines for VST expansion. Figure obtained from Heslop, Sharma & Rooney. *Clinical Oncology*. (2021).¹²⁹

Latency II – Hodgkin and Non-Hodgkin lymphomas

The immunogenicity of the antigens in this latency step is less. In trials using EBVSTs enriched for LMP1 and LMP2 antigens, 28 out of 29 patients receiving these cells as prophylaxis remained in remission three years post-infusion. Additionally, 13 of 21 patients with chemo- and radiotherapy-resistant disease showed clinical responses, with 11 achieving complete remission. Many of these responding patients also exhibited epitope spreading, with increased T cells reacting to other tumor-associated antigens.¹³³ A separate study in South Korea demonstrated that

patients with extranodal NK/T lymphoma in remission after initial therapy who received autologous EBVSTs targeting LMP1/2a as adjunct therapy had a 100% overall survival rate and 90% progression-free survival at four years. These findings suggest that EBVSTs could be promising for type 2 latency diseases.¹³⁴ However, the manufacture of these autologous EBVSTs was time-consuming, taking over three months, which sometimes resulted in patients progressing during this period. Therefore, follow-up studies are trying to simplify the manufacture method (**Figure 14**). The use of donor-derived allogeneic EBVSTs has also been explored in patients who underwent allogeneic HSCT for type 2 latency lymphoma. Results were promising, with a 2-year overall survival rate of 80% for B-cell disease patients, and 50% for T cell disease patients, which is an improvement over historical survival rates in this high-risk group.¹³⁵

Latency I – Burkitt lymphomas

This type of latency tumor presents significant challenges for immunotherapy because they express only the minimally immunogenic EBNA-1 antigen. EBNA-1 has traditionally been considered immunologically inert due to its glycine-alanine repeat domain, which prevents its breakdown and presentation by the MHC.¹³⁶ However, recent findings have identified HLA class I and class II responses targeting EBNA-1, and EBNA1-directed T cells have shown success in treating type I latency PTLD.¹¹⁷

8.3. Banked EBVSTs

To increase the availability of EBVSTs, several groups developed banks of HLA-typed EBVST lines from normal donors. The first report of clinical activity for this product came from Haque et al., who created a bank of polyclonal LCL-induced VSTs and achieved complete responses in three of eight patients with PTLD after SOT.¹¹¹ A follow-up report involving 33 patients showed overall response rates of 64% at 5 weeks and 52% at 6 months, with the degree of HLA match identified as a predictive factor for response.¹³⁷

The Scottish National Blood Transfusion Service has licensed a smaller bank of EBVSTs from 25 donors¹³⁸ and recently processed 132 HLA matching requests and completed 61 allocation reviews.¹³⁹ Additionally, other centers have employed T cells targeting EBV and other viruses (multivirus-VSTs) to treat PTLD (**Table 9**). One concern with using banked cells is the potential presence of residual alloreactive cells, which led to GvHD. However, as indicated in **Table 9**, clinical trials involving banked EBVSTs have shown a low incidence of GvHD. Another issue is that the recipient's immune system may recognize alloantigen's on the infused EBVSTs, which can limit their persistence. Research has demonstrated that banked T cells generally do not persist as long as patient-specific cells, leading to the inclusion of repeated dosing in several treatment regimens to address this challenge.^{96,129}

Table 9. Donor-Banked EBVSTs to treat EBV lymphomas

Cell Type	Patients	CR/PR	%ORR	GvHD	References
Monovirus EBVSTs LCL-induced EBVST					
LCL-induced EBVST	2 PTLD post SOT	2	75	None	(Sun, et al., 2002) ¹⁴⁰
	2 nontransplant	1			
LCL-induced EBVST	33 PTLD post HSCT or SOT	17	52	None	(Haque et al., 2007) ¹³⁷
LCL-induced EBVST	10	8	80	None	(Vickers et al., 2014) ¹³⁸
LCL-induced EBVST	11: 9 PTLD post HSCT or SOT, 2 nontransplant 4 4 PTLD post HSCT or SOT	4	44	None	(Gallot et al., 2014) ¹⁴¹
LCL-induced EBVST	4 PTLD post HSCT or SOT	1	25	1	(Naik et al., 2016) ¹⁴²
Pepmix-induced EBVST	2 PTLD post HSCT or SOT	1	50	None	(Naik et al., 2016) ¹⁴²
Multimer selected	1 PTLD post HSCT or SOT	1	100	None	(Uhlen et al., 2010) ¹⁴³
LCL-induced EBVST	10 PTLD post HSCT or SOT	8	100	None	(Chiou et al., 2018) ¹⁴⁴
LCL-induced EBVST	1 PTLD post HSCT or SOT	1	100	None	(Mika et al., 2019) ¹⁴⁵
LCL-induced EBVST	59: 28 PTLD post HSCT, 20 PTLD post SOT, 11 nontransplant	35	59	None	(Kazi et al., 2019) ¹³⁹
LCL-induced EBVST	46		63	1	(S. Prockop et al., 2020) ⁹⁶
	33 HCT	22(HCT)			
	13 SOT	7 (SOT)			
Multivirus-specific T cells that include EBV					
Transduced monocyte/LCL-induced trivirus VST	9 (treated for EBV) PTLD post HSCT	6	67	3	(A. M. Leen et al., 2013) ¹⁰⁸
Pepmix-induced multivirus VSTs	3 (treated for EBV) PTLD post HSCT	3	100	None	(Tzannou et al., 2017) ¹¹⁰
Pepmix-induced multivirus VSTs	1 (treated for EBV) NKT lymphoma relapse post HSCT	1	100	None	(Withers et al., 2017) ¹⁰⁵

Adapted from Heslop, Sharma & Rooney. *Clinical Oncology*. (2021).¹²⁹

With the promising results previously discussed for both CAR-T therapy and VSTs, specifically EBVSTs, combining these approaches could potentially enhance anti-cancer treatment. Furthermore, as EBV is associated with certain types of cancer, EBVSTs may be suitable hosts for CARs, as CAR-T cells could be directed through the endogenous TCR of EBVSTs, improving their persistence, proliferation and safety *in vivo*.¹⁴⁶

9. CAR-VSTs Therapy

The Baylor College of Medicine group has been one of the pioneers in researching and publishing studies on the fusion of these 2 therapies in recent years.

In 2013, Cruz et al. determined that VSTs against EBV, AdV and/or CMV transduced with CAR.CD19 and administered to patients with B cell neoplasms (4 B-cell ALL, 4 B-cell CLL) were: (i) safe without inducing GvHD, nor elevation of cytokines IL-6, TNF- α and IFN- γ , and (ii) capable of expanding, persisting and accumulating at disease sites.¹⁴⁷

In 2015, Sun et al. determined that carrying out transduction with CAR.GD2 in the VSTs against EBV on the third day of expansion was more efficient, increasing the expression of the CAR by stimulating the TCR of the VSTs and generating a central memory phenotype, causing a greater persistence, than when transducing on day 19.¹⁴⁸

In 2018, Omer et al. identified that the signal from the co-stimulatory molecule CD28 ζ of CAR.GD2 transduced in varicella zoster (VZV) or EBV VSTs promotes the expansion of VSTs, while 4-1BB ζ inhibits the proliferation and function of VSTs, but maintains antitumor efficacy. Therefore, CAR-containing signaling domains can enhance or diminish native TCR function.¹⁴⁹

Lapteva et al. (2019) identified that multi-virus-specific CD19-28 ζ CAR T cells expand rapidly in a virus load-dependent manner, and CAR T cell proliferation was significantly lower in patients without preexisting EBV, CMV, or adenovirus infection. Which shows that TCR stimulation from VSTs (EBV, CMV and AdV) and CAR.CD19 enhance the expansion of effector cells and the persistence of the CAR *in vivo*. Also, this study provides proof of the concept that CAR-T cells can be expanded via their native TCR without lymphodepletion.¹⁴⁶

Omer et al. (2022), demonstrated that by genetically modifying T cells with a costimulatory chimeric antigen receptor, can increase the activity of T cells expressing both native TCR (EBVSTs) and transgenic TCR (sTCR) and improve antitumor responses.⁷⁷

Quach et al. (2022), shows that CD30.CAR EBVSTs can be a safe and effective treatment for CD30⁺ lymphomas, and may avert GvHD and immediate rejection even after multiple infusions. Furthermore, they seek to improve the durability of responses and test whether CD30.CAR EBVST can be used as a platform for other "*off-the-shelf*" CAR-T cell therapies.¹⁵⁰

Currently, the clinical trial #NCT01109095 was completed, but there are 4 more in phase I (recruiting or active phase): #NCT00840853, #NCT03740256, #NCT00085930 and #NCT04288726 to determine the effectiveness of the aforementioned treatments.^{147,150–153}

Therefore, the dual stimulation approach between native TCR and CAR, may increase the efficacy and persistence of CAR-T cells, targeting multiple antigens and reducing the risk of immune escape. However, the challenge of this combination is to generate a product with high specificity, optimal fitness and stemness so that it can persist and proliferate *in vivo*.

10. Partial reprogramming T cells with Yamanaka Factors

In most adoptive cell therapies, increasing age and T cell differentiation are associated with reduced efficacy and reduced benefit in cancer patients. The capacity of T cells for self-renewal, proliferation, persistence, and antitumor activity is negatively affected by aging. Methods have been developed to dedifferentiate cells into induced pluripotent stem cells (iPSCs) that return to a stage of embryonic development characterized by epigenetic youth; however, the resulting cells lose their functional identity. Subsequent redifferentiation of iPSCs into the desired functional T cell phenotype is a complex and time-consuming process.¹⁵⁴ Therefore, recently, the idea of rejuvenating the age of the cells with partial reprogramming (by using Yamanaka factors) has emerged (**Figure 15**).

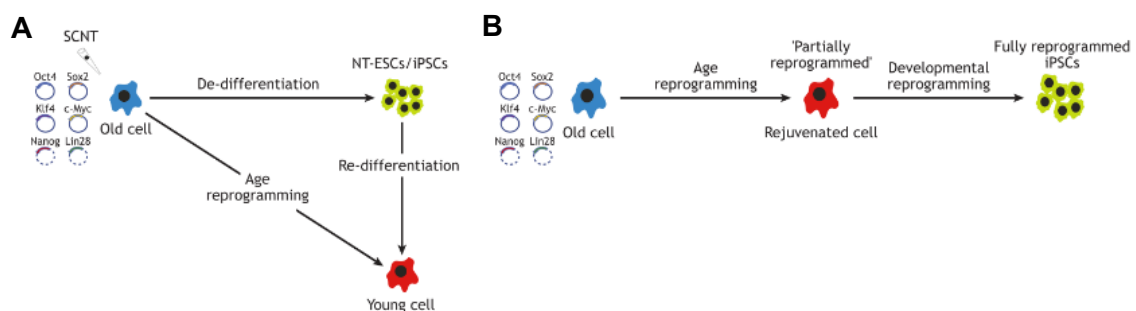


Figure 15. Age reprogramming.

(A) In a complete or nuclear reprogramming, where an old cell (blue) reaches a young one, using transcription factor (OCT4, SOX2, KLF4, c-MYC, NANOG AND LIN28), it is necessary through two phases: de-differentiation and re-differentiation. The first one produces induced pluripotent stem cells (iPSCs) and/or nuclear transfer-derived ESCs (NT-ESCs) (green). Second, yield rejuvenated cells (red). While, age reprogramming aims to skip the de-/re-differentiation cycle, rejuvenating old cells while retaining their specialized functions. (B) In partial reprogramming, the transcription factors are introduced into an old cell (blue), and during the transition to iPSCs (green), there is a stage where age-related markers are reduced or lost, indicating rejuvenation (red). This process conserves the specialized characteristics of the initial cells without becoming fully embryonic. Figure obtained from P. B. Singh & Zhakupova. *Development*. (2022).¹⁵⁴

10.1. Yamanaka factors

Shinya Yamanaka and Takahashi, screened 24 genes as candidates for factors that induce pluripotency in somatic cells. These factors are associated with the mouse embryonic state, by overexpressing them in fibroblasts cultured *in vitro*. In 2006, they select 4/24 transcription factors: OCT4, SOX2, Krüppel-Like factor 4 (KLF4) AND c-MYC (OSKM). This cocktail of four factors named “the Yamanaka factors” or “the Yamanaka cocktail”.^{155,156}

c-MYC, opens chromatin by binding to a methylated region. Additionally, it is involved in self-renewal processes and induces epigenetic changes that cause dedifferentiation or block cell differentiation. **OCT4** is specifically expressed in all pluripotent cells during embryogenesis and undifferentiated embryonic stem cells. It is required to establish and maintain cellular pluripotency. **SOX2** is important for the embryonic development of tissues and organs. It is also expressed in the late phases of embryonic development, especially in neural stem cells. SOX2 interacts with OCT4 to regulate the expression of genes such as NANOG, Fgf4, osteopontin, and lefty, which are involved in maintaining cellular pluripotency. **KLF4**, contains three tandem zinc fingers to interact directly with OCT4 and is expressed at sufficient levels to generate iPSCs.¹⁵⁷ This OKSM allows the reprogramming of murine fibroblasts into cells with properties like those of embryonic stem cells. In 2007, the experiment was successfully reproduced in human fibroblasts.^{155,156}

The original Yamanaka cocktail, consisting of OCT4, SOX2, KLF4, and c-MYC (OSKM), has been extensively used across various studies. However, in 2007, Yu et al. introduced two different factors, NANOG and LIN28.¹⁵⁸ **NANOG**, is a homeodomain transcription factor crucial in the earliest steps of embryogenesis. Interacts with OCT4 and SOX2, to self-renewal and pluripotency by regulating gene expression. High expression of *Nanog* can induce cellular self-renewal, but a low expression causes differentiation. **LIN28**, regulates development, pluripotency and cell growth through the modulation of miRNAs and other signaling pathways.¹⁵⁷

The combination of the 6 transcription factors (OKSMNL) demonstrate a better reprogramming efficiency and makes it possible to reprogram senescent cells and the oldest cells into iPSCs.¹⁵⁵

10.2. Cell source

To date, fibroblasts are the most widely used cell source for reprogramming, with very well-established protocols. Skin biopsy studies and melanocytes have also been studied, and more recently, studies with PBMCs, CD34⁺ hematopoietic stem cells, blood mononuclear cells (MNC) and T lymphocytes, where their reprogramming and culture can be complicated,¹⁵⁵ since the

efficiency of blood reprogramming (0.001-0.0002%) is approximately 10-50 times lower than that of human fibroblast reprogramming.¹⁵⁹

10.3. Reprogramming strategies

Reprogramming strategies, or “delivery strategies”, refers to the methods that introduce the reprogramming factors (Yamanaka factors) into the cells. These strategies can be classified into two categories: integrative and non-integrative systems. The **integrative systems** involve the integration of the vector's genetic material into the host genome. Among integrative systems are viral vectors (e.g. retroviruses and lentiviruses) and non-viral vectors (e.g. linear DNA and transposons). The **non-integrative systems** do not permanently integrate genetic material into the host cell's genome. This can be subclassified as non-integrating viral vectors (e.g. adenovirus and Sendai virus) and non-integrating non-viral vectors (e.g. episomal vectors, proteins, chemical molecules and RNA). **Table 10** shows the disadvantages and advantages of different reprogramming methods.¹⁶⁰

Table 10. Advantages and disadvantages of different reprogramming methods

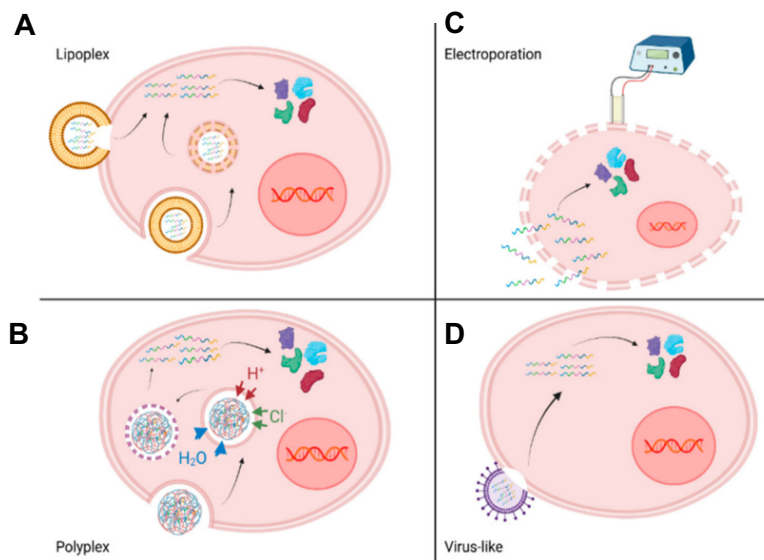
Method	Virus	Advantages	Disadvantages
Retrovirus	Yes	High efficiency	Risk of insertional mutagenesis, transgene reactivation and residual expression Risk of presence of viral particles Can only be used in dividing cells
Lentivirus	Yes	High efficiency Can be used in both dividing and non-dividing cells	Risk of insertional mutagenesis, transgene reactivation and residual expression Risk of presence of viral particles
Adenovirus	Yes	No integration/small risk of integration	Moderate efficiency Need for repeated transductions Risk of presence of viral particles
Sendai virus	Yes	High efficiency Non-transgene, no integration	Risk of presence of viral particles
Conventional and episomal plasmids	No	No integration No viral particles	Very low efficiency Need for repeated transfections
Minicircle	No	Efficiency higher than conventional plasmids No integration No viral particles No bacterial backbone	Low efficiency (lower than viral methods) (Need for repeated transfections)
PiggyBac transposon	No	No viral particles Theoretically possible to excise transgenes	Low efficiency Extra excision step Imperfect excision and transposition Risk of insertional mutagenesis, transgene reactivation and residual expression Possible interactions between piggyBac system and endogenous transposon systems
mRNA	No	Very high efficiency Non-transgene, no integration No viral particles	Need for repeated transfections High cost
Protein	No	Non-transgene, no integration, no exogenous nucleic acids No viral particles	Very low efficiency

Table 10 (continued)

Small molecule compounds	No	Non-transgene, no integration, no exogenous nucleic acids No viral particles Moderate efficiency	Not yet shown in human cells Moderate efficiency
Direct transfection of mature miRNA	No	Non-transgene, no integration No viral particles Moderate efficiency	Moderate efficiency
Lentiviral delivery of miRNA coding DNA	Yes	Very high efficiency	Risk of insertional mutagenesis, transgene reactivation and residual expression

Adapted from Cieřlar-Pobuda et al., *Molecular Cell Research*. (2017).¹⁶⁰

Of the majority of strategies presented, the use of natural mRNA (cap structure, untranslated regions (5'-UTR and 3'-UTR), an open reading frame (ORF), and a polyadenylated tail), has better advantages, since they do not integrate into the genome, and their delivery to the nucleus is not required. In reprogramming, directly delivering synthetic mRNA into somatic cells to induce pluripotency is the most footprint-free and genome integration-free method for generating iPSCs. Moreover, RNA delivery boasts the highest reprogramming efficiency compared to other nonviral and nonintegrative delivery systems. Therefore, RNA delivery uniquely combines safety and efficiency, making it the most promising approach for future clinical applications.¹⁵⁵ The strategies used to introduce mRNA into cells are represented and described in **Figure 16**.

**Figure 16. mRNA-delivery strategies.**

(A) Lipoplexes integrate into the host cell either by direct membrane fusion or by endocytosis, followed by endosomal membrane destabilization. (B) Polyplexes enter the cell via endocytosis and release mRNAs into the cytoplasm through a "proton sponge" effect. (C) In electroporation, a high-voltage current temporarily permeabilizes the membrane, allowing mRNAs to enter the cell through these pores. (D) Virus-like particles (e.g. Sendai virus) introduce mRNAs into the host cell efficiently and specifically, utilizing viral properties without integration or genomic trace. The A and B strategies can classify as chemical methods and C as physical method. Both chemical and physical methods open the pores of the cell membrane to allow the entry of mRNA. Figure obtained from Bailly et al. *Pharmaceutics*. (2022).¹⁵⁵

10.4. Evidence of partial reprogramming in T cells

As mentioned before, studies of partial reprogramming in T cells or PBMCs are very limited and are recently emerging. However, Raul Vizardo and collaborators have presented a study where they reprogrammed exhausted TILs that possess TCR specific for tumor antigens into iPSCs to rejuvenate them, for more potent ACT. For the transfection of the mRNA of Yamanaka factors were performed with the non-integrative viral delivery system (Sendai virus), with a sufficiently high MOI and with the addition of the SV40 oncogene.¹⁶¹

HYPOTHESIS AND OBJECTIVES

It has been demonstrated that dual stimulation of the TCR and CAR enhances the expansion of effector T cells and the persistence of the CAR *in vivo*.^{146,153} Likewise, Cruz et al. (2013) determined that the administration of VSTs against EBV, AdV, and/or CMV transduced with CAR.CD19 to patients with B cell neoplasms (ALL and CLL) was capable of expanding, persisting, and accumulating in the sites of the disease and was safe without inducing GvHD or cytokine release syndrome (IL-6, TNF- α , and IFN- γ).¹⁴⁷

Considering this, our hypothesis is that having T lymphocytes specific to the EBV with the native TCR and that also co-express CAR.CD19 (ARI-0001), enhances the persistence and proliferation of ARI-0001 *in vivo*. Furthermore, it could be an immunotherapy developed by the academy in an “*off-the-shelf*” allogeneic format, wherein the donor is a partially HLA-compatible with the recipient, to treat patients with EBV⁺ associated lymphomas, acute lymphoblastic leukemia with EBV⁺ infection, and as a bridge therapy for patients who are unable to receive autologous ARI-0001.

Taking into consideration what has already been described, the main objective of the doctoral thesis was to optimize the development of specific T lymphocytes against the EBV and subsequently transduce them with the CAR.CD19 construct (ARI-0001).

The specific objectives of this thesis are:

1. *In vitro* optimization of the activation and expansion of EBVSTs ^(Chapter I)

- a. Activation of T cells with overlapping peptides of the EBV virus.
- b. Determination of the most favorable conditions for the expansion of EBVSTs.
- c. TCR- β sequencing to determine the clones of each expanded product.
- d. Characterization of the final product by flow cytometry, and cytotoxicity assays.

2. Validation of activation and expansion of EBVST on a large scale under Good Manufacturing Practices (GMP) ^(Chapter II)

- a. Replicate on a large scale the protocol that has been optimized for the activation and expansion of EBVST in a clean room, under GMP conditions.
- b. TCR- β sequencing to determine the clones of the expanded product.
- c. Characterization of the final product by flow cytometry, ELISpot, and cytotoxicity assays.

3. Optimization of CAR-anti CD19 (ARI-0001) transduction into the EBVST ^(Chapter III and IV)

- a. Optimization of cell maintenance, activation and expansion of cryopreserved EBVSTs for CAR.CD19 (ARI-0001) transduction.

- b. Compare the transduction efficiency of CAR.CD19 (ARI-0001) in EBVSTs vs. normal CD3⁺ T cells.
- c. Compare the CAR.CD19 (ARI-0001) transduction efficiency in EBVSTs cryopreserved at day 12, 15, and 20.
- d. Characterization of the final product by flow cytometry and cytotoxicity assays.
- e. (Proof of concept): Partially reprogram EBVSTs cells to improve their proliferation, fitness and stemness post-thawing, so they can express the CAR.CD19 (ARI-0001).

4. Validation of EBV-specific T cell therapy transduced with the CAR-anti CD19 (ARI-0001) using the CliniMACS Prodigy[®]

- a. Replicate on a large-scale the protocol that has been optimized for the transduction of CAR.CD19 (ARI-0001) into the EBVST by using the CliniMACs Prodigy[®] System.

MATERIALS AND METHODS

1. Samples, cells lines and vectors

Samples: Blood bags with non-optimal volumes from 15 healthy EBV seropositive (IgG⁺IgM⁻) donors were used in accordance with the confidentiality principles of the Banc de Sang i Teixits, Barcelona, Spain, with the favorable approval of the Vall d'Hebron University Hospital Ethics Committee for Research with Medicinal Products (CEIm, project PR[BST]52/217; protocol code:170005). **Table 11** describes the characteristics of the starting material.

Table 11. Initial criteria for starting material

Criteria	Description
Bag aspect	Integrate
Identification	Correct
Serology	IgG ⁺ IgM ⁻
EBV PCR	Negative
Incubation/extraction time	≤ 24 hours
Blood bag volume	200-500mL approximately

*IgG⁺IgM⁻; donor has previously been exposed to EBV, but they are not currently undergoing an acute or recent infection.

PCR, Polymerase chain reaction.

Cell lines: The human cell line NALM6 (CD19⁺, derived from acute lymphoblastic leukemia, ATCC® CRL-3273), was cultured in RPMI-1640 medium (Gibco, Waltham, MA.) supplemented with 10% human serum AB (hSerAB; Banc de Sang i Teixits, Barcelona, Spain), at 37°C and 5% CO₂. It was maintained at a density between 0.2-2x10⁶ cells/mL. Depending on the confluency, weekly passages were performed. The line was tested for mycoplasma, with negative results.

HEK-293T cells (ATCC® CRL-11268), used as packaging cells for the ARI-0001 construct, were cultured in DMEM (Gibco) supplemented with 10% hSAB and 2mM glutamine, at 37°C and 5% CO₂. Passages were performed when confluence was below 90%. The density was maintained between 2-4x10⁴ cells/cm² (5-10x10⁵ total cells for 25cm² or 2-3x10⁶ total cells for 75cm²). HEK-293 T cells were also used to transfect mRNA encoding Yamanaka factors for the proof-of-concept of the partial reprogramming test.

Vector and CAR.CD19 construct (ARI-0001): The CAR.CD19 construct, already cloned into the lentiviral vector and transfected into HEK-293 T cells used in this study, was provided from surplus production of ARI-0001. The complete CAR.CD19 sequence (including signal peptide, A3B1 scFv, CD8 hinge and transmembrane regions 4-1BB, and CD3ζ) was synthesized by GenScript and cloned into a third generation lentiviral vector, pCCL, under the control of EF1α promoter (**Figure 17**). The A3B1 murine anti-CD19 mAb was generated at the Department of Immunology at Hospital Clínic of Barcelona. HEK-293 T cells were transfected with the transfer

vector (pCCL-EF1 α -CAR.CD19) along with the packaging plasmids pMDLg-pRRE (Addgene, 12251), pRSV-Rev (Addgene, 12253), and the envelope plasmid pMD2.G (Addgene, 12259). The number of transducing units (TU/mL) was determined by the limiting dilution method, using HEK 293-T cells.⁵⁴

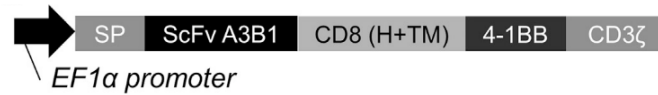


Figure 17. Diagram of A3B1 CAR.CD19 (ARI-0001) construct.

ARI-0001 is a second generation CAR. It has an extracellular target-binding domain directed against CD19 antigen, derived from the monoclonal antibody A3B1. The hinge and transmembrane (H+TM) domains are derived from CD8. The intracellular domain consists of 4-1BB as costimulatory molecule and CD3 ζ for signal transduction. The construct was cloned into a third generation lentiviral vector, pCCL, under the control of the EF1 α promoter. Figure obtained from Castella et al. *Molecular Therapy Methods and Clinical Development* (2019).⁵⁴

2. High-resolution HLA typing

All subjects were typed for HLA class I genes (**Table 12**) and HLA class II genes (**Table 13**). Genome DNA was extracted from peripheral blood using a QIASymphony automated system (Qiagen, Hilden, Germany). HLA typing was performed using next-generation sequencing (NGS) on a MiSeq system with the Reagent Kit v2 (300-cycles) (Illumina, San Diego, CA). Amplicons were generated by in-house multiplex-PCR, and library preparation was done via fragmentation with the NGSgo kit (GenDX, Utrecht, the Netherlands). Data were analyzed using NGSengine Software (GenDX, versions 2.17.0 to 2.22.0) and the IMGT/HLA database.

Table 12. HLA class I alleles in the studied cohort

Donor	HLA-A		HLA-B		HLA-C	
	Allele 1	Allele 2	Allele 1	Allele 2	Allele 1	Allele 2
1	A*11:01	A*33:01	B*14:02	B*35:01	C*04:01	C*08:02
2	A*30:02	A*31:01	B*18:01	B*51:01	C*05:01	C*14:02
3	A*02:01	A*26:01	B*08:01	B*14:01	C*07:01	C*08:02
4	A*02:01	A*11:01	B*18:01	B*27:05	C*01:02	C*12:03
5	A*11:01	A*33:01	B*14:02	B*35:01	C*04:01	C*08:02
6	A*24:02	A*24:02	B*41:02	B*44:03	C*16:01	C*17:03
7	A*02:02	A*26:08	B*15:01	B*41:01	C*03:03	C*17:01
8	A*26:01	A*68:01	B*18:01	B*49:01	C*02:02	C*07:01
9	A*29:02	A*30:01	B*44:03	B*47:01	C*06:02	C*16:01
10	A*24:07	A*30:01	B*08:01	B*35:08	C*04:01	C*07:01
11	A*11:01	A*26:01	B*49:01	B*51:01	C*02:02	C*15:02
12	A*24:02	A*30:02	B*14:01	B*18:01	C*07:02	C*08:02
13	A*01:01	A*32:01	B*08:01	B*35:01	C*04:01	C*07:01
14	A*02:01	A*33:03	B*18:01	B*50:01	C*06:02	C*12:03
15	A*02:01	A*31:01	B*18:01	B*50:01	C*04:01	C*05:01

Table 13. HLA class II alleles in the studied cohort

Donor	HLA-DRB1		HLA-DQA1		HLA-DQB1		HLA-DPA1		HLA-DPB1	
	Allele 1	Allele 2	Allele 1	Allele 2						
1	<i>DRB1*03:01</i>	<i>DRB1*11:01</i>	<i>DQA1*05:01</i>	<i>DQA1*05:05</i>	<i>DQB1*02:01</i>	<i>DQB1*03:01</i>	<i>DPA1*01:03</i>	<i>DPA1*02:01</i>	<i>DPB1*10:01</i>	<i>DPB1*104:01</i>
2	<i>DRB1*03:01</i>	<i>DRB1*13:01</i>	<i>DQA1*01:03</i>	<i>DQA1*05:01</i>	<i>DQB1*02:01</i>	<i>DQB1*06:03</i>	<i>DPA1*01:03</i>	<i>DPA1*01:03</i>	<i>DPB1*02:02</i>	<i>DPB1*04:01</i>
3	<i>DRB1*01:01</i>	<i>DRB1*11:01</i>	<i>DQA1*01:01</i>	<i>DQA1*05:05</i>	<i>DQB1*03:01</i>	<i>DQB1*05:01</i>	<i>DPA1*01:03</i>	<i>DPA1*02:01</i>	<i>DPB1*04:01</i>	<i>DPB1*05:01</i>
4	<i>DRB1*01:01</i>	<i>DRB1*11:04</i>	<i>DQA1*01:01</i>	<i>DQA1*05:05</i>	<i>DQB1*03:01</i>	<i>DQB1*05:05</i>	<i>DPA1*01:03</i>	<i>DPA1*01:03</i>	<i>DPB1*02:01</i>	<i>DPB1*1321:01</i>
5	<i>DRB1*01:01</i>	-	<i>DQA1*01:01</i>	<i>DQA1*01:01</i>	<i>DQB1*05:01</i>	<i>DQB1*05:01</i>	<i>DPA1*01:03</i>	<i>DPA1*02:01</i>	<i>DPB1*13:01</i>	<i>DPB1*104:01</i>
6	<i>DRB1*07:01</i>	<i>DRB1*12:01</i>	<i>DQA1*02:01</i>	<i>DQA1*05:05</i>	<i>DQB1*02:02</i>	<i>DQB1*03:02</i>	<i>DPA1*01:03</i>	<i>DPA1*02:01</i>	<i>DPB1*04:01</i>	<i>DPB1*17:01</i>
7	<i>DRB1*04:05</i>	<i>DRB1*11:01</i>	<i>DQA1*03:03</i>	<i>DQA1*05:05</i>	<i>DQB1*02:02</i>	<i>DQB1*03:01</i>	<i>DPA1*01:03</i>	<i>DPA1*01:03</i>	<i>DPB1*04:01</i>	<i>DPB1*04:02</i>
8	<i>DRB1*13:02</i>	<i>DRB1*16:01</i>	<i>DQA1*01:02</i>	<i>DQA1*01:02</i>	<i>DQB1*06:03</i>	<i>DQB1*06:04</i>	<i>DPA1*01:03</i>	<i>DPA1*02:01</i>	<i>DPB1*04:01</i>	<i>DPB1*10:01</i>
9	<i>DRB1*07:01</i>	<i>DRB1*07:01</i>	<i>DQA1*02:01</i>	<i>DQA1*02:01</i>	<i>DQB1*02:02</i>	<i>DQB1*02:02</i>	<i>DPA1*01:03</i>	<i>DPA1*01:03</i>	<i>DPB1*04:02</i>	<i>DPB1*1321:01</i>
10	<i>DRB1*13:01</i>	<i>DRB1*13:02</i>	-	-	<i>DQB1*05:01</i>	<i>DQB1*06:03</i>	-	-	-	-
11	<i>DRB1*07:01</i>	<i>DRB1*11:01</i>	-	-	<i>DQB1*02:02</i>	<i>DQB1*03:01</i>	-	-	-	-
12	<i>DRB1*04:05</i>	<i>DRB1*11:01</i>	<i>DQA1*03:03</i>	<i>DQA1*05:05</i>	<i>DQB1*03:01</i>	<i>DQB1*03:02</i>	<i>DPA1*01:03</i>	<i>DPA1*01:03</i>	<i>DPB1*351:01</i>	<i>DPB1*1037:01</i>
13	<i>DRB1*03:01</i>	<i>DRB1*13:01</i>	<i>DQA1*01:03</i>	<i>DQA1*05:01</i>	<i>DQB1*02:01</i>	<i>DQB1*06:03</i>	<i>DPA1*01:03</i>	<i>DPA1*02:01</i>	<i>DPB1*01:01</i>	<i>DPB1*04:01</i>
14	<i>DRB1*07:01</i>	<i>DRB1*11:04</i>	-	-	<i>DQB1*02:02</i>	<i>DQB1*03:01</i>	-	-	-	-
15	<i>DRB1*03:01</i>	<i>DRB1*07:01</i>	<i>DQA1*02:01</i>	<i>DQA1*05:01</i>	<i>DQB1*02:01</i>	<i>DQB1*02:02</i>	<i>DPA1*01:03</i>	<i>DPA1*01:03</i>	<i>DPB1*04:01</i>	<i>DPB1*1321:01</i>

3. Isolation of PBMCs

PBMCs were isolated from peripheral blood of healthy EBV-seropositive donors by density gradient centrifugation, using Lymphoprep™ (STEMCELL Technologies, Vancouver, Canada). Blood was diluted 1:2 in 1X Dulbecco's phosphate-buffered saline solution (DPBS) (Lonza, Basilea, Sweden). The final volume depended on the amount of PBMCs required for each experiment (**Table 14**). Subsequently, 15mL of Lymphoprep™ was added to the SepMate® column tubes (STEMCELL Technologies), and 32mL of diluted blood was slowly added. Then, it was centrifuged for 20 minutes at 1.200g at room temperature (RT). The PBMCs were collected by decantation from the upper phase of the column. Two washes were performed with 1X DPBS, to remove any residual platelets and erythrocytes. The pellet was then resuspended in 20mL of 1X DPBS, and counting was performed using a Neubauer chamber.

Table 14. Approximation of the number of cells to be obtained per unit of blood volume

Blood (mL)	1X DPBS (mL)	SepMate® tubes	Lymphoprep™	Isolated PBMCs (10 ⁶)
150	150	9	135	~143-270
200	200	12	180	~325-373
250	250	15	225	~405-649
500	500	31	465	>830

4. Optimization of EBVST generation

The protocol was adapted from methods published by the Center for Cell and Gene Therapy, Baylor College of Medicine, Houston, TX. Fourteen expansions were carried out with different conditions using a Gas Permeable Rapid Expansion (G-Rex®) 24-well plate culture system (Wilson Wolf, St. Paul, MN). With each condition, we aimed to improve and optimize the production of specific T cells against EBV (EBVSTs).

We tested the following variables:

(1) Seeding concentration: 2×10^6 cells/cm² and 4×10^6 cells/cm²

(2) Combinations of cytokines:

- IL-7, IL-15 and IL-2
- IL-7 and IL-15
- IL-7
- IL-2
- IL-15 and IL-21
- IL-7, IL-15 and IL-21
- IL-2 and IL-4

The concentration for each cytokine was 10 ng/mL for IL-7 (R&D Systems) and IL-21 (Miltenyi Biotec, GmbH), 80 U/mL for IL-15 (Miltenyi Biotec), 120 U/mL for IL-2 or Proleukin® (Miltenyi Biotec and Clinigen, Schiphol, the Netherlands) and 200U/mL for IL-4.

(3) Number of stimuli with EBV peptides: 1st stimulation on day 0, 2nd stimulation on day 5 or day 7, and 3rd stimulation on day 12.

(4) Stimuli:

- PepTivator[®] EBV consensus
- PepTivator[®] EBV consensus combined with PepTivator[®] Adenovirus 5 Hexon (AdV5 Hexon)
- PepTivator[®] EBV consensus combined with PepTivator[®] EBNA-1
- PepTivator[®] EBNA-1
- PepTivator[®] LMP2A

The concentration for each PepTivator[®] was 1µg/mL (Miltenyi Biotec).

(5) Expansion media:

- Expansion medium consists of 45% RPMI 1640 (Gibco), 45% Click's EHAA medium (Irvine Scientific, Santa Ana, CA.) and 10% hSAB
- TexMACS[®] GMP medium (Miltenyi Biotec)
- ImmunoCult[™]-XF T Cell Expansion Medium (STEMCELL Technologies)
- TheraPEAK[™] X-VIVO-15 Serum free (Lonza)

(6) Medium changes: days 2, 3, 5, 7, 8, 12 and 15.

(7) Re-stimulation ratios between the cells of the culture and irradiated autologous PBMCs (feeders): 1:4 and 1:1

(8) Culture time (Harvest): 15 or 20 days

Six different experimental designs were conducted with different culture conditions in each one, and PBMC's from different donors were used by each experiment (**Table 15**). Briefly, the optimization process consisted of stimulating 15×10^6 PBMCs/mL with 1µg/mL of the PepTivator[®] for 2 hours in the specified medium at 37°C, 5% CO₂. The cells were then cultured in a G-Rex[®] 24 well plate culture system at 2×10^6 cells/cm² or 4×10^6 cells/cm². On days 5 or 7, the cells were re-stimulated with 30 Grays (Gy) irradiated autologous PBMCs at a ratio of 1:4 or 1:1 (VST:Feeders) and stimulated with the same PepTivator[®] as on day 0. On day 12, a third stimulation was performed, either similar to the second re-stimulation but with a ratio of 1:1 (VST:Feeders), or by simply splitting the cells and changing the medium. The medium change days and cytokine combinations depended on the tested condition. On day 15 or 20, the cells were harvested and cryopreserved.

Table 15. Conditions tested in each optimization

Condition	Seeding density cell/cm ²	Antigen	Days of culture									
			0	2	5	7/8*	12	15	20			
Optimization 1 (Expansion from donor 12)												
A1	2x10 ⁶	EBV consensus	1 st stimulation	IL-7		2 nd stimulation IL-7	3 rd stimulation IL-7/IL-15/IL-2	IL-7/IL-15/IL-2	Harvest			
A2	4x10 ⁶			IL-7				IL-7/IL-15/IL-2				
B1	2x10 ⁶							IL-7		IL-7/IL-15/IL-2		
B2	4x10 ⁶							IL-7		IL-7/IL-15/IL-2		
C1	2x10 ⁶										IL-7/IL-15/IL-2	
C2	4x10 ⁶										IL-7/IL-15/IL-2	
D1	2x10 ⁶			2 nd stimulation IL-7/IL-15/IL-2							IL-7/IL-15/IL-2	
D2	4x10 ⁶										IL-7/IL-15/IL-2	
Optimization 2 (Expansion from donor 13)												
A2	4x10 ⁶	EBV consensus	1 st stimulation	IL-7/IL-15		2 nd stimulation IL-7/IL-15	3 rd stimulation IL-7/IL-15/IL-2	IL-7/IL-15/IL-2	Harvest			
B2				IL-7/IL-15		2 nd stimulation IL-7/IL-15/IL-2						
D2				2 nd stimulation IL-7/IL-15/IL-2								
E				IL-7/IL-15		2 nd stimulation IL-7/IL-15				3 rd stimulation IL-7/IL-15	IL-7/IL-15	
F				IL-7/IL-15		IL-7/IL-15				IL-2		
G										2 nd stimulation IL-7/IL-15/IL-2	3 rd stimulation IL-7/IL-15/IL-2	IL-7/IL-15/IL-2
Optimization 3 (Expansion from donor 14)												
D2	4x10 ⁶	EBV consensus	1 st stimulation		2 nd stimulation [All cells] IL-7/IL-15/IL-2		3 rd stimulation [All cells] IL-7/IL-15/IL-2	IL-7/IL-15/IL-2	Harvest			
D3					2 nd stimulation [0.8M] IL-7/IL-15/IL-2			IL-7/IL-15/IL-2				
D4					2 nd stimulation [All cells] IL-7/IL-15/IL-2			IL-7/IL-15/IL-2				
D5								IL-7/IL-15/IL-2				
H0					IL-7/IL-15					2 nd stimulation [0.8M], ratio 1:4 vs 1:1** IL-7/IL-15	IL-2	Harvest
H1										2 nd stimulation [All cells] IL-7/IL-15		
H2										2 nd stimulation [0.8M] IL-7/IL-15		
H3										EBV consensus + AdV 5 Hexon		

Table 15 (continued)

Condition	Seeding density cell/cm ²	Antigen	Days of culture								
			0	2	5	7/8*	12	15	20		
Optimization 4 (Expansion from donor 1)											
D2	4x10 ⁶	EBV consensus	1 st stimulation		2 nd stimulation [All cells] IL-7/IL-15/IL-2		3 rd stimulation [All cells] IL-7/IL-15/IL-2	IL-7/IL-15/IL-2	Harvest		
D2.1 ***							Split + IL-7/IL-15/IL-2				
D2.2 ****							Split + IL-15/IL-21			IL-15/IL-21	
D2.3							Split + IL-7/ IL-15/IL-21			IL-7/ IL-15/IL-21	
D2.4							IL-2			Harvest and Split +IL-2	
D2.5							IL-2				
H2							Split +IL-2				
H2.1 ***							IL-7/IL-15				2 nd stimulation [All cells] IL-7/IL-15
H2.2											
Optimization 5 (Expansion from donor 3)											
D2.3E	4x10 ⁶	EBV consensus	1 st stimulation		2 nd stimulation [All cells] IL-7/IL-15/IL-2	IL-7/IL-15/IL-2	Split + IL-7/IL-15/IL-2	IL-7/IL-15/IL-2	Harvest		
D2.3X										Split + IL-7/IL-15/IL-2	
D2.3.1										Split + IL-2/IL-4	IL-2/IL-4
D2.3.2										IL-7/IL-15/IL-2	
Optimization 6 (Expansion from donor 9)											
D2.3E	4x10 ⁶	EBV consensus	1 st stimulation		2 nd stimulation [All cells] IL-7/IL-15/IL-2	IL-7/IL-15/IL-2	Split + IL-7/IL-15/IL-2	IL-7/IL-15/IL-2	Harvest		
D2.3X											
D2.3T											
D2.3I											

Notes:

The letters in each experiment have been assigned to distinguish the various conditions tested. In the first optimization, the number "1" indicates a concentration of 2x10⁶ cells/cm², while "2" represents a concentration of 4x10⁶ cells/cm². In the other conditions, the numbers accompany the letters to further differentiate the tested conditions.

*For optimizations 1 to 4, the day of stimulation was 7, while the medium change from optimizations 4 to 6 occurred on day 8.

**Under these conditions we tested two ratios (1:4 vs 1:1, EBVSTs:Feeders) for the 2nd stimulation. The rest of the conditions were tested using a ratio of 1:4.

***The IL-2 cytokine added was Proleukin[®] to compare whether there were any differences with Miltenyi's IL-2, as Proleukin[®] is commonly used in GMP-grade applications.

****The split was performed on day 14 (not shown in the table).

In optimizations 1 to 4, all the conditions were cultured in expansion medium (45% RPMI 1640 + 45% Click's EHAA + 10%hSAB).

The values in [] in optimization 3 represent the total number of cells used to continue the culture.

Each condition is represented by a different color, with the same color scheme carried over to the results section to make visual identification easier

E, Expansion medium; X, TheraPEAK[™] X-VIVO-15 medium; T, TexMACS[™]; I, ImmunoCult[™]-XF T Cell Expansion medium.

Once the condition (D2.3E) was selected, it was replicated 9 times, with each replicate involving the activation and expansion of PBMCs from a different donor (donors 1-9). The protocol consisted of stimulating 15×10^6 PBMCs/mL with $1 \mu\text{g/mL}$ of the PepTivator[®] EBV consensus in expansion medium for 2 hours at 37°C , 5% CO_2 . The PepTivator[®] EBV consensus contains 43 peptides of 8-20 amino acids in length, derived from the lytic and latent EBV proteins, 32 of these are HLA class I and 11 are HLA class II restricted (**Table S1**). The cells were then cultured in a G-Rex[®] 24 well plate culture system at 4×10^6 cells/ cm^2 . On day 5, the cells were re-stimulated with 30 Gy irradiated autologous PBMCs at a ratio of 1:4 (VST:Feeders) and stimulated with the same PepTivator[®] EBV consensus as on day 0. The cells were cultured with fresh media containing IL-2 [120 U/mL], IL-7 [10 ng/mL] and IL-15 [80 U/mL]. Fresh medium with cytokines was changed every 3 to 4 days. On day 12, the cells were counted and adjusted to 4×10^6 cells/ cm^2 . The cells were expanded until day 20 and cryopreserved on days 12, 15 and 20 to be transduced with the CAR.CD19 (ARI-0001) construct (**Figure 18**).

This condition was also tested by stimulating PBMCs with a combination of PepTivator[®] EBV consensus and PepTivator[®] EBNA-1 ($n = 3$, donors 4, 10 and 11), as well as with PepTivator[®] EBNA-1 alone ($n = 1$, donor 4) or PepTivator[®] LMP2A ($n = 2$, donors 6 and 7).

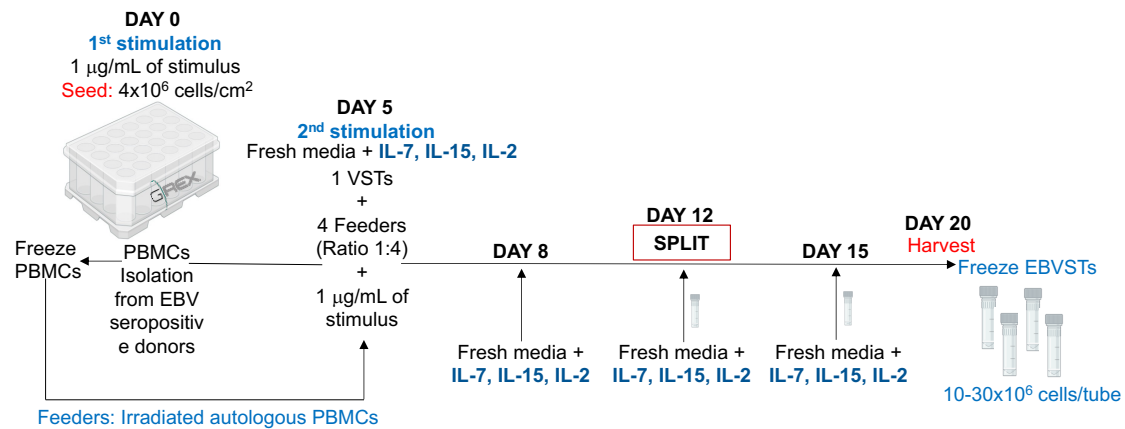


Figure 18. Protocol developed and optimized for the small-scale production of EBVSTs.

PBMCs isolated from EBV-seropositive donors were stimulated on day 0 and 5 with peptide pool from lytic and latent proteins of EBV (PepTivator[®] EBV consensus), Epstein-Barr nuclear antigen-1 (EBNA-1) or Latent membrane protein 2A (LMP2A). Cells were cultured in G-Rex[®] 24 well plate system at a seeding density of 4×10^6 cells/ cm^2 . On day 5, a second stimulation was performed using irradiated autologous PBMCs as feeders (ratio 1:4, VSTs: Feeders). Fresh medium with cytokines (IL-2 [120 U/mL], IL-7 [10 ng/mL], and IL-15 [80 U/mL]) were changed every 3-4 days. On day 12, cells were counted, adjusted (split) to 4×10^6 cells/ cm^2 per well, and expanded until day 20, with cryopreservation on days 12, 15, and 20. Figure created by the author.

5. Large-scale of EBVSTs production

The protocol was replicated on a large scale under GMP conditions using the 10M-CS and 100M-CS G-Rex[®] culture systems. The 10M-CS and 100M-CS formats have membrane surfaces of 10cm² and 100cm², with media capacities of 100 mL and 1 L, respectively. Both are closed systems. The 10M-CS was used for the stimulation phase of the T cells, while the 100M-CS was used for the expansion phase.

Briefly, PBMCs from an EBV-seropositive donor (n = 1, donor 15) were isolated by density centrifugation. Next, 15x10⁶ PBMCs/mL were stimulated with 1µg/ml of PepTivator[®] EBV Select (GMP-grade equivalent to EBV consensus) in expansion medium for 2 hours at 37°C, 5% CO₂. The cells were cultured in three 10M-CS G-Rex[®] units at a density of 4x10⁶ cells/cm² per G-Rex[®]. On day 5, cells were re-stimulated with 30 Gy irradiated autologous PBMCs at a ratio of 1:4 (VST:Feeders) and stimulated with the same PepTivator[®] EBV Select as on day 0. The cells were cultured with fresh media containing Proleukin[®] [120 U/mL], IL-7 [10 ng/mL] and IL-15 [80 U/mL]. Fresh medium with cytokines was changed every 3 to 4 days. On day 12, the cells were counted, pooled and adjusted to 3-4x10⁶ cells/cm² in a single 100M-CS G-Rex[®]. Cells were expanded until day 20 (**Figure 19**). Cryopreservation was performed on days 12, 15 and 20 to transduce them with the CAR.CD19 (ARI-0001) construct.

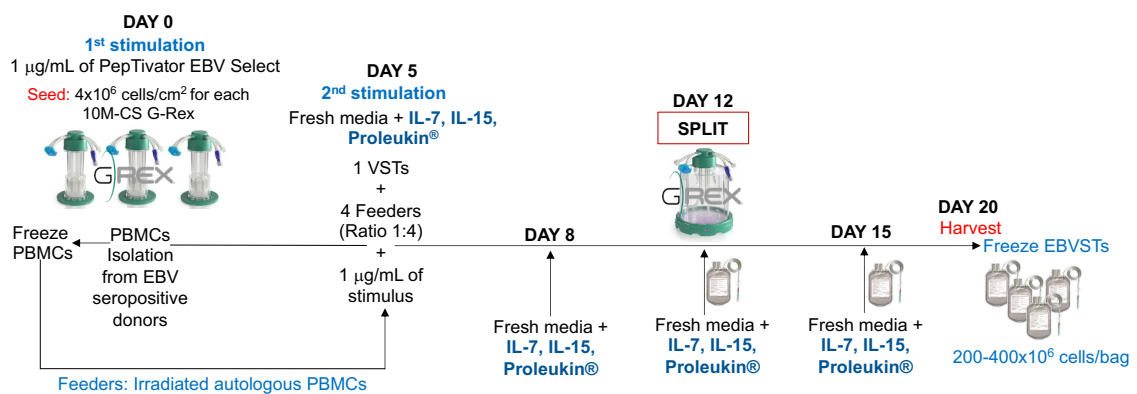


Figure 19. Protocol developed and optimized for large-scale production of EBVSTs.

PBMCs isolated from EBV-seropositive donors were stimulated on days 0 and 5 with PepTivator[®] EBV Select (GMP-grade). Cells were seeded at 4x10⁶ cells/cm² in three 10M-CS G-Rex[®] units. On day 5, a second stimulation was performed using irradiated autologous PBMCs as feeders (ratio 1:4, VSTs: Feeders). Fresh media with cytokines (Proleukin[®] [120 U/mL], IL-7 [10 ng/mL], IL-15 [80 U/mL]) were changed every 3-4 days. On day 12, cells were counted, pooled, and transferred to a 100M-CS G-Rex[®] unit at 3-4x10⁶ cells/cm². Expansion continued until day 20, with cryopreservation on days 12, 15, and 20. Figure created by the author.

6. Optimization of EBVSTs transduction

Based on the established and approved protocol for producing the ARI-0001 (CAR.CD19), we decided to replicate the same protocol *in vitro* as a first test to transduce the CAR.CD19 construct into EBVSTs.

An aliquot of EBVSTs generated on a large scale under GMP conditions and CD3⁺ T lymphocytes were thawed, washed and conditioned overnight (O/N) at 37°C, 5% CO₂ in a T75 cell culture flask (Corning, Somerville, MA) with TexMACSTM medium (Miltenyi Biotec) supplemented with 3% hSAB. The seeding concentration for the conditioning was 3x10⁶ cells/mL. The following day, cells were resuspended at a concentration of 1x10⁶ cells/mL in TexMACSTM medium supplemented with 3% hSAB, IL-7 [155 U/mL] and IL-15 [290 U/mL], in a 24-well plate (Corning). For T cell activation, 25 µL of DynabeadsTM CD3/CD28 (Gibco) per 1x10⁶ cells was used. Before adding the DynabeadsTM, they were washed with TexMACSTM medium and 3% hSAB, as they were initially resuspended in dimethyl sulfoxide (CryoSure-DMSO, Longwood, Zaragoza, Spain). Cells were incubated at 37°C, 5%CO₂. Twenty-four hours after activation, cells were counted and divided into the following conditions at 1x10⁶ cells/mL: (1) Untransduced (UTD) EBVSTs (negative control), (2) CAR.CD19-EBVSTs, and (3) CAR.CD19-CD3⁺ T lymphocytes (positive control), with each condition tested in duplicate. Conditions 2 and 3 were transduced (TD) with the lentivirus containing the CAR.CD19 construct at a multiplicity of infection (MOI) of 5. Two days after transduction, cells were adjusted at 0.8x10⁶ cells/mL with fresh medium and cytokines. On day 6, cells were counted, and the DynabeadsTM were removed from the culture using the MACSiMAGTM Separator. Cells were adjusted again at 0.8x10⁶ cells/mL. On day 8, cells were collected for functional assays (detection of CAR.CD19 and cytotoxicity assay) (**Figure 20**).

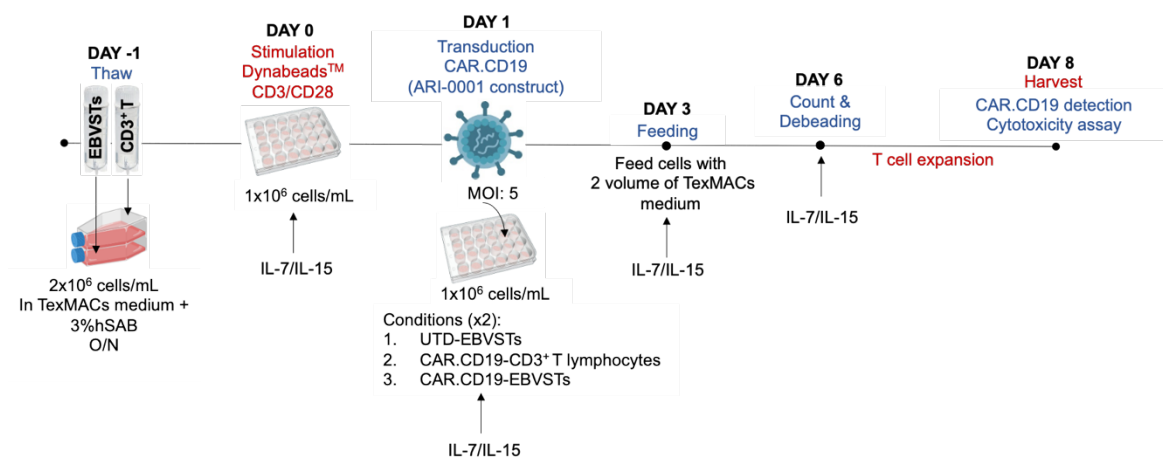


Figure 20. Protocol for the first transduction of CAR.CD19 (ARI-0001) into EBVSTs.

Cells were thawed and cultured overnight in TexMACSTM medium + 3% hSAB at 37°C, 5%CO₂. Cells were activated with DynabeadsTM CD3/CD28, and 24 hours later transduced with CAR.CD19 construct at an MOI of 5. Fresh media with cytokines were added in the indicated days until day 8. CAR.CD19-EBVSTs

expression was compared between CD3⁺ T cells (positive control) and UTD EBVSTs (negative control). hSAB, human Serum AB; MOI, multiplicity of infection; O/N, overnight; UTD, untransduced. Figure created by the author.

Since EBVSTs are previously activated and thawed T cells, the established cell culture conditions for ARI-0001 transduction had to be adapted and optimized for our starting material. Based on this, we tested the following conditions:

- (1) Culture system:** G-Rex[®] 24-well culture versus conventional 24-well plate (Corning).
 - (2) Stimulation method:** Dynabeads[™] CD3/CD28 and soluble monoclonal antibodies (anti-CD3, clone OKT3 and anti-CD28, clone 15E8, Miltenyi Biotec).
 - (3) Antibodies concentrations:**
 - 0.03 µg/mL or 1 µg/mL of anti-CD3 (clone OKT3)
 - 1 µg/mL of anti-CD28 (clone 15E8)
 - (4) Conditioning time:** None, 2 hours and O/N
 - (5) Media:** TexMACS[™] medium supplemented with 3% hSAB, expansion media supplemented with 10% or 3% of hSAB.
 - (6) Combination of cytokines:**
 - IL-7 and IL-15
 - IL-7, IL-15 and IL-2
 - IL-2
- The concentration for each cytokine was 155U/mL for IL-7, 290U/mL for IL-15 and 120 U/mL for IL-2.
- (7) Transduction day:** 24 hours, 48 hours or 72 hours post-activation.
 - (8) Seeding concentration:** 1 to 4x10⁶ cells/mL
 - (9) Cell expansion comparison** of cryopreserved EBVSTs on days 12, 15 and 20
 - (10) CAR.CD19 detection method:**
 - anti-CD19 scFv (Jackson ImmunoResearch Laboratories Inc., Cambridge, UK)
 - CD19 Protein, Fc Tag (Acrobiosystems, Basel, Switzerland).
 - (11) Partial reprogramming of EBVSTs before transduction:** A proof of concept was conducted to determine if partially reprogramming T cells using Yamanaka factors (OKSMNL: OCT4, SOX2, KLF4, c-MYC, LIN28 and NANOG), could enhance cell proliferation post-thaw.

Most of the optimizations were performed with EBVSTs produced on a large scale (donor 15), except for the last one, which was tested with EBVSTs derived from PBMCs of donor 5. For the comparison of cell expansion on days 12, 15, and 20, EBVSTs obtained from the PBMCs of donor 3 were used. For partial reprogramming, EBVSTs from donors 5, 6, and 7 were used.

Proof of concept for partial reprogramming T cells

HEK-293 T cells, PBMCs, CD3⁺ T cells, and EBVSTs were subjected for partial reprogramming. HEK-293 T cells and CD3⁺ T cells were stimulated with DynabeadsTM CD3/CD28. Fresh PBMCs and EBVSTs were stimulated with 1 µg/mL PepTivator[®] EBV consensus, while thawed EBVSTs were stimulated with 0.03 µg/mL anti-CD3 (clone OKT3) and 1 µg/mL anti-CD28 (clone 15E8) antibodies. The stimulation was performed 24 hours before transfection.

GFP-mRNA or mRNA encoding the Yamanaka factors proteins (OCT4, SOX2, KLF4, c-MYC, LIN28 and NANONG) from the StemRNATM 3rd gen reprogramming kit (Stemgent, REPROCELL, Beltsville, MD) was transfected using electroporation or chemical reagents. GFP-mRNA was used as a positive control, and untransfected cells as a negative control. For electroporation, a 4D-NucleofactorTM core unit (Lonza) was used. The chemical reagents tested were TransIT[®] (Mirus, Madison WI, USA), LipofectamineTM RNAiMAX (ThermoFisher Scientific, Waltham, MA) or LipofectamineTM RNAiMAX with Protamine sulfate (Sigma Aldrich, Misuri, USA) at a ratio of 1:3 (**Table 16**).

Cells were cultured in expansion medium with cytokines (10 ng/mL IL-7, 120 U/mL IL-2 and 80 U/mL IL-15) for 10-14 days. Fresh medium with cytokines was changed every 2-3 days. Detection of Yamanaka factor proteins or GFP was performed 24, 48, and 72 hours after transfection using flow cytometry. For PBMCs, only GFP-mRNA was transfected and detected using an immunofluorescence microscope (Leica Microsystems, L'Hospitalet de Llobregat, Spain).

Table 16. Parameters tested with different chemical reagents for transfection

Parameter	Lipofectamine TM RNAiMAX	Lipofectamine TM RNAiMAX + Protamine	TransIT [®]
Seeded cells (cells/mL)	1x10 ⁶	1x10 ⁶	1x10 ⁶
Volume (mL)	0.5	0.5	0.5
Culture plate	24-well plate	24-well plate	24-well plate
Confluency	60-80%	60-80%	60-80%
OKSMNL-mRNA	19.4µL (1.8µg mRNA + 0.4µg micrRNAs)	19.4µL (1.8µg mRNA + 0.4µg micrRNAs)	19.4µL (1.8µg mRNA + 0.4µg micrRNAs)
Transfection reagent volume	2µL RNAiMAX TM + 48µL expansion medium	2µL RNAiMAX TM + 5.4µL Protamine + 42.6µL expansion medium	3.6µL TransIT [®] -mRNA + 3.6µL mRNA Boost + 23.4µL Click's w/o hSAB medium

Abbreviation: w/o, without; OKSMNL, OCT4, SOX2, KLF4, c-MYC, LIN28 and NANONG.

7. Flow cytometry

PBMCs and EBVSTs stained

Surface staining

1x10⁶ cells/mL from PBMCs and EBVSTs from days 5, 12, 15 and 20 were washed with 1X DPBS. The cells were then stained with 100 µL/sample of viability mix (FC receptor block (BD Biosciences, Franklin Lakes, NJ) at 20 mg/mL and Viakrome fixable viability dye diluted 1:200 (Beckman Coulter, Pasadena, CA)). The cells were incubated for 10 minutes at room temperature (RT). Monoclonal antibodies directed against surface markers CD45-PE, CD3-PC5.5, CD56-PC7, CD4-AF750, CD8-KrO (Beckman Coulter), CD45RA-BV605 and CCR7-BV785 (Biolegend, San Diego, CA) were then added and incubated for 20 minutes at RT. The cells were washed and resuspended in 1X DPBS for cytometer acquisition. Stained samples were acquired using a CytoFlex (Beckman Coulter) flow cytometer and analyzed with Kaluza software (Beckman Coulter).

CD107a degranulation assay and intracellular staining

For T cell specificity determination, 1x10⁶ cells/mL were collected and stimulated with 1 µg/mL of PepTivator[®] (EBV consensus, LMP2A or/and EBNA-1) in a 96-well plate. Simultaneously, an anti-CD107a-APC antibody (Beckman Coulter) was added to the culture and incubated at 37°C, 5% CO₂. One hour later, 1 µg/mL of Brefeldin A (10 mg/mL; Sigma Aldrich) and protein transport inhibitor containing monensin (BD Golgi Stop; Pharmingen, Franklin Lakes, NJ) diluted 1:1000 was added to the culture. For the positive control, cells were stimulated with 50 ng/mL of Phorbol 12-myristate 13-acetate (PMA) (Sigma Aldrich) and 1 µg/mL of Ionomycin (Sigma Aldrich). The negative control was not stimulated with any stimulus. After overnight stimulation at 37°C, 5% CO₂, flow cytometry staining was performed. Cells were washed with 1X DPBS, and then FC receptor block (20 mg/mL; BD Biosciences) and Viakrome fixable viability dye diluted 1:200 were added for 10 minutes at RT in the dark. Monoclonal antibodies directed against surface markers CD3-PC5.5, CD56-PC7, CD4-AF750, CD8-KrO, CD45RA-BV605, and CCR7-BV785 were then added and incubated for 20 minutes at RT in the dark. Next, cells were washed and following the manufacturer's instructions for the Fixation/Permeabilization kit (BD Biosciences), antibodies against intracellular antigens IL-2-FITC, IFN-γ-PE, and TNF-α-AF-700 (Beckman Coulter) were added and incubated for 30 minutes at 4°C. Cells were washed and resuspended with 1X DPBS for cytometer acquisition.

For antigen specificity determination of cryopreserved expanded cells, VSTs were thawed and kept for 2 hours at 37°C and 5% CO₂. Then, followed the same stimulation and staining protocol

as used for fresh T cells, as described above. Stained samples were acquired using CytoFlex flow cytometer and analyzed with Kaluza software.

Exhaustion staining

1x10⁶ cells/mL of the final EBVSTs product from donors 3, 4, 6, 7, 10, 11 and 15 were stimulated with 1 µg/mL of PepTivator[®] (EBV consensus or/and EBNA-1) in a 96-well plate. The negative control was not stimulated with any stimulus. After overnight stimulation at 37°C, 5% CO₂, flow cytometry staining was performed as described in the surface staining procedure, with the addition of exhaustion markers: LAG-3-FITC (CD223), CTLA-4-PE (CD152), PD-1-AF-700 (CD279) and TIM-3-APC (CD366) (Biolegend). Stained samples were acquired using CytoFlex flow cytometer and analyzed with Kaluza software.

CAR.CD19-EBVSTs stained

Detection of the scFv extracellular domain

Cells were washed with 1X DPBS and 2% hSAB. Then, 2 µL per 10⁵ cells of biotin-SP-conjugated AffiniPure Goat Anti-Mouse IgG, F(ab')₂ Fragment Specific was added and incubated for 30 minutes at 4°C. After incubation, cells were washed and 1 µL per 10⁵ cells of Streptavidin-PE (ThermoFisher) was added and incubated for 20 minutes at RT. Cells were washed and resuspended with 1X DPBS and 2% hSAB. Stained samples were acquired using a CytoFlex flow cytometer and analyzed with Kaluza software.

Detection of CD19 Protein, Fc Tag

Cells were washed with 1X DPBS and 2% hSAB. Then, Viakrome fixable viability dye, diluted 1:200, was added and incubated for 10 minutes at RT in the dark. After this incubation, 2µL/sample of FITC-Labeled Human CD19 (20-291) Protein, Fc Tag (Acrobiosystems) was added and incubated for 20 minutes at RT. The cells were washed and resuspended with 1X DPBS and 2% hSAB. Stained samples were acquired using a CytoFlex flow cytometer and analyzed with Kaluza software.

Yamanaka factors stained

Detection was performed 24, 48 and 72 hours after transfection. Cells were washed with 1X DPBS and then stained with 100 µL/sample of Viakrome fixable viability dye, diluted 1:200. The cells were incubated for 10 minutes at RT in the dark. Monoclonal antibodies directed against surface markers CD3-PC5.5, CD56-PC7, CD4-AF750 and CD8-KrO were then added and incubated for 20 minutes at RT in the dark. Following this, the cells were washed, and, in accordance with the manufacturer's instructions for the Fixation/Permeabilization kit (BD

Biosciences), antibodies OCT4-AF-488, SOX2-PE, KLF4-APC, c-MYC-AF-750 and GFP-FITC were added and incubated for 30 minutes at 4°C. The cells were then washed and resuspended with 1X DPBS for cytometer acquisition and analyzed with Kaluza software.

Table 17 describes and summarizes the information on the antibodies used.

Table 17. Cytometry panels and antibodies information

Antibody	Dye	Clone	Commercial House	Reference
Superficial Staining				
Viakrome 405	PB	NA	Beckman Coulter	C36614
CD3	PC5.5	UCHT1	Beckman Coulter	A66327
CD4	AF-750	13B8.2	Beckman Coulter	A94682
CD56	PC7	N901	Beckman Coulter	A21692
CD45	PE	J33	Beckman Coulter	A07783
CD8	KrO	B9.11	Beckman Coulter	B00067
CD45RA	BV605	HI100	Biologend	304134
CCR7	BV785	G043H7	Biologend	353230
Intracellular staining				
CD107a	APC	H4A3	Beckman Coulter	328619
IFN-γ	PE	45.15	Beckman Coulter	IM2717U
TNF-α	AF-700	IPM2	Beckman Coulter	B76295
IL-2	FITC	IL2.39.1	Beckman Coulter	B90436
Exhaustion staining				
PD-1	AF-700	EH12.2H7	Biologend	329951
CTLA-4	PE	BNI3	Biologend	369603
TIM-3	APC	F38-2E2	Biologend	345011
LAG-3	FITC	11C3C65	Biologend	369307
Yamanaka factors staining				
OCT4	AF-488	3A2A20	Biologend	653705
c-MYC	AF-750	9E10	R&D Systems	IC3696S
SOX2	PE	245610	R&D Systems	IC2018P
KLF4	APC	Polyclonal Goat IgG	R&D Systems	IC3640A
GFP	FITC	-	ThermoFisher	

Note: For each cytometry panel, the corresponding FMOs were performed. NA, Not apply.

Tetramers staining

Following the staining protocol provided by the Leiden University group, the final products of EBVSTs from donors 3, 4, 6, 10 and 15 were thawed and conditioned in expansion medium at a concentration of $2-3 \times 10^6$ cells/mL for 2 hours at 37°C, 5% CO₂. After 2 hours of conditioning, the cells were harvested, washed and counted. Cells were then transferred to cytometer tubes and concentrated to $1-3 \times 10^6$ cells/0.3 μ L with DPBS/Albuplan[®] dilution (1X DPBS with 0.4% of Albuplan[®] 200g/L (GRIFOLS, Barcelona, Spain)). Next, cells were stained with peptide-MHC tetramer-PE or APC (provided by the Department of Hematology, Leiden University, Medical Center, the Netherlands, **Table 18**) and incubated for 10 minutes in the dark at 37°C, 5% CO₂.

Without washing, a mix of surface markers was added (CD3-PC5.5, CD8-KrO, CD4-AF750, CD56-PC7 and 1:200 of Viakrome 405 Fixable Viability dye) and incubated for 25 minutes in the dark at 4°C. Following this, the cells were washed and resuspended in DPBS/Albuplan®. EBVSTs without peptide-MHC tetramers were used as a negative control. Stained samples were acquired using a CytoFlex (Beckman Coulter) flow cytometer and analyzed with Kaluza software (Beckman Coulter).

Table 18. List of peptide-MHC tetramers used

Donor-derived EBVSTs	Peptide-MHC Tetramer	Peptide sequence	HLA restriction
3	LMP2 A*0201 APC	CLGGLLTMV	A*02:01
	LMP2 A*02:01 PE	FLYALALLL	A*02:01
	BMLF1 A*02:01 PE	GLCTLVAML	A*02:01
	EBNA3C A*0201 PE	LLDFVRFMGV	A*02:01
	BMRF1 TLD A*0201 PE	TLDYKPLSV	A*02:01
	BRLF1 YVL A*0201 PE	YVLDHLIVV	A*02:01
	EBNA3A B*08:01 PE	FLRGRAYGL	B*08:01
	EBNA3A B*0801 PE	QAKWRLQTL	B*08:01
	BZLF1 RAK B*0801 PE	RAKFKQLL	B*08:01
	EBNA1 B*0801 PE	YNLRRGTAL	B*08:01
4	LMP2 A*0201 APC	CLGGLLTMV	A*02:01
	LMP2 A*02:01 PE	FLYALALLL	A*02:01
	BMLF1 A*02:01 PE	GLCTLVAML	A*02:01
	EBNA3C A*0201 PE	LLDFVRFMGV	A*02:01
	BMRF1 TLD A*0201 PE	TLDYKPLSV	A*02:01
	BRLF1 YVL A*0201 PE	YVLDHLIVV	A*02:01
6	BRLF1 A*2402 PE	DYCNVLNKEF	A*24:02
	LMP2 A*2402 PE	TYGPVFMCL	A*24:02
10	EBNA3A B*08:01 PE	FLRGRAYGL	B*08:01
	EBNA3A B*0801 PE	QAKWRLQTL	B*08:01
	BZLF1 RAK B*0801 PE	RAKFKQLL	B*08:01
	EBNA1 B*0801 PE	YNLRRGTAL	B*08:01
15	LMP2-ESE-A*01:01 PE	ESEERPPTY	A*01:01
	EBNA3A-FLQ-A*01:01 PE	FLQRTDLSY	A*01:01
	BZLF1-FTP-A*01:01 PE	FTPDPYQVPF	A*01:01
	LMP2-LTE-A*01:01 PE	LTEWGSGNRTY	A*01:01
	EBNA3A-YTD-A*01:01 PE	YTDHQTTP	A*01:01

Note: The concentration of each peptide-MHC tetramer was 0.2µg/µL. Each peptide-MHC tetramer was provided by the Department of Hematology, Leiden University, Medical Center, the Netherlands.

8. *In vitro* cytotoxicity assay

PHA-Blast generation

Fresh or thawed PBMCs were cultured at 2×10^6 cells/mL in expansion medium and stimulated with phytohemagglutinin (PHA-P) (Sigma-Aldrich), at a concentration of 5 $\mu\text{g/mL}$. On day 3, cells were harvested, counted, and cultured at 2×10^6 cells/mL with IL-2 (100 U/mL, Miltenyi Biotec). On day 7, the PHA-blasts were washed, harvested, and frozen until use.

T cell cytotoxicity assay

PHA-blasts were pulsed (P) or not pulsed (NP) with peptide pools (PepTivator[®] EBV consensus and/or EBNA-1) for 2 hours at 37°C, 5% CO₂. The PHA-blasts were then stained with two different concentrations of CFSE CellTrace (ThermoFisher) following the manufacturer's instructions. Briefly, a 1:5000 dilution was performed for CFSE^{high} and a 1:10 dilution for CFSE^{low}. PHA-blasts were incubated for 5 minutes with the respective CFSE concentrations in the dark. Then, PHA-blasts were washed and co-cultured with thawed EBVSTs overnight at target-to-effector (T:E) cell ratios of 1:20, 1:10, 1:5, and 1:2.5. PHA-blasts without EBVSTs and EBVSTs without PHA-blasts served as controls. 7-AAD (1-Aminoactinomycin D) (BD Biosciences) was added 5 minutes before acquisition using a Cytoflex (Beckman Coulter) flow cytometer. The percentage of specific lysis was calculated as follows:

$$100 - \left(100 * \left[\frac{(\bar{x}P/\bar{x}NP) \text{ with EBVSTs}}{(\bar{x}P/\bar{x}NP) \text{ without EBVSTs}} \right] \right)$$

$\bar{x}P$: average of pulsed PHA-blasts

$\bar{x}NP$: average of not pulsed PHA-blasts

The assay tested different ratios performed on EBVSTs obtained from donor 12. Whereas EBVSTs obtained from donors 4, 7 and 11 were only evaluated at a 1:5 (T:E) ratio.

CAR-EBVST cytotoxicity assay

Transduced (CAR.CD19-EBVSTs and CAR.CD19-CD3⁺ T lymphocytes) and untransduced (EBVST) conditions were co-cultured in a 96-well plate for 16-19 hours with tumor target cell line NALM6 at ratios 1:2 and 1:0.5 (T:E). Additionally, NALM6 cells were cultured alone, without co-culture, to determine basal cell viability. The cells were resuspended in TexMACS[™] and 3% hSAB and each condition was performed in duplicate. The following day, cytotoxicity was assessed by calculating the number of surviving target cells. Cells were transferred to cytometer tubes, washed and stained for 30 minutes in the dark at room temperature with

LIVE/Dead™ Fixable Aqua (ThermoFisher Scientific). The cells were then washed and stained with the CD19-PE antibody for 20 minutes at RT in the dark. Subsequently, the cells were washed and resuspended in 1X DPBS. Stained samples were acquired using the Attune™ NxT flow cytometer (ThermoFisher Scientific). The percentage of alive target cells was calculated as follows:

$$100 * \left(\frac{\bar{x} \text{ acquired events of NALM6 alive in co-culture}}{\bar{x} \text{ acquired events of NALM6 alone}} \right)$$

9. Interferon-gamma (IFN- γ) ELISpot assay

The ELISpot assay was performed only on PBMCs (day 0) and EBVSTs (day 20) product, obtained in a large-scale under GMP conditions. This assay was conducted to measure the T cell response against EBV peptides while in co-culture with autologous PHA-blasts.

The IFN- γ ELISpot assay was carried out using the ELISpotPRO kit (MABTECH, 3420-2AST-2, Nacka, Swedish). The mAb 1-D1K pre-coated 96-well plate was washed and then conditioned with expansion medium for 30 minutes at room temperature. Meanwhile, conditions were prepared as follows:

EBV peptides conditions

- **Positive control:** 0.1×10^6 PBMCs or EBVSTs + 10 $\mu\text{g/mL}$ of PHA-P.
- **Negative control:** 0.1×10^6 PBMCs or EBVSTs resuspended in expansion medium.
- **Sample:** 0.1×10^6 PBMCs or EBVSTs + 1 $\mu\text{g/mL}$ of PepTivator® EBV consensus.

Co-culture conditions

- **Autologous pulsed PHA-Blasts:** 0.1×10^6 PHA-blasts (previously pulsed with 1 $\mu\text{g/mL}$ PepTivator® EBV consensus for 2 hours) resuspended in expansion medium.
- **Autologous non-pulsed PHA-Blasts:** 0.1×10^6 PHA-blasts resuspended in expansion medium.
- **Co-culture, autologous pulsed PHA-blasts and EBVSTs:** 0.1×10^6 pulsed PHA-blasts + 0.1×10^6 EBVSTs.
- **Co-culture, autologous non-pulsed PHA-blasts and EBVSTs:** 0.1×10^6 non-pulsed PHA-blasts + 0.1×10^6 EBVSTs.

After the 30-minutes of plate conditioning, the medium was removed, and each condition was seeded in triplicate, with a final volume of 200 μL /well of expansion medium. The plate was incubated at 37°C, 5% CO₂ for 18-20 hours.

Following the incubation, the spot forming units (SFU) were detected. First, washes were performed with non-sterile 1X DBPS. Then, 100 μ L/well of the IFN- γ antibody solution (diluted 1:200 with 1X DPBS) was added. The plate was incubated for 2 hours at RT in the dark. Subsequently, washes were performed with 200 μ L/well of non-sterile 1X DPBS. Then, 100 μ L/well of the previously filtered and tempered BCIP/NBT substrate solution was added for 4-5 minutes. Visible spots were counted using an automated plate reader (AID ELISpot, GmbH).

10. DNA extraction and TCR- β sequencing

The β chain of the T cell receptor (TCR- β) was characterized in PBMCs from different donors and at days 12, 15 and 20 of expansion using a strategy developed in the Histocompatibility and Immunogenetics Laboratory of the BST. Genomic DNA was obtained using the QIAamp DNA Blood Mini Kit (Qiagen, Hilden, Germany) and around 24,000 T cells per sample were analyzed. A two-step PCR was used to amplify the DNA rearrangements of the Variable (TRBV), Diversity (TRBD) and Joining (TRBJ) genes, and to perform library preparation. Libraries from different samples were pooled together at equimolar concentrations, purified using the MinElute Gel Extraction kit (Qiagen) and sequenced in a Miseq system using a 500-cycle MiSeq Reagent Kit v2 (Illumina, San Diego, CA, USA).

Data analysis was performed using MIXCR¹⁶² and VDJtools¹⁶³ bioinformatics software. MIXCR handled primary analysis, including alignment and clonotype assembly. Secondary analysis was performed with both MIXCR and VDJtools. Only productive clonotypes were considered for the analysis. Normalization of reads per sample was performed before diversity assessment, which was presented as observed diversity, normalized Shannon-Wiener and Inverse Simpson indexes, and D50. Observed diversity indicates the number of unique clonotypes, while D50 represents the number of unique clonotypes covering 50% of the repertoire abundance. The distribution of CDR3 length and usage frequencies of the TRBV and TRBJ genes were also analyzed. The overlap of the TCR- β repertoire was studied in PBMCs samples from different donors and in the final products on day 20. For this analysis, clonotypes with less than 10 reads were discarded to avoid cross-contamination between samples, and those clonotypes with the same CDR3 amino acidic region were considered public TCRs.

Finally, the most frequent clonotypes (> 2%) identified in each sample, as well as those clonotypes shared between the different final products at day 20, were searched in public TCR sequence databases (<http://tools.iedb.org/tcrmatch/>, <https://vdjdb.cdr3.net/> and <https://friedmanlab.weizmann.ac.il/McPAS-TCR/>).

11. Cryopreservation

The isolated PBMCs and the final products obtained (EBVSTs and CAR-EBVSTs) were cryopreserved at a 1:1 dilution with 1X DPBS and cryopreservation solution (40% hSAB + 40% Albuplan[®] 200g/L + 20% DMSO). The small-scale expansions were cryopreserved in cryotubes. The products obtained on a large-scale under GMP conditions were cryopreserved in cryotubes and CryoMACS[®] Freezing Bag 250 (Miltenyi Biotec). The final concentration, whether in tube or bag, was between 10×10^6 cells/mL.

12. EBVSTs thawing and stability

Initially, both PBMCs and EBVSTs were thawed slowly in a 37°C water bath (Grant, Cambridge, UK), then diluted 1:2 with expansion medium and incubated for 10 minutes at 4°C. Next, they were diluted 1:10, washed, and resuspended to the desired concentration. However, we later switched to a rapid thawing method,¹⁶⁴ which consisted of directly diluting the cells 1:10 with pre-warmed expansion medium, washing them, and resuspending them to the desired concentration.

To assess cell stability, EBVSTs obtained from large-scale production under GMP conditions were thawed. Cell viability was compared at 0, 2, 4, 16, and 24 hours when stored at 4°C or RT. A surface staining was also performed to compare the cell phenotype at 0 and 16 hours.

13. Statistical analysis

All data were tabulated in Microsoft Excel version 16.75.2 and presented as the median with an interquartile range. The calculation of fold expansion was based on dividing the number of cells in culture by the number of cells seeded on day 0. GraphPad Prism 5 (GraphPad, San Diego, CA) was used to generate graphs and perform statistical analyses. A Wilcoxon test was performed to compare the differences between days when $n > 1$. Statistical significance was set at: (*) p -value of <0.05 , (**) p -value of <0.001 and (***) p -value of <0.0001 .

RESULTS

Chapter I: *In vitro* optimization of the activation and expansion of EBVSTs

To determine the optimal parameters and conditions for the activation and expansion of EBVSTs, different culture conditions were tested on a small scale using the G-Rex[®] 24-well plate system. PBMCs were used as the starting material for the activation and expansion of T cells. A total of 14 expansions were performed, each corresponding to a different EBV-seropositive healthy donor. The specificity in this study was measured by IFN- γ production following stimulation with EBV antigen. The viability percentage in the cultures was over 90% in all conditions. The gating strategy is shown in the annexes (**Figures S1 and S2**).

1.1. Optimization 1

The first expansion showed that on day 20 of the culture, there was a median of 92.42% (IQR: 95.71-88.91) CD3⁺ T cells under the tested conditions (**Figure 21A**). The conditions in which the medium was changed on days 5 and 7, with the addition of only IL-7 (B1, B2, C1 and C2), resulted in the greatest expansion (**Figure 21B**), resulting in a similar CD4:CD8 ratio (**Figure 21C**).

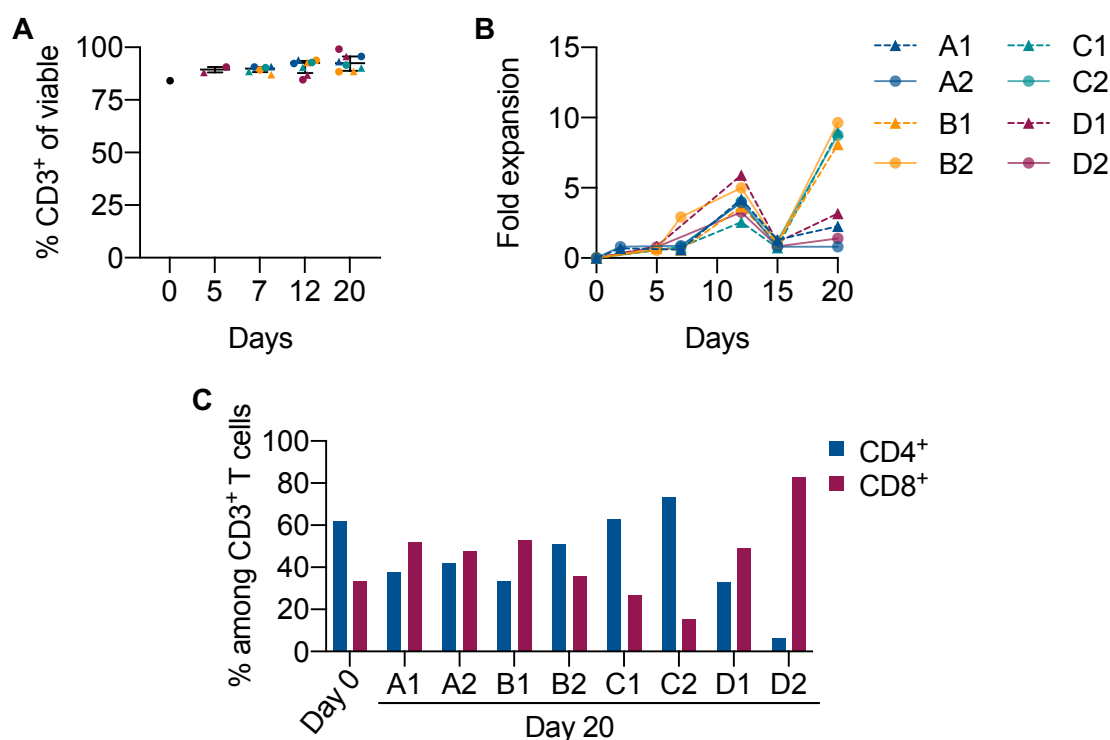


Figure 21. Phenotypic characterization in the 1st expansion of EBVSTs.

(A) Percentage of CD3⁺ T cells under the different conditions tested at various time points during the culture. The black dot at day 0 represents PBMCs isolated from the donor; (B) Fold expansion of total cells at different time points during the culture relative to day 0; (C) Percentage of CD4⁺ and CD8⁺ T cells

subpopulations pre- (day 0) and post-expansion (day 20). Numbers next to the letter of each condition indicate initial seeding concentrations: 1 = 2×10^6 cells/cm², 2 = 4×10^6 cells/cm².

However, the B1, B2, C1, and C2 conditions did not exceed 40% of specificity as measured by IFN- γ production (**Figure 22A**). In contrast, conditions A2 and D2, although they did not expand as much as the other conditions, showed CD8⁺ T cell specificities of 54% and 80%, respectively (**Figure 22A**). CD8-specific T cells from conditions A2 and D2 exhibited 33.62% and 79.42% expression of the CD107a marker, respectively (**Figure 22B**), indicating potential cytotoxic activity and degranulation functionality. Therefore, it was inferred that a higher seeding concentration (4×10^6 cells/cm²) combined with the addition of IL-7, IL-15 and IL-2 cytokines from day 5 onwards promotes the expansion of specific and cytotoxic T cells. Regarding early (day 5) versus late (day 7) re-stimulation, no differences were observed in this expansion.

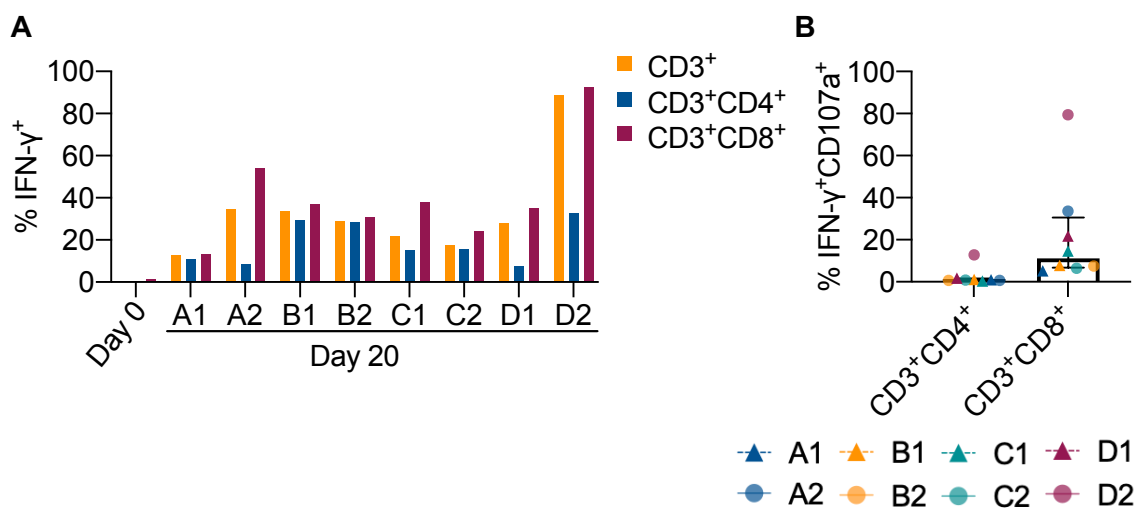


Figure 22. IFN- γ specificity and degranulation marker in the 1st expansion of EBVSTs.

(A) Percentage of IFN- γ production in different T cells subpopulations pre- (day 0) and post-expansion (day 20) (B) Percentage of degranulation marker in IFN- γ ⁺CD4⁺ and IFN- γ ⁺CD8⁺ T cells on day 20 of the culture. Numbers next to the letter of each condition indicate initial seeding concentrations: 1 = 2×10^6 cells/cm², 2 = 4×10^6 cells/cm².

The expression of differentiation phenotype markers revealed that most conditions exhibit effector memory T cell (T_{EM}) markers at the end of the culture (day 20). CD4⁺ T cells tend to retain a higher percentage of naïve T cells (T_{N+SCM}) compared to CD8⁺ T cells (**Figures 23A-B**). Condition D2 also showed 51% central memory T cells (T_{CM}) among IFN- γ ⁺CD8⁺ T cells (**Figure 23D**), making it a promising option.

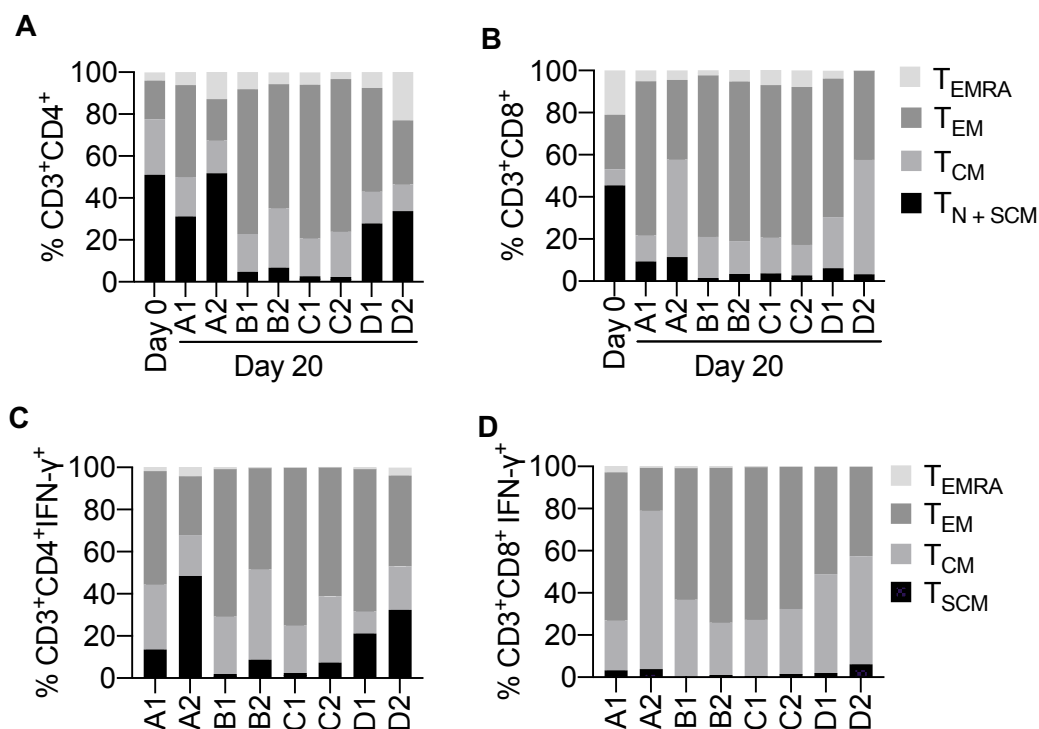


Figure 23. T cell differentiation phenotypes in the 1st expansion of EBVSTs.

Comparison of T cell subset differentiation phenotypes among the different conditions tested in the (A) CD3⁺CD4⁺ and (B) CD3⁺CD8⁺ subpopulations pre- (day 0) and post-expansion (day 20). Comparison of memory T cell subsets in post-expansion IFN-γ⁺ (C) CD4⁺ and (D) CD8⁺ T cells. T_N indicates naïve T cell (CCR7⁺CD45RA⁺); T_{SCM}, T memory stem cells (CCR7⁺CD45RA⁺); T_{CM}, central memory T cell (CCR7⁺CD45RA⁻); T_{EM}, effector memory T cell (CCR7⁺CD45RA⁻); and T_{EMRA}, terminally differentiated effector memory T cell (CCR7⁻CD45RA⁺).

1.2. Optimization 2

Based on these findings, condition D2 was replicated, and conditions A2 and B2 were also retested. New conditions E, F and G were also tested (Table 15, Methods section). It was observed that CD8⁺ T cells predominated in all conditions (Figure 24A). Not adding cytokines for 5 days (D2 condition) or 7 days (G condition) helped maintain a small proportion of CD4⁺ T cells in the culture. IFN-γ production was >88% for both CD3⁺ and CD8⁺ T cell populations (Figure 24B). Regarding the degranulation marker, conditions G and D2 exhibited the highest percentages (60% and 40%, respectively) (Figure 24C). Nevertheless, condition D2 demonstrated a better fold expansion (Figure 24D). Hence, it can be inferred that the combination of IL-15 with IL-7 influences T cell specificity, while adding IL-2 helps to maintain both specificity and T cell expansion.

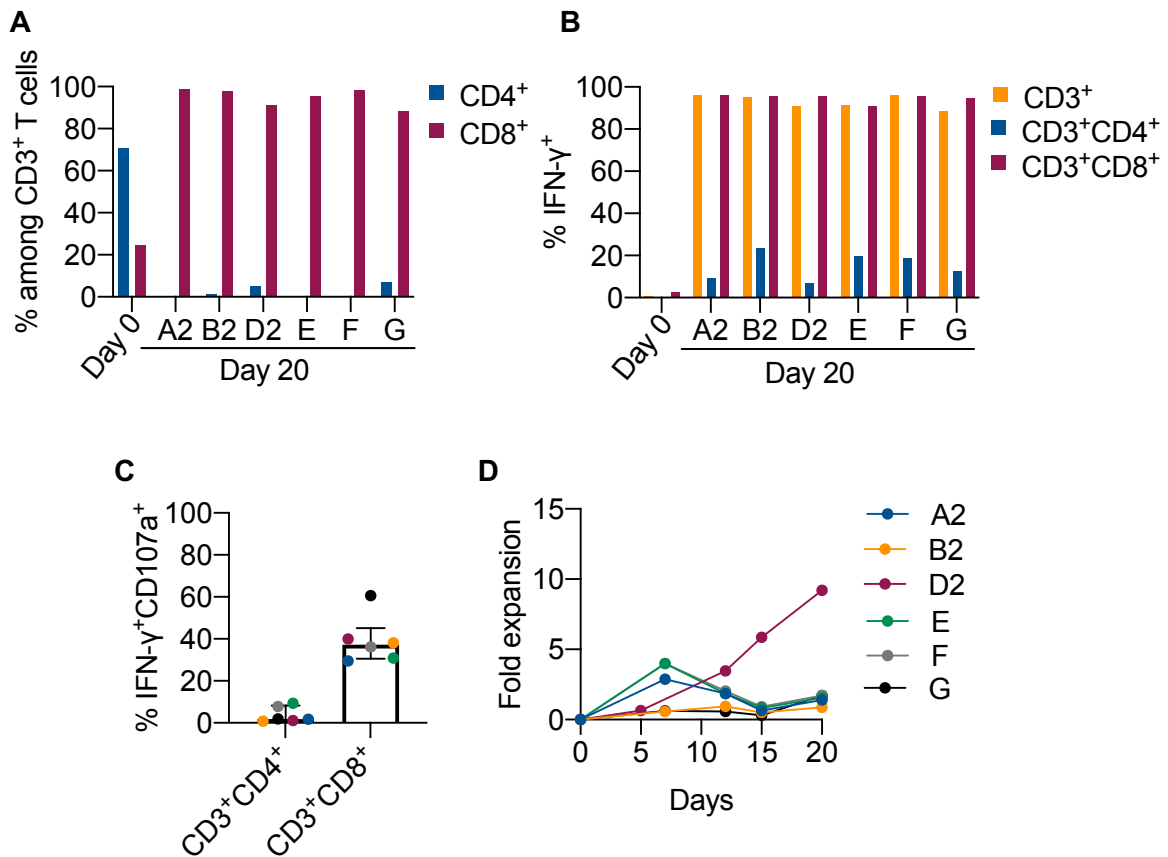


Figure 24. Phenotypic characterization and IFN- γ specificity in the 2nd expansion of EBVSTs.

(A) Percentage of CD4⁺ and CD8⁺ T cell subpopulations pre- (day 0) and post-expansion (day 20). (B) Percentage of IFN- γ production in different T cell subpopulations pre- (day 0) and post-expansion (day 20). (C) Percentage of degranulation marker expression in IFN- γ ⁺CD4⁺ and IFN- γ ⁺CD8⁺ T cells at day 20 of the culture. (D) Fold expansion of total cells at different time points during the culture relative to day 0.

The expression of differentiation phenotype markers showed that condition D2 retains a higher percentage of T_{N+SCM} CD4⁺ T cells (Figure 25A) and T_{SCM} in IFN- γ ⁺CD4⁺ T cells (Figure 25C). Likewise, to optimization 1, condition D2 preserves a T_{CM} phenotype in the CD8⁺ T cell subpopulation (Figure 25B) and IFN- γ ⁺CD8⁺ T cells (Figure 25D) compared to the other conditions. In most conditions, the CD8⁺ T cell population exhibits a T_{EM} phenotype on day 20 (Figures 25B and D).

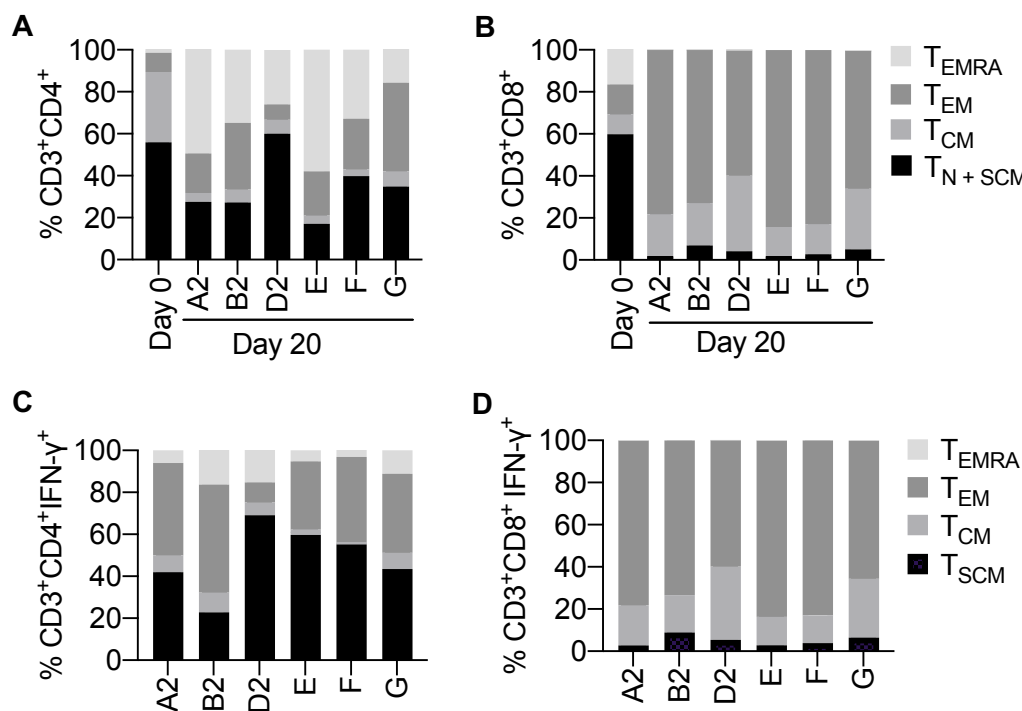


Figure 25. T cell differentiation phenotypes in the 2nd expansion of EBVSTs.

Comparison of T cell subset differentiation phenotypes among the different conditions tested in the (A) CD3⁺CD4⁺ and (B) CD3⁺CD8⁺ subpopulations pre- (day 0) and post-expansion (day 20). Comparison of memory T cell subsets in post-expansion IFN-γ⁺ (C) CD4⁺ and (D) CD8⁺ T cells. T_N indicates naïve T cell (CCR7⁺CD45RA⁺); T_{SCM}, T memory stem cells (CCR7⁺CD45RA⁺); T_{CM}, central memory T cell (CCR7⁺CD45RA⁻); T_{EM}, effector memory T cell (CCR7⁺CD45RA⁻); and T_{EMRA}, terminally differentiated effector memory T cell (CCR7⁻CD45RA⁺).

1.3. Optimization 3

Therefore, antigen stimulation with PepTivator[®] EBV consensus can expand a highly specific product; however, it was necessary to improve both the fold expansion and the percentage of CD4⁺ T cells in the culture. For this reason, in the third expansion, we evaluated the addition of PepTivator[®] AdV5 Hexon, as well as different concentrations and ratios in the re-stimulation step. Additionally, we compared the outcomes of harvesting the culture on day 15 versus day 20 (Table 15, Methods section).

No improvement was observed in the fold expansion among the different conditions tested (Figure 26A). Conditions H0, H1 and H3, where the number of cells was adjusted at day 7 and the culture was maintained from day 2 to day 12 with IL-7 and IL-15, exhibited a percentage of NK cells (CD3⁻CD56⁺) ranging from 6-12% in the final cell product, compared to condition H2 (1.19%), which all cells were re-stimulated. In contrast, conditions D2-D5, which had 5 additional days of culture, resulted in less than 0.83% NK cells, thus producing a purer final product (Figure 26B). No difference was observed in the percentage of CD4⁺ T cells in the condition where the

PepTivator® EBV consensus was combined with the Ad5 Hexon stimulus (**Figure 26C**). Conditions H0 and H1 showed a slight increase in CD4⁺ T cells compared to conditions H2 and H3, though the specificity was slightly lower (**Figure 26D**). However, the phenotype and specificity were not influenced by the 1:4 (H0, H2, H3) vs 1:1(H1) ratio (VSTs:Feeders) in the re-stimulation step. The H2 condition expanded more than H1 (**Figure 26A**). There was no difference in the CD4:CD8 ratio between conditions D2-D5 (**Figure 26C**). Stimulating three times and maintaining the cells for an additional 5 days (conditions D) increased the specificity, mainly in CD4⁺ T cells, compared to conditions H (**Figure 26D**). At the level of degranulation, it appears that a higher number of total cells in the well induces a lower percentage of degranulation (**Figure 26E**).

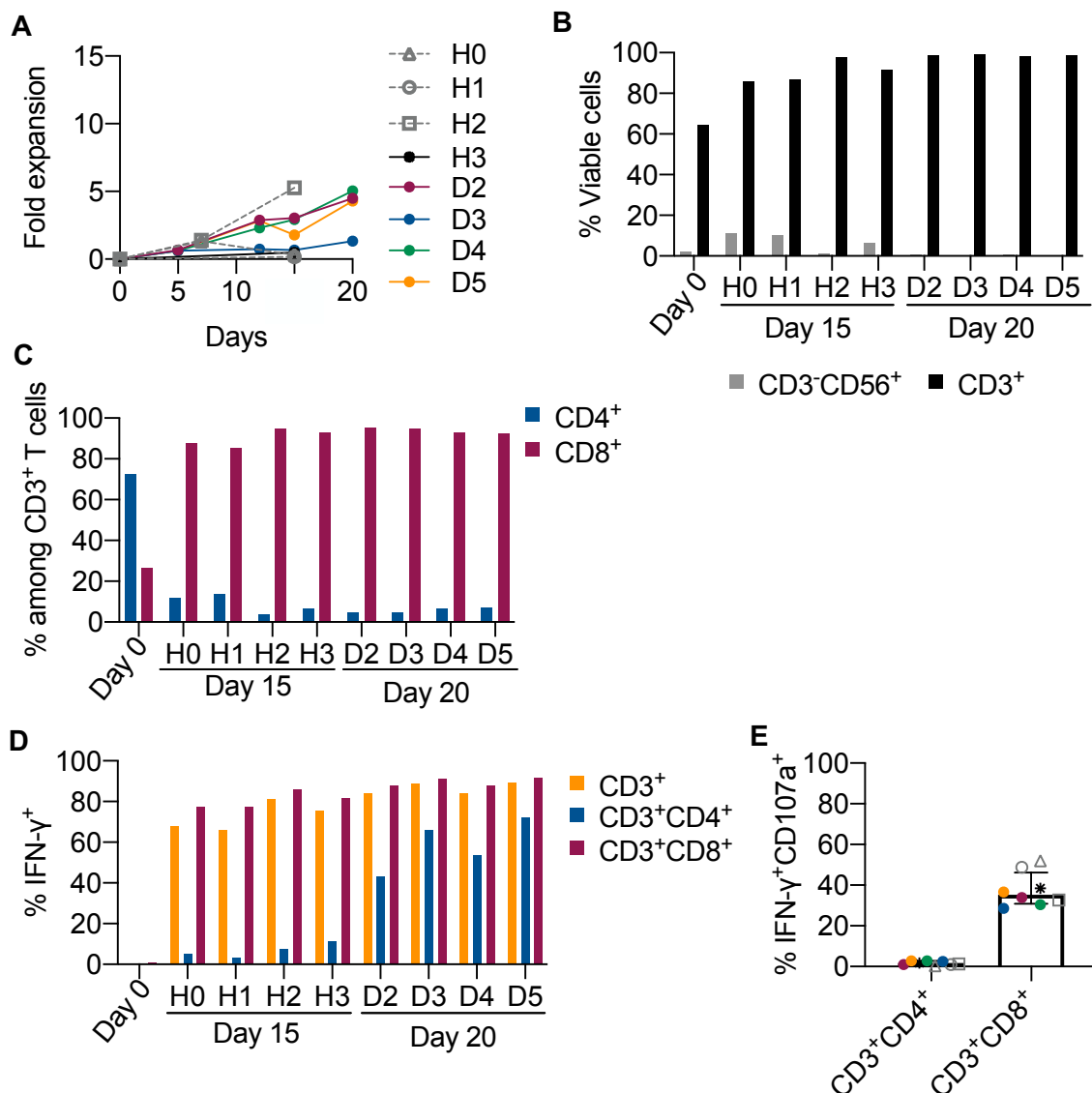


Figure 26. Phenotypic characterization and IFN- γ specificity in the 3rd expansion of EBVSTs.

(A) Fold expansion of total cells at different time points during the culture relative to day 0. (B) Comparison of the percentage of CD3⁺ T cells and NK cells (CD3⁺CD56⁺) in the culture. (C) Percentage of CD4⁺ and CD8⁺ T cell subpopulations pre- (day 0) and post-expansion (day 15 or 20). (D) Percentage of IFN- γ production in different T cell subpopulations pre- (day 0) and post-expansion (day 15 or 20). (E) Percentage

of degranulation marker in IFN- γ ⁺CD4⁺ and IFN- γ ⁺CD8⁺ T cells at day 15 and 20 of the culture. Conditions H were harvested on day 15, while conditions D were harvested on day 20.

Phenotypic analysis showed that conditions harvested on day 15, which were only stimulated twice, retained a higher proportion of CD4⁺ T_{N+SCM} cells (**Figure 27A**). In IFN- γ ⁺CD4⁺ T cells, conditions where the total number of cells was limited during re-stimulation (H0 and H1) preserved the T_{SCM} phenotype (**Figure 27C**). While CD8⁺ and IFN- γ ⁺CD8⁺ T cells predominantly exhibited a T_{EM} cell phenotype in all conditions (**Figures 27B and 27D**).

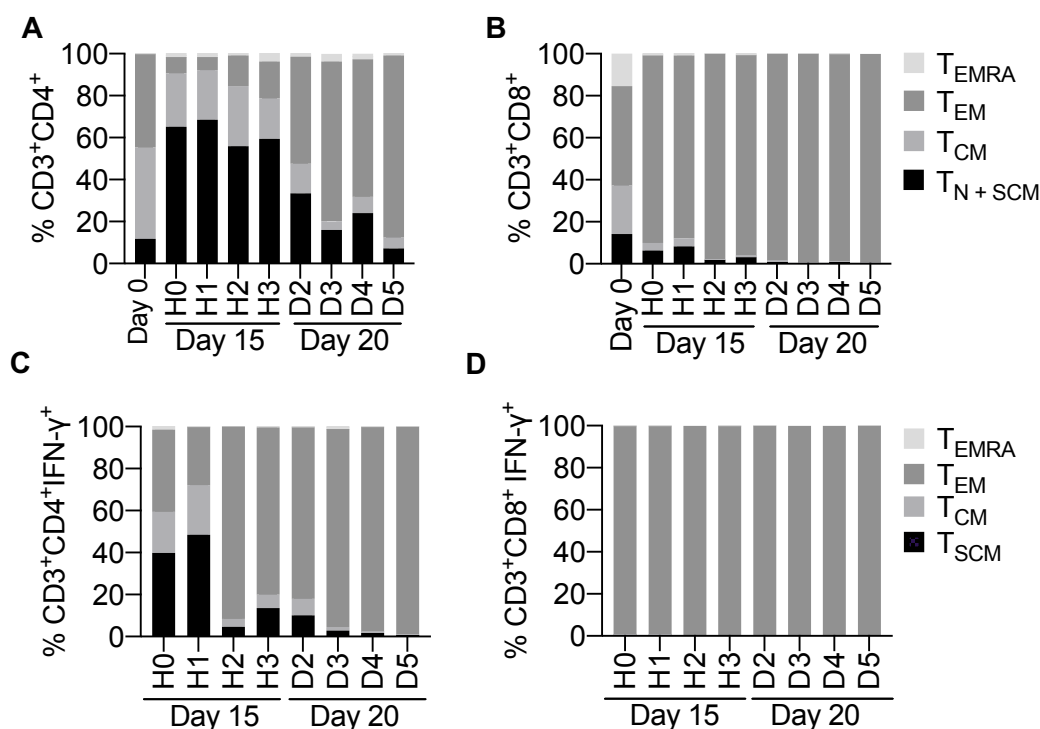


Figure 27. T cell differentiation phenotypes in the 3rd expansion of EBVSTs.

Comparison of T cell subset differentiation phenotypes among the different conditions tested in the (A) CD3⁺CD4⁺ and (B) CD3⁺CD8⁺ subpopulations pre- (day 0) and post-expansion (day 15 or 20). Comparison of memory T cell subsets in post-expansion IFN- γ ⁺ (C) CD4⁺ and (D) CD8⁺ T cells. T_N indicates naïve T cell (CCR7⁺CD45RA⁺); T_{SCM}, T memory stem cells (CCR7⁺CD45RA⁺); T_{CM}, central memory T cell (CCR7⁺CD45RA⁻); T_{EM}, effector memory T cell (CCR7⁻CD45RA⁻); and T_{EMRA}, terminally differentiated effector memory T cell (CCR7⁻CD45RA⁺).

1.4. Optimization 4

In the conditions tested during expansion 4 (**Table 15, Methods section**), it was observed that performing a split led to better fold expansion, with splitting on day 12 (D2.3, D2.4 and D2.5) yielding better results than on day 14 (D2.2.), compared to the conditions where no split was performed (D2 and D2.1) (**Figure 28A**). All conditions had more than 93% CD3⁺ T cells and less than 0.2% NK cells (CD3⁻CD56⁺) (**Figure 28B**). No significant differences were observed between using IL-2 from Miltenyi (D2 and H2) or Proleukin[®] (D2.1 and H2.1). Not performing a

split (D2 or H2) maintained a higher percentage of CD4⁺ T cells (21.68% and 10.32%, respectively) in the culture (**Figure 28C**), however, the specificity was slightly lower (**Figure 28D**). Therefore, we infer that stimulating twice and performing a split on day 12 results in better fold expansion and specificity across all T cell populations, with the combination of IL-7, IL-15 and IL-2 (D2.3) cytokines maintaining a higher percentage of CD4⁺ T cells and better specificity compared to IL-15 and IL-21 (D2.4) or IL-7, IL-15 and IL-21 (D2.5) (**Figures 28A and 28D**).

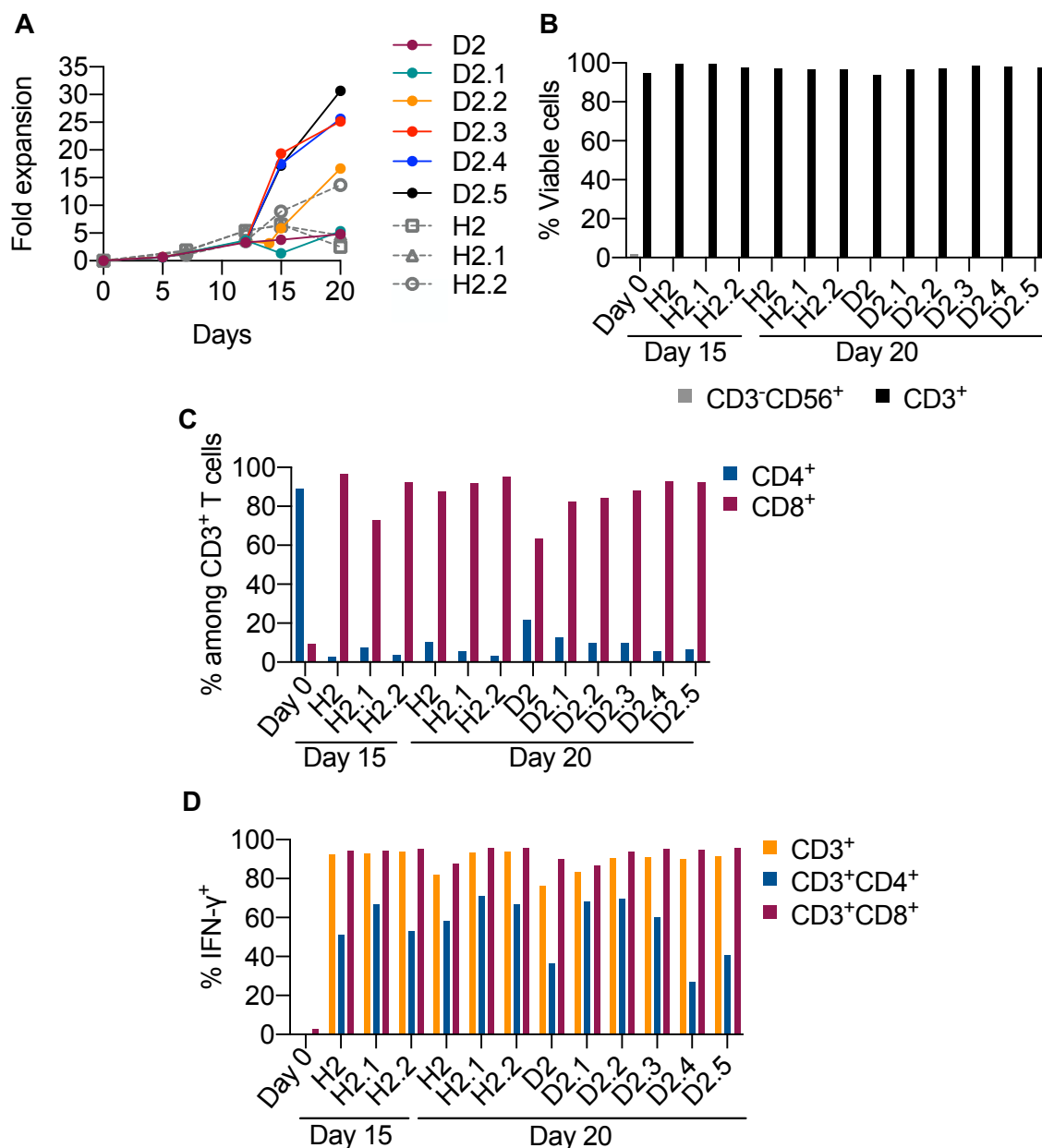


Figure 28. Phenotypic characterization and IFN- γ specificity in the 4th expansion of EBVSTs.

(A) Fold expansion of total cells at different time points during the culture relative to day 0. (B) Comparison of the percentage of CD3⁺T and NK cells (CD3⁺CD56⁺) in the culture. (C) Percentage of CD4⁺ and CD8⁺ T cell subpopulations pre- (day 0) and post-expansion (day 15 or 20). (D) Percentage of IFN- γ production in the different T cell subpopulations pre- (day 0) and post-expansion (day 15 or 20).

The percentage of CD8⁺ T cell degranulation in conditions expanded for 15 days has a median of 35.05% (IQR: 62.26-23.16%) (**Figure 29A**), while by day 20, this percentage increases to 65.82% (IQR: 68.04-44.79%) (**Figure 29B**). It could not be determined whether saturation (performing a split on day 12 or not) of the G-Rex[®] well affects the percentage of the degranulation marker, as no differences were observed between the conditions (D2, D2.3, D2.4 and D2.5). However, performing a split on day 14 (D2.2) or two splits on day 12 and 15 (H2.2) decreases the percentage of degranulation. The H2 condition exhibits a slightly higher percentage of the degranulation marker (71.57%) compared to the D conditions, possibly due to the cytokine combination used. Additionally, it can be inferred that Proleukin[®] decreases the degranulation capacity (D2 vs D2.1 and H2 vs H2.1) (**Figure 29B**).

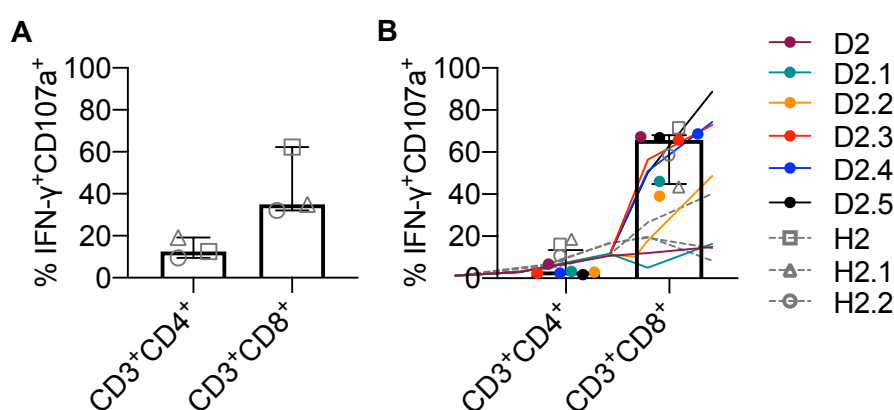


Figure 29. Percentage of degranulation marker in the 4th expansion of EBVSTs.

Degranulation marker in IFN- γ ⁺CD4⁺ and IFN- γ ⁺CD8⁺ T cell populations (**A**) on day 15 and (**B**) on day 20 of the culture.

The results of differentiation phenotype were like those in optimization three. Conditions harvested on day 15 retained a higher proportion of T_N+SCM cells, primarily in the CD4⁺ T cells. While CD8⁺ and both IFN- γ ⁺CD4⁺ and IFN- γ ⁺CD8⁺ T cells predominantly exhibited a T_{EM} cell phenotype on both days 15 and 20. No differences in the memory phenotype were observed in conditions where IL-21 was added (D2.4 and D2.5) (data not shown).

1.5. Optimization 5 and 6

In expansion 5, the results obtained with the tested conditions (**Table 15, Methods section**) showed that cells expanded more effectively with the expansion medium (22.57-fold) compared to TheraPeak[™] X-VIVO[™] 15 medium (0.78-fold). Performing two splits on days 8 and 12 (D2.3.1 condition) led to a decrease in the total number of cells in the culture (15.31-fold) compared to 22.57-fold in the D2.3E condition, where only one split was performed. Adding IL-4 (D2.3.2) during the expansion phase (from day 12 until day 20) resulted in lower fold expansion (11.48-fold) (**Figure 30A**). No differences were observed in the CD4:CD8 ratio, as all conditions

predominantly contained CD8⁺ T cells (>95%) (**Figure 30B**). IFN- γ production in CD4⁺ T cells decreased when cultured in TheraPeakTM X-VIVOTM 15 medium (D2.3X) or when IL-4 was added (D2.3.2). Meanwhile, few differences in IFN- γ production were noted in CD3⁺ and CD8⁺ T cells (**Figure 30C**). It is worth pointing out that specific T cells cultured in TheraPeakTM X-VIVOTM 15 medium exhibited 95.77% expression of the degranulation marker, compared to 3.99% expression in cells cultured in the expansion medium (**Figure 30D**).

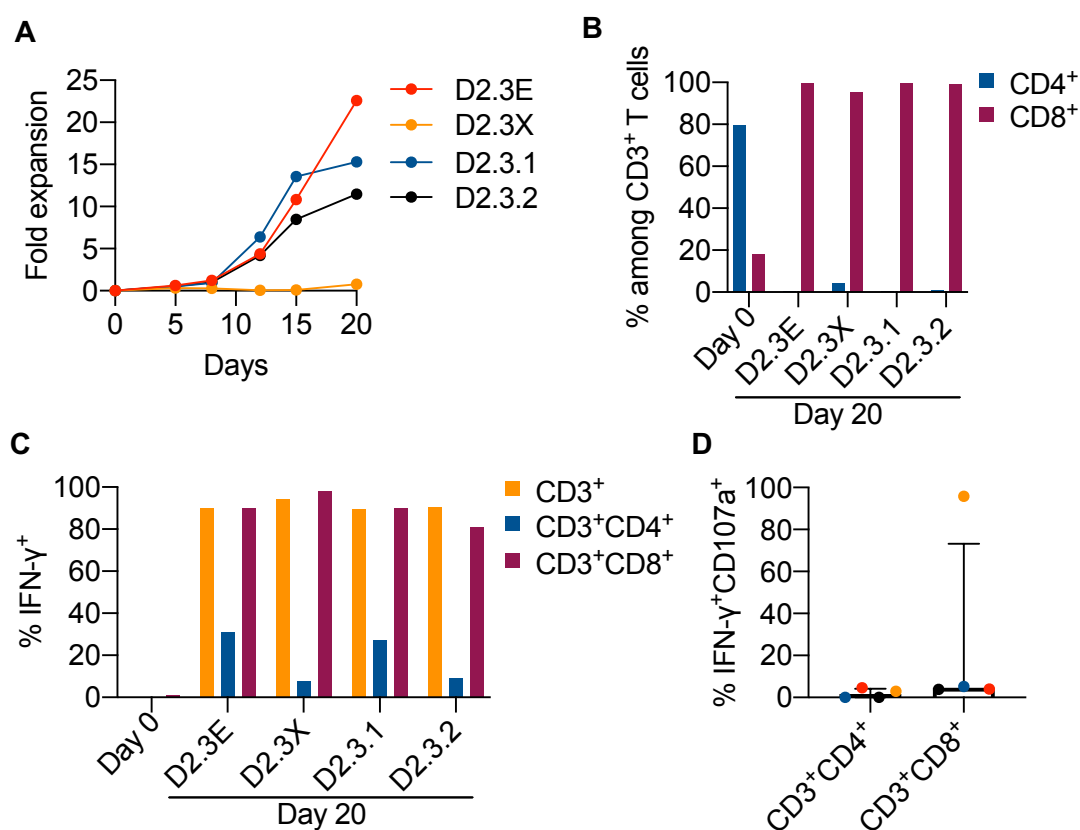


Figure 30. Phenotypic characterization and IFN- γ specificity in the 5th expansion of EBVSTs.

(A) Fold expansion of total cells at different time points during the culture relative to day 0. (B) Percentage of CD4⁺ and CD8⁺ T cell subpopulations pre- (day 0) and post-expansion (day 20). (C) Percentage of IFN- γ production in different T cell subpopulations pre- (day 0) and post-expansion (day 20). (D) Percentage of degranulation marker in IFN- γ ⁺CD4⁺ and IFN- γ ⁺CD8⁺ T cells at day 20 of the culture. E, expansion medium; X, TheraPeakTM X-VIVOTM 15 medium.

In the D2.3.2 condition, where IL-4 and IL-2 were added during the expansion phase, CD4⁺ and IFN- γ ⁺CD4⁺ T cells exhibited 64.74% of T_{N+SCM} and 23.53% of T_{SCM} cell phenotypes, respectively, compared to less than 30% T_{N+SCM} and less than 2.50% T_{SCM} in other conditions. In contrast, CD8⁺ and IFN- γ ⁺CD8⁺ T cells predominantly exhibited a T_{EM} phenotype, exceeding 95% across all conditions (data not shown).

In addition to TheraPeakTM X-VIVOTM 15 medium, we compared serum-free culture media, specifically TexMACSTM and ImmunoCultTM-XF T cell expansion medium (**Table 15, Methods**

section). In this expansion, PBMCs isolated from donor 9 showed remarkably lower fold expansion and it had to be harvested on day 15. However, we observed a slightly increased expansion in those cells cultured in the expansion medium which contained 10% hSAB (**Figure 31A**) and produced a purer product, with 98.96% CD3⁺ T cells, compared to less than 88% in other media (**Figure 31B**). In all conditions, the CD8⁺ T cell phenotype predominated, but the median percentage of CD4⁺ T cells was 22.25% (IQR: 39.46-16.89%) (**Figure 31C**), unlike previous expansions where it was less than 10% (**condition D2.3, Figures 28C and 30B**). Specificity was not as high as in previous expansions; however, cells cultured in both the expansion medium and TheraPeak™ X-VIVO™ 15 medium achieved a specificity of 70% for CD3⁺ T cells and 80% for CD8⁺ T cells (**Figure 31D**). Consistent with previous results (**Figure 30D**), cells cultured in X-VIVO™ 15 exhibited higher percentages of degranulation marker (85.93%) compared to 6.19% of expression in cells cultured in the expansion medium (**Figure 31E**).

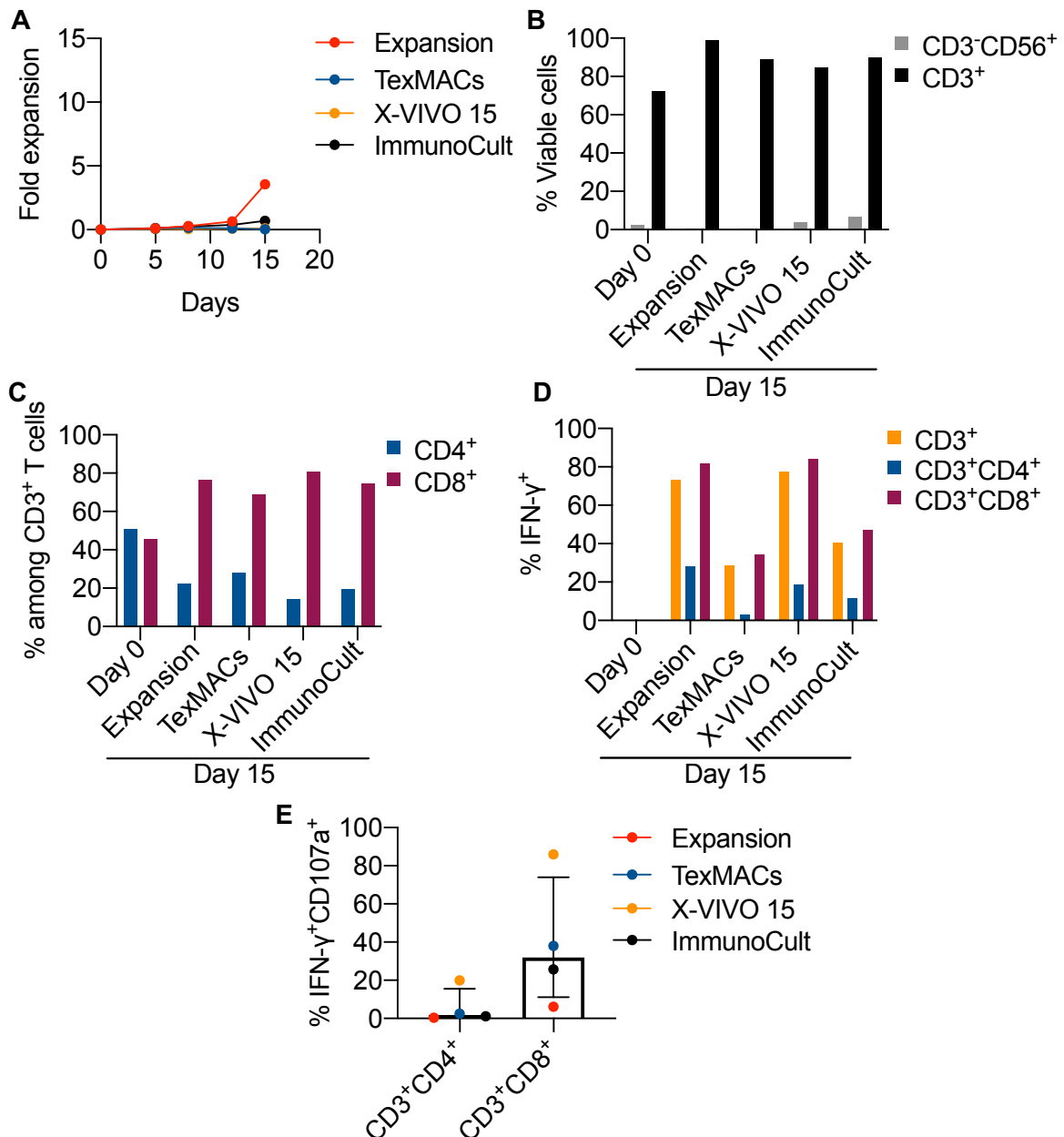
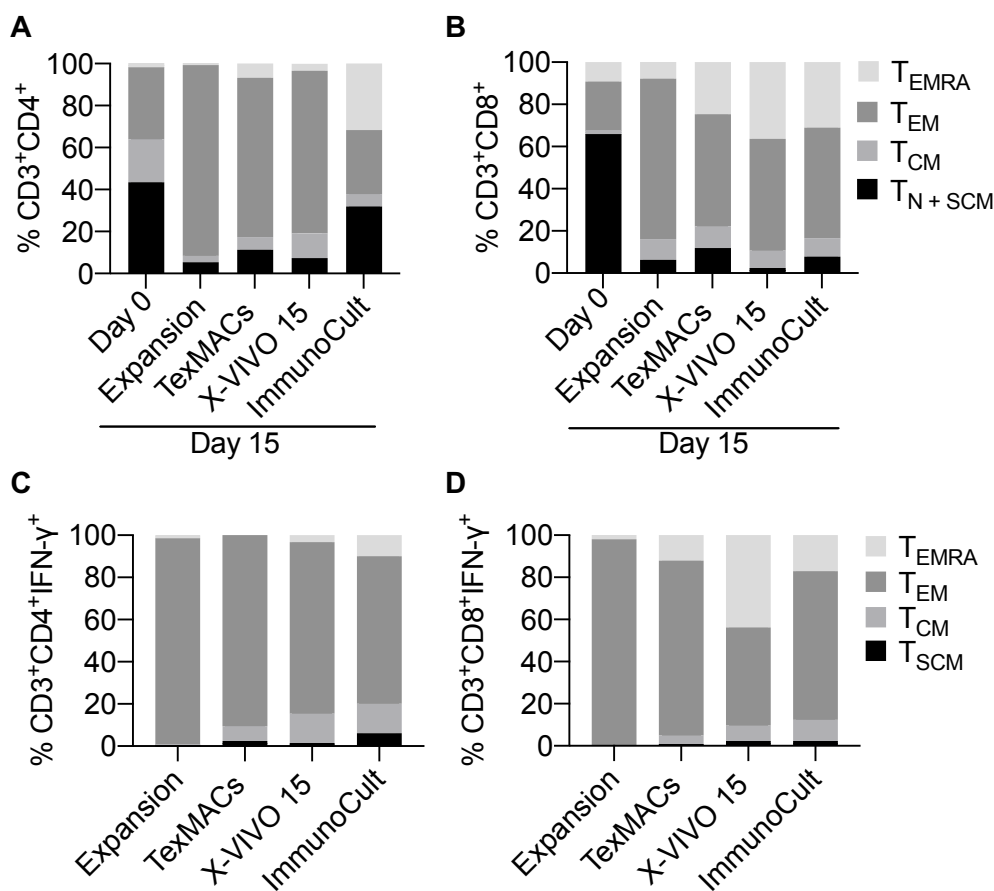


Figure 31. Phenotypic characterization and IFN- γ specificity of the 6th expansion of EBVSTs.

(A) Fold expansion of total cells at different time points during the culture relative to day 0. (B) Percentage of CD4⁺ and CD8⁺ T cell subpopulations pre- (day 0) and post-expansion (day 15). (C) Percentage of IFN- γ production in different T cell subpopulations pre- (day 0) and post-expansion (day 15). (D) Percentage of degranulation marker in IFN- γ ⁺CD4⁺ and IFN- γ ⁺CD8⁺ T cells on day 15 of culture.

The analysis of the differentiation phenotype showed that in most conditions the T_{EM} phenotype predominates; however, in this expansion, a higher proportion of T_{EMRA} phenotype was observed, specifically in the conditions cultured in TheraPeak™ X-VIVO™ 15 and ImmunoCult™-XF T cell expansion medium (Figures 32A-D).

**Figure 32. T cell differentiation phenotypes in the 6th expansion of EBVSTs.**

Comparison of T cell subset differentiation phenotypes among the different conditions tested in the (A) CD3⁺CD4⁺ and (B) CD3⁺CD8⁺ subpopulations pre- (day 0) and post-expansion (day 15). Comparison of memory T cell subsets in post-expansion IFN- γ ⁺ (C) CD4⁺ and (D) CD8⁺ T cells. T_N indicates naïve T cell (CCR7⁺CD45RA⁺); T_{SCM}, T memory stem cells (CCR7⁺CD45RA⁺); T_{CM}, central memory T cell (CCR7⁺CD45RA⁻); T_{EM}, effector memory T cell (CCR7⁻CD45RA⁻); and T_{EMRA}, terminally differentiated effector memory T cell (CCR7⁻CD45RA⁺).

1.6. Selected condition

After testing 32 conditions across six optimizations and observing T cell dynamics in various donors, we identified the optimal parameters for activating and expanding EBVSTs. Consequently, the chosen condition, denoted D2.3E in the optimizations (**Figure 33A**), was replicated in 9 donors; however, the results from 2 of them were excluded because they did not meet (1) the HLA class I restriction for the EBV overlapping peptide pool used for cell activation (PepTivator[®] EBV consensus) and (2) had a percentage of NK cells (CD3⁻CD56⁺) exceeding 20%.

Three out of the 7 expansions achieved a total cell fold expansion in culture greater than 20-fold, reaching up to 25.14-fold (**Figure 33B**). Cells from donor 2 exhibited a lower fold expansion (4.8), which could be attributed to the donor's HLA genotype, as this donor presented only one HLA class I allele restricted for the EBV overlapping peptide pool used for cell activation (PepTivator[®] EBV consensus) (**Table 12, Methods section and Table S1, Annexes section**). All conditions demonstrated a viability in culture greater than 90%, with more than 95% of CD3⁺ T cells at day 20 of culture (**Figure 33C**). Phenotypic characterization revealed that the majority of PBMCs were initially CD4⁺ T cells, with a median of 70.87% (IQR: 79.66-64.51%). However, after two stimulations and 12 days in culture in the presence of IL-7, IL-15 and IL-2, the cell population dynamics shifted significantly in most donors, resulting in a final product predominantly composed of CD8⁺ T cells (median of 93.50%, IQR: 99.29%-78.62%) (**Figure 33D**). Interestingly, donor 2, who showed less expansion, had a phenotype characterized by a higher proportion of CD4⁺ T cells compared to CD8⁺ T cells.

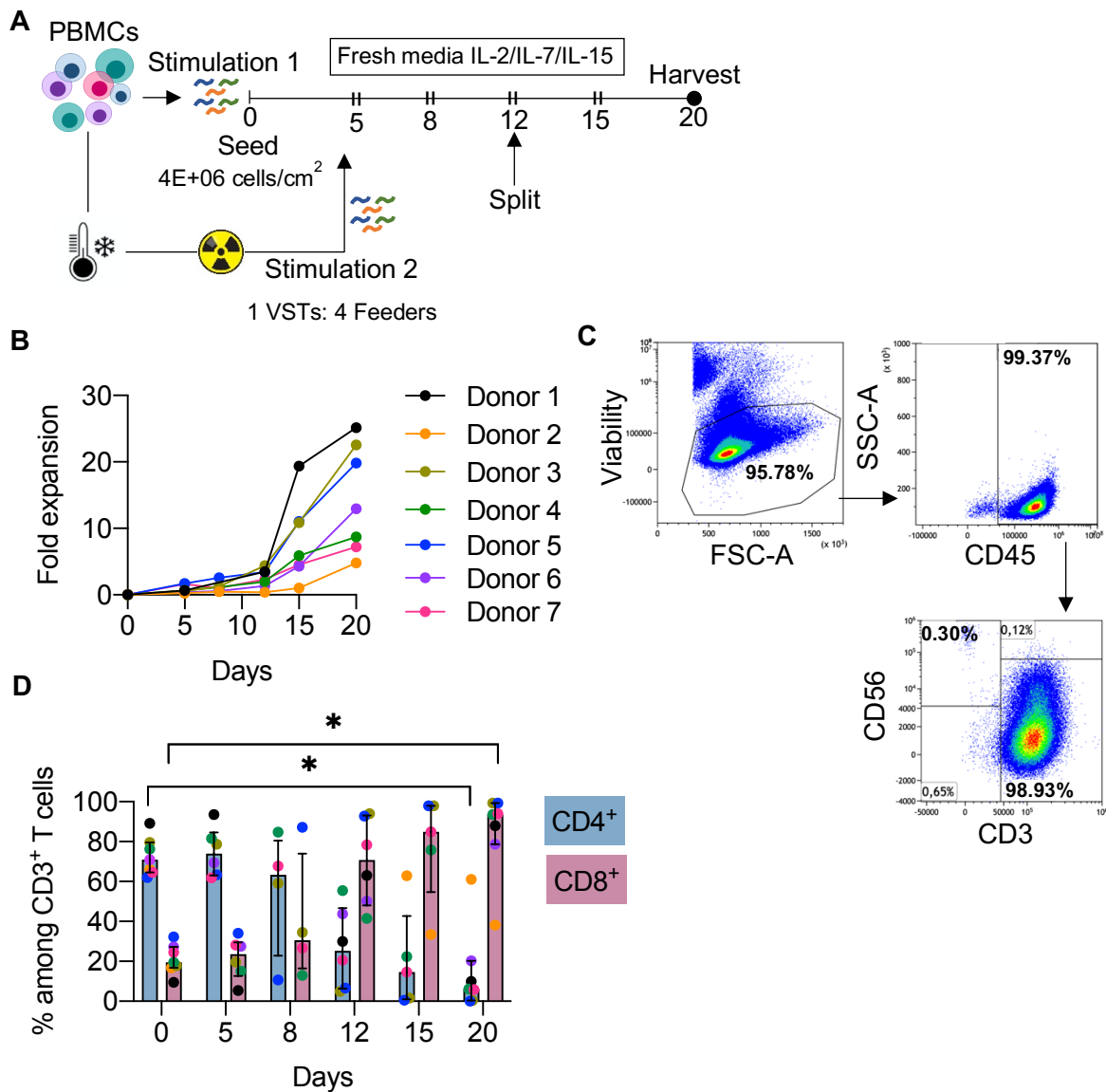


Figure 33. Optimized protocol to produce EBVSTs and characterization of the expanded product.

(A) Schematic diagram of the optimized protocol for the T cell activation and expansion of EBVSTs. Cells were cultured in expansion media in the presence of IL-7, IL-15 and IL-2. (B) Fold expansion of total cells at different time points during culture relative to day 0. Each color represents a different donor sample. (C) Representative flow cytometry dot plots showing viability, CD45⁺ expression, CD3⁺ T cells and NK cells (CD3⁺CD56⁺) from donor 5. (D) Percentage of CD4⁺ and CD8⁺ T cell subpopulations pre-expansion (day 0) and post-expansion at different time points during culture. Each value is represented as the median with interquartile range. The Wilcoxon test was performed to determine significant differences between each day of culture relative to day 0. Statistical significance was set at: (*) *p*-value of <0.05, (**) *p*-value of <0.001 and (***) *p*-value of <0.0001.

IFN- γ production increased in CD3⁺ and CD8⁺ T cells starting on day 12 and became significantly more specific by day 20 compared to day 0 (Figure 34A). For CD4⁺ T cells, the highest increase in INF- γ was observed on day 20. The degranulation marker on day 20 of culture showed a median of 24.02% (IQR: 65.82%-8.99%) for CD8⁺ specific T cells (Figure 34B). Additionally, in donors

4, 5 and 6, TNF- α and IL-2 production was evaluated in IFN- γ producing T cells (**Figures 34C-D**).

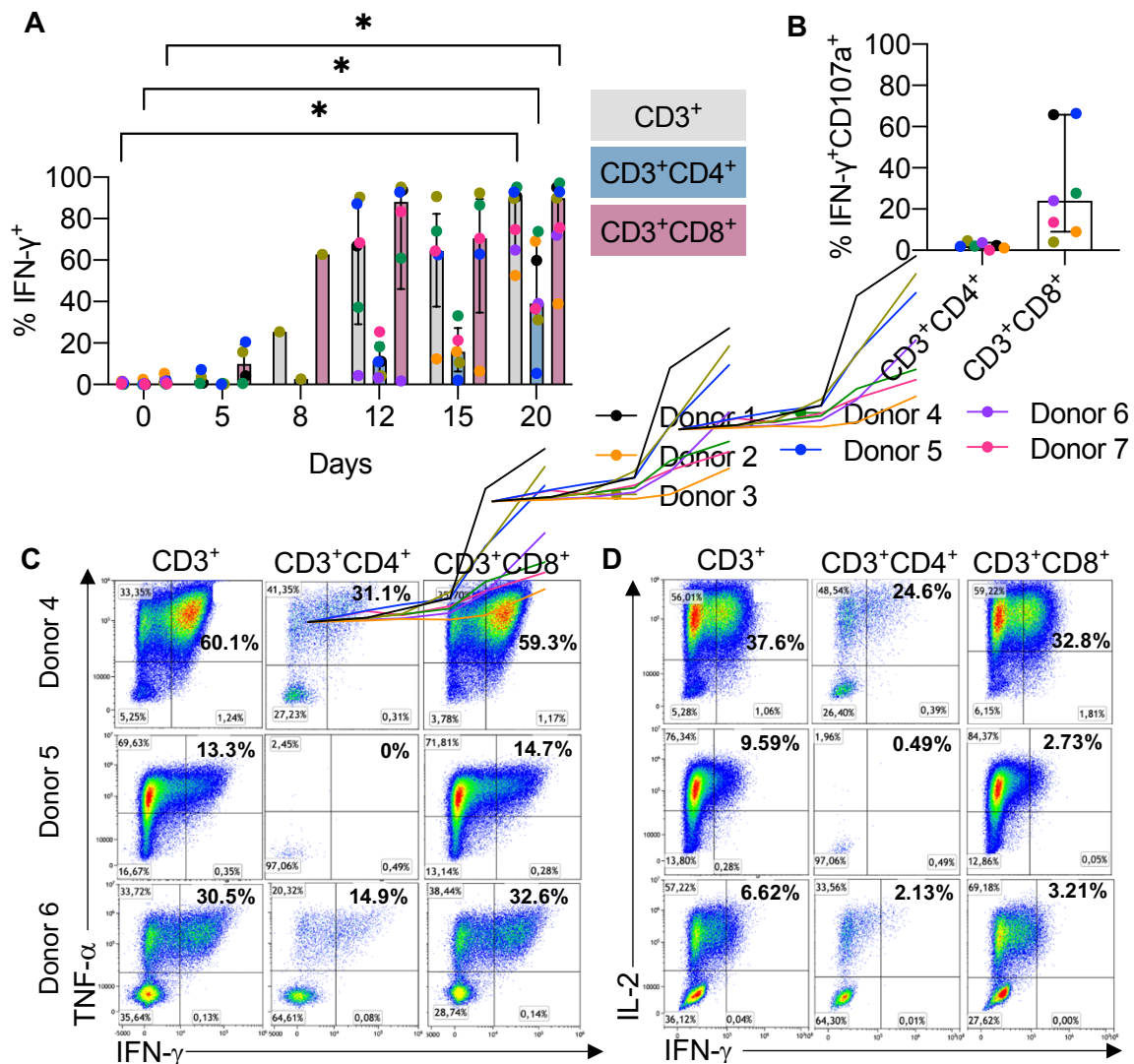


Figure 34. Polyfunctional EBV-specific T cells.

(A) Percentage of IFN- γ production in the different T cell subpopulations pre-expansion (day 0) and post-expansion at different time points during culture. The Wilcoxon test was performed to determine significant differences between each day of culture relative to day 0. Statistical significance was set at: (*) p -value of <0.05 , (**) p -value of <0.001 and (***) p -value of <0.0001 . (B) Percentage of degranulation marker in IFN- γ ⁺CD4⁺ and IFN- γ ⁺CD8⁺ T cells on day 20 of culture. Each value is represented as the median with IQR of the replicates ($n = 7$). (C) Production of TNF- α and (D) IL-2 in IFN- γ -producing CD4⁺ and CD8⁺ T cells from donors 4, 5 and 6 on day 20 of culture. Each color represents a different donor sample.

In order to determine the clonality and diversity of the expanded EBVST products, T cell receptor beta (TCR- β) was sequenced from all donors. A median of 24,617 (IQR: 25,070.03-23,805.52) T cells were amplified for days 0, 12, 15, and 20, resulting in a total of 98,783.50 (IQR: 142,927-79,305.25) sequenced reads. The alignment success rate was 89.31% (IQR: 90.12-86.51%), with

a depth coverage of 64,843.5 (IQR:84,126.50-50,192.50) for productive clonotypes, meaning the reads obtained after alignment and the exclusion of non-productive clonotypes.

The observed diversity (**Figure 35A**), normalized Shannon-Wiener index (**Figure 35B**), inverse Simpson index (**Figure 35C**) and D50 index (**Figure 35D**) showed a greater diversity on day 0 compared to the expanded T cells on days 12, 15, and 20, consistent with our findings of increased T cell specificity from day 12 onwards. Interestingly, the repertoire of donor 5 (blue color), from day 12 was lower compared to the other donors. This is likely due to a dominant clonotype present on day 0 that was possibly specific to the EBV virus, as by day 20, more than 90% of the reads belonged to this same clonotype (**Figure S3**).

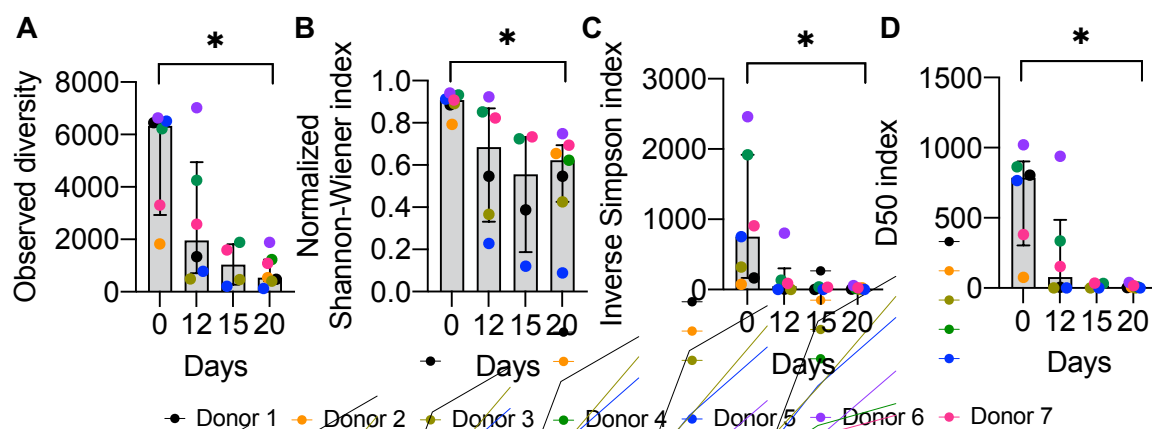


Figure 35. Comparative analysis of EBVSTs TCR- β diversity pre- and post-expansion.

Bar graphs showing (A) Observed diversity (B) Normalized Shannon-Wiener index (C) Inverse Simpson index and (D) D50 index. Each color represents a different donor. Data are presented as the median with interquartile range of the replicates (n = 7). T cells on day 0 (pre-expansion) corresponding to the PBMCs isolated from each donor.

In the TCR- β sequencing analysis, the average length of the CDR3 region was between 42 and 44 nucleotides, corresponding to 14-15 amino acids, with a normal distribution and measurements within the expected values for a diverse TCR repertoire (**Figure S4A**). By day 20, although the amino acid sequences remained within the expected range, the normal distribution was altered due to the expansion of T cells, as each expansion presented different clonotypes (**Figure S4B**).

On the other hand, the repertoire of T cells from the PBMCs on day 0 showed a higher diversity of VJ segment combinations, suggesting greater repertoire diversity (**Figures 36A-B**).

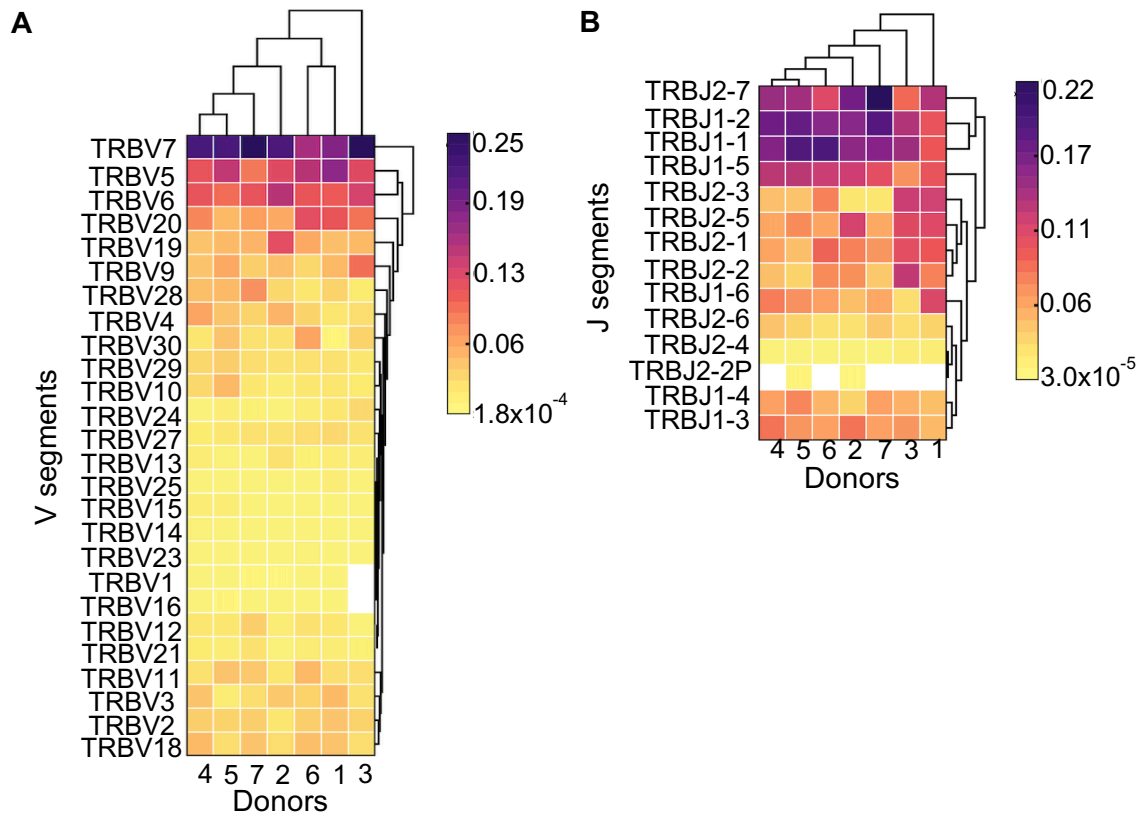


Figure 36. Comparison of V and J gene segments usage frequencies in TCR- β analysis of PBMCs from different donors.

Heatmap for (A) TRBV segments and (B) TRBJ segment expression from PBMCs on day 0. The scale color represents the usage frequencies in each TRBV and TRBJ segments.

While, by day 20, the EBVSTs exhibited a reduced diversity of specific V and J segment combinations. The expanded clonotypes were not consistently composed of the same TRBV and TRBJ segments. However, TRBV-5, TRBV-6, and TRBV-7 were identified in the expanded clonotypes from various donors, and these segments were also the most frequent at day 0 (**Figures 37A-B**). These findings confirm the results of clonal diversity.

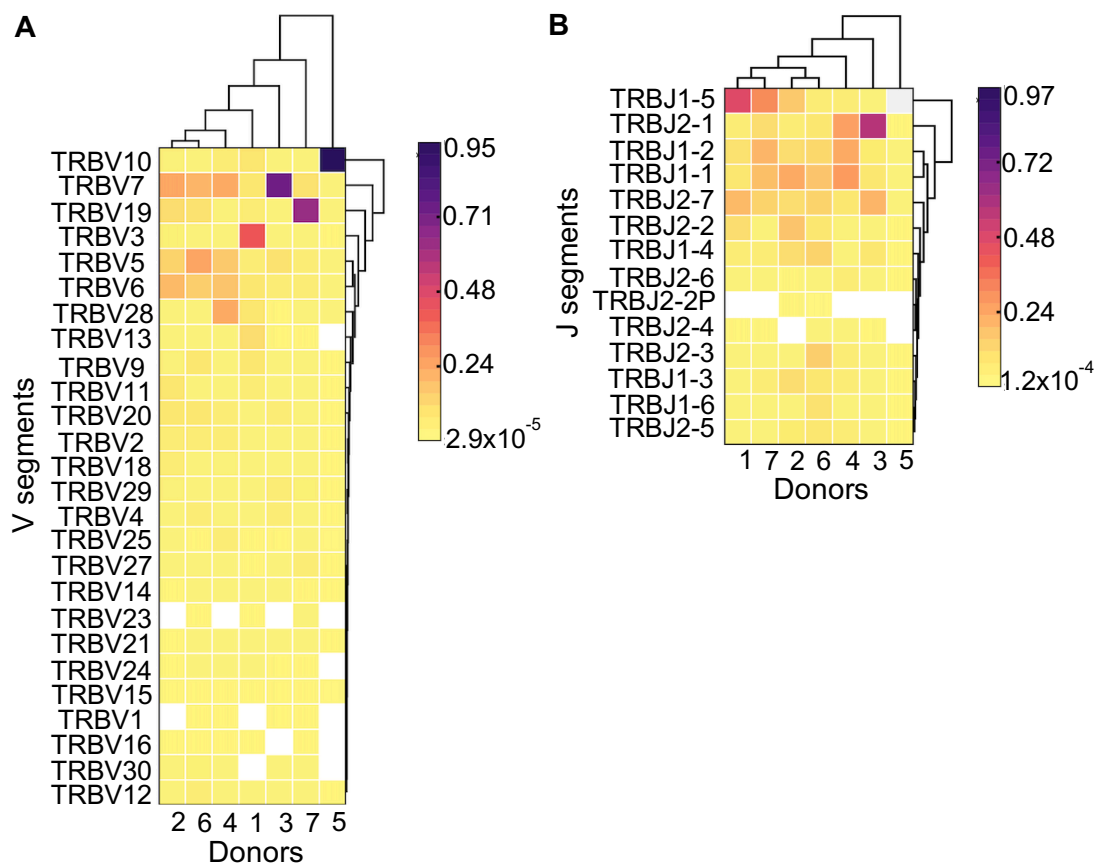


Figure 37. Comparison of V and J gene segments usage frequencies in TCR- β from expanded EBVSTs from different donors.

Heatmap for (A) TRBV segments and (B) TRBJ segment expression from EBVSTs on day 20. The scale color represents the usage frequencies in each TRBV and TRBJ segments.

On day 20, a median of 6 clonotypes were found with a frequency greater than 2%, which occupied a median abundance of 49.30% of repertoire. In contrast, these clonotypes accounted for only 0.63% of the repertoire on day 0. Public CDR3 amino acid sequences were found in all donors on day 0 and day 20. On day 0, they share a mean of 1.5 clonotypes among them (from 0 to 6) (**Figure 38A**), while on day 20 the mean number of shared clonotypes decreases to 0.57 (from 0 to 4) (**Figure 38B**). Among the clonotypes shared on day 20, we observe that donor 7 shares clonotypes with most donors, while donors 2 and 3 share clonotypes with only one other donor. Interestingly, donors 1 and 5 share several clonotypes with each other (**Figure 38B**). The clonotypes shared among donors are shown in **Table 19**, along with the description of the antigen, epitope sequence and HLA restriction. Additionally, it can be observed that the CDR3 amino acid sequences are similar between those that recognize each antigen.

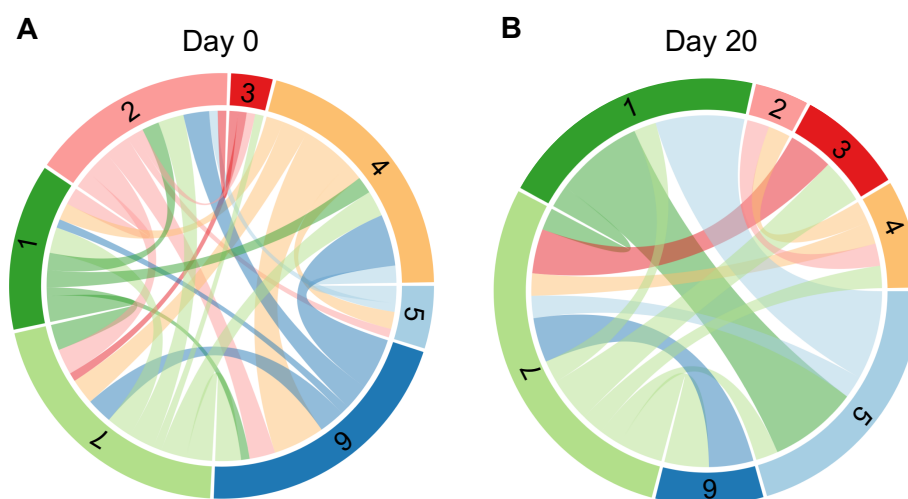


Figure 38. Comparison of TCR- β clonotypes diversity in expanded EBVSTs from 7 donors. Diversity of shared clonotypes between donors in (A) PBMCs on day 0 and (B) expanded EBVSTs on day 20.

Table 19. CDR3 amino acid sequences shared in expanded products on day 20

CDR3 aa sequence	Donors	EBV antigen	Epitope	HLA restriction*
CSVGTGGTNEKLFF	3 and 7	BMLF1	GLCTLVAML	<i>A*02:01</i>
CSVGSGGTNEKLFF				
CASGTGDSNQPQHF	1 and 5	BZLF1	EPLPQGQLTAY	<i>B*35:01</i>
CASSTGDSNQPQHF				
CAISTGDSNQPQHF				
CASSTGDNNQPQHF				
CASSERGHQETQYF	2 and 4			
CASSFEVNTGELFF	4 and 7			
CASSLGADMDGYTF	6 and 7			
CASSLGGETQYF	5 and 7		Not reported	
CASSLGVNQPQHF	1 and 7			
CASSSGSSYEQYF	6 and 7			

Data obtained from public TCR sequence databases (<http://tools.iedb.org/tcrmatch/>, <https://vdjdb.cdr3.net/> and <https://friedmanlab.weizmann.ac.il/McPAS-TCR/>). aa, amino acid.

*HLA typing on Table 12.

We performed tetramer staining to identify and confirm that the CD8⁺ T cells expanded in our EBVST products express a specific TCR capable of recognizing EBV antigens. The expanded EBVSTs from donor 3 predominantly recognized the YVLDHLIVV and CLGGLLTMV epitopes, which correspond to the BRLF1 and LMP2A antigens, respectively. Additionally, they recognized other epitopes to a lesser extent, including GLCTLVAML from the BMLF1 antigen, presented by the donor's HLA class I allele *A*02:01*, consistent with the results from the TCR- β analysis (Figure 39A). EBVSTs expanded from the same donor, also recognized the RAKFKQLL and

FLRGRAYGL epitopes, corresponding to the BZLF1 and EBNA-3 antigens presented by *B*08:01* allele (**Figure 39B**). In the case of donor 6, the expanded EBVSTs recognized to a lesser extent the epitopes of BRLF1 and LMP2A antigens presented by *HLA-A*24:02* (**Figure 39C**).

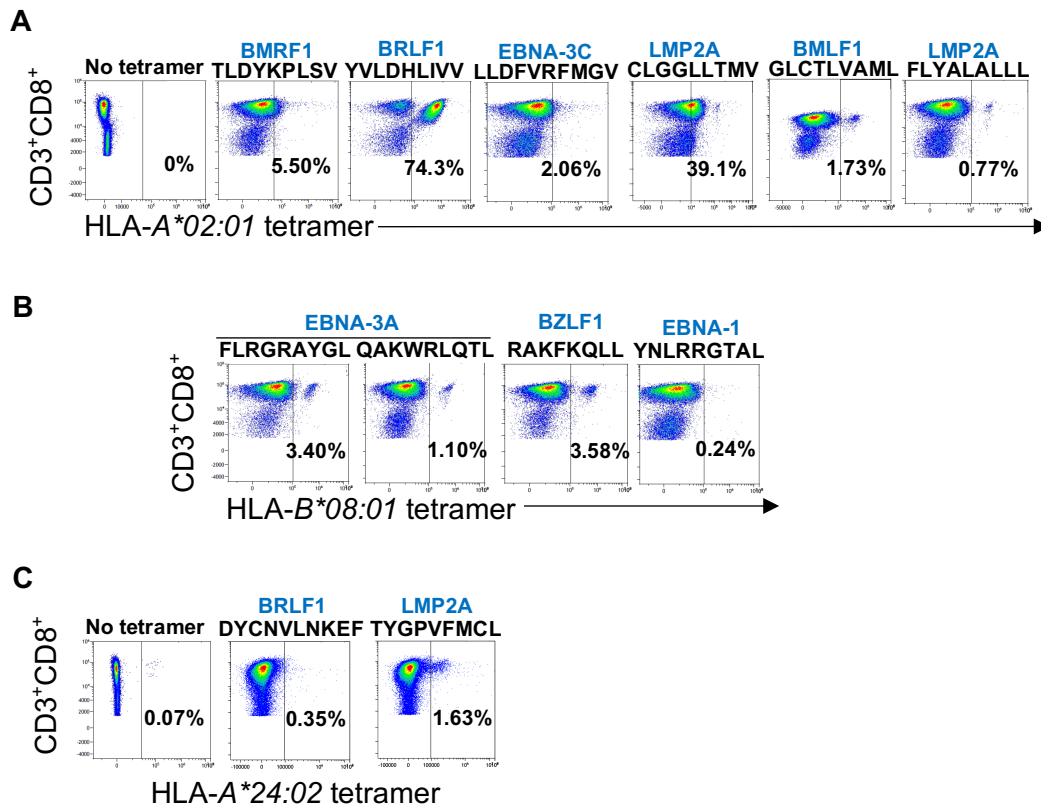


Figure 39. HLA class I tetramer analysis of EBV-specific CD8⁺ T cells in the expanded EBVSTs.

Representative plots of tetramer staining in two expanded EBVSTs products, analyzed using flow cytometry. Expanded EBVSTs from (A) donor 3, showing binding to different HLA-A*02:01-peptide complex, and (B) HLA-B*08:01-peptide complex. (C) Expanded EBVSTs from donor 6, showing binding to different HLA-A*24:02-peptide complex. The epitope (amino acid sequence) and antigen (in blue) for each tetramer used are described above each plot. No tetramer indicates negative control.

The T cell phenotype study showed that as the culture days progressed, the T_{N+SCM} population decreases while the T_{EM} cell population increases (**Figures 40A-D**). By day 20, approximately 20% of T_{N+SCM} cells were retained in the CD4⁺ T cell population (**Figure 40A**), whereas this percentage was minimal in the CD8⁺ T cell population (**Figure 40B**), as was observed for the T_{CM}. The T_{EMRA} cell phenotype accounted for less than 6% of the T cell subpopulations. Consequently, EBVST cells primarily exhibited a memory effector phenotype starting from day 15 in both CD4⁺ and CD8⁺ T cells (**Figure 40A-B**), and from day 12 in the IFN- γ ⁺CD4⁺ and IFN- γ ⁺CD8⁺ T cells (**Figure 40C-D**).

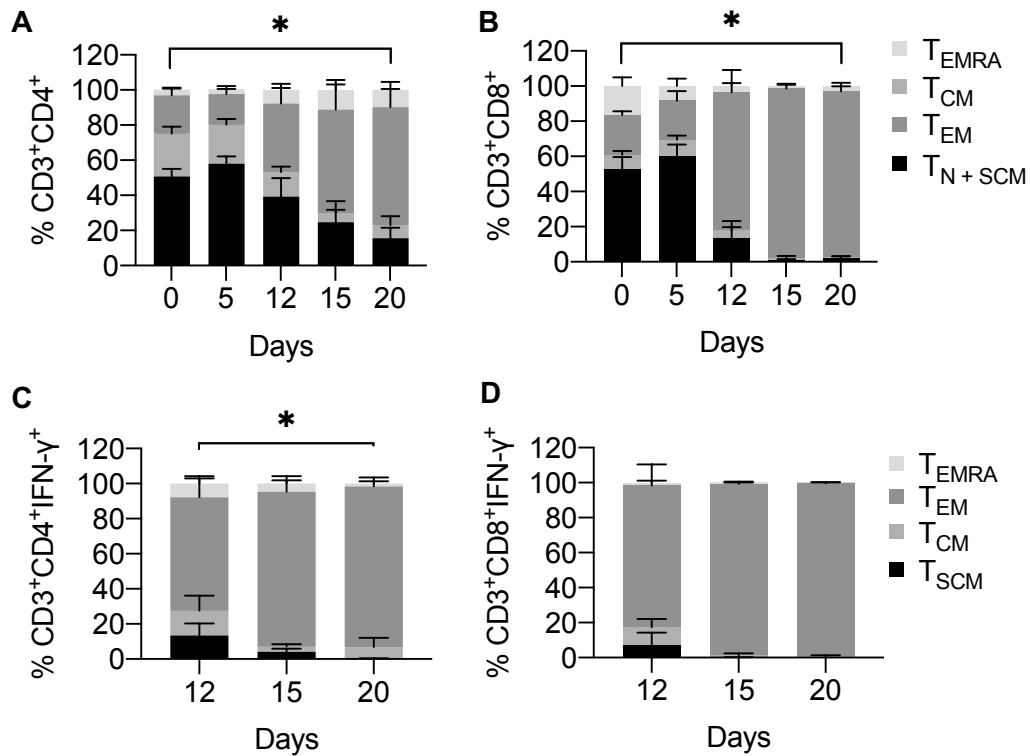


Figure 40. T cell differentiation phenotypes in the optimized condition for generating EBVSTs.

Comparison of T cell subsets differentiation phenotype pre-expansion (day 0) and post-expansion at different time points during culture (**A**) $CD4^+$ and (**B**) $CD8^+$ T cells. Comparison of memory T cell subsets during the expansion phase for (**C**) $CD3^+CD4^+IFN-\gamma^+$ and (**D**) $CD3^+CD8^+IFN-\gamma^+$ T cells. T_N indicates naïve T cell ($CCR7^+CD45RA^+$); T_{SCM} , T memory stem cells ($CCR7^+CD45RA^+$); T_{CM} , central memory T cell ($CCR7^+CD45RA^-$); T_{EM} , effector memory T cell ($CCR7^-CD45RA^-$); and T_{EMRA} , terminally differentiated effector memory T cell ($CCR7^-CD45RA^+$). The figures are represented as the median with IQR of the replicates ($n = 7$). T cell subsets of $CD4^+$ and $CD8^+$ T cell populations were only compared at day 0, whereas $IFN-\gamma$ T cell populations were compared at days 12, 15, and 20. The Wilcoxon test was performed to determine significant differences between each day of culture relative to day 0. Statistical significance was set at: (*) p -value of <0.05 , (**) p -value of <0.001 and (***) p -value of <0.0001

Although the phenotype study did not show a high percentage of T_{EMRA} cells, we decided to evaluate the exhaustion markers TIM-3, LAG-3, PD-1 and CTLA-4 in two expansions from donors 6 and 7. A low level of expression of exhaustion markers was observed, except for donor 7, who exhibited a high percentage of LAG-3 (51.87%) in the $CD8^+$ T cell population (**Figure 41**).

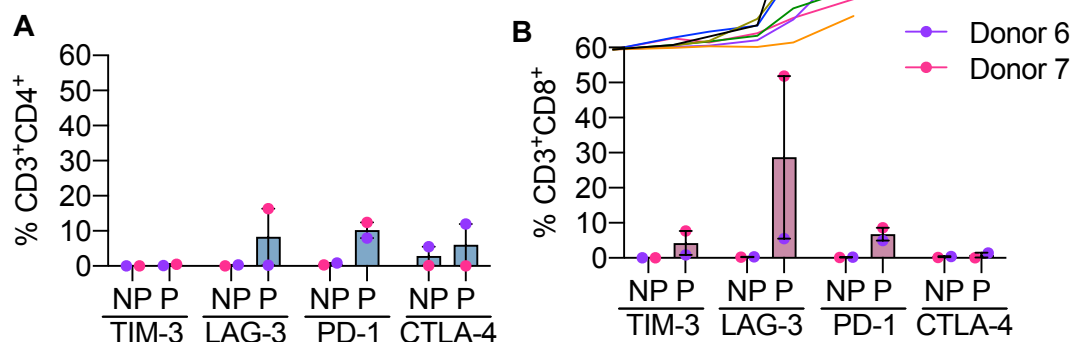


Figure 41. Expression of exhaustion markers in CD4⁺ and CD8⁺ T cells from EBVSTs.

Expression of cell surface markers (TIM-3, LAG-3, PD-1, CTLA-4) on (A) CD4⁺ and (B) CD8⁺ T cells, characterized at day 20, with cells either pulsed (P) overnight with PepTivator[®] EBV consensus or non-pulsed (NP). Data are presented as percentages of each surface marker, with median and IQR.

1.7. Selected condition using different stimuli for PBMC activation

Using the optimized protocol, we evaluated and compared the activation and expansion of EBVSTs with EBNA-1, LMP2A and combination of EBNA-1 + PepTivator[®] EBV consensus antigens. EBNA-1 and LMP2A are significant targets in the context of EBV-related tumors. Additionally, we aimed to determine whether these antigens contribute to an increase in the CD4⁺ T cell population in our product, as the literature suggests that both antigens are involved in the EBV-specific CD4⁺ memory T cell response.^{165–167}

A comparison of the PepTivator[®] EBV consensus, EBNA-1 and the combination of EBNA-1 + PepTivator[®] EBV consensus was conducted in the expansion of EBVSTs from donor 4. It was observed that the combination of both stimuli enhanced fold expansion (**Figure 42A**). However, when this combined stimulus was repeated with two donors (10 and 11), the fold expansion achieved was 18.37 and 9.90, respectively, compared to 25.67-fold observed in donor 4 (**Figure 42B**). In the case of LMP2A stimulus, activation and expansion were conducted with donors 6 and 7. It was noted that T cells expanded slightly less compared to those stimulated with PepTivator[®] EBV consensus (**Figure 42C**).

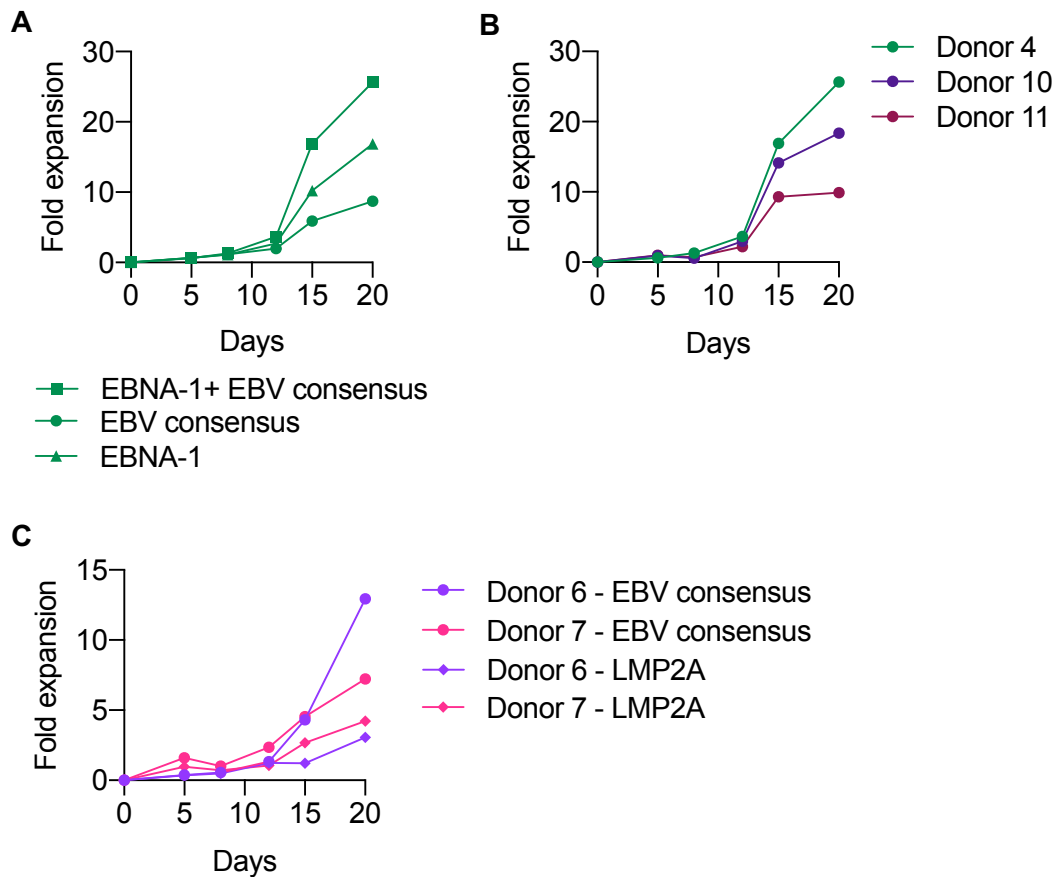


Figure 42. Comparison of the fold expansion of EBVSTs with different stimuli.

(A) Fold expansion in the T cells from donor 4 stimulated with PepTivator® EBV consensus, EBNA-1 and combination of both (EBNA-1 + PepTivator® EBV consensus). (B) Fold expansion in T cells from donors 4, 10 and 11, stimulated with the combination of EBNA-1 + PepTivator® EBV consensus. (C) Fold expansion in T cells from donors 6 and 7, stimulated with PepTivator® EBV consensus and LMP2A.

The stimuli PepTivator® EBV consensus, EBNA-1 + PepTivator® EBV consensus and LMP2A showed a predominant CD8⁺ T cell phenotype at day 20 of the culture. Even so, in the final product of T cells activated with EBNA-1+PepTivator® EBV consensus and LMP2A, there was a higher percentage of CD4⁺ T cells (median 11.88% and 25.95%, respectively) than when using PepTivator® EBV consensus alone (median 8%). In contrast, using only the EBNA-1 stimulus to activate and expand T cells predominantly resulted in CD4⁺ T cells (Figure 43A). The IFN- γ specificity of the three T cell populations (CD3⁺, CD4⁺ and CD8⁺) (Figure 43B) and CD107a (Figure 43E) were higher when the PepTivator® EBV consensus stimulus was included. While the production of TNF- α (Figure 43C) and IL-2 (Figure 43D) is favored when T cells are activated with EBNA-1+PepTivator® EBV consensus stimuli together.

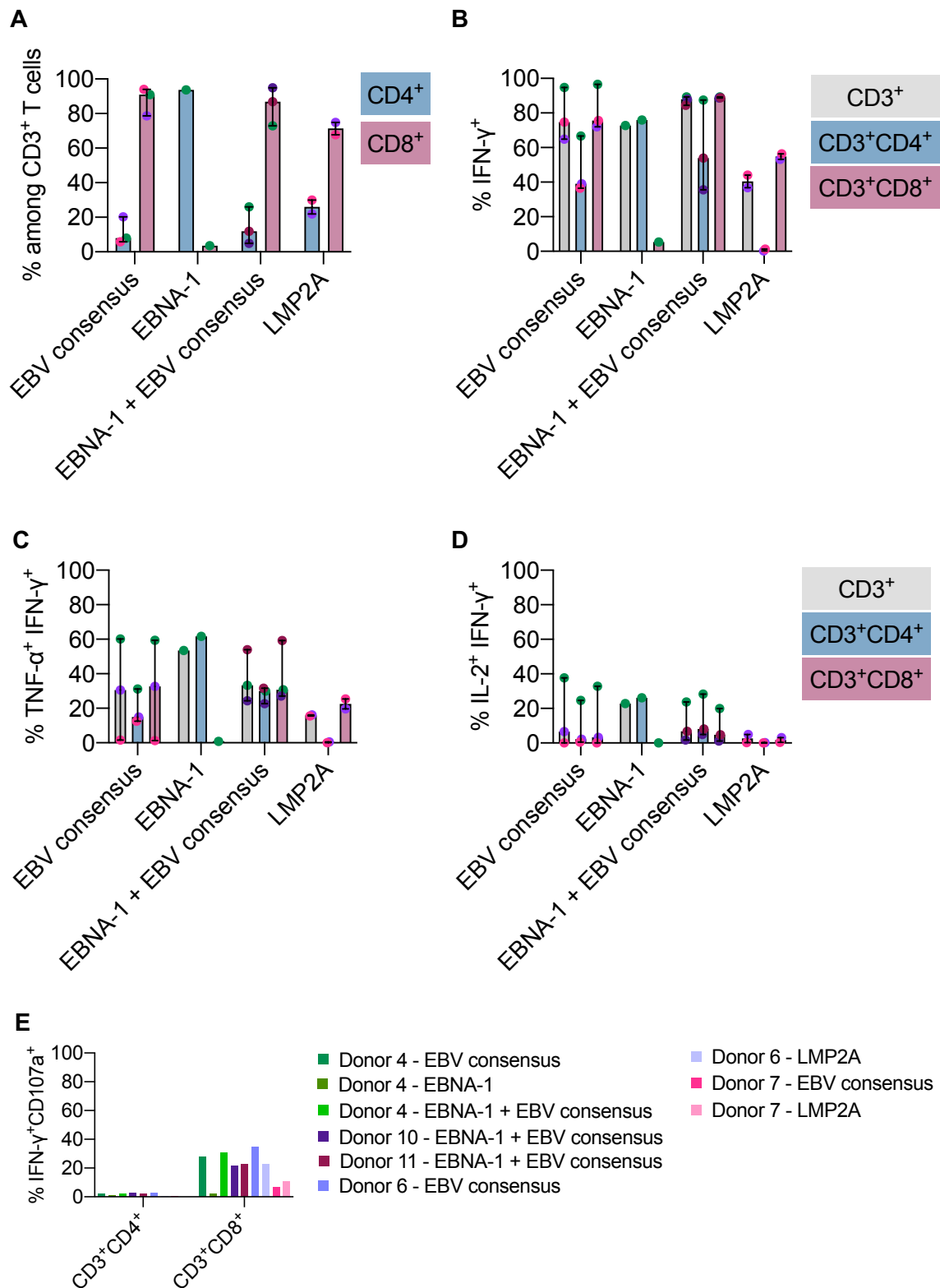


Figure 43. Comparison of EBVSTs characterization and specificity under different stimuli.

(A) Percentage of CD4⁺ and CD8⁺ T cell subpopulations post-expansion (day 20). (B) Percentage of IFN- γ production in different T cell subpopulations post-expansion (day 20). (C) Percentage of TNF- α production in different T cell subpopulations post-expansion (day 20). (D) Percentage of IL-2 production in different T cell subpopulations post-expansion (day 20). (E) Percentage of degranulation marker in IFN- γ ⁺CD4⁺ and IFN- γ ⁺CD8⁺ T cells at day 20 of culture.

In vitro cytotoxicity assays of the expanded products from donors 4 (**Figure 44A-B**) and 11 (**Figure 44C-D**) demonstrated that EBVSTs activated and expanded with EBNA-1+ PepTivator[®] EBV consensus at day 20 exhibited specific lysis of $54.47\pm 1.92\%$ and 56.53 ± 0.98 , respectively, against peptide-pulsed PHA-blasts generated from the same donors.

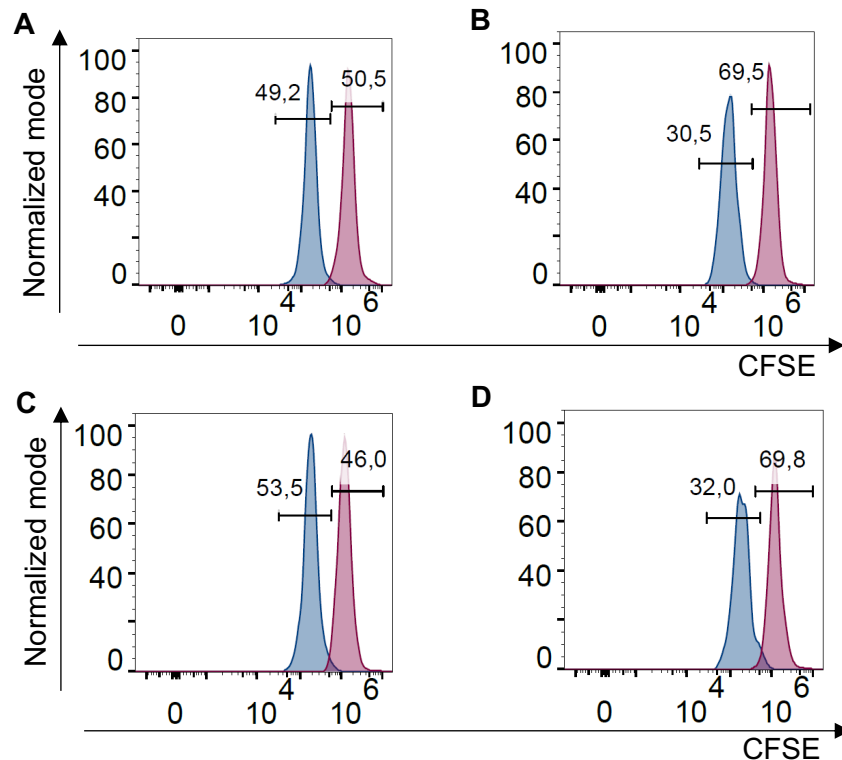


Figure 44. PHA-blast cytotoxicity assay in the final EBVSTs product.

(A) PHA-blast without EBVSTs (control) from donor 4. (B) Co-culture between PHA-blasts and EBVSTs from donor 4 at a ratio 1:5 (Target:Effector). (C) PHA-blast without EBVSTs (control) from donor 11. (D) Co-culture between PHA-blasts and EBVSTs from donor 11 at a ratio 1:5 (Target:Effector). The blue peak represents PHA-blasts pulsed with PepTivator[®] EBV consensus, and the red peak represents non-pulsed-peptide PHA-blasts. Three replicates of each condition were performed, but only replicate 1 is shown.

Comparison of the TCR- β analysis of EBVSTs showed a higher percentage of reads in clonotypes when cells were stimulated with PepTivator[®] EBV consensus (**Figure 45A-B**), compared to stimulation with EBNA-1 alone (**Figure 45C**). Of the clonotypes expanded with the EBNA-1 + PepTivator[®] EBV consensus combination, 5 were shared with cells expanded with PepTivator[®] EBV consensus alone, while none identified in the product expanded with EBNA-1 alone. Two clonotypes with the following CDR3 sequences: CASSSQGGGYGYTF and CASSLVHNEQFF, are described in the literature as recognizing the FLYALALL and YVLDHLIVV epitopes of the LMP2A and BRLF1 antigens, respectively, presented by the HLA class I allele *A*02:01* expressed by the donor. These findings are supported by the tetramer assay (**Figure 45D**).

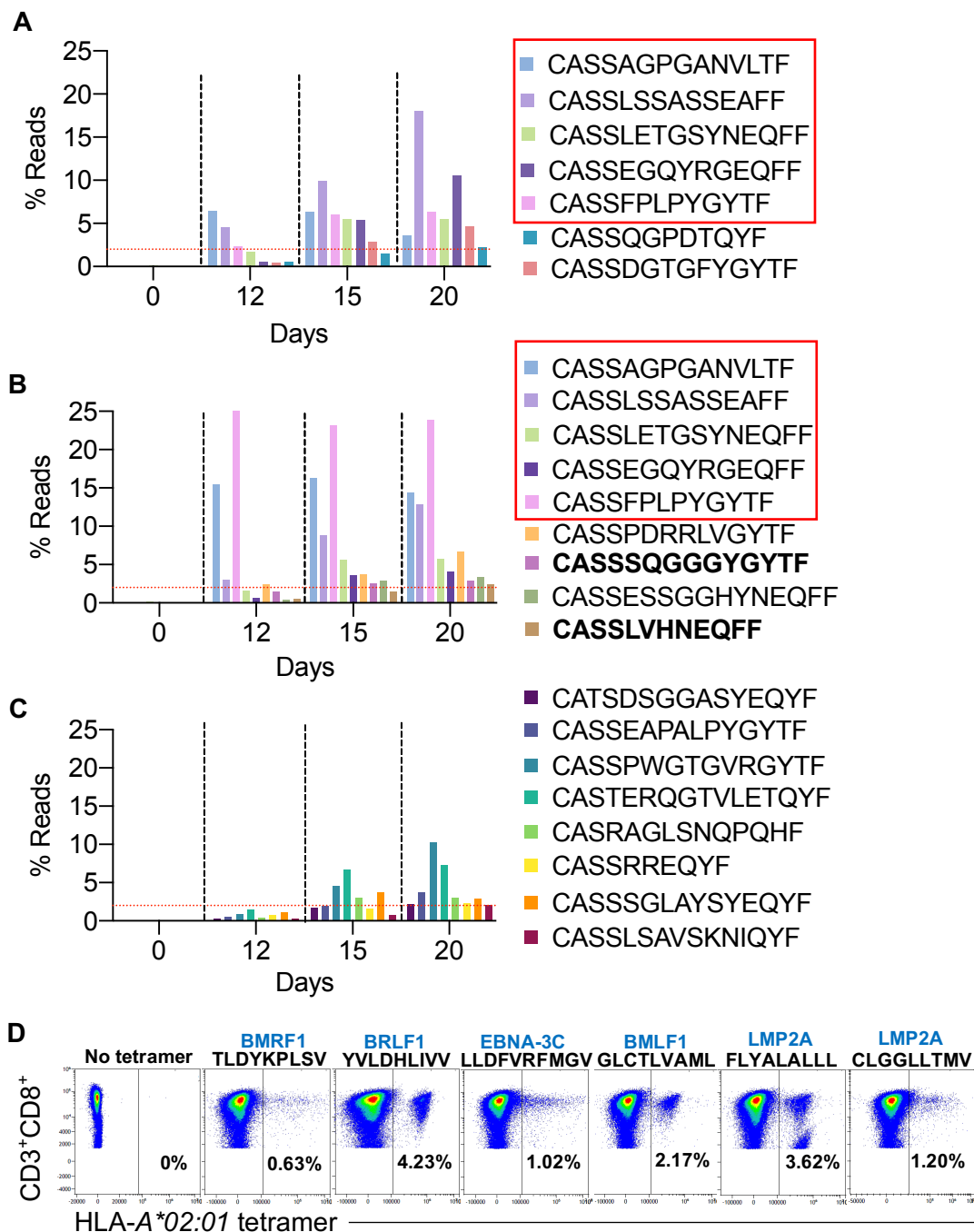


Figure 45. Comparison of TCR- β analysis and tetramer assay of EBVSTs under different stimuli.

(A) CDR3 sequences of clonotypes with more than 2% reads (red dotted line) obtained at days 0, 12, 15 and 20 with PepTivator[®] EBV consensus stimulus. (B) CDR3 sequences of clonotypes with more than 2% reads obtained with EBNA-1+PepTivator[®] EBV consensus stimuli. (C) CDR3 sequences of clonotypes with more than 2% reads obtained with EBNA-1 stimulus. (D) Representative dot plots of tetramer staining in the EBVSTs product at day 20, activated and expanded with EBNA-1+PepTivator[®] EBV consensus. CDR3 sequences in bold from the TCR- β , represent the clonotypes described in the literature. The epitope (amino acid sequence) and antigen (in blue) of each tetramer used are described above each plot. No tetramer indicates negative control. This comparison was with the EBVSTs obtained from donor 4.

In the EBVSTs, stimulated with EBNA-1+PepTivator[®] EBV consensus, from donor 10, five clonotypes with more than 2% reads were expanded. One of these clonotypes, with the CDR3 amino acid sequence CASSLGQAYEQYF, is described in the literature as recognizing the FLRGRAYGL epitope of the EBNA-3A antigen, presented by the HLA class I allele *B*08:01* expressed by the donor. These results are confirmed by the tetramer assay (**Figure 46**).

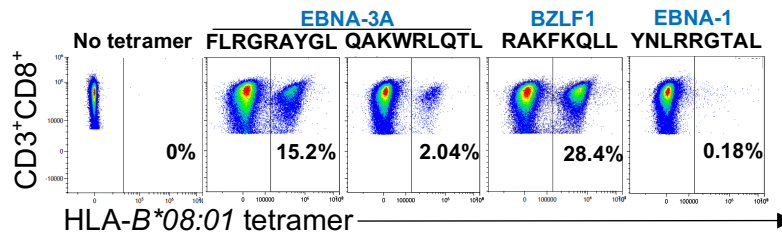


Figure 46. Tetramer assay of expanded EBVSTs with EBNA-1+PepTivator[®] EBV consensus stimuli. Representative dot plots of tetramer staining in the EBVSTs product at day 20 from donor 10. The epitope (amino acid sequence) and antigen (in blue) of each tetramer used are described above each plot. No tetramer indicates negative control.

Meanwhile, the EBVSTs, stimulated with EBNA-1+PepTivator[®] EBV consensus, from donor 11, four different clonotypes with more than 2% reads were expanded. Two of these clonotypes, with the CDR3 amino acid sequence CASSLTSAGELFF and CASSLSSASGELFF, are described in the literature as recognizing the AVFDRKSDAK epitope of the EBNA-4 antigen, presented by the HLA class I allele *A*11:01*. However, we did not have the HLA-peptide complex tetramer to confirm this result. In the TCR- β analysis of LMP2A, the expanded clonotypes were not found to be described in the literature to recognize EBV antigens.

At day 20 of culture, regardless of the stimulus used for activation and expansion, the majority of T cells exhibited T_{EM} phenotype (**Figure 47A-D**). However, CD8⁺ T cells stimulated and expanded with EBNA-1 not only displayed T_{EM} phenotype but also included T_{N+SCM}, T_{CM} and T_{EMRA} phenotypes (**Figure 47B and D**). In contrast, the LMP2A stimulus resulted in more than 3% of T_{EMRA} in CD4⁺ and CD8⁺ T cells (**Figure 47A-B**) as in IFN- γ ⁺CD4⁺ T cells (**Figure 47C**).

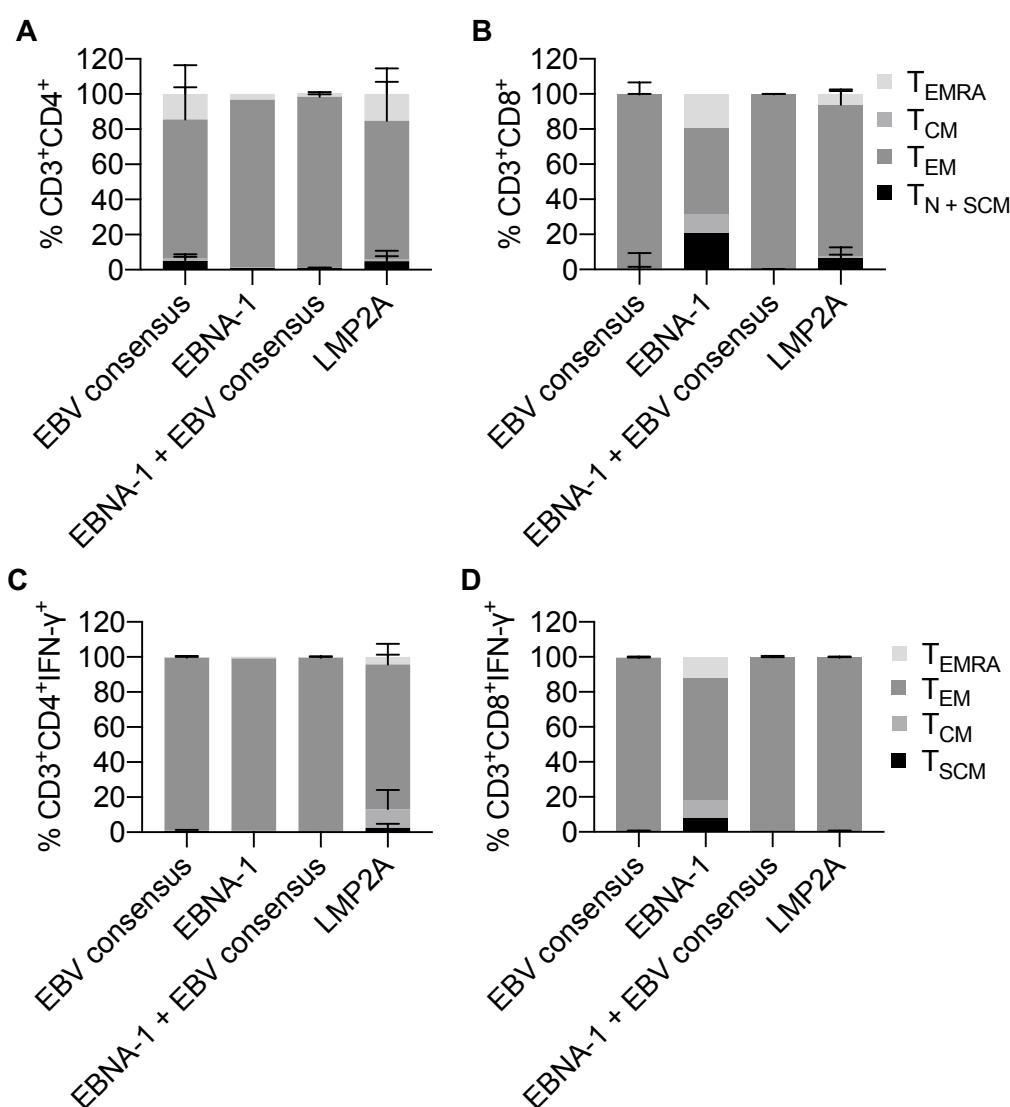


Figure 47. Comparison of T cell differentiation phenotypes under different stimuli.

Differentiation phenotype subsets in (A) CD4⁺ and (B) CD8⁺ T cells post-expansion (day 20). (C) Memory CD3⁺CD4⁺IFN- γ ⁺ T cells and (D) CD3⁺CD8⁺IFN- γ ⁺ T cells post-expansion (day 20). T_N indicates naïve T cell (CCR7⁺CD45RA⁺); T_{SCM}, T memory stem cells (CCR7⁺CD45RA⁺); T_{CM}, central memory T cell (CCR7⁺CD45RA⁻); T_{EM}, effector memory T cell (CCR7⁻CD45RA⁻); and T_{EMRA}, terminally differentiated effector memory T cell (CCR7⁻CD45RA⁺). Data are presented as median and interquartile range of the replicates (n = 3, donor 4, 10 and 11 for EBNA-1 and EBV consensus; and n = 2, donor 6 and 7 for LMP2A).

Exhaustion markers indicated that CD8⁺ T cells exhibited a median expression of 51.28% (IQR:60.04%-44.88%) for LAG-3 and 7.11% (IQR:15.13%-3.23%) for PD-1 (Figure 48A). In contrast, CD4⁺ T cells showed a median expression of 21.25% (IQR: 21.37%-1.56%) for LAG-3 and 17.85% (IQR:18.16%-7.62%) for PD-1 (Figure 48B).

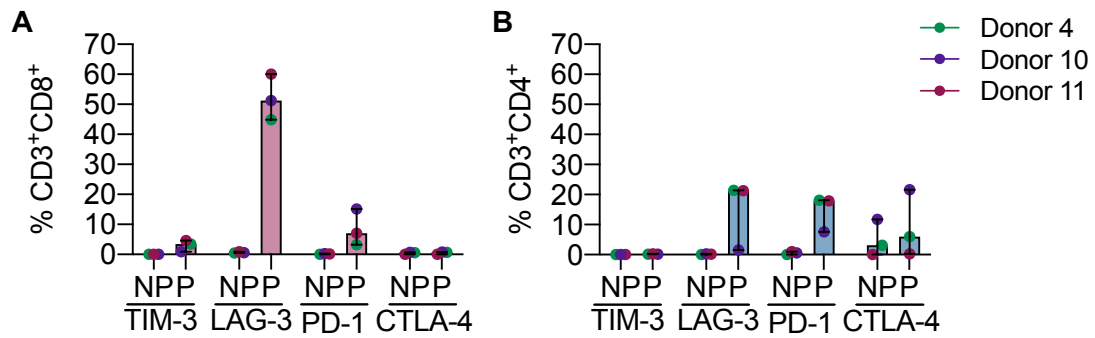


Figure 48. Expression of exhaustion markers in CD8⁺ and CD4⁺ T cells from EBVSTs stimulated with PepTivator[®] EBV consensus/EBNA-1.

Expression of cell surface markers (TIM-3, LAG-3, PD-1, CTLA-4) on (A) CD4⁺ and (B) CD8⁺ T cells, characterized at day 20. Cells were either pulsed (P) overnight with PepTivator[®] EBV consensus and EBNA-1 or non-pulsed (NP). Data is presented as the median and IQR of the replicates (n = 3, donor 4, 10 and 11).

Chapter II: Large-scale activation and expansion of EBVSTs under GMP

After optimizing and replicating a protocol to generate EBVSTs on a small scale, we proceeded to scale it up and conduct the process under GMP conditions ($n = 1$). The large-scale culture achieved a fold expansion of 145.1, which is 11.2 times greater than that observed in the previous optimization experiments (**Figure 49A**). The proliferation kinetics were like those observed on a small scale, with a noticeable increase in cell proliferation from day 12 onwards. Therefore, our culture process appears to have two distinct phases: activation (days 0 to 12) and expansion (days 12 to 20). Cell viability throughout the 20 days of culture was consistently above 90% (**Figure 49B**). As with the small-scale process, the population kinetics remained consistent, resulting in a final product at day 20 with 98.25% CD3⁺ T cells, 94.55% CD8⁺ T cells and 4.0% CD4⁺ T cells (**Figure 49C**).

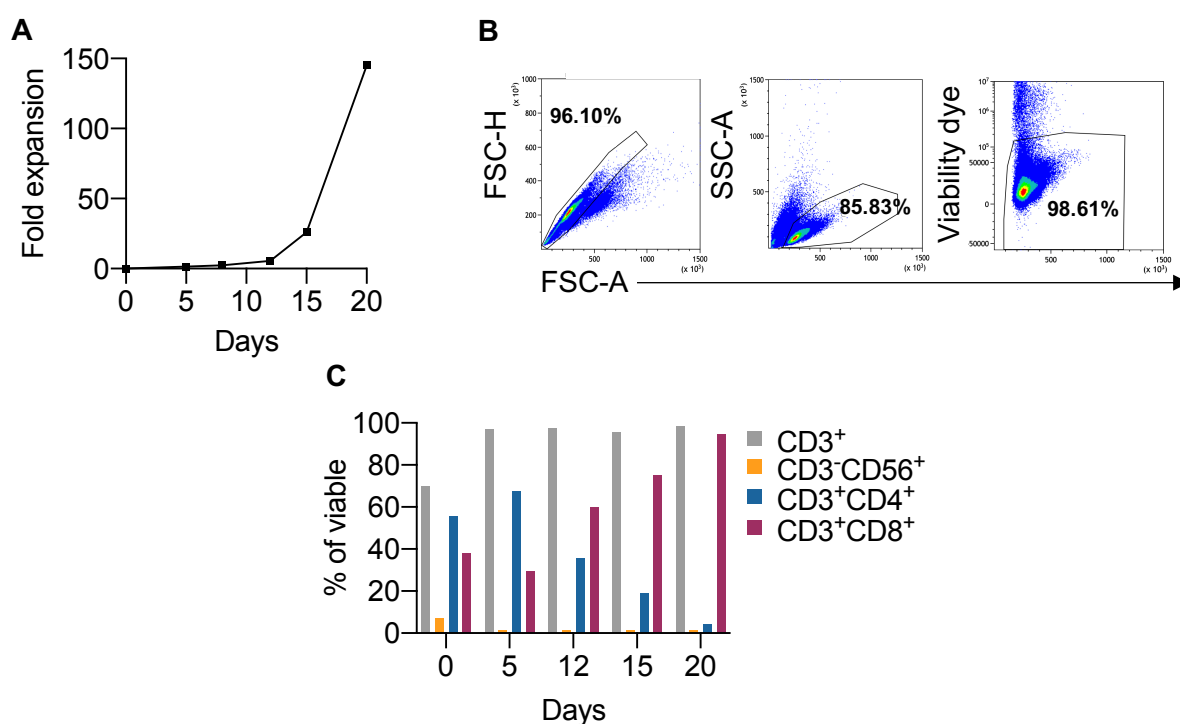


Figure 49. Phenotypic characterization in EBVSTs expanded on a large scale.

(A) Fold expansion of total cells at different time points during culture relative to day 0. (B) Representative flow cytometry dot plots of singlets, lymphocytes and viability at day 20. (C) Percentage of NK cells (CD3⁻CD56⁺) and T cell subpopulations (CD3⁺, CD4⁺ and CD8⁺) at different time points during culture.

IFN- γ production at day 20 was lower compared to the percentages obtained on a small scale; however, the EBVSTs product remained highly specific (**Figure 50A**). Additionally, IFN- γ -

producing T cells also produce TNF- α (Figure 50B) and IL-2 (Figure 50C). Specific CD8⁺ T cells exhibited 39.7% expression of the anti-CD107a degranulation marker (Figure 50D).

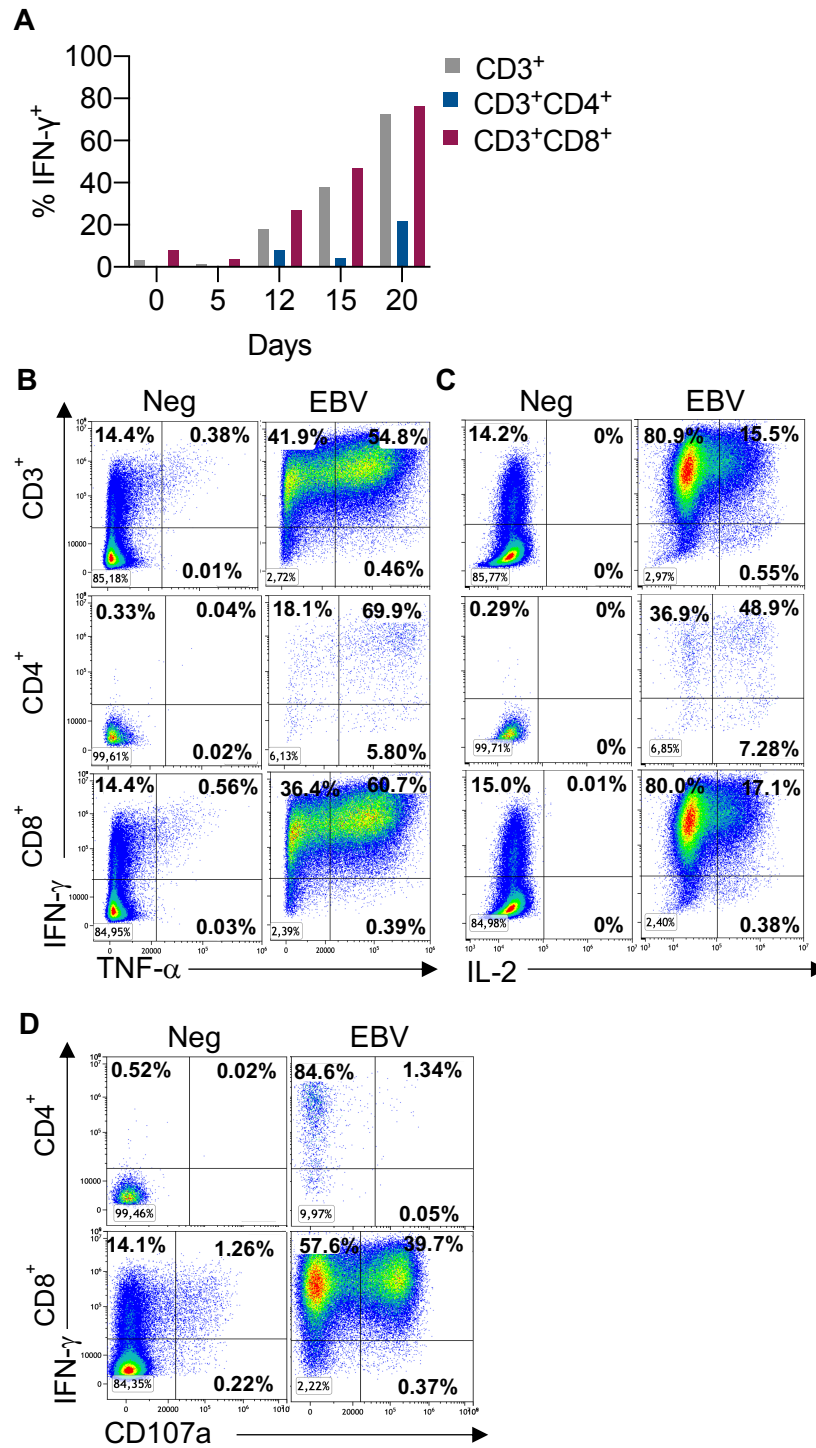


Figure 50. Specificity and degranulation marker of EBVSTs expanded on a large scale.

(A) Percentage of IFN- γ production in various T cell subpopulations pre-expansion (day 0) and post-expansion at different time points during culture. (B) Representative flow cytometry dot plots showing the percentage of TNF- α and (C) IL-2 co-expression in IFN- γ -producing CD3⁺, CD4⁺ and CD8⁺ T cells, stimulated (PepTivator[®] EBV) and non-stimulated (Neg, negative) at day 20. (D) Percentage of

degranulation marker in the $\text{IFN-}\gamma^+\text{CD4}^+$ and $\text{IFN-}\gamma^+\text{CD8}^+$ T cells on day 20 of the culture in stimulated (PepTivator[®] EBV select) and non-stimulated (Neg, negative) conditions.

The ELISpot assay demonstrated that on day 0, PBMCs produce a low amount of $\text{IFN-}\gamma$ (127 ± 12.5 SFU/ 10^5 PBMCs) in response to stimulation with the PepTivator[®] EBV select (**Figure 51A**). After activation and expansion of these cells to generate EBVSTs, a significant increase in $\text{IFN-}\gamma$ production (985.3 ± 54 SFU/ 10^5 EBVSTs) was observed in response to stimulation with the same peptide pools. This increase is clearly detected when using a density of 10^5 cells per well, indicating a robust specific immune response following T cell expansion (**Figure 51B**).

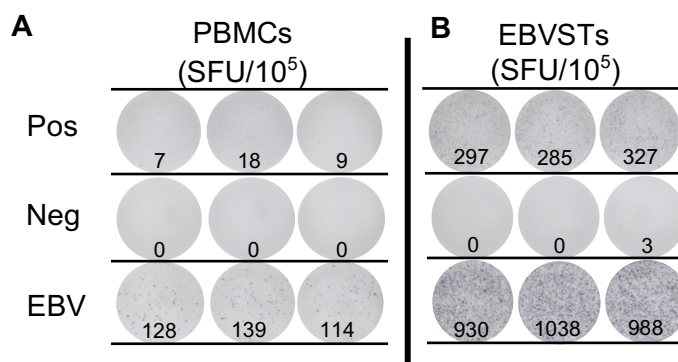


Figure 51. ELISpot assay comparison before and after stimulation and expansion of EBVSTs.

(A) ELISpot responses against PepTivator[®] EBV select pre activation and expansion of PBMCs (day 0), and (B) post-expansion (day 20), response at 10^5 cells/well. Positive control (Pos) cells were stimulated with PHA-A, and negative control (Neg) cells were left unstimulated. Each condition shows SFU (spot-forming units) for triplicates.

The cytotoxicity assay demonstrated that EBVSTs exhibit a specific lysis of $69.61\%\pm 6.40$ against peptide-pulsed PHA-blasts generated from the same donors (**Figure 52A-B**). The ELISpot assay further corroborated these findings, showing that EBVSTs produce a significantly increased amount of $\text{IFN-}\gamma$ (1009.33 ± 28.5 SFU/ 10^5 cells) when co-cultured with PHA-blasts pulsed with PepTivator[®] EBV consensus antigen compared to their production in the absence of the antigen (co-culture with non-pulsed PHA blasts), which yielded only 1.67 ± 0.57 SFU/ 10^5 cells (**Figure 52C**).

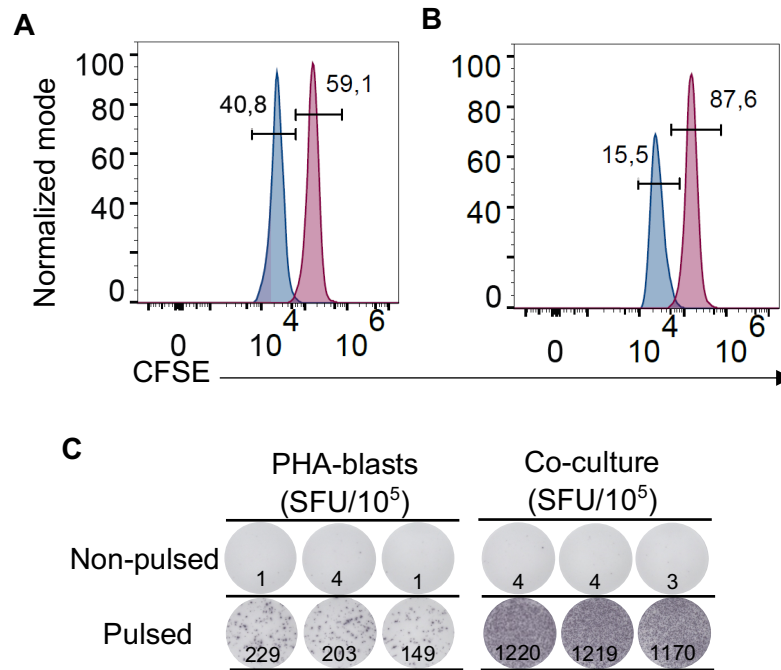


Figure 52. PHA-blast cytotoxicity assay of EBVSTs expanded on a large scale.

(A) PHA-blast without EBVSTs (control). (B) Cytotoxicity assay at a 1:5 ratio of PHA-blasts:EBVSTs. The blue peak represents PHA-blasts pulsed with PepTivator® EBV consensus, while the red peak represents non-pulsed PHA-blast. Three replicates were conducted for each condition, replicate 1 is shown. (C) ELISpot responses of EBVSTs in co-culture with either pulsed or non-pulsed PHA-blasts using PepTivator® EBV consensus. The co-culture was conducted at a 1:1 ratio (PHA-blast:EBVSTs). SFU (spot-forming units) from triplicates assays are shown for each condition.

As expected, observed diversity (**Figure 53A**), the normalized Shannon-Wiener index (**Figure 53B**), and the inverse Simpson index (**Figure 53C**) demonstrated greater clonal diversity at day 0 compared to the expanded T cells at day 20. This is consistent with our findings of increased T cell specificity by day 20. Additionally, the D50 index indicated that in the expanded EBVSTs at day 20, fewer clonotypes accounted for 50% of the total repertoire (**Figure 53D**). Shared clonotype analysis revealed a significant proportion of clonotypes were common across the repertoires of the expanded EBVSTs at days 12, 15 and 20 (**Figure 53E**). The Jaccard index further confirmed this similarity in the TCR- β repertoires, showing that the repertoires at day 12 and day 15 were similar, with even greater similarity between days 15 and 20 (**Figure 53F**).

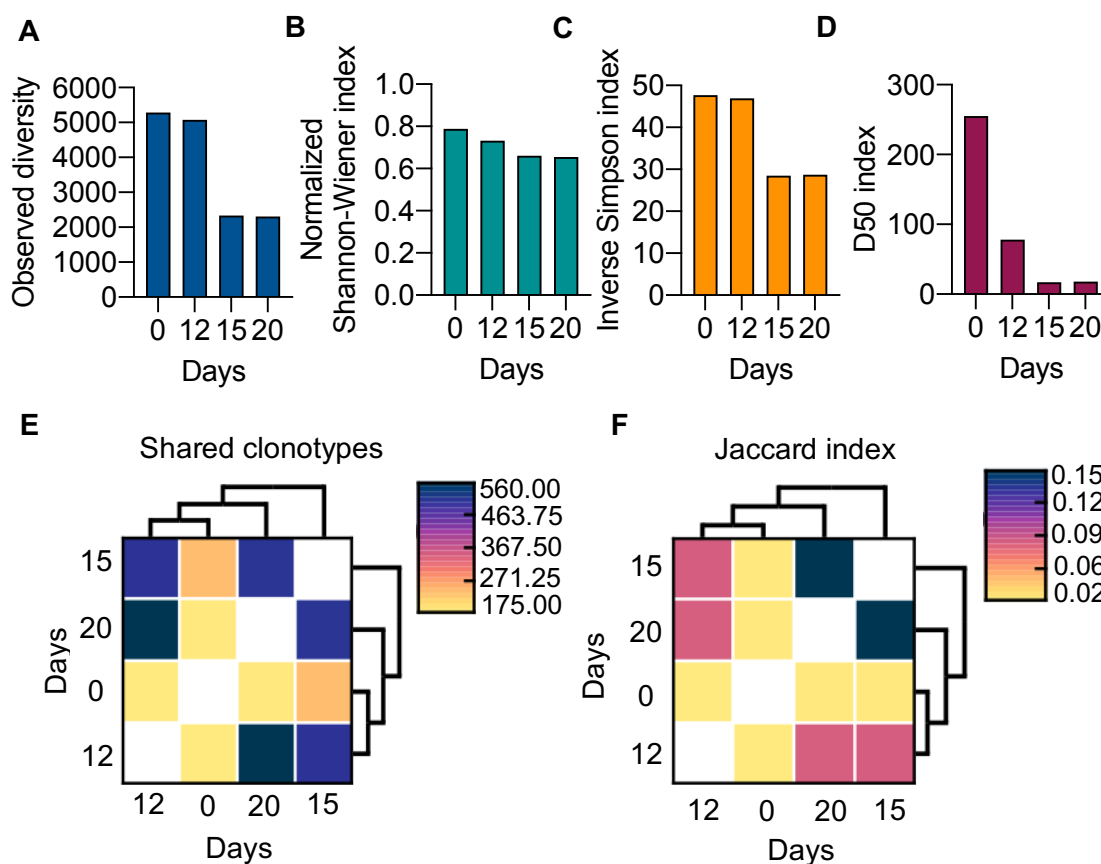


Figure 53. TCR- β diversity pre- and post-large-scale expansion of EBVSTs.

Bar graphs showing (A) Observed diversity, (B) Normalized Shannon-Wiener index, (C) Inverse Simpson index, and the (D) D50 index. (E) Correlation heatmap of shared clonotypes and (F) Jaccard index between different days of culture.

Moreover, a comparison of the most frequent clonotypes at days 0, 12, 15 and 20, focusing on clonotypes present in at least 2% of the reads, revealed that one clonotype present with a frequency greater than 10% on day 0 had decreased by day 20, probably because it is a non-specific EBV clonotype. In contrast, other clonotypes with a lower representation at day 0, increased in frequency after T cell activation and expansion against EBV (Figure 54A). The CDR3 amino acid sequences of two clonotypes (CSAGSGGTNEKLFF and CASSVVGDEQYF) that were above 2% of reads on day 20 are described in the literature as recognizing the GLCTLVAML epitope of the BMLF1 antigen, which is presented by the HLA class I allele *A*02:01* expressed by the donor. This was confirmed using tetramers, where 19.4% of the EBVSTs predominantly bound to the GLCTLVAML-HLA *A*02:01* complex (Figure 54B).

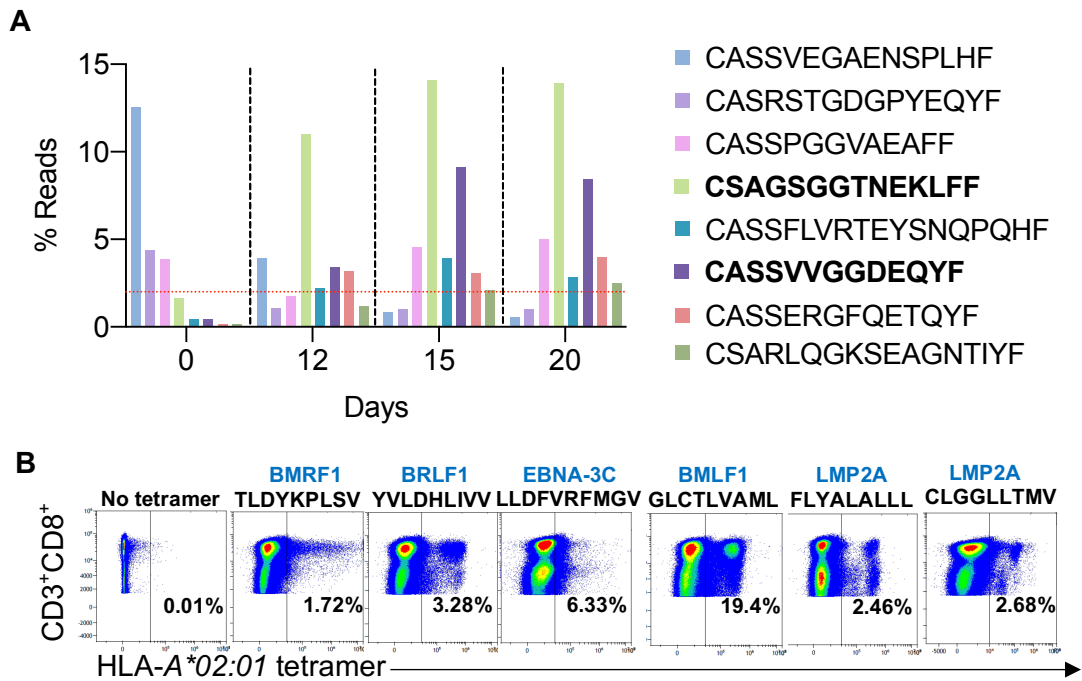


Figure 54. TCR-β clonotypes and tetramer assay of EBVSTs expanded on a large scale.

(A) Bar graph representing percentage of reads for each T cell clonotype by CDR3 amino acid sequences that constitute at least 2% (red dotted line) pre-expansion (day 0) and post-expansion stimulated with PepTivator® EBV select (days 12, 15 and 20). CDR3 sequences highlighted in bold represent clonotypes that are described in the literature. (B) Representative dot plots from the tetramer staining of the EBVSTs product at day 20. The epitope (amino acid sequence) and antigen (in blue) corresponding to each tetramer noted above each plot. No tetramer indicates negative control.

As observed on a small scale, the EBVSTs predominantly exhibited a T_{EM} phenotype (Figure 55).

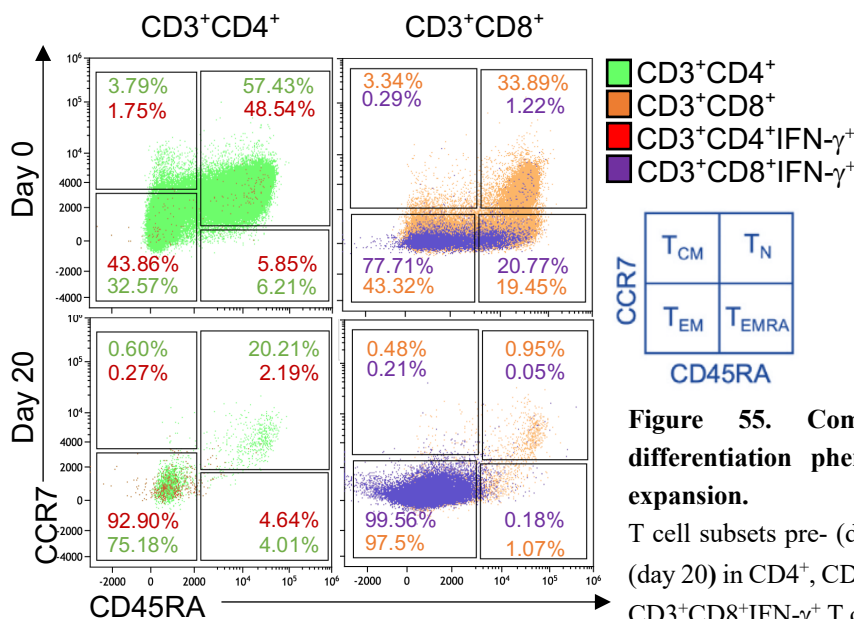


Figure 55. Comparison of T cell differentiation phenotype pre- and post-expansion.

T cell subsets pre- (day 0) and post-expansion (day 20) in CD4⁺, CD8⁺, CD3⁺CD4⁺IFN-γ⁺ and CD3⁺CD8⁺IFN-γ⁺ T cells.

The expression of exhaustion markers in the initial PBMCs did not exceed 0.2% (**Figure 56A**). The CD4⁺ T cells of the EBVSTs produced by day 20 showed low expression of exhaustion markers, while the CD8⁺ T cells expressed 27.3% of LAG-3 and 13.7% of TIM-3 (**Figure 56B**).

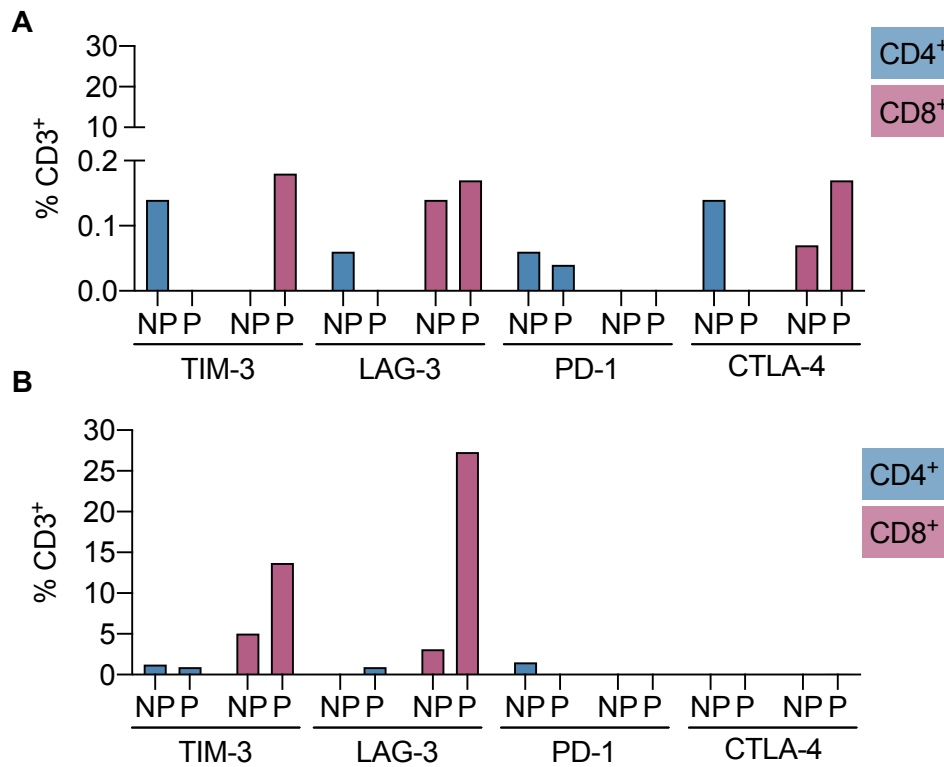


Figure 56. Expression of T cell exhaustion markers pre- and post-expansion of EBVSTs on a large scale.

Expression of cell surface markers (TIM-3, LAG-3, PD-1, CTLA-4) on (A) CD4⁺ and CD8⁺ T cells in the PBMCs, and (B) CD4⁺ and CD8⁺ T cells from EBVSTs produced on day 20. T cells were either pulsed (P) overnight with PepTivator[®] EBV select or non-pulsed (NP).

Chapter III: Transduction *in vitro* of anti-CD19 CAR in thawed EBVSTs

Based on the satisfactory results obtained from the EBVSTs manufactured on a large scale, which are the intermediate product in the proposed therapy, we proceeded with the transduction step. The EBVSTs cryopreserved on day 20, were thawed and transduced *in vitro* ($n = 1$) with the CAR.CD19 construct from ARI-0001 at $\text{MOI} = 5$. Cells from the three conditions tested (untransduced, EBVSTs transduced and CD3^+ T cells transduced) did not expand as expected on day 8 (**Figure 57A**). Despite the limiting number of cells, it was observed that on day 8 the $\text{CD4}:\text{CD8}$ phenotype had been reversed in the EBVSTs, since the viable T cells were mainly CD4^+ instead of CD8^+ T cells (**Figure 57B**).

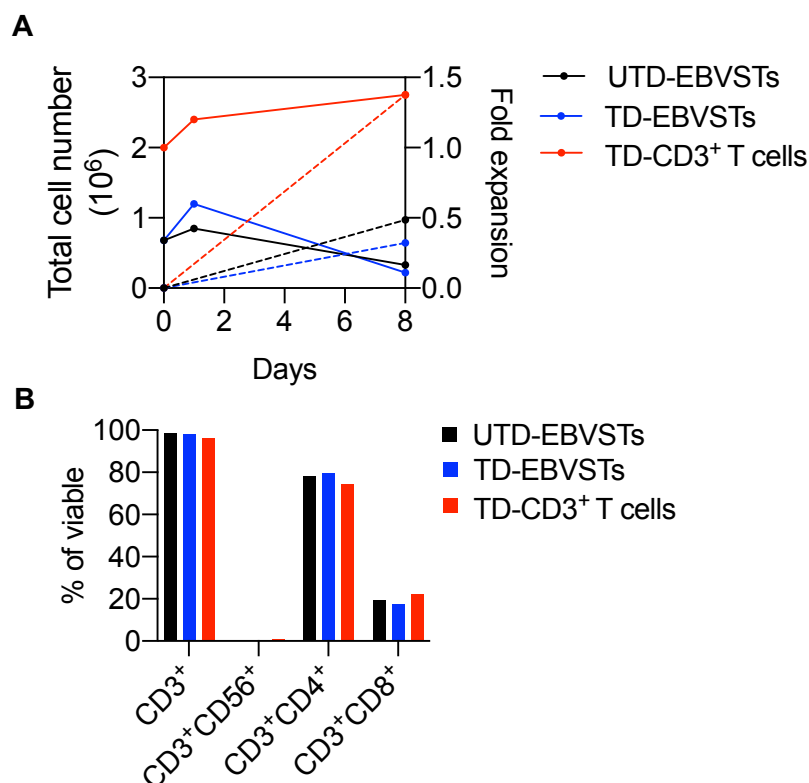


Figure 57. Expansion and characterization of CAR.CD19 (ARI-0001)-transduced EBVSTs.

(A) Expansion kinetics of total cells (continue line) and fold expansion (dashed lines), comparing UTD-EBVSTs, TD-EBVSTs and TD- CD3^+ T cells, after 8 days of culture. (B) Percentage of $\text{CD3}^+\text{CD56}^+$ and T cells subpopulations (CD3^+ , CD4^+ and CD8^+) of the final product post transduction (day 8). UTD, untransduced EBVSTs; TD, transduced.

However, the CD4⁺ and CD8⁺ T cells could express 46.09% of CAR.CD19, like 45.12% of the positive control (CD3⁺ T cells transduced), where the CD3⁺ T cells had not been pre-activated (Figure 58A). Unfortunately, it was not determined whether the expression of CAR.CD19 is from CD4⁺ T cells, CD8⁺ T cells or both. The cytotoxicity assay demonstrated that, after 19h of co-culture, EBVSTs at 2:1 (E:T) ratio were capable of killing 96% of the target cells (NALM6, CD19⁺) and 61.29% at a 0.5:1 ratio (Figure 58B). Therefore, it is seen that pre-activated and thawed EBVSTs may be able to express CAR.CD19 with a high potency against NALM6.

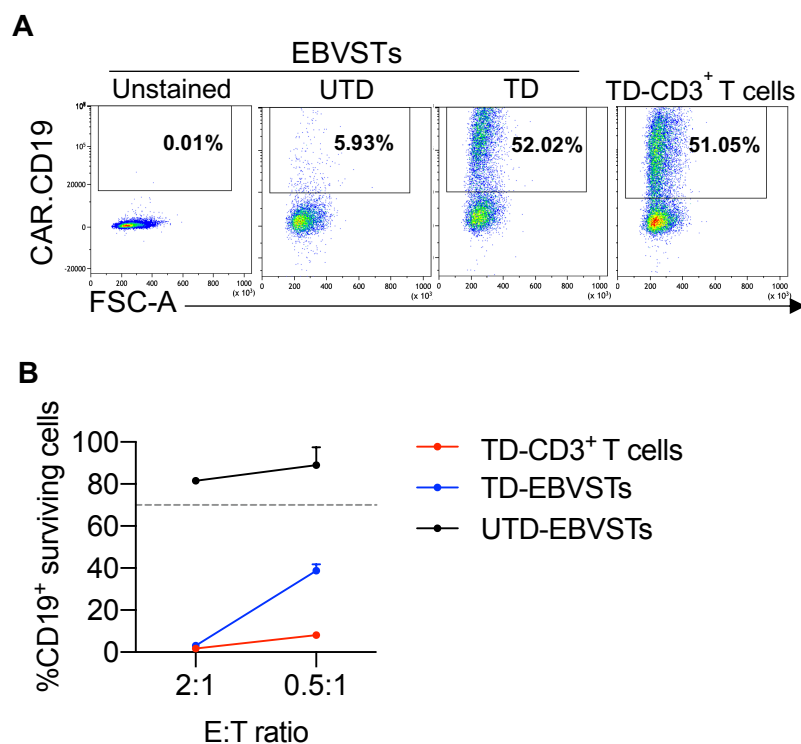


Figure 58. Expression of CAR.CD19 (ARI-0001) and final product potency.

(A) Representative flow cytometry dot plots showing the percentage of CAR.CD19⁺ expression by CD3⁺ T cells in each condition tested. (B) Cytotoxicity assay after 19h of T cells (CD3⁺ or EBVSTs) co-culture with NALM6 cells, at the indicated ratios. Data are represented with the mean \pm SD of the duplicates. The dashed line indicates the minimum ARI-0001-cell cytotoxicity level for a product to be considered valid. UTD, untransduced EBVSTs; TD, transduced. E:T, effector: target cells.

Chapter IV: *In vitro* optimization of cell culture conditions for anti-CD19 CAR transduction in thawed EBVSTs

Although it was possible to transduce the pre-activated and thawed EBVSTs with CAR.CD19 (ARI-0001), it was necessary to adapt the transduction protocol and improve culture conditions to maintain the phenotype and specificity of the EBVSTs, as well as to obtain a sufficient final number of viable cells for patient treatment, and guarantee their ability to expand *in vivo*. The results of the parameters evaluated in the attempt to improve the culture conditions and an efficient transduction in pre-activated and thawed EBVSTs are detailed below.

4.1. Stability of large-scale manufactured EBVSTs

Viability after thawing was 80%, and was maintained after 2 and 4 hours, whether the EBVSTs were stored at room temperature or at 4°C. However, after 4 hours at RT, viability begins to decrease to 77.85%, and drops to 67.86% at 24 hours. In contrast, at 4°C, viability is maintained around 80-90% after 16 and 24 hours (**Figure 59A**). Flow cytometry showed no differences in cell phenotyping between pre-thaw and post-thaw (0 and 16 hours) (**Figure 59B**).

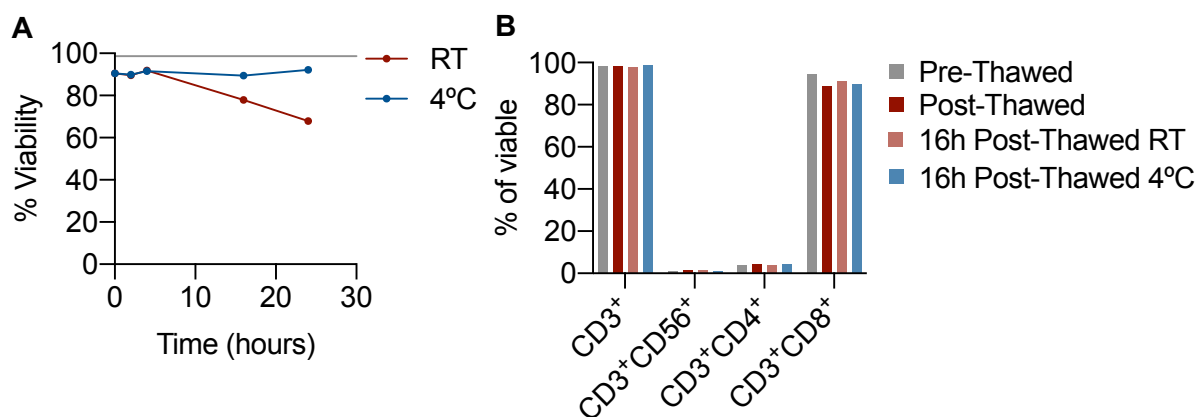


Figure 59. Comparison of EBVSTs stability at room temperature and at 4°C.

(A) Percentage of viability at 0, 2, 4, 16, and 24 hours post-thaw. The gray solid line represents the percentage of viability in EBVSTs prior to freezing (B) Percentage of cell phenotype before and after (at 0 and 16 hours) thawing. RT, room temperature.

4.2. Thawed EBVSTs potency

After confirming that the EBVSTs were stable and maintained their cellular phenotype, their potency (measured by IFN- γ production and degranulation marker expression) was assessed to determine whether the thawing process impacted their functional characteristics across six

different productions. Cellular phenotype did not exhibit many differences (**Figure 60A**), as previously noted (**Figure 59B**). However, specificity in IFN- γ production showed a decrease, ranging from 1.18% to 58.56% (**Figure 60B**). Interestingly, the percentage of the degranulation marker remained stable or, in some cases, even increased (**Figure 60C**).

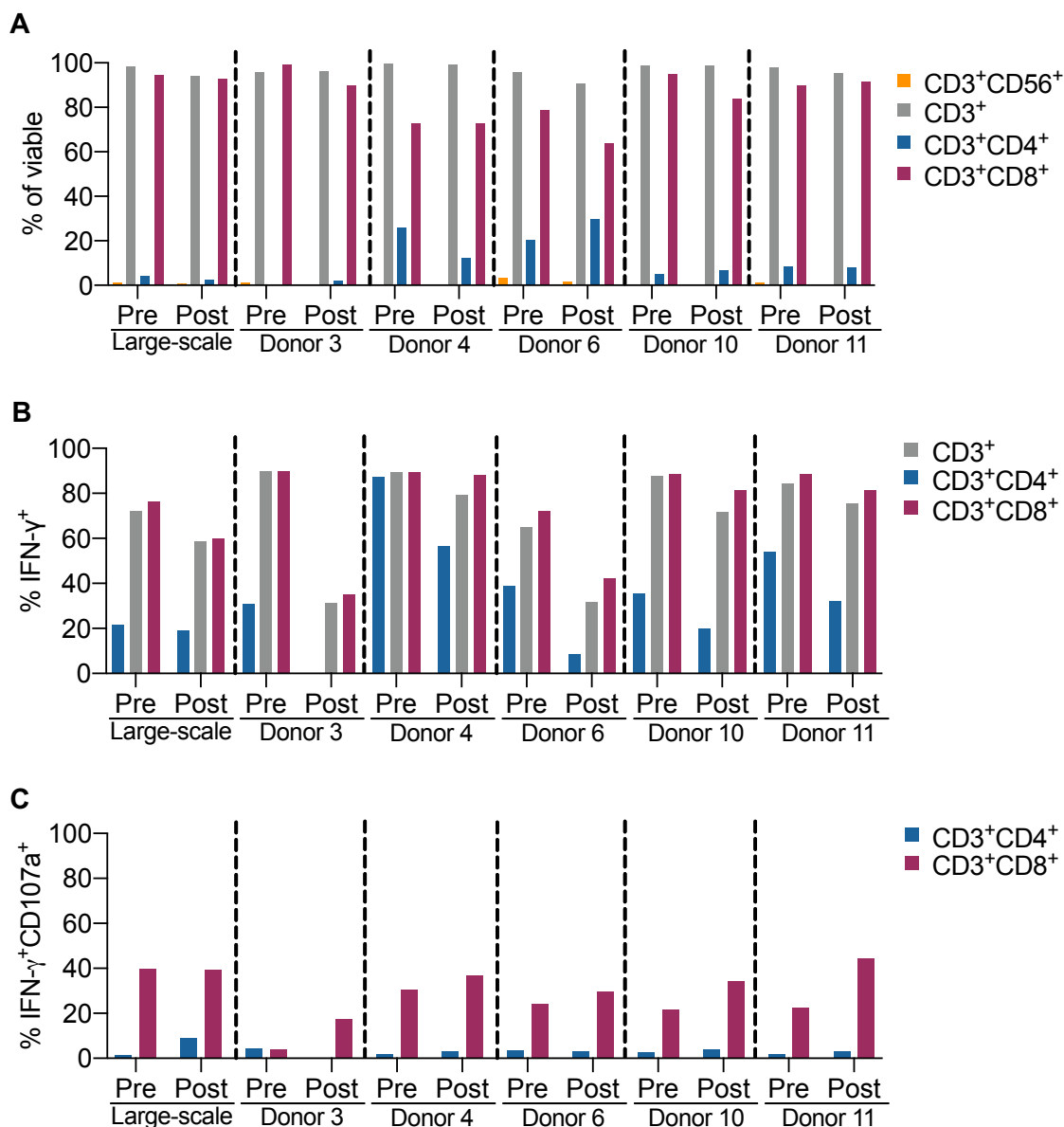


Figure 60. Comparison of T cell phenotype and potency pre- and post-thawing.

(A) Percentage of T cell phenotype pre- and post- thawing. (B) IFN- γ production pre- and post-thawing. (C) Percentage of degranulation marker (CD107a) in IFN- γ ⁺CD4⁺ and IFN- γ ⁺CD8⁺ T cells pre- and post-thawing.

4.3. Optimizing the expansion and culture conditions of post-thaw EBVSTs

After confirming that the EBVSTs largely retain their phenotype and, to a lesser extent, their IFN- γ production, we decided to expand the cells and analyze their kinetics upon re-stimulation after thawing. This approach aimed to identify the factors contributing to the phenotype change during

the first transduction and to explore whether potency could be enhanced during subsequent cultivation.

It was observed that EBVSTs expanded slightly better with 10% hSAB compared to 3% and conditioning them O/N rather than for 2 hours also improved expansion. However, the overall fold expansion remained lower than desired. Additionally, EBVSTs without stimulation by Dynabeads™ or cytokines in the medium began to die after 48h (**Figure 61**).

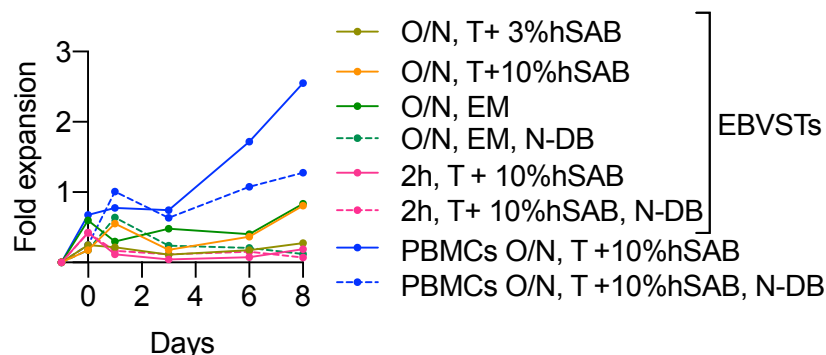


Figure 61. Comparison of the fold expansion of EBVSTs stimulated with Dynabeads™.

Fold expansion of EBVSTs after thawing, cultured in different media with Dynabeads™ (DB, solid line) and without stimulation (N-DB, dashed line) at various time points of culture.

We found that EBVSTs require stimulation with Dynabeads™ on the same day as thawing, as an overnight period without stimulation causes a reversal of the CD4:CD8 ratio. Conversely, when conditioned overnight and cultured without Dynabeads™, the phenotype remained consistent in the few viable cells. There were no differences in phenotype between TexMACS™ medium with 10% or 3% hSAB and the expansion medium (**Figure 62A**).

IFN- γ production was lower in EBVSTs that were left to condition overnight under. However, in unstimulated EBVSTs, the few remaining cells after 8 days of culture maintained, and even improved their specificity by 10%. Due to limitations in cell numbers, the specificity could not be assessed in EBVSTs conditioned for 2 hours (**Figure 62B**).

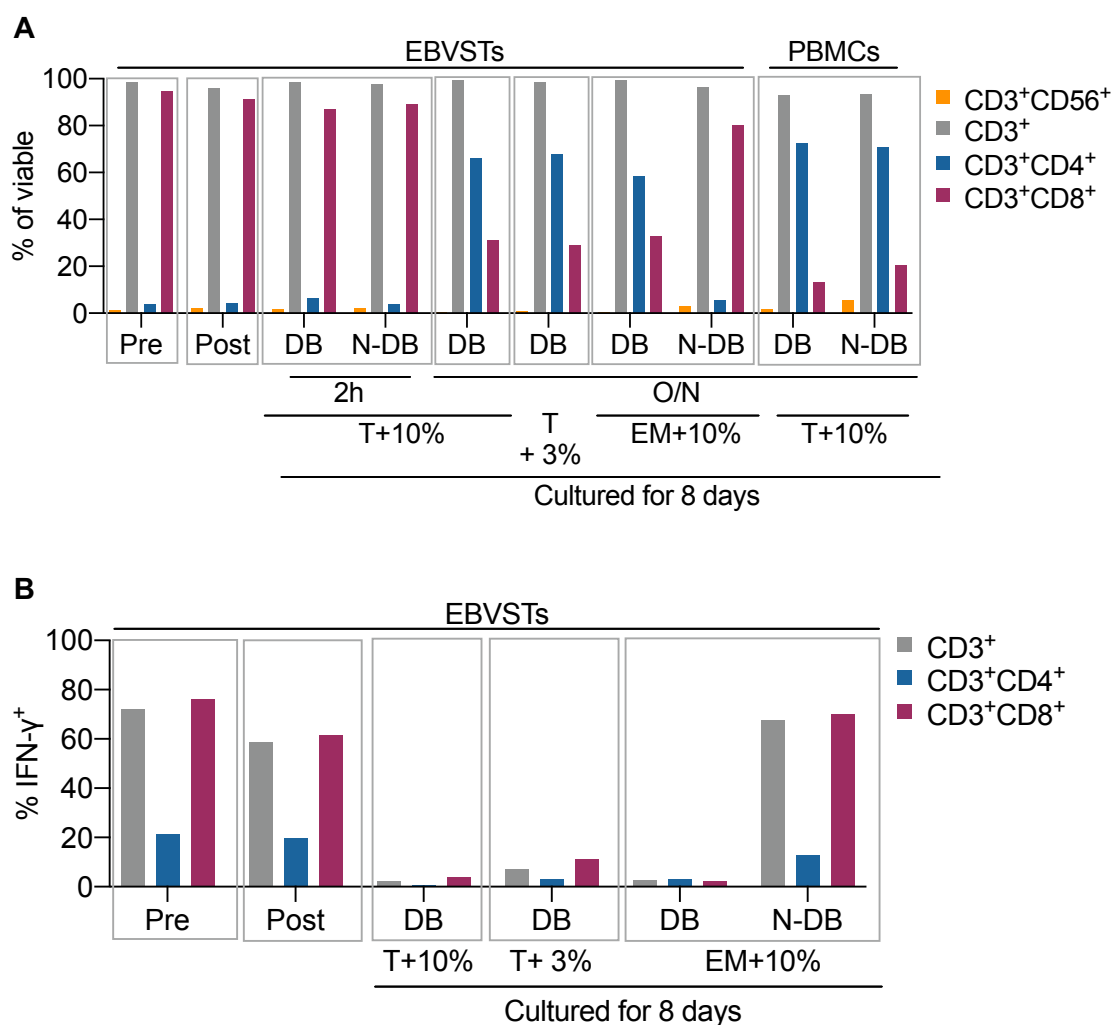


Figure 62. Comparison of phenotype and potency of EBVSTs stimulated with Dynabeads™.

(A) Percentage of cell phenotype pre-, post-thawing, as well as 8 days after culture with different media. (B) IFN- γ production pre-, post-thawing, as well as 8 days after culture with different media. PBMCs were used as a positive control. The seeding concentration for all conditions was 1×10^6 cells/mL. T, TexMACS™ medium; EM, expansion medium; 3% or 10%, percentage of human serum AB (hSAB) in the medium; O/N, overnight; DB, Dynabeads™; N-DB, non-Dynabeads™.

After testing the culture media and selecting the expansion medium for EBVSTs culture post-thawing, we decided to test various cytokines combinations and conditioning times. Stimulating the cells with Dynabeads™ 48 hours after thawing resulted in decreased cell expansion compared to stimulation after overnight conditioning. Interestingly, EBVSTs cultured with IL-7, IL-15 and 2 and stimulated 48 hours after thawing initially shows sustained expansion but then decline. Conversely, cells cultured with IL-2 alone and conditioned O/N began to expand slightly more than the positive control (PBMCs) from day 6 onward. Additionally, expansion kinetics increased on day 9 for conditions with IL-7 and IL-15 combination, and IL-2 alone, while it decreased with IL-7, IL-15 and IL-2 combination. However, optimal expansion is still not achieved (**Figure 63A**). Flow cytometry phenotyping revealed that Dynabeads™ stimulation reversed or equalized

the CD4:CD8 ratio compared to EBVSTs before and after thawing. The CD8⁺ T cell population remained slightly more predominant when cultured with IL-2 alone and conditioned overnight (**Figure 63B**). While maintaining a CD4⁺ T cell population in the culture is important, Dynabeads™ stimulation reduces specificity in CD3⁺, CD4⁺ and CD8⁺ T cell populations across all conditions tested. However, the IL-7 and IL-15 combination proved to be slightly more specific compared to using IL-2 alone or IL-7, IL-15 and IL-2. Consequently, IL-7 and IL-15 is the combination used for ARI-0001 production (**Figure 63C**).

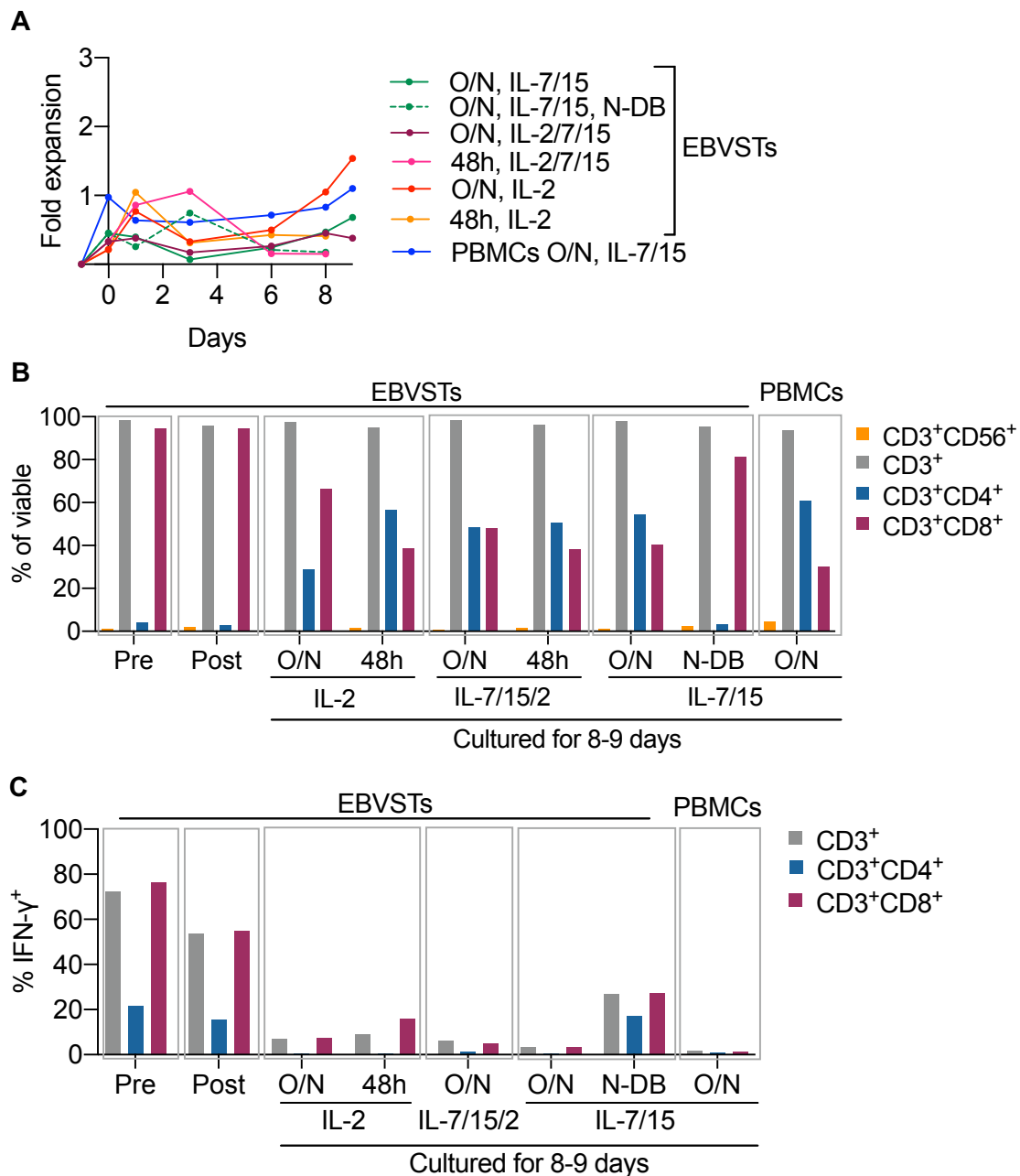


Figure 63. Comparison of the characterization of post-thaw EBVSTs stimulated with Dynabeads™. (A) Fold expansion at different culture time points in EBVSTs stimulated with Dynabeads™ (DB, solid line) after 48 hours or O/N, and without stimulation (N-DB, dashed line), cultured in expansion medium with different cytokine combinations (IL-7/IL-15/IL-2, IL-7/IL-15 and IL-2 alone). (B) Percentage of cell

phenotype pre-thaw, post-thaw, and at days 8-9 after culture. **(C)** IFN- γ production pre-thaw, post-thaw, and at days 8-9 after culture. The seeding concentration for all conditions was 1×10^6 cells/mL. PBMCs were used as a positive control. EM, expansion medium; O/N, overnight. The conditions with 48 hours conditioning and those without stimulus ended the culture on day 8 due to cell death.

Observing the non-specific effects of DynabeadsTM stimulation on EBVSTs, we tested different stimuli based on the recommendations of Li & Kurlander (2010)¹⁶⁸. Additionally, we compared whether the expansion kinetics improved with or without conditioning time.

When stimulated with DynabeadsTM, expansion kinetics improve from day 9 onward (**Figure 64A**). Interestingly, on day 9, CD4⁺ T cells were the predominant population, but by day 13, CD8⁺ T cells became predominant (**Figure 64B**). However, neither population shows IFN- γ production (**Figure 64C**). In contrast, stimulation with soluble antibodies consistently results in CD8⁺ T cell predominance across all conditions (**Figure 64B**), with better IFN- γ production (**Figure 64C**). Conditions without prior conditioning showed improved T cell expansion (**Figure 64A**) and a 15.18% increase in specificity compared to post-thaw CD3⁺ T cells (**Figure 64C**). The conditions stimulated with PepTivator[®] EBV consensus, either alone or in combination with EBNA-1, failed to activate and expand properly, leading to the discontinuation of these conditions after day 6. A higher seeding concentration slightly improved expansion, although the overall kinetics remained unchanged, and an optimal fold expansion has yet to be identified (**Figure 64A**).

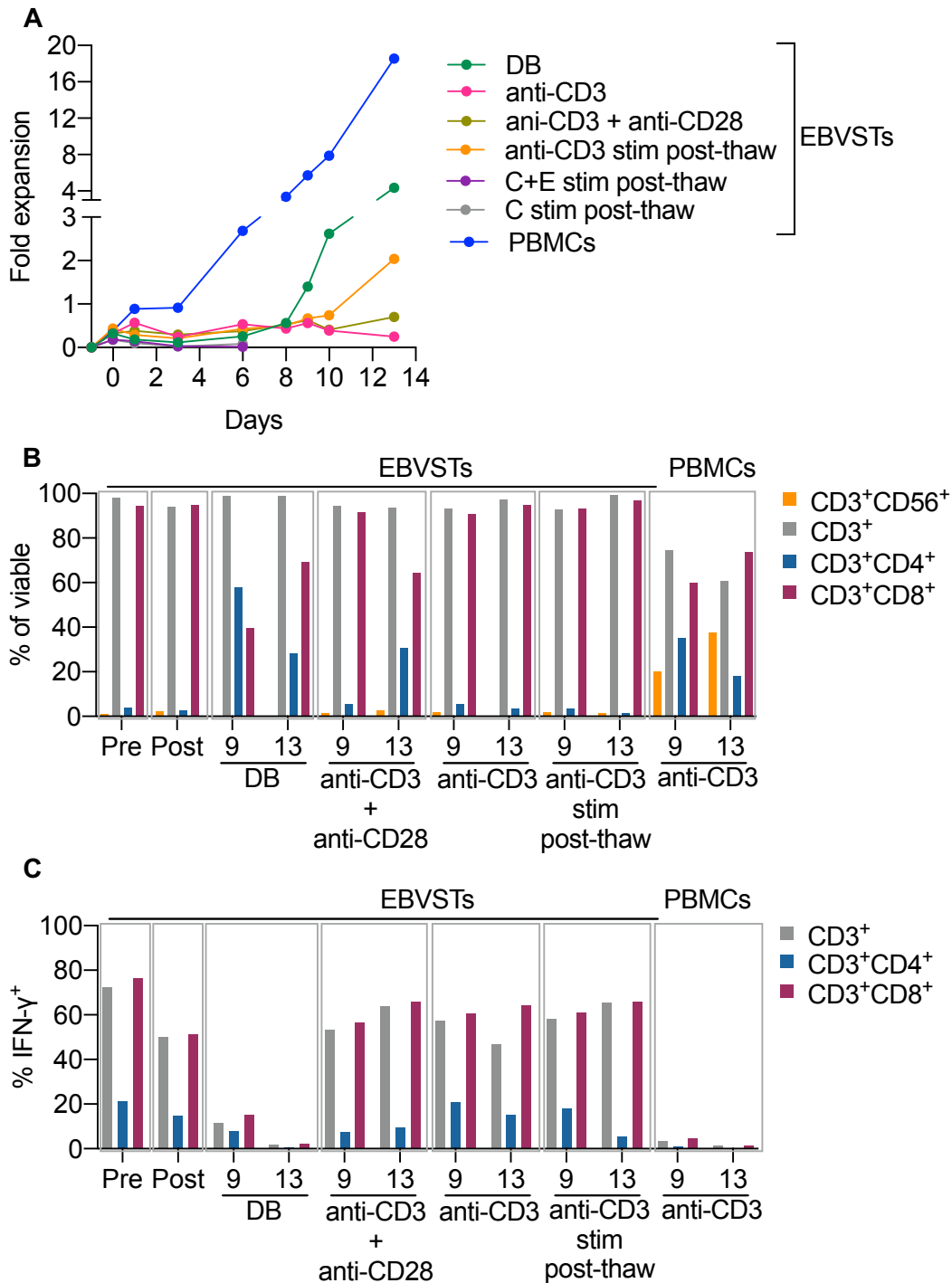


Figure 64. Comparison of the characterization of post-thaw EBVSTs stimulated with different stimuli.

All conditions were cultured in expansion medium with IL-7 and IL-15, at a seeding concentration of 2×10^6 cells/mL. **(A)** Fold expansion comparison between O/N and no conditioning time (stimulated post-thaw) under different stimuli conditions (Dynabeads™ (DB) or soluble antibodies (anti-CD3 alone or anti-CD3 + anti-CD28). **(B)** Percentage of cell phenotype pre-, post-thawing, as well as 9 and 13 days after culture. **(C)** IFN- γ production pre-, post-thawing, as well as 9 and 13 days after culture. PBMCs were used as a positive control. O/N, overnight; stim, stimulated.

4.4. Transduction

After successfully maintaining the phenotype and improving the specificity of the initial EBVSTs post-thawing and after 9 or 13 days of culture, we proceeded with transduction using the CAR.CD19 of ARI-0001 construct.

The fold expansion of both transduced and non-transduced EBVSTs remained below 0.5, lower than the control (PBMCs), which reached a fold expansion of 3.24 by day 14. In contrast to the expansion kinetics described in the previous section, cell death became apparent starting from day 10. Therefore, the use of the G-Rex® 24-well plate did not enhance the fold expansion (**Figure 65A**). Despite this, using the anti-CD3 stimulus, the phenotype was maintained even after the introduction of CAR.CD19 (**Figure 65B**). The EBVSTs with CAR.CD19 maintained a specificity of 74.98% in CD3⁺ T cells, consistent with pre-thawing production, and demonstrated a notable increase of 16.18% compared to 58.80% post-thawing (**Figure 65C**). However, neither the EBVSTs nor the transduced PBMCs expressed CAR.CD19 by day 14 (**Figure 65D**).

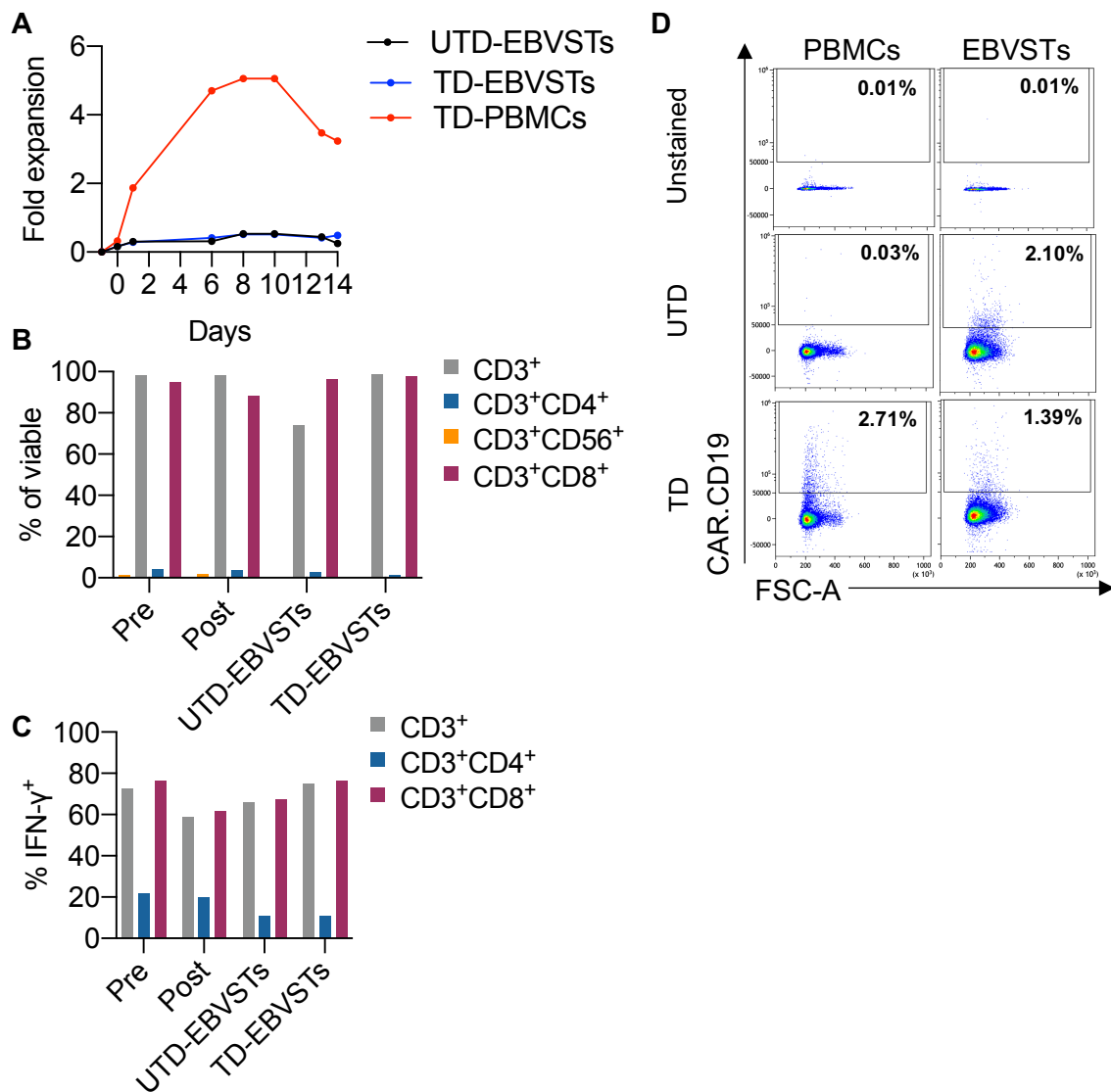


Figure 65. Characterization of EBVSTs stimulated with anti-CD3 and transduced with CAR.CD19. Cells were cultured in a 24-well G-Rex® plate in expansion medium in the presence of IL-7 and IL-15. The initial seeding concentration was 2×10^6 cells/mL. **(A)** Fold expansion, comparing UTD-EBVSTs, TD-EBVSTs and TD-PBMCs (control) after 14 days of culture. **(B)** Percentage of CD3⁺CD56⁺ and T cells subpopulations (CD3⁺, CD4⁺ and CD8⁺) in the final product post-transduction (day 14), compared to EBVSTs pre- and post- thawing. **(C)** Percentage of IFN- γ in CD3⁺, CD4⁺ and CD8⁺ T cells in the final product post-transduction (day 14), compared to EBVSTs pre- and post- thawing. **(D)** Representative flow cytometry dot plots showing the percentage of CAR.CD19⁺ expression in CD3⁺ T cells from each condition tested. UTD, untransduced; TD, transduced.

Since no expression of CAR.CD19 was observed at day 14, we compared expression levels at days 6, 8, and 14. We detected an expression of 3.06% on day 6 and 6.01% on day 8. Although the expression increased by 2.95%, it remained very low, especially considering that the mean (\pm SD) expression in the ARI-0001 study was $30.6 \pm 13.44\%$ between 7 and 10 days of culture. Consequently, expression was not evaluated on day 14 (**Figure 66A**). Regarding fold expansion, there were peaks between days 6 and 8, possibly because 10^5 cells were taken from each condition to evaluate CAR.CD19 expression, and then they began to expand. However, the overall expansion remained low (**Figure 66B**). The phenotype after introducing CAR.CD19 and maintaining the cells in culture for 14 days was still consistent across all conditions (**Figure 66C**). However, the specificity was lower in transduced EBVSTs compared to non-transduced EBVSTs. Due to limited cell numbers after thawing, post-thaw specificity could not be assessed (**Figure 66D**).

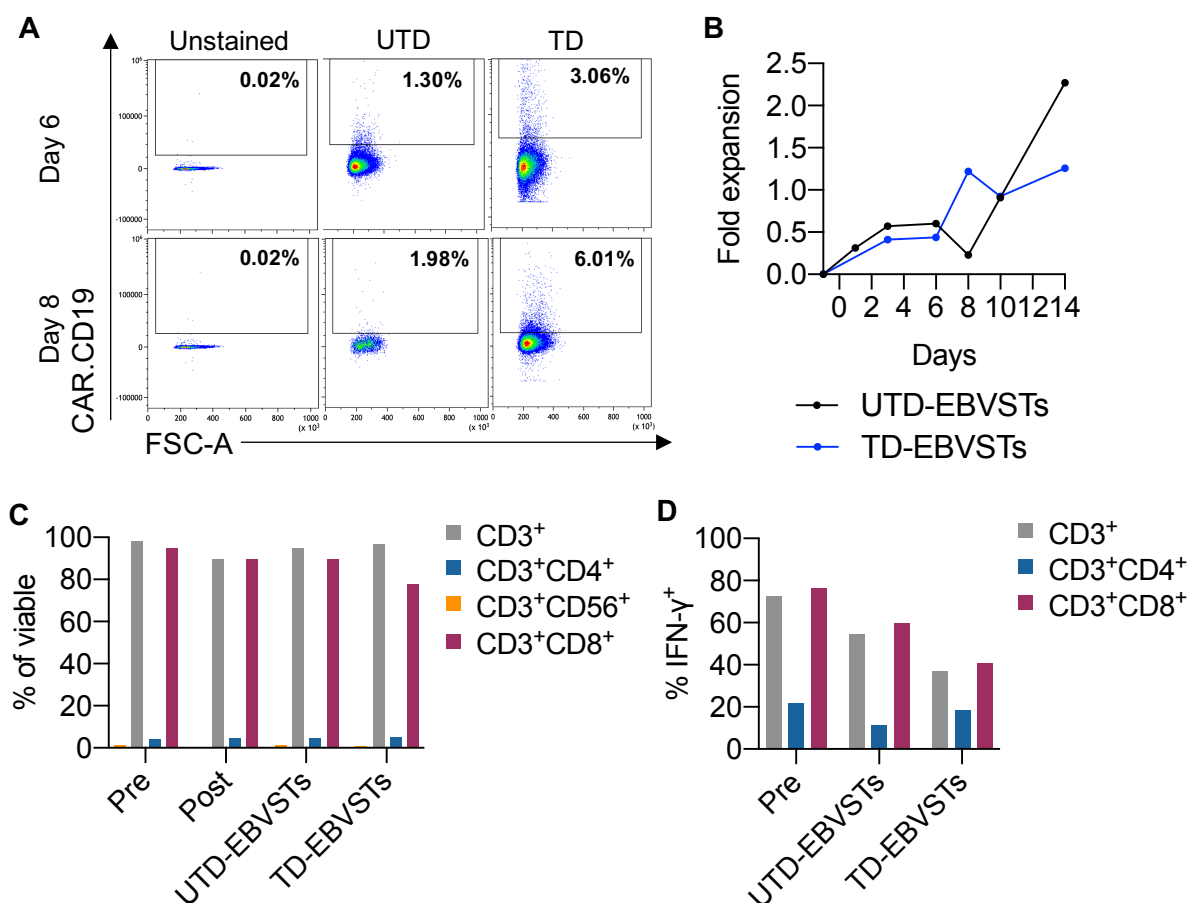
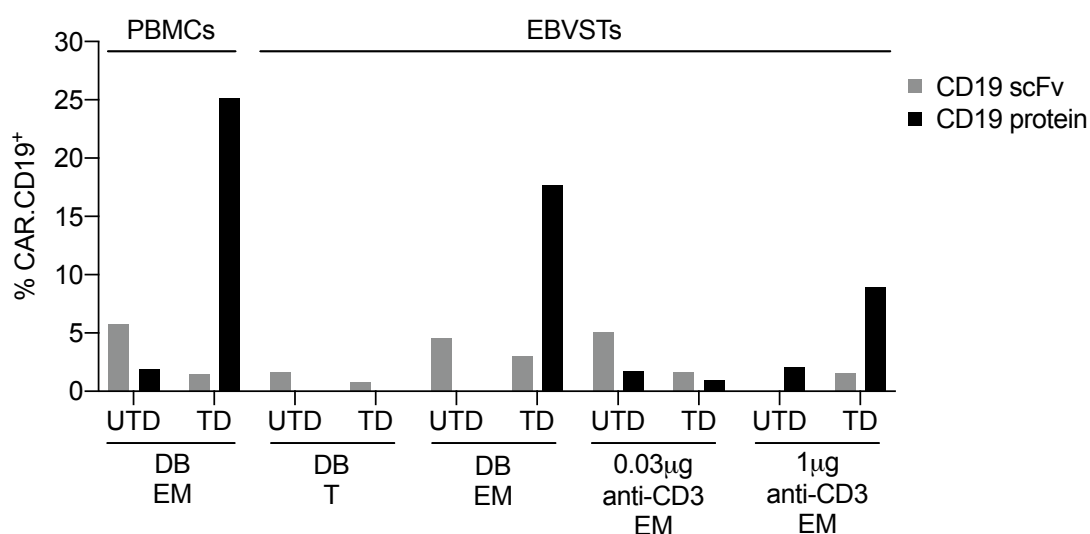


Figure 66. CAR.CD19 expression and characterization at different time points during culture.

Cells were cultured in a 24-well plate in expansion medium in the presence of IL-7 and IL-15. The initial seeding concentration was 4×10^6 cells/mL. (A) Representative flow cytometry dot plots showing and comparing the percentage of CAR.CD19⁺ expression in CD3⁺ T cells from at day 6 vs. day 8 for each condition tested. (B) Fold expansion comparison between UTD-EBVSTs and TD-EBVSTs after 14 days of culture. (C) Percentage of NK cells (CD3⁻CD56⁺) and T cells subpopulations (CD3⁺, CD4⁺ and CD8⁺) in the final product post-transduction (day 14), compared to EBVSTs pre- and post- thawing. (D) Percentage of IFN- γ in CD3⁺, CD4⁺ and CD8⁺ T cells in the final product post-transduction (day 14), compared to EBVSTs pre-thawing. UTD, untransduced; TD, transduced.

Although the phenotype and specificity of the EBVSTs have been maintained, using the anti-CD3 stimulus to re-activate the T cells, we have observed a loss of CAR.CD19 expression compared to the results obtained in first transduction of EBVSTs (**Figure 58A, Chapter 3**). Consequently, we retested the transduction process by comparing various factors, including culture medium, human AB serum percentage, stimulation methods (DynabeadsTM vs. soluble antibodies), and CAR.CD19 detection methods.

Staining of CAR.CD19-expressing cells with FITC-labeled Human CD19 (20-291) Protein, Fc Tag (Acrobiosystems) resulted in a higher fluorescence signal compared to staining with biotin-SP-conjugated AffiniPure Goat Anti-Mouse IgG, F(ab')₂ Fragment Specific (Jackson ImmunoResearch Laboratories Inc.), which detects the scFv domain of the CAR. Additionally, CAR.CD19 expression was observed to be higher when EBVSTs were activated with DynabeadsTM, and to a lesser extent when the concentration of soluble anti-CD3 antibody was increased. In the control (PBMCs), a 25.16% expression of CAR.CD19 was seen when PBMCs were stimulated with DynabeadsTM (**Figure 67**).

**Figure 67. Comparison of CAR.CD19 expression using different detection methods.**

CAR.CD19 expression by detecting the scFv domain and the Fc-tagged region of the recombinant CD19 protein under different conditions tested. Cells were cultured in a 24-well plate in expansion medium (EM)

or TexMACSTM (T), both supplemented with 3%hSAB, in the presence of IL-7 and IL-15. The initial seeding concentration was 2×10^6 cells/mL. This transduction was performed using EBVSTs from donor 5, whereas the first transduction (results of Chapter III) was performed with EBVSTs from donor 15, which were produced on a large scale.

Under conditions where CAR.CD19 was expressed, we identified that both CD4⁺ and CD8⁺ T cells expressed CAR, with higher expression in CD4⁺ T cells (**Figure 68**).

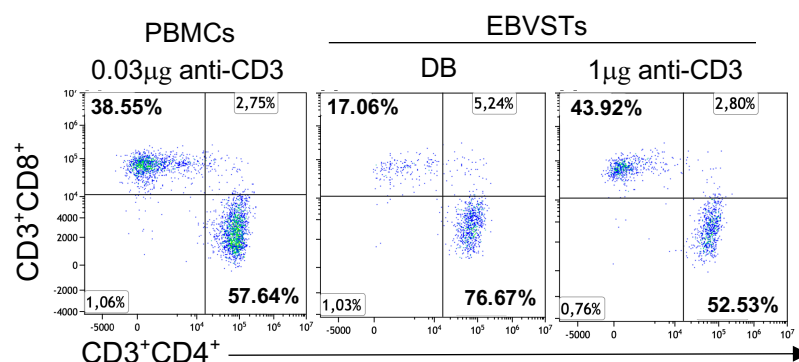


Figure 68. Comparison of T cell subpopulations in transduced conditions.

Representative flow cytometry dot plots showing the percentage of CD4⁺ and CD8⁺ T cells under the three conditions where CAR.CD19⁺ expression was greater than 8%, using detection of the Fc-tagged region of recombinant CD19 protein.

Comparing all conditions, transduced EBVSTs stimulated with anti-CD3 at a concentration of 0.03 μg/mL maintained their phenotype and specificity after thawing. However, when stimulated at a higher concentration (1 μg/mL), the CD4⁺ and CD8⁺ T cells exhibited 25.71% and 73.42%, respectively (**Figure 69A**), reducing specificity by half (**Figure 69B**). In the case of DynabeadsTM, as seen in previous experiments, CD4⁺ T cells outnumbered CD8⁺ T cells (**Figure 69A**), and neither population showed IFN-γ production after 9 days in culture (**Figure 69B**). The fold expansion remained suboptimal, and in some conditions, we could not perform labeling to assess phenotype and specificity due to the limited number of final cells (**Figure 69C**).

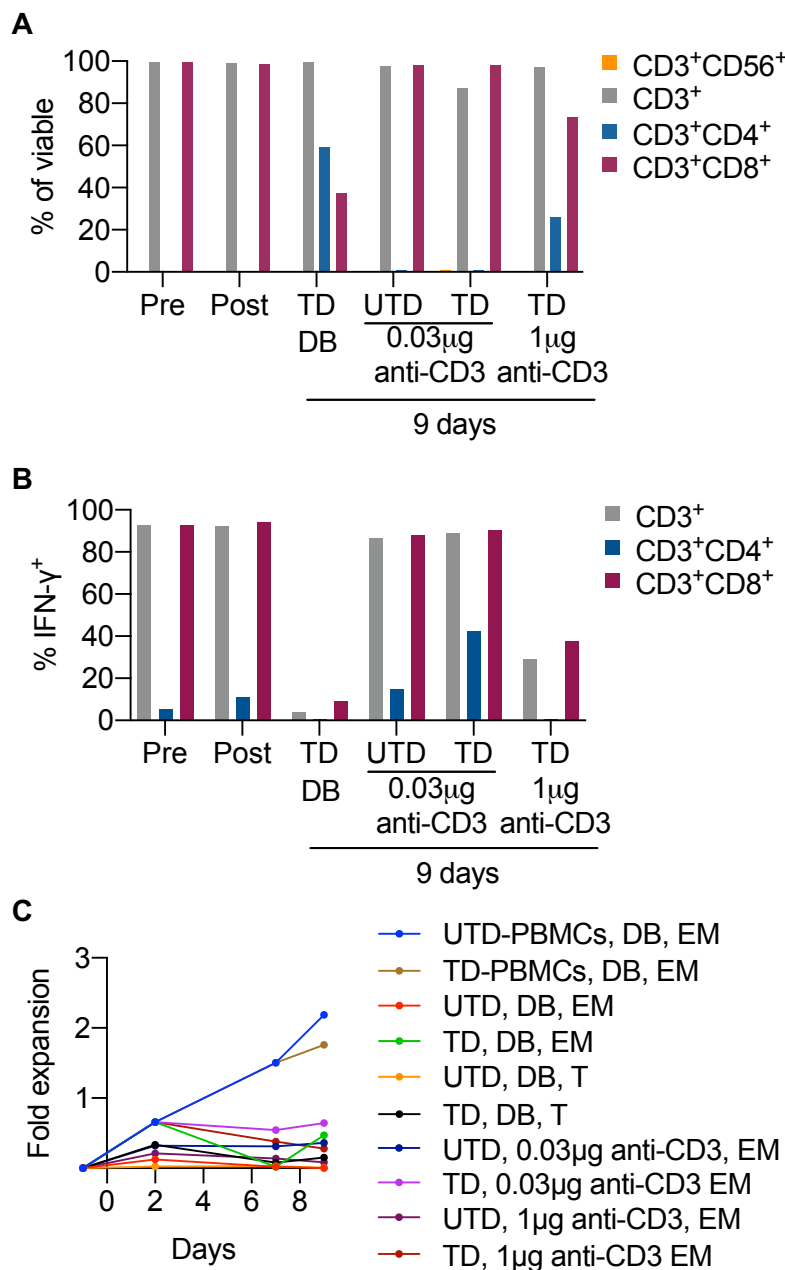


Figure 69. Characterization of transduced EBVSTs with different stimuli and culture media.

(A) Percentage of NK cells (CD3⁻CD56⁺) and T cell subpopulations (CD3⁺, CD4⁺ and CD8⁺) in the final product post-transduction (day 9), compared to EBVSTs pre- and post-thawing. (B) Percentage of IFN-γ⁺ in CD3⁺, CD4⁺ and CD8⁺ T cells in the final product post-transduction (day 9), compared to EBVSTs pre- and post-thawing. (C) Fold expansion comparison at different time points across the various conditions tested. Cells were cultured in a 24-well plate in expansion medium (EM) or TexMACS™ (T), both supplemented with 3%hSAB, in the presence of IL-7 and IL-15. The initial seeding concentration was 2x10⁶ cells/mL. UTD, untransduced; TD, transduced. DB, Dynabeads™; 0.03µg/mL or 1µg/mL indicates the concentration of anti-CD3 antibody used.

Simultaneously, we compared the fold expansion of cryopreserved EBVSTs on days 12, 15, and 20 to assess whether increased T cell differentiation phenotype correlates with reduced

proliferative capacity. Although differences were observed between the different days, an optimal fold expansion was not achieved by day 14 (**Figure 70**).

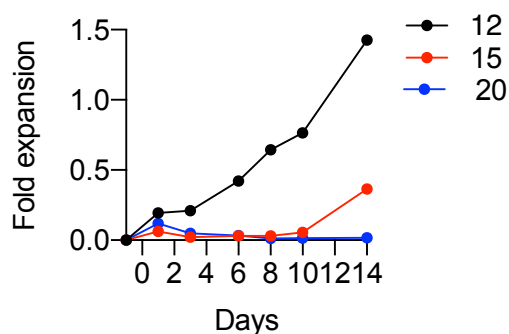


Figure 70. Comparison of the fold expansion in cryopreserved EBVSTs on days 12, 15, and 20.

Cells were thawed and cultured in a 24-well plate in expansion medium supplemented with 10%hSAB and IL-7 and IL-15 for 14 days. The initial seeding concentration was 2×10^6 cells/mL.

4.5. Proof of concept: Partially reprogram EBVST cells with Yamanaka factors

We decided to conduct a proof-of-concept study, since the findings on the optimization of the transduction protocol discussed in sections 4.3 and 4.4 of Chapter 4 are still not optimal for scaling and reproducing the protocol in the CliniMACS Prodigy[®] system. This study aims to determine whether partial reprogramming (7-12 days) of EBVSTs using Yamanaka factors (OCT4, SOX2, KLF4, c-MYC, LIN28, and NANOG) can improve cellular stemness and fitness while maintaining the initial phenotype and specificity of the EBVSTs. The goal is to enable EBVSTs to proliferate more effectively and enhance their antitumor potency both *in vitro* and *in vivo*. We employed a non-integrative method using mRNA encoding the Yamanaka factors. For mRNA transfection, we compared two methods: a physical approach using electroporation and a chemical approach using lipofectamine.

First, we tested the transfection process using RNAiMAX in HEK 293T cells to verify the functionality of the mRNA kit containing Yamanaka factors and to detect these factors by flow cytometry. After 24 hours of transfection, we observed the expression c-MYC (30.7%) and SOX2 (26.3%). The expression of GFP, which served as our control, was 97.7% (**Figure 71**).

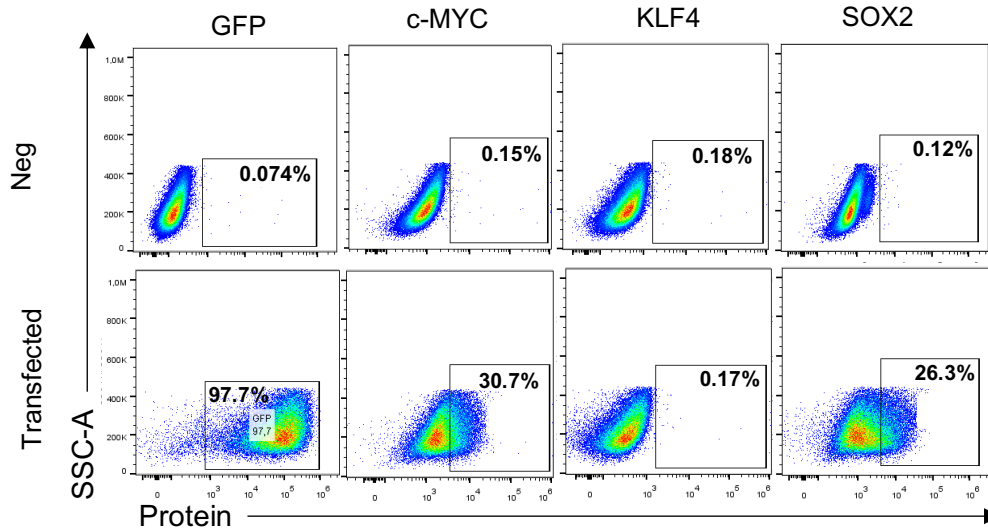


Figure 71. Expression of Yamanaka factors in HEK 293T cells transfected with RNAiMAX.

Representative flow cytometry dot plots showing the percentage of three Yamanaka factors (c-MYC, KLF4, SOX2) and the control Green Fluorescent Protein (GFP) 24 hours post-transfection compared to non-transfected HEK 293T cells. Cells were cultured in RPMI 1640 supplemented with 10%hSAB.

Second, we compared the electroporation method and RNAiMAX for transfecting CD3⁺ T cells. Using mRNA-GFP as a control, we found that electroporation was more effective, achieving 87.9% GFP expression compared to 0.077% with RNAiMAX. When transfecting with Yamanaka factors, we did not observe high levels of expression for the evaluated factors. However, electroporation resulted in slightly higher expression, with 3.16% for SOX2 and 2.13% for KLF4, compared to RNAiMAX (**Figure 72A**). Nevertheless, we noted that electroporation caused greater cellular damage and impaired proliferation compared to RNAiMAX (**Figure 72B**).

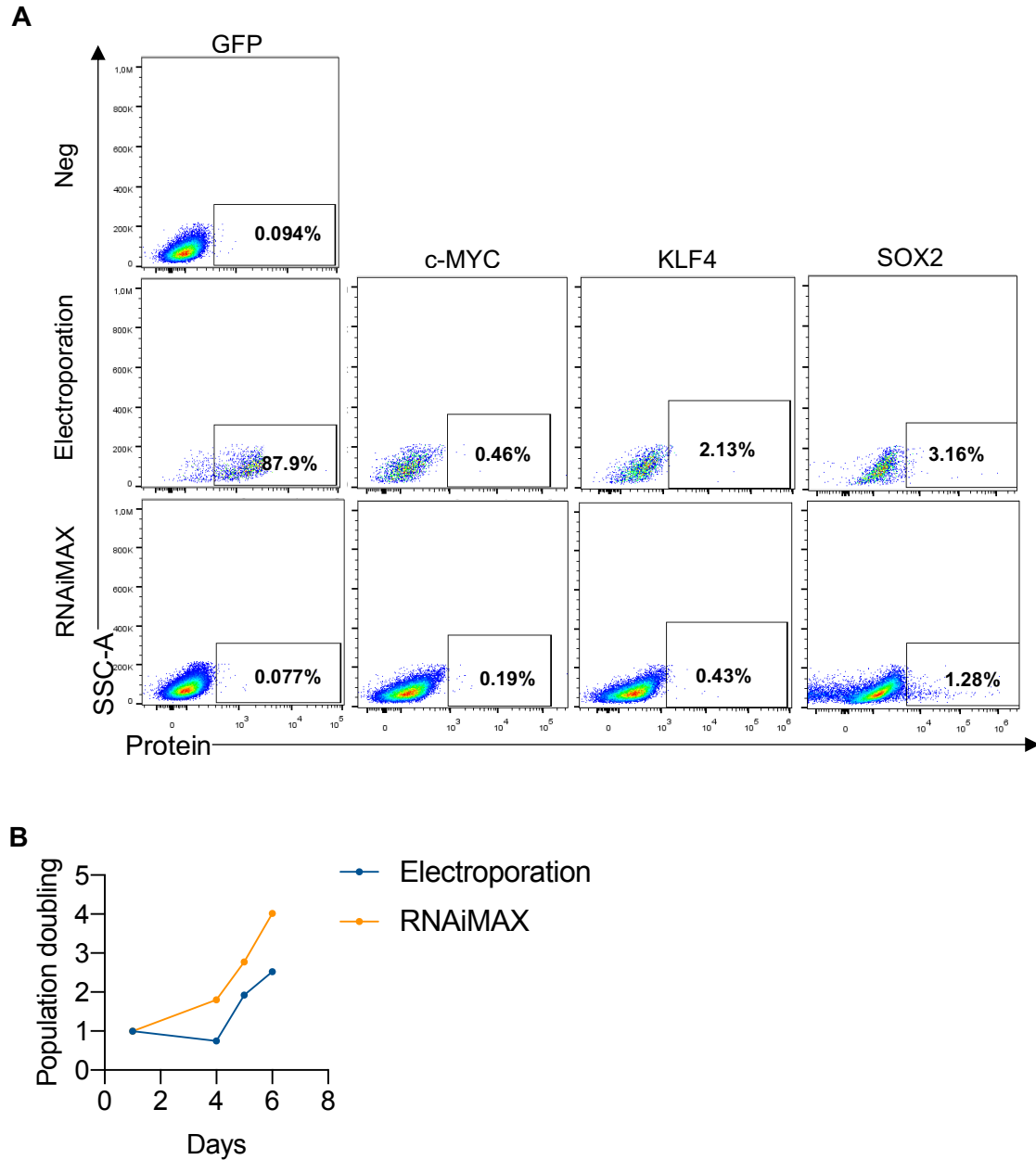


Figure 72. Yamanaka factors expression in transfected CD3⁺ T cells.

(A) Representative flow cytometry dot plots showing the percentage of expression for three Yamanaka factors (c-MYC, KLF4, SOX2) and the control Green Fluorescent Protein (GFP) 24 hours post-transfection using electroporation versus RNAiMAX in CD3⁺ T cells. (B) Population doubling after transfection. Cells were cultured in RPMI 1640 supplemented with 10%hSAB for 6 days.

Third, comparing the different chemical reagents for mRNA transfection in post-thawing EBVSTs from donor 5, we observed that TransIT[®] resulted in a slightly higher fold expansion compared to the others (**Figure 73A**). However, after thawing and re-expanding, RNAiMAX performed better, though an optimal fold expansion has yet to be achieved (**Figure 73B**). There were no differences in viability, but a considerable decrease in the number of lymphocytes was observed after thawing and re-expanding (**Figure 73C**).

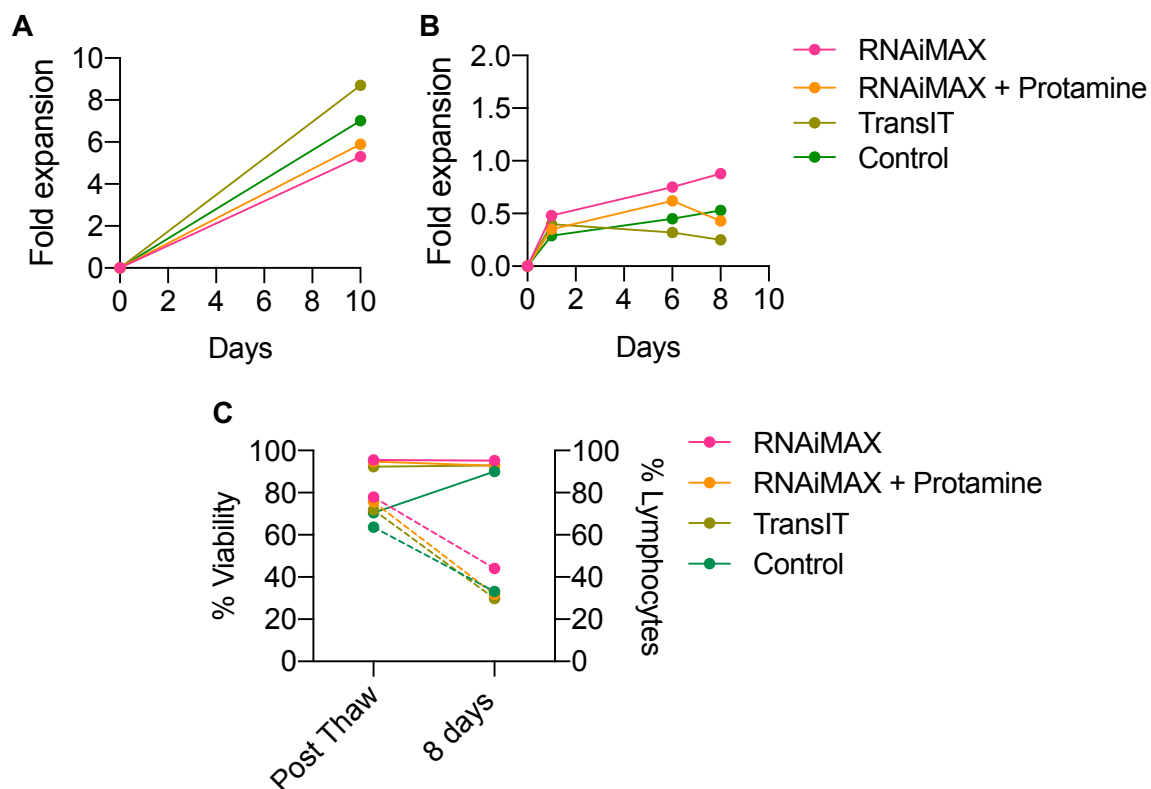


Figure 73. Fold expansion and viability in EBVSTs transfected using chemical methods.

Comparison of (A) Fold expansion of EBVSTs thawed, transfected and culture for 10 days. (B) Fold expansion after thawing the transfected EBVSTs. (C) Percentage of viability and lymphocyte post-thawing and after 8 days of culture for transfected EBVSTs. Control consists of untransfected EBVSTs

When comparing transfection with TransIT[®] using a double dose of mRNA concentration and on different days, no significant effect was observed on reprogramming or the proliferation of post thawing EBVSTs. Then, we transfected PBMCs with mRNA-GFP using Trans-IT[®], and 24 hours later, immunofluorescence confirmed the presence of GFP in some cells. We hypothesized that these cells were not T cells due to their larger size (**Figure 74A-B**).

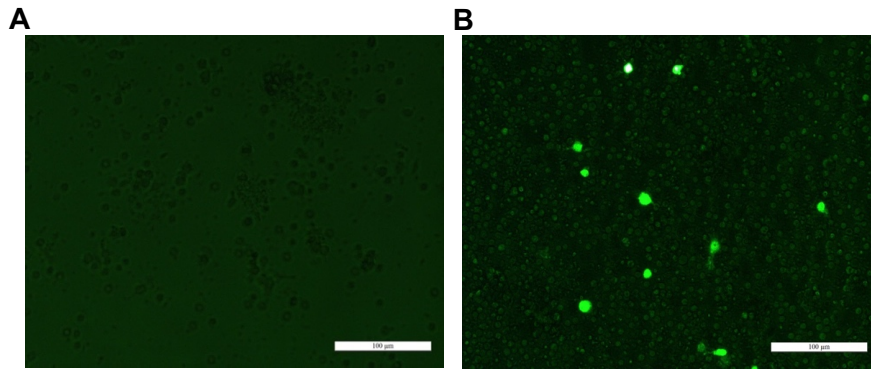


Figure 74. Transfection of PBMCs with mRNA encoding GFP using TransIT®.
(A) Negative control: untransfected PBMCs **(B)** PBMCs transfected with mRNA-GFP after 24 hours.

Finally, we attempted to transfect less differentiated EBVSTs on days 8 and 12 using both methods (electroporation and TransIT®). Unfortunately, all EBVSTs transfected via electroporation died, while with TransIT®, only those transfected on day 8 died. In EBVSTs transfected with TransIT® on day 12, we observed 4.16% GFP and 2.25% SOX2 expression 24 hours post-transfection; however, the negative control showed 1% expression, indicating no significant expression of mRNA (**Figure 75**). The phenotype and specificity of the cells were maintained, but no significant improvement in cell proliferation was observed.

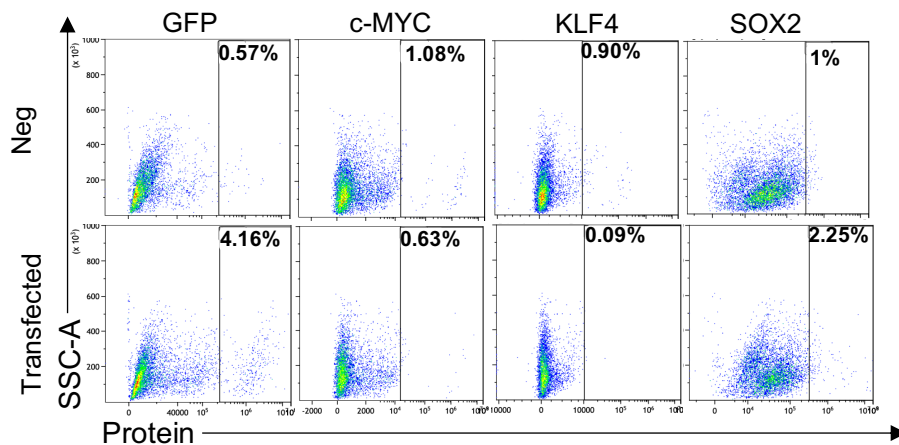


Figure 75. Comparison of Yamanaka factors expression in EBVSTs transfected via TransIT®.
 Representative flow cytometry dot plots showing the percentage of expression for three Yamanaka factors (c-MYC, KLF4, SOX2) and the control Green Fluorescent Protein (GFP) 24 hours post-transfection. The EBVSTs were from day 12 of culture and were not cryopreserved.

Starting from a pre-activated and thawed intermediate product (EBVSTs), the transduction process is more complex. Despite the promising findings and results obtained in each optimization in the transduction step, we have not yet achieved an optimal fold expansion and reproducible expression of EBVST-expressing CAR.CD19 (ARI-0001). As a result, we have not completed the fourth objective of the doctoral thesis.

DISCUSSION

CAR-T therapy targeting the CD19 antigen in the treatment of B-cell neoplasms has shown positive clinical outcomes, offering an alternative therapeutic path to patients whom conventional treatments have failed. However, this therapy still has some limitations, such as severe side effects, loss of the target antigen, lack of proliferation and persistence of CAR-T cells *in vivo*, and to date it is only approved as an autologous therapy.¹⁶⁹ Some of these limitations have been overcome by VSTs therapy which have demonstrated good tolerance rates and low levels of GvHD,¹⁷⁰ extensively proliferation after infusion in HSCT recipients, to control viral infections in immunocompromised patients, and have the potential to be an allogenic “*off-the-shelf*” therapy.^{74,131,171} In this thesis, we aimed to combine both therapies, taking advantage of the VSTs characteristics to the potent cancer CAR-T therapy. The EBVSTs co-expressing a tumor-specific transgenic CAR targeting CD19 could enhance and direct the antitumor response, improving proliferation and long-term persistence in the patient,^{77,147,149} while also controlling viral infections associated with the targeted virus.

The combination of these two therapies is an emerging area of research, with the group from Baylor College of Medicine being one of the pioneers. We have based the optimization for producing this cell therapy on their findings, as well as on the experience of the Banc de Sang i Teixits in producing VSTs against CMV, BKV and SARS-CoV-2.^{85–87,113,172} However, unlike the protocols published to date, our optimization focused on (1) producing EBVSTs from PBMCs of healthy EBV-seropositive donors without the need for prior selection or purification of T cells, significantly reducing production costs, (2) activation and re-stimulation using overlapping peptides in combination with irradiated autologous PBMCs, avoiding the use of lymphoblastic lines, dendritic cells, or other APCs, and most importantly, (3) performing CAR.CD19 transduction in cryopreserved EBVSTs, with the future goal of creating an “*off-the-shelf*” EBVST bank, which could become an allogeneic therapy itself or an intermediate product for other CARs transduction, (4) using our own CAR.CD19 construct (ARI-0001), and (5) exploring the application or introduction of Yamanaka factors for the partial reprogramming of EBVSTs, with the aim of improving stemness and fitness for their subsequent transduction with CAR.CD19.

We outline below the key parameters considered in the development of CAR.CD19-EBVST therapy and estimate that, we could create a therapy with the potential to treat patients with: (1) ALL (CD19⁺) with EBV⁺ infection (2) Lymphomas associated to EBV⁺ infection, and (3) as a bridge therapy for patients unable to immediately receive autologous CAR-T.

EBVSTs production

In the EBVSTs protocol optimization, we identified that a high initial seeding density, along with the absence of cytokines during the first activation of primary T cells, are key culture conditions

for an optimal viability and to enhance specificity of EBVSTs. On one hand, high seeding density of resting state PBMCs, equal to or greater than 1×10^6 cells/mL, is needed to ensure effective T cell activation. Lower densities reduce cell-to-cell contact, which may result in incomplete or no T cell activation. Additionally, T cells activated at low cell density exhibit higher levels of reactive oxygen species (ROS) compared to those cultured at high density, which may induce apoptosis.¹⁷³ On the other hand, the absence of cytokines during the first activation was designed to prevent overstimulation and the proliferation of non-specific cells, as T cells activated at high density secrete autocrine catalase, cytokines like IL-2, and other growth factors that are crucial for their proliferation and survival.^{173,174} Therefore, by maintaining high cell density without cytokines, the accumulation of these autocrine products was facilitated, indirectly promoting the selection of cells with greater proliferation potential and specificity during the first 5 days.

For the activation and stimulation of T cells, we chose an optimized peptide pool of EBV by Miltenyi Biotec (PepTivator[®] EBV consensus) designed for the efficient *in vitro* T cell stimulation, since it contains 43 peptides ranging from 8-20 amino acids in length, derived from 15 lytic and latent phase proteins of the virus. Thirty-two of the peptides are HLA class I-restricted and 11 are HLA class II-restricted. Given that the pool includes more HLA class I-restricted peptides, and it has been reported that EBV tends to elicit a predominantly CD8⁺ T cell response, the dominance of CD8⁺ T cells in our final product was expected. However, we aimed for the CD4⁺ T cell population in our final EBVST product to be between 15-25%, as dendritic cells transmit help signals from CD4⁺ T cells to CD8⁺ T cells during priming, optimizing the magnitude and quality of the cytotoxic cellular response.¹⁷⁵ Additionally, a study by Ahrends et al. (2019), identified that CD4⁺ T cells are necessary for the generation of both T_{CM} and T_{EM} memory CD8⁺ cytotoxic T lymphocytes.¹⁷⁶ Therefore, in Optimization 3, we added AdV 5 hexon stimulation in combination with the PepTivator[®] EBV consensus, but we did not observe any changes in the CD4:CD8 ratio or memory phenotype. We hypothesize that there may have been competition between the peptides, as the PepTivator[®] EBV consensus involves 15 different proteins against various EBV antigens, while for AdV, we only included peptides against AdV5 hexon.

In contrast, when we combined the EBNA-1 antigen with the PepTivator[®] EBV consensus, the CD4⁺ T cells increased in our final product, accompanied by a high IFN- γ production in CD3⁺, CD4⁺, and CD8⁺ T cells. Moreover, by stimulating PBMCs with EBNA-1 alone, we obtained a predominantly CD4⁺ T cell product with high IFN- γ production in T cell populations. Our final T cell product reached higher IFN- γ percentages compared to the study by Bonifacius et al. (2023), where they produced EBVSTs using the same peptides combinations as we did but employed the CliniMACS[®] cytokine capture system IFN- γ selection method⁹⁹. Activation and expansion with LMP2A also increase the proportion of CD4⁺ T cells in the final product, consistent with the

findings of Su et al. (2002)¹⁷⁷. Our protocol, therefore, demonstrates the ability to expand specific CD4⁺ T cells, and it works for both a peptide mix targeting multiple antigens or a single viral antigen of the same EBV. EBNA-1 and LMP2A were chosen because they cannot only be processed and presented through the MHC class II pathway, inducing a consistent CD4⁺ T cell immune response, but are also expressed in Burkitt's lymphoma Hodgkin's lymphoma and carcinoma.^{178,179} These antigens not only promote the expansion of CD4⁺ T cells, which are important for the maintenance of CD8⁺ T cells, but the expanded specific CD4⁺ T cells themselves could also participate in the antitumor process of the therapy under development, helping control tumor growth *in vivo*.¹⁸⁰

However, it is important to consider that the cellular response is highly complex and donor dependent. As we observed, the PBMCs activated and expanded with the PepTivator[®] EBV consensus from one of the processed donors (donor 2) resulted in EBVSTs that were predominantly CD4⁺ T cells in the final product. We hypothesize that this could be attributed to the donor's HLA genotype, as this donor had only one HLA class I allele restricted to the group of overlapping EBV peptides used for cellular activation, making it likely that the HLA class II alleles were more dominant.¹⁷⁹

The combination of cytokines added to the medium from day 5 was another key culture condition. Currently, various cytokines are used to promote the differentiation and division of T cells *in vitro*, but the ideal conditions for maximizing the expansion and functional improvement of peptide-stimulated T cell products have yet to be fully established. Cellular products used in clinical trials have generally supplemented T cell cultures with the growth-promoting cytokines IL-2, IL-15, IL-4, and IL-7.^{92,181–183} The combination of IL-7 and IL-15 emerged as important cytokines for the homeostasis and maintenance of a T_{SCM} or T_{CM} and T_{EM} memory T cell phenotype, leading to long-lived cells capable of persisting *in vivo*.¹⁸⁴ This persistence is crucial to maintain a robust immune response over time, especially in the case of chronic infections or viral reactivations such as CMV, EBV, or AdV. IL-7 and IL-15 together support the survival and homeostatic proliferation of memory T cells without inducing the harmful effects of excessive T cell activation.^{185–188} In our case, we compared both combinations, IL-7 and IL-15, and IL-7, IL-15 and IL-2, and obtained consistent and better results when combining all three cytokines. With IL-7 and IL-15, we achieved a slightly higher percentage of T_{SCM} and T_{CM}, particularly in CD4⁺ T cells by day 15, compared to the addition of IL-7, IL-15, and IL-2. However, CD8⁺ T cells showed similar expression levels across both conditions. Therefore, the IL-7, IL-15 and IL-2 combination was selected, as the synergy of these three cytokines promoted a purer product, with a lower percentage of NK cells in the final product. Moreover, adding IL-2 favors T cell expansion, as increased competition from NK cells and T cells reduces the availability of IL-15.¹⁸⁹

To increase the T_{CM} population, we tested adding IL-4 in combination with IL-2, and IL-21 in combination with IL-7 and/or IL-15 from day 12 (expansion phase), since J. Sun et al. (2015), and Gerdemann et al. (2012), used the IL-7 and IL-4 combination, obtaining a high percentage of T_{CM} phenotype^{94,148}. However, we did not observe a difference in T cell memory subsets using IL-7 and IL-4 combination compared to IL-7, IL-15 and IL-2. Zeng et al. (2005), demonstrated that IL-21 acts synergistically with IL-15 by regulating and promoting the expansion of CD8⁺ memory T cells (CD44^{high}) and naïve T cells (CD44^{low}), increasing IFN- γ production *in vitro* and tumor regression in an *in vivo* experiment with mice bearing large B16 melanomas, showing that this combination of cytokines was effective¹⁹⁰. However, we did not observe any differences when adding IL-15 and IL-21 or IL-7, IL-15 and IL-21. We have to consider that the cytokines combinations can condition the final T cell phenotype depending not only on which cytokines are used, but also the timing in the culture process and T cell activation stage. Our results suggest that adding these cytokines during the expansion phase (day 12 to 20) may not have an effect on the differentiated T cells. Although, our final T cell product did not reach a higher proportion of T_{CM}, several studies have shown that VSTs with a high percentage of T_{EM} phenotype are efficient, safe, less alloreactive, and capable of persisting *in vivo*.^{108,109,191}

Regarding culture media, there are various options available on the market, and different strategies are currently in use to expand T cells *in vitro*. We used expansion medium for producing EBVSTs, consisting of 45% RPMI-1640, 45% Click's EHAA and 10% hSAB provided by the Banc de Sang i Teixits. In order to overcome possible human serum batch-to-batch inconsistencies, and taking into account that during the transduction phase, the production of ARI-0001 is carried out in TexMACS[®] supplemented with 3%hSAB, we considered testing other commercial media. H. Xu et al. (2018), achieved high fold expansion by culturing CD3⁺ T cells, activated with anti-CD3/anti-CD28, with X-VIVO 15 (without serum) compared to RPMI-1640 supplemented with 10%hSAB.¹⁹² We tested X-VIVO 15 and presented much lower fold expansion compared to the expansion medium used. This difference may not only be because of the media, but also due to the stimulus used to activate the T cells or to the concentration of the cytokines, since they added 1000U/mL of IL-2, while we only added 120U/mL. Additionally, we compared other serum-free media to the expansion media used. In the experiment performed, T cells did not present an expected fold expansion in any media tested, this could be because of the donor's HLA genotype that does not present any HLA restriction to the PepTivator[®] EBV consensus, so the activation phase was inadequate. This may be a limitation when using commercial predesigned peptides. Nevertheless, there was a difference in T cell expansion between the media tested, resulting that the expansion medium showed higher fold expansion than the other media tested. Our results are aligned with MacPherson et al. (2022), as TexMACS[®] and ImmunoCult yielded a lower T cell expansion factor and a higher percentage of effector T

cells (CD45RO⁺CCR7⁻) compared to AIM-V medium and RPMI-1640 supplemented with 5% of human serum.¹⁹³ In contrast, Tischer et al. (2014), successfully produced CMV-specific T cells at a clinical grade cultured in TexMACS[®] without serum supplementation but using the CliniMACS cytokine capture system after re-stimulation with an overlapping peptide pool of the immunodominant CMVpp65 antigen.⁸⁴

After establishing these factors for the culture design, the optimized protocol for generating EBVSTs is straightforward and does not require large numbers of lymphocytes in the initial cell source, compared to other processes that require a leukapheresis as a starting material. Additionally, the PBMCs isolated from non-leukapheresis blood bags can be used to obtain a T cell pure and specific product, with enough cell amount to be cryopreserved.

The expansion methodology used in this study successfully obtained polyclonal EBVSTs composed of both CD4⁺ and CD8⁺ T cells with polyfunctional characteristics, as they could produce IFN- γ , TNF- α , and IL-2. Although we observed an overexpression of exhaustion markers, particularly LAG-3 and PD-1, which are known to inhibit T cell function and production of effector cytokines,^{194,195} the T cells were able to produce cytokines once stimulated with the specific peptides not only at day 20 of expansion culture with also after thawed, consistent with Mora-Buch et al. (2023).¹¹³ Moreover, the EBVSTs retained their cytotoxic potency after being cryopreserved, as *in vitro* cytotoxicity assays demonstrated that they specifically recognized and killed only PHA-blasts pulsed with EBV peptides. For future productions, additional controls must be considered to demonstrate that T cell products are non-alloreactive. This could involve pulsing PHA-blasts with antigens unrelated to EBV, co-culturing with allogeneic cells with partial HLA compatibility, and conducting *in vivo* cytotoxicity and tolerance assays.

Based on TCR sequencing, we demonstrated that the decrease in diversity and increase in T cell clonality suggest that the activation, proliferation, and expansion of T cells occurred as expected in response to the EBV antigen, which is consistent with clonal expansion in response to viral antigens.¹⁹⁶ We further demonstrated that some of the expanded clonotypes have been previously described in the recognition of EBV-specific antigens, as confirmed using tetramers. However, several clonotypes in our final products are still not described in the literature. Single cell sequencing of these cell products could be an option to better characterize the specific T cells. Additionally, we hypothesized that the EBVSTs expanded from the seven donors would share a greater number of common clones. Nevertheless, competition among antigens during T cell clonal expansion is influenced by the diverse TCR- β repertoire of the initial PBMCs, as well as antigen presentation through different HLA molecules of different donors. Moreover, we want to emphasize that TCR sequencing not only allows for the characterization of the T cell repertoire

in terms of clonal diversity and identification of expanded clonotypes but can also be used as a crucial tool to evaluate and track these clonotypes over time once infused in the patient, especially in clinical settings. Studies conducted by Frank et al. (2023) and Keller et al. (2019), demonstrate that TCR sequencing is a valuable tool for monitoring the persistence, expansion, and activity of clonotypes after the administration of VSTs to patients, which can help predict treatment efficacy and clinical outcomes.^{112,197} So, in our project, it can also be used to monitor the persistence of the CAR co-expressed in the EBVSTs.

It is worth noting that the expansion methodology allows the cryopreservation of a sufficient number of EBV-specific T cells. The use of the G-Rex[®] system allowed us to culture cells in a larger volume of medium compared to traditional plates, resulting in higher cell density without the need for continuous medium changes. The permeable silicone gas membrane at the base of the G-Rex[®] plate permits O₂ and CO₂ to be exchanged directly from the cells layer, providing a constant supply of oxygen and nutrients directly to the cells and reducing the need for frequent medium changes.¹⁹⁸ Additionally, in line with Lapteva & Vera (2011) and Gotti et al. (2022), we obtained comparable results when we replicated the protocol on a large-scale production under GMP conditions, with the exception of specificity.^{199,200} In the small scale optimizations using the G-Rex[®] plate, T cells were already highly specific by day 12, whereas in large scale production, specificity increases toward the end of the culture. In relation to this results, T cells showed lower expression of exhaustion markers. We hypothesize that this effect could be due to GMP-grade reagents, which are formulated to meet stringent safety and quality control standards, including the presence of stabilizing agents and the purity processes, potentially leading to a reduction in specificity. However, this was tested under GMP conditions only once, so we cannot conclude whether this percentage is reproducible in other donors. In the future, it may be worthwhile considering to replicate the activation and expansion of PBMCs from the same donor in parallel, on both small and large scale. In our case, we did not replicate this in other donors, as we decided to test the transduction with the EBVSTs obtained from the first production, and if successful, proceed with subsequent productions.

Finally, this expansion methodology can be extrapolated to other viruses (e.g. CMV, BK...) to generate an *off-the-shelf* therapy using the ReDoCel donor registry.¹⁰⁰

Co-expression of CAR.CD19 into the EBVSTs

After optimizing a successful EBVSTs generation protocol and producing a GMP-grade product at large scale, we proceeded to co-express CAR.CD19 in the EBVSTs. Interestingly, the initial attempt following the ARI-0001 production protocol, we observed that the EBVSTs co-expressed 50% of CAR.CD19. Unfortunately, we could not determine whether this co-expression occurred

in CD4⁺ T cells, CD8⁺ T cells, or both. However, we identified that after transduction cells in the culture were predominantly CD4⁺ T cells, indicating that the CD4:CD8 ratio was reversed. Additionally, the CAR.CD19-EBVST product was capable of killing 96% of NALM6 cells at a 2:1 ratio, aligning with the potency acceptance criteria for ARI-0001.⁵⁴ Due to the limited number of the final CAR.CD19-EBVSTs product, it was not possible to assess the potency of the product in additional control cell lines (CD19⁺EBV⁺, CD19⁻EBV⁺). The use of these additional cell lines as controls could provide information indicating that our CAR.CD19-EBVST product is not only capable of killing CD19⁺ tumor cells but also those that are CD19⁺EBV⁺ or exclusively EBV-infected T cells.

In the production of EBVSTs, resulting in mainly CD8⁺ T cell product in most of the expansions performed, we hypothesized that the transduction process would impact the CD4:CD8 ratio by slightly increasing the CD4⁺ T cell population, but not completely reversing it. We believe the increase in CD4⁺ T cells could be attributed to: (1) the DynabeadsTM stimulation, which is more generalized as it activates both the TCR/CD3 and the CD28 co-stimulatory receptor. While this method is effective for T cell activation and expansion, it is not antigen specific. Therefore, re-stimulation of EBVSTs with DynabeadsTM is not effective for maintaining specificity and function. (2) The CD8⁺ T cells, being in more activated state than CD4⁺ T cells, may have died in greater ratio in the overnight culture without stimulation or cytokines.

To address the issue of phenotype in the EBVSTs, we compared the stability, phenotype, and specificity of the EBVSTs before and after thawing. We confirmed that DynabeadsTM stimulation was one factor inducing the expansion or survival of CD4⁺ T cells in the final product, as well as decreasing their specificity, while using soluble antibodies (either anti-CD3 alone or in combination with anti-CD28) maintains the initial phenotype and specificity. In line with our findings, Li & Kurlander (2010), identified that stimulation with anti-CD3/anti-CD28 beads is more effective for expanding CD4⁺ T cells, while soluble antibodies offer significant advantages for expanding CD8⁺ T cells, particularly if they have been previously stimulated with antigens *in vitro* or *in vivo*.¹⁶⁸

We compared the optimal concentration of anti-CD3 alone or combined with anti-CD28, and we demonstrated that using anti-CD3 alone at a low concentration (0.3 µg/mL vs 1 µg/mL) effectively maintained the specificity and phenotype of the EBVSTs for 8-14 days in culture after thawing. Considering the production with the CliniMACS Prodigy[®], in contrast to DynabeadsTM, soluble anti-CD3 is available in GMP format and does not need to be removed from the culture. Additionally, studies from the Baylor College group, which is a reference group in the field, used anti-CD3 antibodies for stimulating VSTs during transduction.^{26,77} However, during transduction,

activating the EBVSTs with anti-CD3 did not result in optimal CAR.CD19 expression. We considered an optimal value to be $\geq 20\%$. In both ARI-0001 and the clinical trial by Cruz et al. (2019), it was established that 20% is sufficient to achieve a therapeutic effect against CD19-expressing B-cell malignancies.^{54,147}

We hypothesize that the lack of CAR.CD19 expression may be due to the following reasons:

(1) Although the first attempt of transduction the EBVSTs was successful with about 50% of cells expressing the construct, we cannot rule out the possibility that using a lentiviral vector with a freeze-thaw cycle might have affected the transduction efficiency, as studies have shown that lentiviral vectors are sensitive to external factors such as heat, osmotic pressure, and freeze-thaw cycles.²⁰¹

(2) There was a lack of information regarding the expression kinetics of the CAR.CD19 in VSTs. It could be internalized or lost, as it was detected only after 14 days of culture. However, when we compared the stability of expression on the same EBVSTs in other transduction attempts on days 6 and 8, it was not detected.

(3) There might have been interference between the anti-CD3 antibody and the biotin-SP-conjugated AffiniPure Goat Anti-Mouse IgG, F(ab')₂ Fragment Specific, which detects the scFv domain of the CAR:

- The stimulus with anti-CD3 antibody (clone OKT3) could cause steric hindrance, potentially blocking or masking CAR detection through scFv, particularly if the CAR and CD3 are in proximity.
- The activation of T cells with anti-CD3 antibody could generate strong downstream signaling, which might alter surface expression or lead to CAR internalization. This could reduce the ability to detect CAR expression if the receptor is being modulated or downregulated due to strong TCR signaling.

To verify this hypothesis, we decided to compare CAR expression by stimulating with both Dynabeads™ and anti-CD3 antibody and using two detection methods (scFv and CD19, Fc Tag). Although higher CAR.CD19 expression was observed using the CD19, Fc Tag method, we cannot conclude that anti-CD3 antibody interferes with the expression and detection of CAR.CD19. This is because, even when stimulating EBVSTs with Dynabeads™, no CAR.CD19 expression was observed using the scFv detection method, which is the traditional method for detecting the transduction efficiency in ARI-0001. However, we can infer that re-stimulating EBVSTs with the soluble anti-CD3 antibody at a concentration of 0.3 $\mu\text{g}/\text{mL}$ is insufficient for CAR.CD19 construct expression in EBVSTs, as a concentration of 1 $\mu\text{g}/\text{mL}$ resulted in double the expression, and Dynabeads™ yielded a 25% increase. Therefore, finding a balance between maintaining phenotype, specificity, and achieving CAR.CD19 expression in EBVSTs after thawing remains a challenge. More experiments are needed to confirm or refute our hypotheses.

Since this is an emerging therapy, there are not many studies available for comparison. In the case of Baylor College, in trials for autologous therapy, they performed transduction during the production of VSTs and J. Sun et al. (2015), demonstrated that transduction is more effective during early stages of VST production.¹⁴⁸ In contrast, our approach to creating an allogenic and "off-the-shelf" therapy, has a more challenging step to optimize transduction starting from previously frozen and activated VSTs.

In parallel, we evaluated the factors that could influence cell expansion, also taking into account the specifications of ARI-0001 to ensure a sufficient cell product for optimal treatment. Based on previous ARI-0001 production, we initially estimated that an optimal expansion would range from 6 to 52-fold, starting from an intermediate product of 100×10^6 EBVST (required for CliniMACS Prodigy[®]), resulting in a final CAR.CD19-EBVST product of 600 to $5,200 \times 10^6$ total cells. These values would allow us to cover a single dose, or fractionated doses as specified for ARI-0001 (0.5 to 1×10^6 cells/kg for adult patients with ALL, and 5×10^6 cells/kg for pediatric patients with ALL and adults with NHL/CLL).⁵⁴⁻⁵⁸

Despite our efforts, the observed expansion of the transduced EBVSTs was lower than expected. However, when considering the infusion doses of VSTs (1×10^7 VSTs/m² to 5×10^8 VSTs/m²),^{95,110,133,139,142} or even more relevant, the current results from clinical trials of the enhanced combined VSTs-CAR therapy (1×10^6 to 4×10^8 CAR-VSTs/m²),^{147,150-153} the total final number of cells required per production batch to treat a single patient would be significantly lower than the initially estimated 600×10^2 total cells. In particular, Heslop et al. (2010) observed that after infusing between $1-5 \times 10^7$ EBVSTs/m² into 114 patients to prevent or treat EBV-PTLD, achieved a sustained complete remissions in the majority of patients and using a genetic marking component demonstrated that functional EBVSTs persisted for up to 12-15 years, with 79 patients alive after 3 to 15 years of follow-up.⁹⁵ Cruz et al. (2013), infusing 1.9×10^7 - 1.13×10^8 CAR-VSTs/m² a complete response was achieved in the majority of patients treated for ALL, and CAR.CD19-VST infusions were found to be safe in all patients, did not induce GvHD, and expanded in the presence of EBV reactivation, with VSTs persisting for an average of 8 weeks in the blood and up to 9 weeks in disease sites.¹⁴⁷ Thus, based on the patient's progression, tolerability, and treatment efficiency, as well as the consideration of infusing multiple or fractionated doses in certain cases, a minimum production of $200-300 \times 10^6$ total cells CAR.CD19-EBVSTs would be necessary to treat a patient. Furthermore, starting with an intermediate product of 200×10^6 EBVSTs instead of 100×10^6 EBVSTs in the CliniMACS Prodigy[®] could be considered, as large-scale production yields a significantly higher total number of EBVSTs.

As part of our efforts to enhance EBVST expansion post-thaw and consequently improve CAR.CD19 expression, along with the microenvironment that impacts both processes, we evaluated the influence of the culture medium used. A study by Eberhardt et al. (2023), demonstrated that after 12 days of culturing CD19.CAR T cells, expansion, viability, and exhaustion markers did not differ between CAR T cells generated in serum-free media compared to standard media containing FBS. Furthermore, CAR T cells generated in serum-free media exhibited greater cytotoxicity than those cultivated with FBS.²⁰² Consistent with our findings, we observed that perform transduction with either TexMACS[®] or expansion media supplemented with 3% serum, there were higher CAR.CD19 expression compared to using expansion media with 10% serum. However, expansion did not reach the expected cell numbers. Additionally, we tested different cytokine combinations without improving previous results, therefore we used the established IL-7 and IL-15 cytokine combination for ARI-0001 production, as CAR-T cells cultured in the presence of these cytokines have demonstrated greater expansion and persistence *in vivo*.²⁰³ Regarding the activation method, it has been observed that stimulating with Dynabeads[™] provides a better expansion factor compared to soluble antibodies.^{192,203,204} Although we observed that Dynabeads[™] led to better expansion in some optimizations, the results were not consistent.

Another important parameter to consider is culture timing, EBVSTs thawed on day 12 showed higher expansion compared to those thawed on days 15 and 20; however, the fold expansion did not reach cell numbers expected. We did not test the expression of exhaustion markers on days 12 and 15, so we cannot confirm whether the cells exhibit exhaustion or if it is due to the differentiation state in which the cells are. Nevertheless, cryopreservation itself has an important effect by itself, regardless of the day it is performed. A study by Owen et al. (2007), indicated that long-term cryopreservation has detrimental effects on IFN- γ responses in T cells, as well as causing a decrease, though more limited, in CD8⁺ T cell responses. These losses were more pronounced in cells stored for over a year compared to those stored for less than six months.²⁰⁵ In our case, we have not tested whether there is an effect on the expansion and IFN- γ production in EBVSTs products stored at different times; but we have observed that IFN- γ production decreases after thawing. In some cases, the percentage of decrease was higher, but after 8-14 days post-thawing culture, some IFN- γ production levels were restored or even increased. Another study, conducted by Baboo et al. (2019), demonstrated that the freezing and thawing process also influences product quality, concluding that a rapid thawing method is more beneficial for T cells when DMSO is used as a cryoprotectant.¹⁶⁴ Consequently, we changed our slow thawing method to a rapid one. However, we did not observe improvement in cell expansion.

We sought to address the challenges of post-thaw T cells expansion and improve the CAR.CD19 expression by reprogramming EBVSTs with Yamanaka factors to change the cell differentiation status and improve their stemness and fitness. Nevertheless, reprogramming T cells, especially antigen-specific T cells, is a highly complex and underexplored process, with an extremely low reprogramming efficiency (approximately 0.0008–0.01%).²⁰⁶ Most reprogramming protocols use fibroblasts as the cell source for differentiation into iPSCs.^{156,158,160,207}

Islam et al. (2023), developed an optimal method for selectively reprogramming tumor antigen-specific T cells from heterogeneous TIL populations, as well as reprogramming PBMCs into iPSCs. They transfected cells using the Sendai CytoTune-iPS 2.0 kit, which contained Yamanaka factors (OCT4, SOX2, KLF4, AND c-MYC) and added the oncogene SV40 (large T antigen) at a high MOI.¹⁶¹ We tested a non-integrative, non-transgenic transfection methods that do not involve viruses to avoid viral particles in the final product, ensuring a safe cell product. Therefore, we chose to transfect mRNA using methods like electroporation or chemical approaches. However, to date, there are no previous studies on reprogramming successfully T cells using these strategies. From our results, we observed that electroporation allows greater mRNA uptake in T cells, but it damages the cells, leading to slower and reduced expansion. Among the chemical methods, Trans-IT[®] appears to be more effective than RNAiMAX, as it resulted in higher mRNA-GFP expression in EBVSTs, as well as in SOX2. However, the post-thaw expansion still did not meet our expectations. We hypothesize that a higher dose of mRNA is required to produce a significant effect in the EBVSTs. Therefore, we will synthesize our own mRNA encoding Yamanaka factors.

Recently, Doan et al. (2024), identified 41 genes that were more active in CAR-T cells associated with good treatment responses compared to those with poor responses. These genes appeared to be regulated by a master switch protein called FOXO1.²⁰⁸ Chan et al. (2024), then modified CAR-T cells to produce more FOXO1, which altered their genetic activity to resemble memory T stem cells, known for their ability to quickly recognize and respond to cancer targets. When these modified cells were injected into mice with various types of cancer, the increased FOXO1 enhanced the CAR-T cells ability to reduce both solid tumors and blood cancers. Additionally, these stem-like cells not only reduced tumors more effectively but also persisted longer *in vivo* compared to standard CAR-T cells.²⁰⁹ These findings open new possibilities to explore other transcription factors beyond the Yamanaka cocktail.

Furthermore, other strategies to modify the differentiation status of the cells could be explored, such as using Urolithin A (UA) to expand T_{SCM} cells, as demonstrated by the group of Denk et al. (2022).²¹⁰ Also, blocking the molecules responsible for cellular exhaustion could be another

approach. Lak et al. (2022), showed that the production of antigen-specific CD8⁺ T cells can be enhanced through the combined blockade of TIM3 and PD-L1/PD-1, achieving significantly improved antigen-specific T cell expansion without inducing dysfunction.²¹¹ Additionally, it would be necessary to replicate our experiments, potentially testing different concentrations of anti-CD3, conditions of serum supplementation, MOI, including more T cell activation markers in the flow cytometry characterization, or even conducting a transcriptomic and metabolomic analysis, to gain deeper insight into the functional status of these cells and identifying the balance between activation and cell culture environment to achieve optimal CAR expression and T cell expansion.

Although we were unable to resolve the issue of EBVST expansion after thawing and co-expressing CAR.CD19 in EBVSTs activated with anti-CD3, and validate the manufacture in the CliniMACS Prodigy[®], the findings open the door to further exploration of this emerging strategy. Additionally, they highlight the potential of combining both therapies to achieve co-expression of native TCR and CAR, which could help overcome the current limitations of CAR-T therapy and potentially extrapolated to other tumor targets.

CONCLUSIONS

1. A protocol was successfully optimized and developed for generating Epstein-Barr virus-specific T cells, demonstrating scalability to GMP standards, providing an *in vitro* safe, pure, specific and polyfunctional product.
2. TCR- β analysis is a valuable tool for assessing the diversity and clonality of expanded products and identifying clonotypes that can recognize EBV antigens presented by donor HLA molecules.
3. The Epstein-Barr virus-specific T cells were able to express CAR.CD19 and effectively kill target cells (NALM6). However, stimulation using DynabeadsTM modified the CD4:CD8 ratio and decreased the specificity of the T cells.
4. Optimization during the transduction process revealed that stimulation with a soluble anti-CD3 antibody, without prior T cell conditioning, retained the phenotype and specificity of Epstein-Barr virus-specific T cells but decreased CAR.CD19 co-expression. Additionally, cellular expansion was limited due to the use of pre-activated, thawed EBVSTs as starting source.
5. Further improvements are needed to enhance cell expansion and increase CAR.CD19 expression in Epstein-Barr virus-specific T cells. Once these challenges are resolved, the manufactured product can be validated using the CliniMACS Prodigy[®].

BIBLIOGRAPHY

1. Sociedad Española de Oncología Médica (SEOM), Red Español de Registros de Cáncer (REDECAN). Las cifras del cáncer en España 2024. https://seom.org/images/publicaciones/informes-seom-de-evaluacion-de-farmacos/LAS_CIFRAS_2024.pdf. Published 2024.
2. Hill BT. Etiology of Cancer. In: *Clinical Ophthalmic Oncology: Basic Principles, Third Edition*. ; 2019:11-17. doi:10.1007/978-3-030-04489-3
3. Gonzalez-Meneses López A. Bases genéticas y moleculares en el cáncer infantil. In: *Pediatría Integral*. Vol XX. ; 2016:359-366.
4. Savage P. Chemotherapy curable malignancies and cancer stem cells: A biological review and hypothesis. *BMC Cancer*. 2016;16(1):1-11. doi:10.1186/s12885-016-2956-z
5. Baskar R, Itahana K. Radiation therapy and cancer control in developing countries: Can we save more lives? *Int J Med Sci*. 2017;14(1):13-17. doi:10.7150/ijms.17288
6. Lu J, Jiang G. The journey of CAR-T therapy in hematological malignancies. *Mol Cancer*. 2022;21(1):1-15. doi:10.1186/s12943-022-01663-0
7. Rodriguez-Abreu D, Bordoni A, Zucca E. Epidemiology of hematological malignancies. *Ann Oncol*. 2007;18(SUPPL. 1):i3-i8. doi:10.1093/annonc/mdl443
8. Alaggio R, Amador C, Anagnostopoulos I, et al. The 5th edition of the World Health Organization Classification of Haematolymphoid Tumours: Lymphoid Neoplasms. *Leukemia*. 2022;36(7):1720-1748. doi:10.1038/s41375-022-01620-2
9. Chang JHC, Poppe MM, Hua CH, Marcus KJ, Esiashvili N. Acute lymphoblastic leukemia. *Pediatr Blood Cancer*. 2021;68(S2):1-7. doi:10.1002/pbc.28371
10. Malard F, Mohty M. Acute lymphoblastic leukaemia. *Lancet*. 2020;395(10230):1146-1162. doi:10.1016/S0140-6736(19)33018-1
11. DeAngelo DJ. The use of novel monoclonal antibodies in the treatment of acute lymphoblastic leukemia. *Hematol (United States)*. 2015;2015(1):400-405. doi:10.1182/asheducation-2015.1.400
12. Díaz-Regañón I. Neoplasias hematológicas. *Libr neoplasias hematológicas para el diagnóstico leucemias agudas*. 2018;65:667-677.
13. Terwilliger T, Abdul-Hay M. Acute lymphoblastic leukemia: a comprehensive review and 2017 update. *Blood Cancer J*. 2017;7(6). doi:10.1038/BCJ.2017.53
14. Kikushige Y. Pathogenesis of chronic lymphocytic leukemia and the development of novel therapeutic strategies. *J Clin Exp Hematop*. 2020;60(4):146-158. doi:10.3960/jslrt.20036
15. Chiorazzi N, Chen SS, Rai KR. Chronic lymphocytic leukemia. *Cold Spring Harb Perspect Med*. 2021;11(2):1-35. doi:10.1101/cshperspect.a035220

16. Ekström-Smedby K. Epidemiology and etiology of non-Hodgkin lymphoma - A review. *Acta Oncol (Madr)*. 2006;45(3):258-271. doi:10.1080/02841860500531682
17. Singh R, Shaik S, Negi BS, et al. Non-Hodgkin's lymphoma: A review. *J Fam Med Prim Care*. 2020;9(4):1834-1840. doi:10.4103/jfmpe.jfmpe_1037_19
18. Shankland KR, Armitage JO, Hancock BW. Non-Hodgkin lymphoma. *Lancet*. 2012;380(9844):848-857. doi:10.1016/S0140-6736(12)60605-9
19. Chihara D, Nastoupil LJ, Williams JN, Lee P, Koff JL, Flowers CR. New insights into the epidemiology of non-Hodgkin lymphoma and implications for therapy. *Expert Rev Anticancer Ther*. 2015;15(5):531-544. doi:10.1586/14737140.2015.1023712
20. Brian C.-H. Chiu NH. *Non-Hodgkin Lymphoma: Pathology, Imaging, and Current Therapy*. (Evens, Andre M.; Blum KA, ed.). Switzerland: Springer International; 2015. doi:10.1007/978-3-319-13150-4
21. Gisselbrecht C, Van Den Neste E. How I manage patients with relapsed/refractory diffuse large B cell lymphoma. *Br J Haematol*. 2018;182(5):633-643. doi:10.1111/bjh.15412
22. Abramson JS. Anti-CD19 CAR T-Cell Therapy for B-Cell Non-Hodgkin Lymphoma. *Transfus Med Rev*. 2020;34(1):29-33. doi:10.1016/j.tmr.2019.08.003
23. Wang HW, Balakrishna JP, Pittaluga S, Jaffe ES. Diagnosis of Hodgkin lymphoma in the modern era. *Br J Haematol*. 2019;184(1):45-59. doi:10.1111/bjh.15614
24. Ansell SM. Hodgkin lymphoma: A 2020 update on diagnosis, risk-stratification, and management. *Am J Hematol*. 2020;95(8):978-989. doi:10.1002/ajh.25856
25. Weiss LM, Strickler JG, Warnke RA, Purtilo DT, Sklar J. Epstein-Barr viral DNA in tissues of Hodgkin's disease. *Am J Pathol*. 1987;129(1):86-91.
26. Ramos CA, Ballard B, Zhang H, et al. Clinical and immunological responses after CD30-specific chimeric antigen receptor-redirected lymphocytes. *J Clin Invest*. 2017;127(9):3462-3471. doi:10.1172/JCI94306
27. Abbas AK, Lichtman AH, Pillai S. *Basic Immunology: Functions and Disorders of the Immune System*. Fifth. Elsevier; 2016.
28. Mellman I, Chen DS, Powles T, Turley SJ. The cancer-immunity cycle: Indication, genotype, and immunotype. *Immunity*. 2023;56(10):2188-2205. doi:10.1016/j.immuni.2023.09.011
29. Cruz-Tapias P, Castiblanco J, Manuel Anaya J. Major histocompatibility complex: Antigen processing and presentation. In: Manuel Anaya J, Shoenfeld Y, Rojas-Villarraga A, Cervera R, eds. *Autoimmunity From Bench to Bedside*. First. Colombia: El Rosario University Press; 2013:169-183.
30. Mariuzza RA, Agnihotri P, Orban J. The structural basis of T-cell receptor (TCR) activation: An enduring enigma. *J Biol Chem*. 2020;295(4):914-925. doi:10.1074/jbc.REV119.009411

31. Rossjohn J, Gras S, Miles JJ, Turner SJ, Godfrey DI, McCluskey J. T cell antigen receptor recognition of antigen-presenting molecules. *Annu Rev Immunol.* 2015;33:169-200. doi:10.1146/annurev-immunol-032414-112334
32. Sun Y, Li F, Sonnemann H, et al. Evolution of cd8+ t cell receptor (Tcr) engineered therapies for the treatment of cancer. *Cells.* 2021;10(9):1-19. doi:10.3390/cells10092379
33. Charmsaz S, Collins DM, Perry AS, Prencipe M. Novel strategies for cancer treatment: Highlights from the 55th IACR annual conference. *Cancers (Basel).* 2019;11(8):1-11. doi:10.3390/cancers11081125
34. Anurathapan U, Leen AM, Brenner MK, Vera JF. Engineered T cells for cancer treatment. *Cytotherapy.* 2014;16(6):713-733. doi:10.1016/j.jcyt.2013.10.002
35. Zhang P, Zhang G, Wan X. Challenges and new technologies in adoptive cell therapy. *J Hematol Oncol.* 2023;16(1):1-55. doi:10.1186/s13045-023-01492-8
36. Cappell KM, Kochenderfer JN. A comparison of chimeric antigen receptors containing CD28 versus 4-1BB costimulatory domains. *Nat Rev Clin Oncol.* 2021;18(11):715-727. doi:10.1038/s41571-021-00530-z
37. Abbasi S, Totmaj MA, Abbasi M, et al. Chimeric antigen receptor T (CAR-T) cells: Novel cell therapy for hematological malignancies. *Cancer Med.* 2023;12(7):7844-7858. doi:10.1002/cam4.5551
38. Jogalekar MP, Rajendran RL, Khan F, Dmello C, Gangadaran P, Ahn BC. CAR T-Cell-Based gene therapy for cancers: new perspectives, challenges, and clinical developments. *Front Immunol.* 2022;13(July):1-15. doi:10.3389/fimmu.2022.925985
39. Ghazi B, El Ghanmi A, Kandoussi S, Ghouzlani A, Badou A. CAR T-cells for colorectal cancer immunotherapy: Ready to go? *Front Immunol.* 2022;13(November):1-23. doi:10.3389/fimmu.2022.978195
40. Sterner RC, Sterner RM. CAR-T cell therapy: current limitations and potential strategies. *Blood Cancer J.* 2021;11(4). doi:10.1038/s41408-021-00459-7
41. Uscanga-Palomeque AC, Chávez-Escamilla AK, Alvizo-Báez CA, et al. CAR-T Cell Therapy: From the Shop to Cancer Therapy. *Int J Mol Sci.* 2023;24(21). doi:10.3390/ijms242115688
42. Torres AM. Síntesis y estado actual de la terapia con CARTs. 2016. Facultad de Medicina, Universidad de Zaragoza, España.
43. Kawalekar OU, O'Connor RS, Fraietta JA, et al. Distinct Signaling of Coreceptors Regulates Specific Metabolism Pathways and Impacts Memory Development in CAR T Cells. *Immunity.* 2016;44(2):380-390. doi:10.1016/j.immuni.2016.01.021
44. Tokarew N, Ogonek J, Endres S, von Bergwelt-Baildon M, Kobold S. Teaching an old dog new tricks: next-generation CAR T cells. *Br J Cancer.* 2019;120(1):26-37. doi:10.1038/s41416-018-0325-1

45. Eshhar Z, Waks T, Gkoss G, Schindler DG. Specific activation and targeting of cytotoxic lymphocytes through chimeric single chains consisting of antibody-binding domains and the γ or ζ subunits of the immunoglobulin and T-cell receptors. *Proc Natl Acad Sci U S A*. 1993;90(2):720-724. doi:10.1073/pnas.90.2.720
46. Smith AJ, Oertle J, Warren D, Prato D. Chimeric antigen receptor (CAR) T cell therapy for malignant cancers: Summary and perspective. *J Cell Immunother*. 2016;2(2):59-68. doi:10.1016/j.jocit.2016.08.001
47. Kagoya Y, Tanaka S, Guo T, et al. A novel chimeric antigen receptor containing a JAK-STAT signaling domain mediates superior antitumor effects. *Nat Med*. 2018;24(3):352-359. doi:10.1038/nm.4478
48. Labbé RP, Vessillier S, Rafiq QA. Lentiviral vectors for t cell engineering: Clinical applications, bioprocessing and future perspectives. *Viruses*. 2021;13(8):1-22. doi:10.3390/v13081528
49. Milone MC, O'Doherty U. Clinical use of lentiviral vectors. *Leukemia*. 2018;32(7):1529-1541. doi:10.1038/s41375-018-0106-0
50. Mirones I, Moreno L, Pati A, Moraleda JM, Luisa M, Pérez-martínez A. Inmunoterapia con células CAR-T en hematooncología pediátrica. *An Pediatr (Barc)*. 2020;93(1):59.e1-59.e10.
51. Wang JY, Wang L. CAR-T cell therapy: Where are we now, and where are we heading? *Blood Sci*. 2023;5(4):237-248. doi:10.1097/BS9.0000000000000173
52. Mitra A, Barua A, Huang L, Ganguly S, Feng Q, He B. From bench to bedside: the history and progress of CAR T cell therapy. *Front Immunol*. 2023;14(May):1-14. doi:10.3389/fimmu.2023.1188049
53. Chen Y, Abila B, Kamel YM. CAR-T : What Is Next ? *Cancers (Basel)*. 2023;15(663):1-20. doi:doi.org/10.3390/cancers15030663
54. Castella M, Boronat A, Martín-Ibáñez R, et al. Development of a Novel Anti-CD19 Chimeric Antigen Receptor: A Paradigm for an Affordable CAR T Cell Production at Academic Institutions. *Mol Ther Methods Clin Dev*. 2019;12(March):134-144. doi:10.1016/j.omtm.2018.11.010
55. Ortiz-Maldonado V, Alonso-Saladrigues A, Español-Rego M, et al. Results of ARI-0001 CART19 cell therapy in patients with relapsed/refractory CD19-positive acute lymphoblastic leukemia with isolated extramedullary disease. *Am J Hematol*. 2022;97(6):731-739. doi:10.1002/ajh.26519
56. Castella M, Caballero-Baños M, Ortiz-Maldonado V, et al. Point-of-care CAR T-cell production (ARI-0001) using a closed semi-automatic bioreactor: Experience from an academic phase i clinical trial. *Front Immunol*. 2020;11(March):1-13. doi:10.3389/fimmu.2020.00482

57. Ortíz-Maldonado V, Rives S, Castellà M, et al. CART19-BE-01: A Multicenter Trial of ARI-0001 Cell Therapy in Patients with CD19+ Relapsed/Refractory Malignancies. *Mol Ther.* 2021;29(2):636-644. doi:10.1016/j.ymthe.2020.09.027
58. Ortiz-Maldonado V, Frigola G, Español-Rego M, et al. Results of ARI-0001 CART19 Cells in Patients With Chronic Lymphocytic Leukemia and Richter's Transformation. *Front Oncol.* 2022;12(January):1-7. doi:10.3389/fonc.2022.828471
59. Frigault MJ, Maus M V. State of the art in CAR T cell therapy for CD19+ B cell malignancies. *J Clin Invest.* 2020;130(4):1586-1594. doi:10.1172/JCI129208
60. Zhao L, Cao YJ. Engineered T Cell Therapy for Cancer in the Clinic. *Front Immunol.* 2019;10(October). doi:10.3389/fimmu.2019.02250
61. Gattinoni L, Finkelstein SE, Klebanoff CA, et al. Removal of homeostatic cytokine sinks by lymphodepletion enhances the efficacy of adoptively transferred tumor-specific CD8+ T cells. *J Exp Med.* 2005;202(7):907-912. doi:10.1084/jem.20050732
62. Brudno JN, Kochenderfer JN. Toxicities of chimeric antigen receptor T cells: Recognition and management. *Blood.* 2016;127(26):3321-3330. doi:10.1182/blood-2016-04-703751
63. Klebanoff CA, Khong HT, Antony PA, Palmer DC, Restifo NP. Sinks, suppressors and antigen presenters: how lymphodepletion enhances T cell-mediated tumor immunotherapy. *Trends Immunol.* 2005;26(2):111-117. doi:10.1016/j.it.2004.12.003
64. Santomaso BD, Park JH, Salloum D, et al. Clinical and Biologic Correlates of Neurotoxicity Associated with CAR T Cell Therapy in Patients with B-cell Acute Lymphoblastic Leukemia (B-ALL). *Cancer Discov.* 2019;8(8):958-971. doi:10.1158/2159-8290.CD-17-1319
65. Yáñez L, Sánchez-Escamilla M, Perales MA. CAR T cell toxicity: Current management and future directions. *HemaSphere.* 2019;3(2). doi:10.1097/HS9.0000000000000186
66. Maus M V., Grupp SA, Porter DL, June CH. Antibody-modified T cells: CARs take the front seat for hematologic malignancies. *Blood.* 2014;123(17):2625-2635. doi:10.1182/blood-2013-11-492231
67. Brudno JN, Somerville RPT, Shi V, et al. Allogeneic T cells that express an anti-CD19 chimeric antigen receptor induce remissions of B-cell malignancies that progress after allogeneic hematopoietic stem-cell transplantation without causing graft-versus-host disease. *J Clin Oncol.* 2016;34(10):1112-1121. doi:10.1200/JCO.2015.64.5929
68. Gardner R, Wu D, Cherian S, et al. Acquisition of a CD19-negative myeloid phenotype allows immune escape of MLL-rearranged B-ALL from CD19 CAR-T-cell therapy. *Blood.* 2016;127(20):2406-2410. doi:10.1182/blood-2015-08-665547
69. Hamieh M, Dobrin A, Cabriolu A, et al. CAR T cell trogocytosis and cooperative killing regulate tumour antigen escape. *Nature.* 2019;568(62):112-116. doi:10.1038/s41586-019-1054-1

70. Quail D, Joyce J. Microenvironmental regulation of tumor progression and metastasis. *Nat Med*. 2013;19(11):1423-1437. doi:10.1038/nm.3394
71. Larson RC, Maus M V. Recent advances and discoveries in the mechanisms and functions of CAR T cells. *Nat Rev Cancer*. 2021;21(3):145-161. doi:10.1038/s41568-020-00323-z
72. Lonez C, Breman E. Allogeneic CAR-T Therapy Technologies: Has the Promise Been Met? *Cells*. 2024;13(2). doi:10.3390/cells13020146
73. Egri N, Ortiz de Landazuri I, San Bartolomé C, Ortega JR, Español-Rego M, Juan M. CART manufacturing process and reasons for academy-pharma collaboration. *Immunol Lett*. 2020;217(September 2019):39-48. doi:10.1016/j.imlet.2019.10.014
74. Quach DH, Lulla P, Rooney CM. Banking on virus-specific T cells to fulfill the need for off-the-shelf cell therapies. *Blood*. 2023;141(8):877-885. doi:10.1182/blood.2022016202
75. Motta CM, Keller MD, Bollard CM. Applications of virus-specific T cell therapies post-BMT. *Semin Hematol*. 2023;60(1):10-19. doi:10.1053/j.seminhematol.2022.12.002
76. Kaeuferle T, Krauss R, Blaeschke F, Willier S, Feuchtinger T. Strategies of adoptive T - cell transfer to treat refractory viral infections post allogeneic stem cell transplantation. *J Hematol Oncol*. 2019;12(1):1-10. doi:10.1186/s13045-019-0701-1
77. Omer B, Cardenas MG, Pfeiffer T, et al. A Costimulatory CAR Improves TCR-based Cancer Immunotherapy. *Cancer Immunol Res*. 2022;10(4):512-524. doi:10.1158/2326-6066.CIR-21-0307
78. Riddell SR, Watanabe KS, Goodrich JM, Li CR, Agha ME, Greenberg PD. Restoration of Viral Immunity in Immunodeficient Humans by the Adoptive Transfer of T Cell Clones. *Science (80-)*. 1992;257(5067):238-241. doi:10.1126/science.1352912
79. Barrett AJ, Prockop S, Bollard CM. Virus-Specific T Cells: Broadening Applicability. *Biol Blood Marrow Transplant*. 2018;24(1). doi:10.1016/j.bbmt.2017.10.004
80. Saglio F, Hanley PJ, Bollard CM. The time is now: Moving toward virus-specific T cells after allogeneic hematopoietic stem cell transplantation as the standard of care. *Cytotherapy*. 2014;16(2):149-159. doi:10.1016/j.jcyt.2013.11.010
81. Bollard CM, Heslop HE. T cells for viral infections after allogeneic hematopoietic stem cell transplant. *Blood*. 2016;127(26):3331-3340. doi:10.1182/blood-2016-01-628982
82. Harding C V., Canaday D, Ramachandra L. Choosing and Preparing Antigen-Presenting Cells. In: *Current Protocols in Immunology*. Vol 88. ; 2010:1-30. doi:10.1002/0471142735.im1601s88
83. Lodge A. What Are Irradiated PBMCs. Eureka, a dose of Science. <https://www.criver.com/eureka/what-are-irradiated-pbmc>. Published 2023. Accessed September 3, 2024.
84. Tischer S, Priesner C, Heuft HG, et al. Rapid generation of clinical-grade antiviral T cells: Selection of suitable T-cell donors and GMP-compliant manufacturing of antiviral T cells.

- J Transl Med.* 2014;12(1). doi:10.1186/s12967-014-0336-5
85. Alonso L, Rudilla F, Gimeno R, et al. Successful treatment of post-transplant CMV meningoencephalitis with third-party CMV virus-specific T cells: Lessons learned. *Pediatr Transplant.* 2019;23(8):1-4. doi:10.1111/petr.13584
 86. Alonso L, Méndez-Echevarría A, Rudilla F, et al. Failure of Viral-Specific T Cells Administered in Pre-transplant Settings in Children with Inborn Errors of Immunity. *J Clin Immunol.* 2021;41(4):748-755. doi:10.1007/s10875-020-00961-w
 87. Sempere A, Castillo N, Rudilla F, et al. Successful BK virus-specific T cell therapy in a kidney transplant recipient with progressive multifocal leukoencephalopathy. *Am J Transplant.* 2024;24(9):1698–1702. doi:https://doi.org/10.1016/j.ajt.2024.05.003
 88. Walter EA, Greenberg PD, Gilbert MJ, et al. Reconstitution of Cellular Immunity against Cytomegalovirus in Recipients of Allogeneic Bone Marrow by Transfer of T-Cell Clones from the Donor. *N Engl J Med.* 1995;333(16):1038-1044. doi:10.1056/nejm199510193331603
 89. Leen AM, Myers GD, Sili U, et al. Monoculture-derived T lymphocytes specific for multiple viruses expand and produce clinically relevant effects in immunocompromised individuals. *Nat Med.* 2006;12(10):1160-1166. doi:10.1038/nm1475
 90. Green A, Rubinstein JD, Grimley M, Pfeiffer T. Virus-Specific T Cells for the Treatment of Systemic Infections Following Allogeneic Hematopoietic Cell and Solid Organ Transplantation. *J Pediatric Infect Dis Soc.* 2024;13(Suppl 1):S49-S57. doi:10.1093/jpids/piad077
 91. Papadopoulou A, Gerdemann U, Katari UL, et al. Activity of Broad-Spectrum T Cells as Treatment for AdV, EBV, CMV, BKV, and HHV6 Infections after HSCT Anastasia. 2014;6(242). doi:10.1126/scitranslmed.3008825
 92. Gerdemann U, Katari UL, Papadopoulou A, et al. Safety and clinical efficacy of rapidly-generated trivirus-directed T cells as treatment for adenovirus, EBV, and CMV infections after allogeneic hematopoietic stem cell transplant. *Mol Ther.* 2013;21(11):2113-2121. doi:10.1038/mt.2013.151
 93. Hanley PJ, Melenhorst JJ, Nikiforow S, et al. CMV-specific T cells generated from naïve T cells recognize atypical epitopes and may be protective in vivo. *Sci Transl Med.* 2015;7(285). doi:10.1126/scitranslmed.aaa2546
 94. Gerdemann U, Keirnan JM, Katari UL, et al. Rapidly generated multivirus-specific cytotoxic T lymphocytes for the prophylaxis and treatment of viral infections. *Mol Ther.* 2012;20(8):1622-1632. doi:10.1038/mt.2012.130
 95. Heslop HE, Slobod KS, Pule MA, et al. Long-term outcome of EBV-specific T-cell infusions to prevent or treat EBV-related lymphoproliferative disease in transplant recipients. *Blood.* 2010;115(5):925-935. doi:10.1182/blood-2009-08-239186

96. Prockop S, Doubrovina E, Suser S, et al. Off-the-shelf EBV-specific T cell immunotherapy for rituximab-refractory EBV-associated lymphoma following transplantation. *J Clin Invest.* 2020;130(2). doi:10.1172/JCI121127
97. Olson A, Lin R, Marin D, Rafei H, Bdaiwi MH, Thall PF. Third-Party BK Virus-Specific Cytotoxic T Lymphocyte Therapy for Hemorrhagic Cystitis Following Allogeneic Transplantation abstract. *J Clin Oncol.* 2021;39(24):2710-2719. doi:https://doi.org/10.1200/JCO.20.02608 J
98. Pfeiffer T, Tzannou I, Wu M, et al. Posoleucel, an Allogeneic, Off-the-Shelf Multivirus-Specific T-Cell Therapy, for the Treatment of Refractory Viral Infections in the Post-HCT Setting. *Clin Cancer Res.* 2023;29(2):3240330. doi:10.1158/1078-0432.CCR-22-2415
99. Bonifacius A, Lamottke B, Tischer-Zimmermann S, et al. Patient-tailored adoptive immunotherapy with EBV-specific T cells from related and unrelated donors. *J Clin Invest.* 2023;133(12):1-14. doi:10.1172/JCI163548
100. Rudilla F, Carrasco-Benso MP, Pasamar H, et al. Development and characterization of a cell donor registry for virus-specific T cell manufacture in a blood bank. *HLA.* 2024;103(3):1-12. doi:10.1111/tan.15419
101. Dave H, Luo M, Blaney JW, et al. Toward a Rapid Production of Multivirus-Specific T Cells Targeting BKV, Adenovirus, CMV, and EBV from Umbilical Cord Blood. *Mol Ther Methods Clin Dev.* 2017;5(June):13-21. doi:10.1016/j.omtm.2017.02.001
102. Hanley PJ, Cruz CRY, Savoldo B, et al. Functionally active virus-specific T cells that target CMV, adenovirus, and EBV can be expanded from naive T-cell populations in cord blood and will target a range of viral epitopes. *Blood.* 2009;114(9):1958-1967. doi:10.1182/blood-2009-03-213256
103. Abraham AA, John TD, Keller MD, et al. Safety and feasibility of virus-specific T cells derived from umbilical cord blood in cord blood transplant recipients. *Blood Adv.* 2019;3(14):2057-2068. doi:10.1182/bloodadvances.2019000201
104. Withers B, Clancy L, Burgess J, et al. Establishment and Operation of a Third-Party Virus-Specific T Cell Bank within an Allogeneic Stem Cell Transplant Program. *Biol Blood Marrow Transplant.* 2018;24(12). doi:10.1016/j.bbmt.2018.08.024
105. Withers B, Blyth E, Clancy LE, et al. Long-term control of recurrent or refractory viral infections after allogeneic HSCT with third-party virus-specific T cells. *Blood Adv.* 2017;1(24):2193-2205. doi:10.1182/bloodadvances.2017010223
106. Tzannou I, Watanabe A, Naik S, et al. “mini” bank of only 8 donors supplies CMV-directed T cells to diverse recipients. *Blood Adv.* 2019;3(17):2571-2580. doi:10.1182/bloodadvances.2019000371
107. Richard J, O’Reilly M, Susan Prockop M, Aisha N. Hasan M, Guenther Koehne, MD P, Ekaterina Doubrovina M. Virus-Specific T-Cell Banks for “Off the Shelf” Adoptive

- Therapy of Refractory Infections. *Bone Marrow Transplant*. 2016;51(9):1163-1172. doi:10.1038/bmt.2016.17.VIRUS-SPECIFIC
108. Leen AM, Bollard CM, Mendizabal AM, et al. Multicenter study of banked third-party virus-specific T cells to treat severe viral infections after hematopoietic stem cell transplantation. *Blood*. 2013;121(26):5113-5123. doi:10.1182/blood-2013-02-486324
 109. Melenhorst JJ, Leen AM, Bollard CM, et al. Allogeneic virus-specific T cells with HLA alloreactivity do not produce GVHD in human subjects. *Blood*. 2010;116(22). doi:10.1182/blood-2010-06-289991
 110. Tzannou I, Papadopoulou A, Naik S, et al. Off-the-shelf virus-specific T cells to treat BK virus, human herpesvirus 6, cytomegalovirus, Epstein-Barr virus, and adenovirus infections after allogeneic hematopoietic stem-cell transplantation. *J Clin Oncol*. 2017;35(31):3547-3557. doi:10.1200/JCO.2017.73.0655
 111. Haque T, Wilkie GM, Taylor C, et al. Treatment of Epstein-Barr-virus-positive post-transplantation lymphoproliferative disease with partly HLA-matched allogeneic cytotoxic T cells. *Lancet*. 2002;360(9331):436-442. doi:10.1016/S0140-6736(02)09672-1
 112. Keller MD, Darko S, Lang H, et al. T-cell receptor sequencing demonstrates persistence of virus-specific T cells after antiviral immunotherapy. *Br J Haematol*. 2020;187(2):206-218. doi:10.1111/bjh.16053.T
 113. Mora-Buch R, Tomás-Marín M, Enrich E, et al. Virus-Specific T Cells From Cryopreserved Blood During an Emergent Virus Outbreak for a Potential Off-the-Shelf Therapy. *Transplant Cell Ther*. 2023;29(9). doi:10.1016/j.jtct.2023.06.001
 114. Nelson AS, Heyenbruch D, Rubinstein JD, et al. Virus-specific T-cell therapy to treat BK polyomavirus infection in bone marrow and solid organ transplant recipients. *Blood Adv*. 2020;4(22):5745-5754. doi:10.1182/bloodadvances.2020003073
 115. Leen AM, Christin A, Myers GD, et al. Cytotoxic T lymphocyte therapy with donor T cells prevents and treats adenovirus and Epstein-Barr virus infections after haploidentical and matched unrelated stem cell transplantation. *Blood*. 2009;114(19):4283-4292. doi:10.1182/blood-2009-07-232454
 116. Doubrovina E, Oflaz-Sozmen B, Prockop SE, et al. Adoptive immunotherapy with unselected or EBV-specific T cells for biopsy-proven EBV+ lymphomas after allogeneic hematopoietic cell transplantation. *Blood*. 2012;119(11):2644-2656. doi:10.1182/blood-2011-08-371971
 117. Icheva V, Kayser S, Wolff D, et al. Adoptive transfer of Epstein-Barr virus (EBV) nuclear antigen 1-specific T cells as treatment for EBV reactivation and lymphoproliferative disorders after allogeneic stem-cell transplantation. *J Clin Oncol*. 2013;31(1):39-48. doi:10.1200/JCO.2011.39.8495

118. Prockop SE, Hasan A, Doubrovina E, et al. Third-party cytomegalovirus-specific T cells improved survival in refractory cytomegalovirus viremia after hematopoietic transplant. *J Clin Invest.* 2023;133(10):1-16. doi:10.1172/JCI165476
119. Pei XY, Zhao XY, Chang YJ, et al. Cytomegalovirus-Specific T-Cell Transfer for Refractory Cytomegalovirus Infection after Haploidentical Stem Cell Transplantation: The Quantitative and Qualitative Immune Recovery for Cytomegalovirus. *J Infect Dis.* 2017;216(8):945-956. doi:10.1093/infdis/jix357
120. Jiang W, Clancy LE, Avdic S, et al. Third-party CMV- and EBV-specific T-cells for first viral reactivation after allogeneic stem cell transplant. *Blood Adv.* 2022;6(17):4949-4966. doi:10.1182/bloodadvances.2022007103
121. Feucht J, Opherk K, Lang P, et al. Adoptive T-cell therapy with hexon-specific Th1 cells as a treatment of refractory adenovirus infection after HSCT. *Blood.* 2015;125(12):1986-1994. doi:10.1182/blood-2014-06-573725
122. Rubinstein JD, Zhu X, Leemhuis T, et al. Virus-specific T cells for adenovirus infection after stem cell transplantation are highly effective and class II HLA restricted. *Blood Adv.* 2021;5(17):3309-3321. doi:10.1182/BLOODADVANCES.2021004456
123. Creidy R, Moshous D, Touzot F, et al. Specific T cells for the treatment of cytomegalovirus and/or adenovirus in the context of hematopoietic stem cell transplantation. *J Allergy Clin Immunol.* 2016;138(3):920-924.e3. doi:10.1016/j.jaci.2016.03.032
124. Damania B, Kenney SC, Raab-Traub N. Epstein-Barr virus: Biology and clinical disease. *Cell.* 2022;185(20):3652-3670. doi:10.1016/j.cell.2022.08.026
125. Yu H, Robertson ES. Epstein–Barr Virus History and Pathogenesis. *Viruses.* 2023;15(3). doi:10.3390/v15030714
126. AbdelAziz Soliman SH, Orlacchio A, Verginelli F. Viral manipulation of the host epigenome as a driver of virus-induced oncogenesis. *Microorganisms.* 2021;9(6):1-42. doi:10.3390/microorganisms9061179
127. Münz C. Latency and lytic replication in Epstein–Barr virus-associated oncogenesis. *Nat Rev Microbiol.* 2019;17(11):691-700. doi:10.1038/s41579-019-0249-7
128. Babcock GJ, Hochberg D, Thorley-Lawson DA. The expression pattern of Epstein-Barr virus latent genes in vivo is dependent upon the differentiation stage of the infected B cell. *Immunity.* 2000;13(4):497-506. doi:10.1016/S1074-7613(00)00049-2
129. Heslop HE, Sharma S, Rooney CM. Adoptive T-Cell Therapy for Epstein-Barr Virus – Related Lymphomas. *Clin Oncol.* 2021;39(2):514-524. doi:https://doi.org/10.1200/JCO.20.01709
130. Rooney CM, Ng CYC, Loftin S, et al. Use of gene-modified virus-specific T lymphocytes to control Epstein-Barr-virus-related lymphoproliferation. *Lancet.* 1995;345(8941):9-13.

- doi:10.1016/S0140-6736(95)91150-2
131. Jalili A, Hajifathali A, Mohammadian M, et al. Virus-Specific T Cells: Promising Adoptive T Cell Therapy Against Infectious Diseases Following Hematopoietic Stem Cell Transplantation. *Adv Pharm Bull.* 2023;13(3):469-482. doi:10.34172/apb.2023.046
 132. Mahadeo K, Baiocchi R, Beitinjaneh A, et al. Tabelecleucel for allogeneic haematopoietic stem-cell or solid organ transplant recipients with Epstein–Barr viruspositive post-transplant lymphoproliferative disease after failure of rituximab or rituximab and chemotherapy (ALLELE): a phase 3, multicentr. *Lancet Oncol.* 2024;25(3):376-387.
 133. Bollard CM, Gottschalk S, Torrano V, et al. Sustained complete responses in patients with lymphoma receiving autologous cytotoxic T lymphocytes targeting Epstein-Barr virus latent membrane proteins. *J Clin Oncol.* 2014;32(8):798-808. doi:10.1200/JCO.2013.51.5304
 134. Cho SG, Kim N, Sohn HJ, et al. Long-term Outcome of Extranodal NK/T Cell Lymphoma Patients Treated with Postremission Therapy Using EBV LMP1 and LMP2a-specific CTLs. *Mol Ther.* 2015;23(8):1401-1409. doi:10.1038/mt.2015.91
 135. McLaughlin LP, Rouce R, Gottschalk S, et al. EBV/LMP-specific T cells maintain remissions of T- and B-cell EBV lymphomas after allogeneic bone marrow transplantation. *Blood.* 2018;132(22):2351-2361. doi:10.1182/blood-2018-07-863654
 136. Levitskaya J, Coram M, Levitsky V, et al. Inhibition of antigen processing by the internal repeat region of the Epstein-Barr virus nuclear antigen-1. *Nature.* 1995;375(22):685-688.
 137. Haque T, Wilkie GM, Jones MM, et al. Allogeneic cytotoxic T-cell therapy for EBV-positive posttransplantation lymphoproliferative disease: Results of a phase 2 multicenter clinical trial. *Blood.* 2007;110(4):1123-1131. doi:10.1182/blood-2006-12-063008
 138. Vickers MA, Wilkie GM, Robinson N, et al. Establishment and operation of a good manufacturing practice-compliant allogeneic Epstein-Barr virus (EBV)-specific cytotoxic cell bank for the treatment of EBV-associated lymphoproliferative disease. *Br J Haematol.* 2014;167(3):402-410. doi:10.1111/bjh.13051
 139. Kazi S, Mathur A, Wilkie G, et al. Long-term follow up after third-party viral-specific cytotoxic lymphocytes for immunosuppression- and Epstein-Barr virus-associated lymphoproliferative disease. *Haematologica.* 2019;104(8):356-359. doi:10.3324/haematol.2018.207548
 140. Sun Q, Burton R, Reddy V, Lucas KG. Safety of allogeneic Epstein-Barr virus (EBV)-specific cytotoxic T lymphocytes for patients with refractory EBV-related lymphoma. *Br J Haematol.* 2002;118(3):799-808. doi:10.1046/j.1365-2141.2002.03683.x
 141. Gallot G, Vollant S, Saïagh S, et al. T-cell therapy using a bank of EBV-specific Cytotoxic T cells: Lessons from a phase I/II feasibility and safety study. *J Immunother.* 2014;37(3):170-179. doi:10.1097/CJI.0000000000000031

142. Naik S, Nicholas S, Martinez C, et al. Adoptive Immunotherapy for Primary Immunodeficiency Disorders with Virus-Specific T-lymphocytes. *J Allergy Clin Immunol.* 2016;135(5):1498-1505. doi:10.1016/j.jaci.2015.12.1311
143. Uhlin M, Okas M, Gertow J, Uzunel M, Brismar TB, Mattsson J. A novel haplo-identical adoptive CTL therapy as a treatment for EBV-associated lymphoma after stem cell transplantation. *Cancer Immunol Immunother.* 2010;59(3):473-477. doi:10.1007/s00262-009-0789-1
144. Chiou FK, Beath S V., Wilkie GM, Vickers MA, Morland B, Gupte GL. Cytotoxic T-lymphocyte therapy for post-transplant lymphoproliferative disorder after solid organ transplantation in children. *Pediatr Transplant.* 2018;22(2):1-7. doi:10.1111/ptr.13133
145. Mika T, Strate K, Ladigan S, et al. Refractory Epstein-Barr Virus (EBV)-Related Post-transplant Lymphoproliferative Disease: Cure by Combined Brentuximab Vedotin and Allogeneic EBV-Specific T-Lymphocytes. *Front Med.* 2019;6(December):1-5. doi:10.3389/fmed.2019.00295
146. Lapteva N, Gilbert M, Diaconu I, et al. T Cell Receptor Stimulation Enhances the Expansion and Function of CD19 Chimeric Antigen Receptor-Expressing T Cells. *Clin Cancer Res.* 2020;25(24):7340-7350. doi:10.1158/1078-0432.CCR-18-3199
147. Cruz CRY, Micklethwaite KP, Savoldo B, et al. Infusion of donor-derived CD19-redIRECTED virus-specific T cells for B-cell malignancies relapsed After allogeneic stem cell transplant: A phase 1 study. *Blood.* 2013;122(17):2956-2973. doi:10.1182/blood-2013-06-506741
148. Sun J, Huye LE, Lapteva N, et al. Early transduction produces highly functional chimeric antigen receptor-modified virus-specific T-cells with central memory markers: A Production Assistant for Cell Therapy (PACT) translational application. *J Immunother Cancer.* 2015;3(1). doi:10.1186/s40425-015-0049-1
149. Omer B, Castillo PA, Tashiro H, et al. Chimeric antigen receptor signaling domains differentially regulate proliferation and native T cell receptor function in virus-specific T cells. *Front Med.* 2018;5(343):1-13. doi:10.3389/fmed.2018.00343
150. Quach DH, Ramos CA, Lulla PD, et al. CD30.CAR-Modified Epstein-Barr Virus-Specific T Cells (CD30.CAR EBVSTs) Provide a Safe and Effective Off-the-Shelf Therapy for Patients with CD30-Positive Lymphoma. *Blood.* 2022;140(Supplement 1):412-414. doi:10.1182/blood-2022-160244
151. Ahmed N, Brawley V, Hegde M, et al. HER2-specific chimeric antigen receptor–modified virus-specific T cells for progressive glioblastoma: A phase 1 dose-escalation trial. *JAMA Oncol.* 2017;3(8). doi:10.1001/jamaoncol.2017.0184
152. Makawita S, Gibbs JM, McFadden DR, et al. Binary Oncolytic Adenovirus in Combination With HER2-Specific Autologous CAR VST, Advanced HER2 Positive

- Solid Tumors (VISTA). *J Clin Oncol.* 2024;42(16).
<https://clinicaltrials.gov/ct2/show/NCT03740256>.
153. Teppert K, Wang X, Anders K, Evaristo C, Lock D, Künkele A. Joining Forces for Cancer Treatment: From “TCR versus CAR” to “TCR and CAR.” *Int J Mol Sci.* 2022;23(23). doi:10.3390/ijms232314563
 154. Singh PB, Zhakupova A. Age reprogramming: cell rejuvenation by partial reprogramming. *Dev.* 2022;149(22). doi:10.1242/dev.200755
 155. Bailly A, Milhavet O, Lemaitre J-M. RNA-Based Strategies for Cell Reprogramming toward Pluripotency To cite this version : HAL Id : hal-03565865 RNA-Based Strategies for Cell Reprogramming toward Pluripotency. *Pharmaceutics.* 2022;14(317):1-25.
 156. Takahashi K, Yamanaka S. Induction of Pluripotent Stem Cells from Mouse Embryonic and Adult Fibroblast Cultures by Defined Factors. *Cell.* 2006;126(4):663-676. doi:10.1016/j.cell.2006.07.024
 157. Aguirre M, Escobar M, Forero Amézquita S, et al. Application of the Yamanaka Transcription Factors Oct4, Sox2, Klf4, and c-Myc from the Laboratory to the Clinic. *Genes (Basel).* 2023;14(9). doi:10.3390/genes14091697
 158. Yu J, Vodyanik MA, Smuga-Otto K, et al. Induced pluripotent stem cell lines derived from human somatic cells. *Science (80-).* 2007;318(5858):1917-1920. doi:10.1126/science.1151526
 159. Staerk, J, et al. Reprogramming of peripheral blood cells to induced pluripotent stem cells. *Cell Stem Cell.* 2010;7(1):20-24. doi:10.1016/j.stem.2010.06.002
 160. Ciešlar-Pobuda A, Knoflach V, Rinh M V., et al. Transdifferentiation and reprogramming: Overview of the processes, their similarities and differences. *Mol Cell Res.* 2017;1864(7):1359-1369. doi:10.1016/j.bbamcr.2017.04.017
 161. Islam SMR, Maeda T, Tamaoki N, et al. Reprogramming of Tumor-reactive Tumor-infiltrating Lymphocytes to Human-induced Pluripotent Stem Cells. *Cancer Res Commun.* 2023;3(5):917-932. doi:10.1158/2767-9764.crc-22-0265
 162. Bolotin DA, Poslavsky S, Mitrophanov I, et al. MiXCR: Software for comprehensive adaptive immunity profiling. *Nat Methods.* 2015;12(5):380-381. doi:10.1038/nmeth.3364
 163. Shugay M, Bagaev D V., Turchaninova MA, et al. VDJtools: Unifying Post-analysis of T Cell Receptor Repertoires. *PLoS Comput Biol.* 2015;11(11):1-16. doi:10.1371/journal.pcbi.1004503
 164. Baboo J, Kilbride P, Delahaye M, et al. The Impact of Varying Cooling and Thawing Rates on the Quality of Cryopreserved Human Peripheral Blood T Cells. *Sci Rep.* 2019;9(1):1-13. doi:10.1038/s41598-019-39957-x
 165. Liu M, Wang R, Xie Z. T cell-mediated immunity during Epstein–Barr virus infections in children. *Infect Genet Evol.* 2023;112(January). doi:10.1016/j.meegid.2023.105443

166. Pender MP. The essential role of Epstein-Barr virus in the pathogenesis of multiple sclerosis. *Neuroscientist*. 2011;17(4):351-367. doi:10.1177/1073858410381531
167. Martinez OM, Krams SM. The Immune Response to Epstein Barr Virus and Implications for Posttransplant Lymphoproliferative Disorder. *Transplantation*. 2017;101(9):2009-2016. doi:10.1097/TP.0000000000001767
168. Li Y, Kurlander RJ. Comparison of anti-CD3 and anti-CD28-coated beads with soluble anti-CD3 for expanding human T cells: Differing impact on CD8 T cell phenotype and responsiveness to restimulation. *J Transl Med*. 2010;8(1):104. doi:10.1186/1479-5876-8-104
169. Kim SJ, Yoon SE, Kim WS. Current Challenges in Chimeric Antigen Receptor T-cell Therapy in Patients With B-cell Lymphoid Malignancies. *Ann Lab Med*. 2024;44(3):210-221. doi:10.3343/alm.2023.0388
170. Feuchtinger T, Matthes-Martin S, Richard C, et al. Safe adoptive transfer of virus-specific T-cell immunity for the treatment of systemic adenovirus infection after allogeneic stem cell transplantation. *Br J Haematol*. 2006;134(1):64-76. doi:10.1111/j.1365-2141.2006.06108.x
171. Koldehoff M, Eiz-Vesper B, Maecker-Kolhoff B, et al. Long-Term Follow-Up after Adoptive Transfer of BK-Virus-Specific T Cells in Hematopoietic Stem Cell Transplant Recipients. *Vaccines*. 2023;11(4). doi:10.3390/vaccines11040845
172. Grau-Vorster M, López-Montañés M, Cantó E, et al. Characterization of a Cytomegalovirus-Specific T Lymphocyte Product Obtained Through a Rapid and Scalable Production Process for Use in Adoptive Immunotherapy. *Front Immunol*. 2020;11(February). doi:10.3389/fimmu.2020.00271
173. Ma Q, Wang Y, Lo ASY, Gomes EM, Junghans RP. Cell density plays a critical role in ex vivo expansion of T cells for adoptive immunotherapy. *J Biomed Biotechnol*. 2010;2010. doi:10.1155/2010/386545
174. Sandstrom PA, Buttke TM. Autocrine production of extracellular catalase prevents apoptosis of the human CEM T-cell line in serum-free medium. *Proc Natl Acad Sci U S A*. 1993;90(10):4708-4712. doi:10.1073/pnas.90.10.4708
175. Borst J, Ahrends T, Bąbała N, Melief CJM, Kastenmüller W. CD4+ T cell help in cancer immunology and immunotherapy. *Nat Rev Immunol*. 2018;18(10):635-647. doi:10.1038/s41577-018-0044-0
176. Ahrends T, Busselaar J, Severson TM, et al. CD4+ T cell help creates memory CD8+ T cells with innate and help-independent recall capacities. *Nat Commun*. 2019;10(1):1-13. doi:10.1038/s41467-019-13438-1
177. Su Z, Peluso M V., Raffegerst SH, Schendel DJ, Roskrow MA. Antigen presenting cells transfected with LMP2a RNA induce CD4+ LMP2a-specific cytotoxic T lymphocytes

- which kill via a fas-independent mechanism. *Leuk Lymphoma*. 2002;43(8):1651-1662. doi:10.1080/1042819021000002992
178. Bickham K, Münz C, Tsang ML, et al. EBNA1-specific CD4+ T cells in healthy carriers of Epstein-Barr virus are primarily Th1 in function. *J Clin Invest*. 2001;107(1):121-130. doi:10.1172/JCI10209
 179. Leen A, Meij P, Redchenko I, et al. Differential Immunogenicity of Epstein-Barr Virus Latent-Cycle Proteins for Human CD4 + T-Helper 1 Responses . *J Virol*. 2001;75(18):8649-8659. doi:10.1128/jvi.75.18.8649-8659.2001
 180. Fu T, Kui SV, Wang RF. Critical role of EBNA1-specific CD4+ T cells in the control of mouse Burkitt lymphoma in vivo. *J Clin Invest*. 2004;114(4):542-550. doi:10.1172/JCI22053
 181. Durkee-Shock J, Lazarski CA, Jensen-Wachspress MA, et al. Transcriptomic analysis reveals optimal cytokine combinations for SARS-CoV-2-specific T cell therapy products. *Mol Ther Methods Clin Dev*. 2022;25(June):439-447. doi:10.1016/j.omtm.2022.04.013
 182. Gerdemann U, Vera JF, Rooney CM, Leen AM. Generation of multivirus-specific T cells to prevent/treat viral infections after allogeneic hematopoietic stem cell transplant. *J Vis Exp*. 2011;10(51):1-6. doi:10.3791/2736
 183. Lazarski CA, Datar AA, Reynolds EK, Keller MD, Bollard CM, Hanley PJ. Identification of new cytokine combinations for antigen-specific T-cell therapy products via a high-throughput multi-parameter assay. *Cytotherapy*. 2021;23(1):65-76. doi:10.1016/j.jcyt.2020.08.006
 184. Cox MA, Kahan SM, Zajac AJ. Anti-viral CD8 T cells and the cytokines that they love. *Virology*. 2013;435(1):157-169. doi:10.1016/j.virol.2012.09.012
 185. Gong W, Hoffmann JM, Stock S, et al. Comparison of IL-2 vs IL-7/IL-15 for the generation of NY-ESO-1-specific T cells. *Cancer Immunol Immunother*. 2019;68(7):1195-1209. doi:10.1007/s00262-019-02354-4
 186. Kaneko S, Mastaglio S, Bondanza A, et al. IL-7 and IL-15 allow the generation of suicide gene modified alloreactive self-renewing central memory human T lymphocytes. *Blood*. 2009;113(5):1006-1015. doi:10.1182/blood-2008-05-156059
 187. Liu Q, Sun Z, Chen L. Memory T cells: strategies for optimizing tumor immunotherapy. *Protein Cell*. 2020;11(8):549-564. doi:10.1007/s13238-020-00707-9
 188. Xu Y, Zhang M, Ramos CA, et al. Closely related T-memory stem cells correlate with in vivo expansion of CAR.CD19-T cells and are preserved by IL-7 and IL-15. *Blood*. 2014;123(24):3750-3759. doi:10.1182/blood-2014-01-552174
 189. Yang Y, Lundqvist A. Immunomodulatory Effects of IL-2 and IL-15; Implications for Cancer Immunotherapy 1 2. *Cancers (Basel)*. 2020;12(3586):1-20. doi:10.3390/cancers12123586

190. Zeng R, Spolski R, Finkelstein SE, et al. Synergy of IL-21 and IL-15 in regulating CD8+ T cell expansion and function. *J Exp Med*. 2005;201(1):139-148. doi:10.1084/jem.20041057
191. Rocha FA, Silveira CRF, dos Santos AF, Stefanini ACB, Hamerschlag N, Marti LC. Development of a highly cytotoxic, clinical-grade virus-specific T cell product for adoptive T cell therapy. *Cell Immunol*. 2024;395-396(June 2023). doi:10.1016/j.cellimm.2023.104795
192. Xu H, Wang N, Cao W, Huang L, Zhou J, Sheng L. Influence of various medium environment to in vitro human T cell culture. *Vitr Cell Dev Biol - Anim*. 2018;54(8):559-566. doi:10.1007/s11626-018-0273-3
193. MacPherson S, Keyes S, Kilgour MK, et al. Clinically relevant T cell expansion media activate distinct metabolic programs uncoupled from cellular function. *Mol Ther Methods Clin Dev*. 2022;24(March):380-393. doi:10.1016/j.omtm.2022.02.004
194. Wherry EJ, Kurachi M. Molecular and cellular insights into T cell exhaustion. *Nat Rev Immunol*. 2015;15(8):486-499. doi:10.1038/nri3862
195. Ma J, Yan S, Zhao Y, Yan H, Zhang Q, Li X. Blockade of PD-1 and LAG-3 expression on CD8+ T cells promotes the tumoricidal effects of CD8+ T cells. *Front Immunol*. 2023;14(September):1-13. doi:10.3389/fimmu.2023.1265255
196. Sanromán F, Joshi K, Au L, Chain B, Turajlic S. TCR sequencing: applications in immuno-oncology research. *Immuno-Oncology Technol*. 2023;17(C):1-9. doi:10.1016/j.iotech.2023.100373
197. Frank ML, Lu K, Erdogan C, et al. T-Cell Receptor Repertoire Sequencing in the Era of Cancer Immunotherapy. *Clin Cancer Res*. 2023;29(6):994-1008. doi:10.1158/1078-0432.CCR-22-2469
198. Vera JF, Brenner LJ, Gerdemann U, et al. Accelerated production of antigen-specific T-cells for pre-clinical and clinical applications using Gas-permeable Rapid Expansion cultureware (G-Rex). *J Immunother*. 2010;33(3):305-315. doi:10.1097/CJI.0b013e3181c0c3cb.
199. Lapteva N, Vera JF. Optimization manufacture of virus- and tumor-specific T cells. *Stem Cells Int*. 2011;2011:17-20. doi:10.4061/2011/434392
200. Gotti E, Tettamanti S, Zaninelli S, et al. Optimization of therapeutic T cell expansion in G-Rex device and applicability to large-scale production for clinical use: GMP-compliant polyclonal T cell expansion in G-Rex. *Cytotherapy*. 2022;24(3):334-343. doi:10.1016/j.jcyt.2021.11.004
201. Luostarinen A, Kailaanmäki A, Turkki V, et al. Optimizing lentiviral vector formulation conditions for efficient ex vivo transduction of primary human T cells in chimeric antigen receptor T-cell manufacturing. *Cytotherapy*. 2024;26:1084-1094.

- doi:10.1016/j.jcyt.2024.04.002
202. Eberhardt F, Hückelhoven-Krauss A, Kunz A, et al. Impact of serum-free media on the expansion and functionality of CD19.CAR T-cells. *Int J Mol Med*. 2023;52(1):1-13. doi:10.3892/ijmm.2023.5261
 203. Watanabe N, Mo F, McKenna MK. Impact of Manufacturing Procedures on CAR T Cell Functionality. *Front Immunol*. 2022;13(April):1-11. doi:10.3389/fimmu.2022.876339
 204. Lu TL, Pugach O, Somerville R, et al. A Rapid Cell Expansion Process for Production of Engineered Autologous CAR-T Cell Therapies. *Hum Gene Ther Methods*. 2016;27(6):209-218. doi:10.1089/hgtb.2016.120
 205. Owen RE, Sinclair E, Emu B, et al. Loss of T cell responses following long-term cryopreservation. *J Immunol Methods*. 2007;326(1-2):93-115. doi:10.1016/j.jim.2007.07.012
 206. Seki T, Yuasa S, Fukuda K. Generation of induced pluripotent stem cells from a small amount of human peripheral blood using a combination of activated T cells and Sendai virus. *Nat Protoc*. 2012;7(4):718-728. doi:10.1038/nprot.2012.015
 207. Nakagawa M, Koyanagi M, Tanabe K, et al. Generation of induced pluripotent stem cells without Myc from mouse and human fibroblasts. *Nat Biotechnol*. 2008;26(1):101-106. doi:10.1038/nbt1374
 208. Doan AE, Mueller KP, Chen AY, et al. *FOXO1 Is a Master Regulator of Memory Programming in CAR T Cells*. Vol 629. Springer US; 2024. doi:10.1038/s41586-024-07300-8
 209. Chan JD, Scheffler CM, Munoz I, et al. FOXO1 enhances CAR T cell stemness, metabolic fitness and efficacy. *Nature*. 2024;629(8010):201-210. doi:10.1038/s41586-024-07242-1
 210. Denk D, Petrocelli V, Conche C, et al. Expansion of T memory stem cells with superior anti-tumor immunity by Urolithin A-induced mitophagy. *Immunity*. 2022;55(11):2059-2073.e8. doi:10.1016/j.immuni.2022.09.014
 211. Lak S, Janelle V, Djedid A, et al. Combined PD-L1 and TIM3 blockade improves expansion of fit human CD8+ antigen-specific T cells for adoptive immunotherapy. *Mol Ther Methods Clin Dev*. 2022;27(December):230-245. doi:10.1016/j.omtm.2022.09.016

ANNEXES

Table S1. Information of PepTivator® EBV consensus pool

Lytic and latent EBV proteins	HLA class I-restriction	HLA class II-restriction
LMP2A	HLA-A*02	HLA-DR
BRLF1	HLA-A*03	
BMLF1 (EB2)	HLA-A*11	
BNLF1 (LMP1)	HLA-A*24	
BERF3 (EBNA6)	HLA-A*26	
BERF1 (EBNA3)	HLA-B*07	
BERF2 (EBNA4)	HLA-B*08	
BALF2 (DNBI)	HLA-B*15	
BMRF1	HLA-B*18	
BZLF1	HLA-B*27	
BNRF1 (MTP)	HLA-B*35	
EBNA 1	HLA-B*40	
BLLF1 (gp350)	HLA-B*44:02	
BXLF2		
EBNA2		

Note: Contains 43 peptides of 8-20 amino acids in length. 32 of these peptides are MHC class I and 11 peptides are MHC class II restricted. The sequences of these peptides were derived from the following 15 different lytic and latent EBV proteins. Table obtained from the data sheet of Miltenyi's product (Ref. 130-099-764 or 130-103-462).

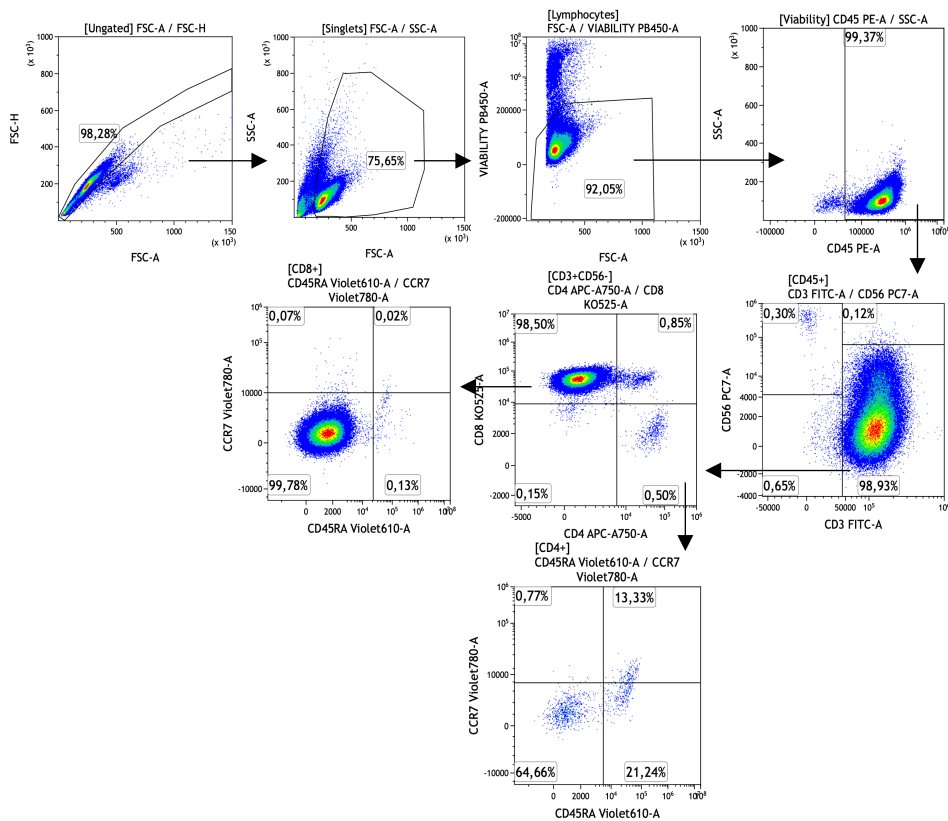


Figure S1. Flow cytometry analysis strategy for surface staining, analyzed using Kaluza software from Beckman Coulter. Example from the expansion of donor 5.

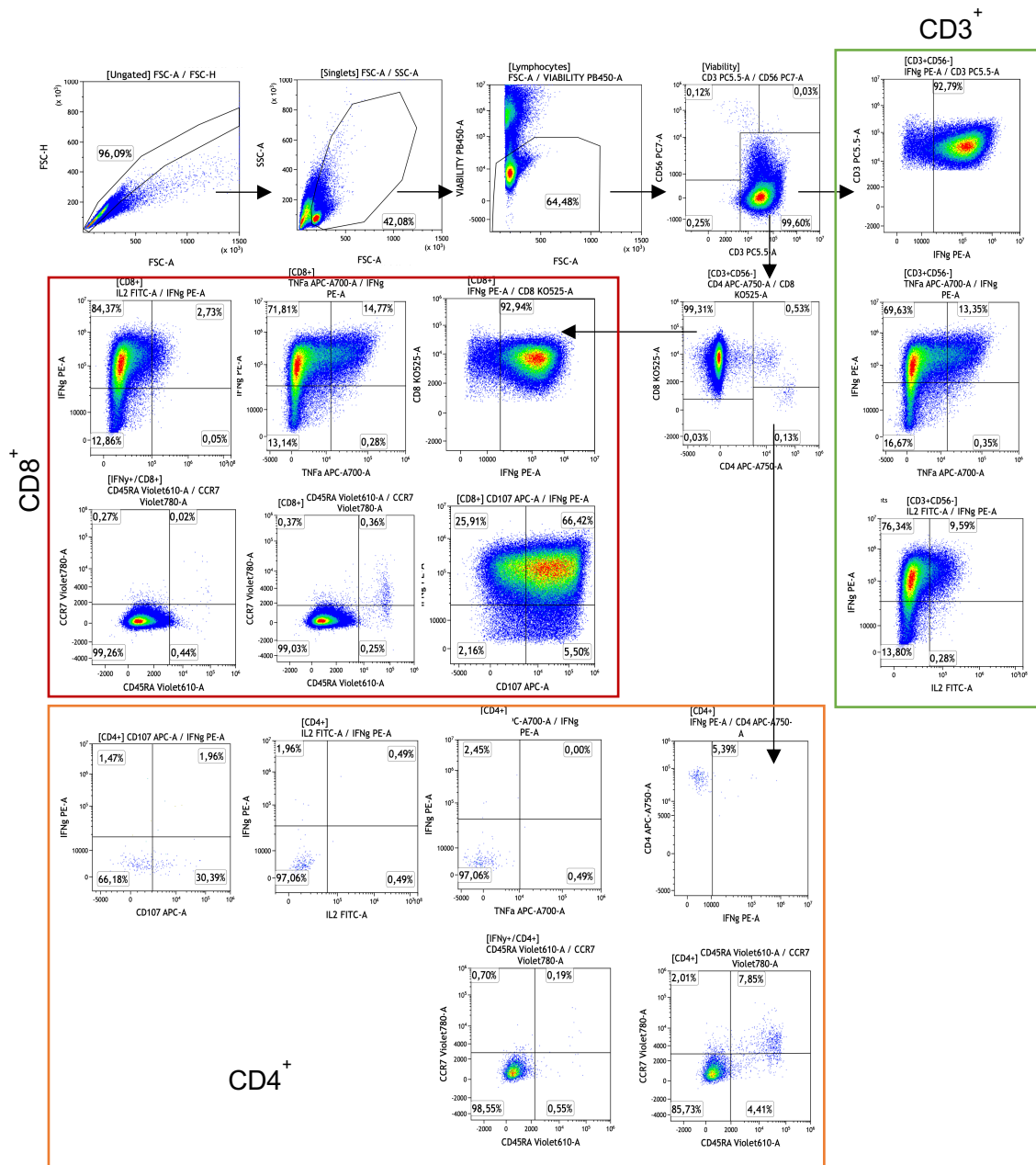


Figure S2. Flow cytometry analysis strategy for CD107a degranulation assay and intracellular staining, analyzed using Kaluza software from Beckman Coulter. Example from the expansion of donor 5.

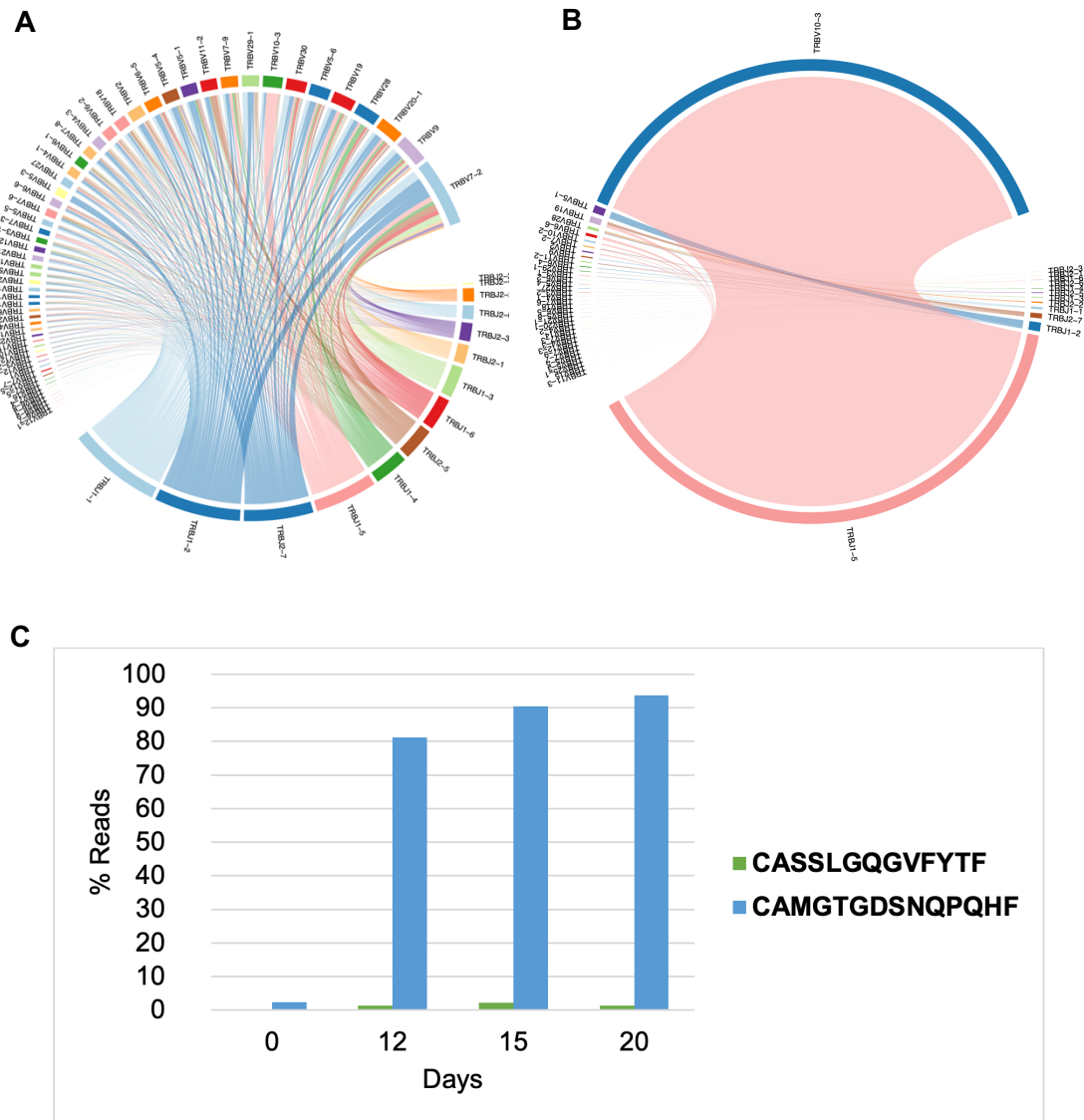


Figure S3. TCR- β analysis of the EBVSTs expanded product obtained from donor 5 (A) TCR- β clonotypes diversity shared pre-expansion (day 0) and (B) post-expansion (day 20) (C) CDR3 sequences of clonotypes with more than 2% reads (red dotted line) obtained at days 0, 12, 15 and 20 with PepTivator[®] EBV consensus stimulus. CDR3 sequences in bold from the TCR- β , represent the clonotypes described in the literature: CASSLGQGVFYTF is described that recognizes the EBNA-4 antigen restricted to HLA-A*11:01 and CAMGTGDSNQPQHF is described that recognizes the BZLF1 antigen restricted to HLA-B*35:01. Both HLA alleles are expressed in donor 5 (Table 12, Methods Section).

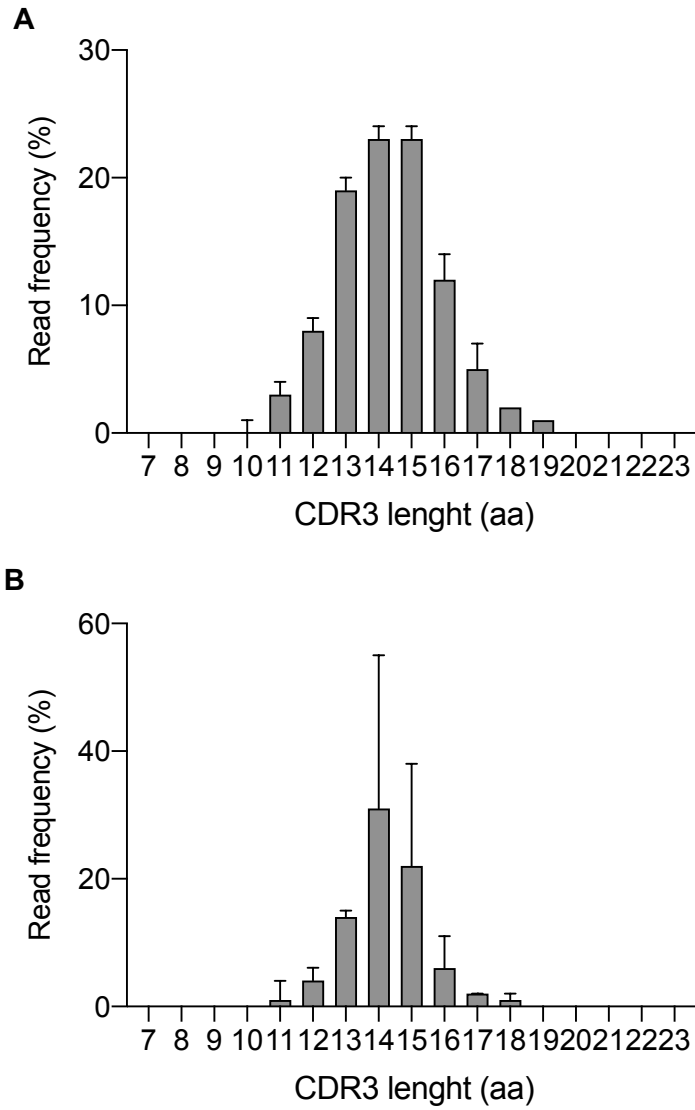


Figure S4. Distribution of CDR3 amino acid sequence length in the TCR- β analysis (A) Length of amino acids with a normal distribution for a diverse TCR repertoire were expanded in the PBMCs pre-expansion (day 0) **(B)** Length of amino acids, with altered distribution due to the expansion of EBVSTs on day 20.